

**Ruthenium Carbonyl Complexes Containing
Ligands Derived From Pyridine And
Pyridine-2-thione.**

A thesis presented for the degree of

DOCTOR OF PHILOSOPHY

of the

University of London

by

BRUCE COCKERTON

1993

Department of Chemistry, University College London.

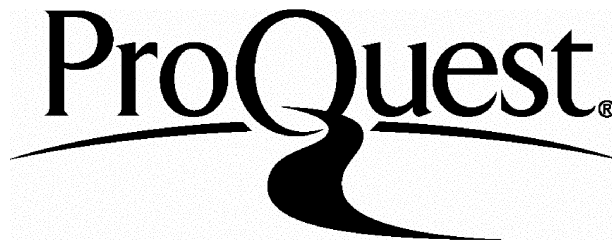
ProQuest Number: 10045548

All rights reserved

INFORMATION TO ALL USERS

The quality of this reproduction is dependent upon the quality of the copy submitted.

In the unlikely event that the author did not send a complete manuscript and there are missing pages, these will be noted. Also, if material had to be removed, a note will indicate the deletion.



ProQuest 10045548

Published by ProQuest LLC(2016). Copyright of the Dissertation is held by the Author.

All rights reserved.

This work is protected against unauthorized copying under Title 17, United States Code.
Microform Edition © ProQuest LLC.

ProQuest LLC
789 East Eisenhower Parkway
P.O. Box 1346
Ann Arbor, MI 48106-1346

ABSTRACT

This thesis describes the synthesis and characterisation of some ruthenium carbonyl complexes containing ligands derived from pyridine and pyridine-2-thione. These complexes have been characterised by infrared, ^1H and ^{13}C NMR and mass spectroscopy, elemental analysis and X-ray crystallography.

Chapter One is an introduction to the coordination chemistry of pyridine and pyridine-2-thione and contains a brief survey of transition metal complexes containing these ligands.

Chapter Two concerns the separation and structural characterisation of the two isomers of $[\text{Re}_2\text{Ru}_2(\mu_4\text{-S})(\mu\text{-C}_5\text{H}_4\text{N})(\mu\text{-pyS})(\text{CO})_{13}]$. This compound reacts with $[\text{Ru}_3(\text{CO})_{12}]$ to give $[\text{Re}_2\text{Ru}_2(\mu_4\text{-S})(\mu\text{-H})(\mu\text{-C}_5\text{H}_4\text{N})(\text{CO})_{14}]$, the crystal structure of which was determined. The effect of altered conditions on the reaction between $[\text{Re}_2(\mu\text{-pyS})_2(\text{CO})_6]$ and $[\text{Ru}_3(\text{CO})_{12}]$ was investigated.

Chapters Three and Five concern the synthesis of high nuclearity clusters via thermolysis of $[\text{Ru}_3\text{H}(\text{pyS})(\text{CO})_9]$ and reaction of $[\text{Ru}_3(\text{CO})_{12}]$ with $[\text{Ru}(\text{pyS})_2(\text{CO})_2]$. The 2D NMR spectrum of $[\text{Ru}_4(\mu_4\text{-S})(\mu\text{-C}_5\text{H}_4\text{N})_2(\text{CO})_{12}]$ and the crystal structures of $[\text{Ru}_6(\mu_4\text{-S})_2(\mu\text{-C}_5\text{H}_4\text{N})_2(\text{CO})_{18}]$ and $[\text{Ru}_6(\mu_4\text{-S})(\mu\text{-SH})(\mu_3\text{-pyS})(\text{CO})_{17}]$ are discussed.

Chapter Four describes the reaction between $[\text{Ru}_3(\text{CO})_{12}]$ and pyridine. At $120\text{ }^\circ\text{C}$, $[\text{Ru}_2(\mu\text{-C}_5\text{H}_4\text{N})_2(\text{CO})_6]$ is produced as head-to-head and head-to-tail isomers. The crystal structures of the 4-methylpyridine osmium analogues were determined. At $180\text{ }^\circ\text{C}$, $[\text{Ru}_2(\mu\text{-C}_5\text{H}_4\text{N})(\mu\text{-C}_{10}\text{H}_7\text{N}_2)(\text{CO})_5]$ is produced, shown by X-ray diffraction to contain a bridging ortho-metallated bipy ligand

formed by coupling of two 2-pyridyl ligands. A similar reaction with 4-methylpyridine gave an analogous compound as well as $[\text{Ru}_2\text{Cl}(\mu\text{-H})(\mu\text{-MeC}_5\text{H}_3\text{N})_2(\text{Me}_2\text{C}_{10}\text{H}_6\text{N}_2)(\text{CO})_3]$. At 180 °C, increased reaction times result in Ru–Ru bond cleavage, giving $[\text{RuCl}_2(\text{CO})_2(\text{py})_2]$ and $[\text{RuCl}_2(\text{CO})(\text{py})_3]$. $[\text{Ru}_2(\mu\text{-C}_5\text{H}_4\text{N})_2(\text{CO})_6]$ was treated with 4-methylpyridine giving mono- or dinuclear compounds, depending on the isomer used. The crystal structure of $[\text{Ru}_2\text{HCl}(\mu\text{-MeC}_5\text{H}_3\text{N})_2(\text{C}_{10}\text{H}_8\text{N}_2)(\text{CO})_3] \cdot \text{H}_2\text{O}$ was determined.

In summary, the pyridine-2-thionato ligand was found to coordinate in doubly- and triply-bridging modes, or to undergo S–C cleavage to give μ_4 -sulphido complexes containing 2-pyridyl ligands. Pyridine was found to react with $[\text{Ru}_3(\text{CO})_{12}]$ to give a range of products containing monodentate or ortho-metallated pyridyl ligands, as well as undergoing coupling reactions at ruthenium centres to give bipyridyl ligands.

CONTENTS

Abstract	2
Contents	4
Acknowledgements	7
List of Abbreviations	8
List of Tables	9
List of Figures	11

CHAPTER ONE	13
--------------------	----

**An Introduction to the Coordination Chemistry of Pyridine
and Pyridine-2-thione**

1.1	Introduction	14
1.2	Physical properties of pyridine-2-thione	15
1.3	Transition metal complexes of pyridine-2-thione and pyridine-2-thionato ligands	20
1.4	Complexes containing monodentate pySH or pyS ligands	21
1.5	Complexes containing chelating pyS ligands	23
1.6	Complexes containing doubly-bridging pyS ligands	24
1.7	Complexes containing triply-bridging pyS ligands	26
1.8	Complexes containing quadruply-bridging pyS ligands	27
1.9	Cleavage of the C-S bond of the pyS ligand	27
1.10	Physical properties of pyridine	28
1.11	Transition metal complexes of pyridine	29

CHAPTER TWO 33

Mixed Tetranuclear Rhenium-Ruthenium Compounds

2.1	Introduction	34
2.2	Separation of the isomers of $[\text{Re}_2\text{Ru}_2\text{S}(\text{C}_5\text{H}_4\text{N})(\text{pyS})(\text{CO})_{13}]$	44
2.3	Effect of altered reaction conditions on product ratios	55
2.4	Reaction of $[\text{Re}_2\text{Ru}_2\text{S}(\text{C}_5\text{H}_4\text{N})(\text{pyS})(\text{CO})_{13}]$ with $[\text{Ru}_3(\text{CO})_{12}]$	57
2.5	Experimental	67

CHAPTER THREE 73

Higher Nuclearity Ruthenium Carbonyl Complexes Derived

From $[\text{Ru}(\text{pyS})_2(\text{CO})_2]$ and $[\text{Ru}_3(\text{CO})_{12}]$

3.1	Introduction	74
3.2	Results and Discussion	80
	(i) Syntheses	80
	(ii) Characterisation	80
3.3	Experimental	105

CHAPTER FOUR 108

Dinuclear Ruthenium and Osmium Carbonyl Complexes

Derived From Pyridine and 4-Methylpyridine

4.1	Introduction	109
4.2	Results and Discussion	111
	(i) Crystal structures of the two isomers of $[\text{Os}_2(\text{CO})_6(\text{MeC}_5\text{H}_3\text{N})_2]$	111
	(ii) The ruthenium dimers $[\text{Ru}_2(\text{CO})_6(\text{C}_5\text{H}_4\text{N})_2]$	116

(iii)	The reaction of $[\text{Ru}_3(\text{CO})_{12}]$ with pyridine and 4-methylpyridine under more forcing conditions	120
(iv)	The reaction of $[\text{Ru}_3(\text{CO})_{12}]$ with pyridine under very forcing conditions	132
(v)	The reactions of $[\text{Ru}_2(\text{CO})_6(\text{C}_5\text{H}_4\text{N})_2]$ with 4-methylpyridine	136
4.3	Experimental	158
CHAPTER FIVE		169
Higher Nuclearity Ruthenium Carbonyl Complexes Derived From $[\text{Ru}_3\text{H}(\text{pyS})(\text{CO})_9]$		
5.1	Introduction	170
5.2	Results and Discussion	175
5.3	Other compounds produced from the thermolysis of $[\text{Ru}_3\text{H}(\text{pyS})(\text{CO})_9]$ under an atmosphere of CO	185
5.4	Other reactions	187
5.5	Experimental	192
Appendix : Fractional Atomic Coordinates for the Crystal Structures		196
General Experimental		205
References		206

ACKNOWLEDGEMENTS

I would like to express my heartfelt gratitude to my supervisor, Professor Deeming, for his invaluable advice, for his constant enthusiasm and for his words of encouragement in all aspects of this work. I would also like to thank Dr. Tocher for all his help with the X-ray crystallography.

I am very grateful to members of the Deeming Group, past and present, for helpful suggestions as well as entertaining distractions from research, especially Tara, Jane, Caroline, Dave and Simon. The efforts of all the technical staff are also very much appreciated for their assistance in this work especially Alan Stones, Gillian Maxwell and Steve Corker in the analytical department and Margaret Murzek for the mass spectroscopy.

Finally, I would like to say thankyou to all my friends in the department for helping to make my time at UCL so enjoyable, and especially to Duncan, Rob, Elliot, Dan, Pete and Navjot and to Russell for being such a groovy flatmate.

List of Abbreviations Used in This Thesis

Å	angstrom
acac	acetylacetonate anion
bipy	2,2'-bipyridine
b.p.	boiling point
cm	centimetre
cp	cyclopentadienyl (C ₅ H ₅)
cp*	pentamethylcyclopentadienyl (C ₅ Me ₅)
°	degrees
d	doublet
dmp	2-(dimethylaminomethyl)phenyl
EI	Electron Impact
FAB	Fast Atom Bombardment
h	hour
HPLC	High Performance Liquid Chromatography
Hz	hertz
Me	methyl
Mepy	4-methylpyridine
min	minute
NMR	Nuclear Magnetic Resonance
Ph	phenyl
ppm	parts per million
py	pyridine
pySH	pyridine-2-thione
pyS	pyridine-2-thionato
s	singlet
t	triplet
TLC	Thin Layer Chromatography
δ	chemical shift
v	wavenumber (cm ⁻¹)
λ	wavelength

List of Tables

1.1	¹ H NMR Data for Pyridine and Pyridine-2-thione	18
2.1	Bond Lengths and Angles for [Re ₂ Ru ₂ S(C ₅ H ₄ N)(pyS)(CO) ₁₃]	50
2.2	Effect of Altered Conditions on Product Ratios for the Reaction between [Ru ₃ (CO) ₁₂] and [Re ₂ (pyS) ₂ (CO) ₆]	55
2.3	Binomial Probability Distribution and Observed Yields in <i>m</i> -xylene	57
2.4	Bond Lengths and Angles for [Re ₂ Ru ₂ (S)(H)(C ₅ H ₄ N)(CO) ₁₄]	61
2.5	¹ H NMR Data for the New Compounds	65
2.6	Infrared Data for the New Compounds	66
3.1	Bond Lengths and Angles for [Ru ₆ (S) ₂ (C ₅ H ₄ N) ₂ (CO) ₁₈]	85
3.2	Colours of Some Polynuclear Sulphido Ruthenium Carbonyl Clusters	90
3.3	Infrared Data for the New Compounds	101
3.4	¹ H NMR Data for the New Compounds Recorded in CDCl ₃	102
3.5	¹ H NMR Data for the New Compounds Recorded in d ⁶ -acetone	103
3.6	¹³ C NMR Data for the New Compounds	104
4.1	Bond Lengths and Angles for [Os ₂ (CO) ₆ (MeC ₅ H ₃ N) ₂]	114
4.2	Comparison of the ¹³ C NMR Chemical Shifts of Pyridine and [Ru ₂ (CO) ₆ (C ₅ H ₄ N) ₂]	118
4.3	Bond Lengths and Angles for [Ru ₂ (CO) ₅ (C ₅ H ₄ N)(C ₁₀ H ₇ N ₂)]	123
4.4	Bond Lengths and Angles for [Ru ₂ HCl(CO) ₃ (MeC ₅ H ₃ N) ₂ (C ₁₀ H ₈ N ₂)] · H ₂ O	142
4.5	¹ H NMR Data for the New Compounds	151

4.6	^{13}C NMR Data for $[\text{Ru}_2(\text{CO})_6(\text{C}_5\text{H}_4\text{N})_2]$	154
4.7	Infrared Data for the New Compounds	155
4.8	Mass, Infrared and ^{13}C NMR Spectroscopic Data for $[\text{RuCl}_2(\text{CO})_2(\text{py})_2]$ and $[\text{RuCl}_2(\text{CO})(\text{py})_3]$	156
4.9	^1H NMR Data for $[\text{RuCl}_2(\text{CO})_2(\text{py})_2]$ and $[\text{RuCl}_2(\text{CO})(\text{py})_3]$	157
5.1	Bond Lengths for $[\text{Ru}_6(\text{S})(\text{SH})(\text{pyS})(\text{CO})_{17}]$	177
5.2	Bond Angles for $[\text{Ru}_6(\text{S})(\text{SH})(\text{pyS})(\text{CO})_{17}]$	179
5.3	^1H NMR Data for $[\text{Ru}_6(\text{S})(\text{SH})(\text{pyS})(\text{CO})_{17}]$	190
5.4	Infrared Data for $[\text{Ru}_6(\text{S})(\text{SH})(\text{pyS})(\text{CO})_{17}]$	190
5.5	Spectroscopic Data for the Unidentified Compounds	191
A1	Atomic Coordinates for $[\text{Re}_2\text{Ru}_2\text{S}(\text{C}_5\text{H}_4\text{N})(\text{pyS})(\text{CO})_{13}]$	197
A2	Atomic Coordinates for $[\text{Re}_2\text{Ru}_2(\text{S})(\text{H})(\text{C}_5\text{H}_4\text{N})(\text{CO})_{14}]$	198
A3	Atomic Coordinates for $[\text{Ru}_6(\text{S})_2(\text{C}_5\text{H}_4\text{N})_2(\text{CO})_{18}]$	199
A4	Atomic Coordinates for $[\text{Ru}_2(\text{CO})_5(\text{C}_5\text{H}_4\text{N})(\text{C}_{10}\text{H}_7\text{N}_2)]$	200
A5	Atomic Coordinates for $[\text{Ru}_2\text{HCl}(\text{CO})_3(\text{MeC}_5\text{H}_3\text{N})_2(\text{C}_{10}\text{H}_8\text{N}_2)] \cdot \text{H}_2\text{O}$	201
A6	Atomic Coordinates for $[\text{Os}_2(\text{CO})_6(\text{MeC}_5\text{H}_3\text{N})_2]$	202
A7	Atomic Coordinates for $[\text{Ru}_6(\text{S})(\text{SH})(\text{pyS})(\text{CO})_{17}]$	203

List of Figures

1.1	Prototropic Exchange in Pyridine-2-thione	14
1.2	Dimeric Structure of Pyridine-2-thione	16
1.3	X-ray and Neutron Diffraction Structures of Pyridine-2-thione	17
1.4	Coordination Modes for Pyridine-2-thione and Pyridine-2-thionato Ligands	19
Scheme 2.1	Reaction of $[\text{Ru}_3(\text{CO})_{12}]$ with $[\text{Re}_2(\text{pyS})_2(\text{CO})_6]$	41
2.1	Structure of $[\text{ReRu}_3\text{S}(\text{C}_5\text{H}_4\text{N})(\text{CO})_{14}]$	42
2.2	Structure of $[\text{Re}_3\text{RuS}(\text{C}_5\text{H}_4\text{N})(\text{pyS})_2(\text{CO})_{11}]$	43
2.3	Structure of $[\text{Re}_2\text{Ru}_2\text{S}(\text{C}_5\text{H}_4\text{N})(\text{pyS})(\text{CO})_{13}]$ Isomer A	47
2.4	Structure of $[\text{Re}_2\text{Ru}_2\text{S}(\text{C}_5\text{H}_4\text{N})(\text{pyS})(\text{CO})_{13}]$ Isomer B	48
2.5	Structure of $[\text{Re}_2\text{Ru}_2\text{S}(\text{C}_5\text{H}_4\text{N})(\text{pyS})(\text{CO})_{13}]$ Isomer B Showing Correct and Incorrect 2-pyridyl Orientations	49
2.6	Structure of $[\text{Re}_2\text{Ru}_2(\text{S})(\text{H})(\text{C}_5\text{H}_4\text{N})(\text{CO})_{14}]$	59
2.7	Alternative View of $[\text{Re}_2\text{Ru}_2(\text{S})(\text{H})(\text{C}_5\text{H}_4\text{N})(\text{CO})_{14}]$ Showing Probable Hydride Position	60
3.1	Structure of $[\text{Ru}_6(\text{S})_2(\text{C}_5\text{H}_4\text{N})_2(\text{CO})_{18}]$	82
3.2	Alternative Views of $[\text{Ru}_6(\text{S})_2(\text{C}_5\text{H}_4\text{N})_2(\text{CO})_{18}]$	83
3.3	The Three Isomers of $[\text{Ru}_6(\text{S})_2(\text{C}_5\text{H}_4\text{N})_2(\text{CO})_{18}]$	84
3.4	The Three Isomers of $[\text{Ru}_4\text{S}(\text{C}_5\text{H}_4\text{N})_2(\text{CO})_{12}]$	95
3.5	^1H NMR Spectra of $[\text{Ru}_4\text{S}(\text{C}_5\text{H}_4\text{N})_2(\text{CO})_{12}]$	96
3.6	Two-dimensional ^1H NMR Spectrum of $[\text{Ru}_4\text{S}(\text{C}_5\text{H}_4\text{N})_2(\text{CO})_{12}]$	97

4.1	Structures of the Two Isomers of $[\text{Os}_2(\text{CO})_6(\text{MeC}_5\text{H}_4\text{N})_2]$	113
4.2	Isomers of $[\text{Ru}_2(\text{CO})_6(\text{C}_5\text{H}_4\text{N})_2]$	116
4.3	Structure of $[\text{Ru}_2(\text{CO})_5(\text{C}_5\text{H}_4\text{N})(\text{C}_{10}\text{H}_7\text{N}_2)]$	122
4.4	^1H NMR spectrum of $[\text{Ru}_2(\text{CO})_5(\text{C}_5\text{H}_4\text{N})(\text{C}_{10}\text{H}_7\text{N}_2)]$	125
4.5	Probable Structure of $[\text{Ru}_2\text{HCl}(\text{CO})_3(\text{MeC}_5\text{H}_3\text{N})_2(\text{Me}_2\text{C}_{10}\text{H}_6\text{N}_2)]$	129
4.6	Probable Structure of $[\text{RuCl}_2(\text{CO})_2(\text{py})_2]$	133
4.7	Possible Structures of $[\text{RuCl}_2(\text{CO})(\text{py})_3]$	134
4.8	^1H NMR spectra of $[\text{Ru}_2\text{HCl}(\text{CO})_3(\text{MeC}_5\text{H}_3\text{N})_2(\text{Me}_2\text{C}_{10}\text{H}_6\text{N}_2)]$ and $[\text{Ru}_2\text{HCl}(\text{CO})_3(\text{MeC}_5\text{H}_3\text{N})_2(\text{C}_{10}\text{H}_8\text{N}_2)] \cdot \text{H}_2\text{O}$	138
4.9	Two-dimensional ^1H NMR spectra of $[\text{Ru}_2\text{HCl}(\text{CO})_3(\text{MeC}_5\text{H}_3\text{N})_2(\text{Me}_2\text{C}_{10}\text{H}_6\text{N}_2)]$ and $[\text{Ru}_2\text{HCl}(\text{CO})_3(\text{MeC}_5\text{H}_3\text{N})_2(\text{C}_{10}\text{H}_8\text{N}_2)] \cdot \text{H}_2\text{O}$	139
4.10	Structure of $[\text{Ru}_2\text{HCl}(\text{CO})_3(\text{MeC}_5\text{H}_3\text{N})_2(\text{C}_{10}\text{H}_8\text{N}_2)] \cdot \text{H}_2\text{O}$	140
4.11	Structure of $[\text{Ru}_2\text{HCl}(\text{CO})_3(\text{MeC}_5\text{H}_3\text{N})_2(\text{C}_{10}\text{H}_8\text{N}_2)] \cdot \text{H}_2\text{O}$ Showing Probable Hydride Position.	141
4.12	Possible Mechanism for Ru–Ru Cleavage	150
5.1	Structure of $[\text{Ru}_3\text{H}(\text{pyS})(\text{CO})_9]$	170
5.2	Structure of $[\{\text{Ru}_3\text{H}(\text{pyS})(\text{CO})_7\}_3]$	171
5.3	Structure of $[\text{Ru}_6(\text{S})(\text{SH})(\text{pyS})(\text{CO})_{17}]$	176
5.4	Structure of $[\text{Ru}_6(\text{S})(\text{EtNCSNHEt})(\text{EtNCSNHEt})(\text{CO})_{16}]$	184
5.5	Structure of $[\{\text{Os}_3\text{S}_2(\text{CO})_8\}_2]$	186
5.6	Structure of $[\text{Ru}_6(\text{H})(\text{S})(\text{SC}(\text{NPh})\text{NPh})(\text{CO})_{16}]$	187

CHAPTER ONE

An Introduction to the Coordination Chemistry of Pyridine-2-thione and Pyridine.

1.1 Introduction.

Nitrogen-containing heterocyclic compounds possessing exocyclic functional groups capable of coordination and undergoing prototropic exchange (Figure 1.1) belong to a class of ligands described as ambidentate.¹ These ligands have more than one possible mode of coordination and are of considerable interest because of their diverse use in synthetic chemistry and because of the insight into the nature of the metal-ligand bond that their behaviour provides.² In addition, interest in these ligand systems has increased since the discovery that *cis*-platin and related complexes are powerful anti-carcinogens.³ This property is thought to arise from the coordination of these transition metal complexes to the purine and pyrimidine bases in DNA,^{4,5} and as a consequence the coordination chemistry of these ligands and their sulphur-containing analogues has been extensively studied.⁵

Pyridine-2-thione is a simple member of the class of nitrogen heterocycles possessing an exocyclic functionality and undergoes prototropic exchange as shown in Figure 1.1.

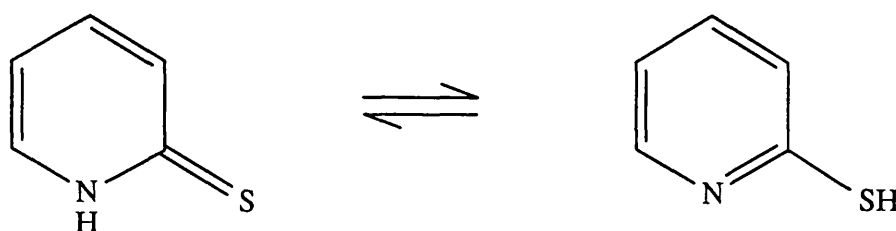


Figure 1.1 Prototropic exchange between the two tautomeric forms of pyridine-2-thione.

As a ligand, pyridine-2-thione gives rise to an extensive chemistry with

considerable structural diversity since it can coordinate in the neutral thione form or the deprotonated thionato form. In both instances there are many different ways in which the ligand can coordinate (Figure 1.4). We have chosen to use pyridine-2-thione as a ligand because of the wide variety exhibited in its coordination to metal atoms and in particular, because of its potential to undergo further modification once it is already bound to metal centres. These modifications are typified by changes in the coordination mode of the ligand *via* the utilisation of a lone-pair of electrons on the sulphur atom or, more commonly in this thesis, C-S cleavage which leads to separate μ_4 -S and 2-pyridyl ligands. The regular occurrence of the 2-pyridyl ligand in our work with pyridine-2-thione prompted us to investigate more extensively the reactions of pyridine itself with ruthenium carbonyl. In the following pages is a discussion of the chemistry and coordination modes of pyridine-2-thione and pyridine ligands and a brief survey of the transition metal complexes in which they are observed.

1.2 *Physical Properties of Pyridine-2-thione.*

Pyridine-2-thione is a yellow crystalline compound (m.p. 128-130 °C) which is sparingly soluble in water and diethylether but readily dissolves in most polar organic solvents.⁶ The compound is a weak acid ($pK_a = 9.97$) and exists in equilibrium with the thiol form,^{6,8} as shown in Figure 1.1.

The equilibrium position between the tautomers pyridine-2-thione and pyridine-2-thiol is very sensitive to the nature of the solvent, the thione form predominating in aqueous, methanol or acetone solution,⁸⁻¹⁰ while in low

polarity solvents the equilibrium is more towards the thiol form.¹¹ Spectroscopic evidence suggests that in chloroform and cyclohexane solutions, particularly at high concentrations, pyridine-2-thione exists as H-bonded dimers (Figure 1.2).^{9,18}

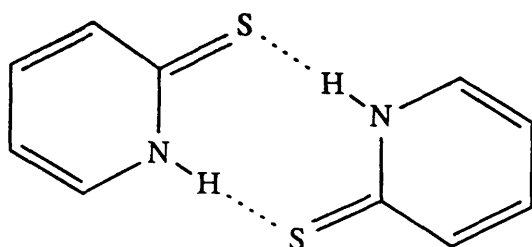


Figure 1.2 Hydrogen-bonded dimeric structure of pyridine-2-thione.

The crystal structure of pyridine-2-thione was first reported by Penfold in 1953.¹² It was found that the C-S bond distance was 1.68(2) Å and by using weighted contributions of the various tautomers to the ground state structure, Penfold calculated that it contained 65% double bond character. The thione structure was further supported by the large variations observed for the C-C bond distances in the ring. Since the thiol form is aromatic, one might expect to find essentially equal bond lengths for this tautomer. The molecules in the crystal were found to exist in pairs and it was suggested that they were joined by weak H-bonding. A more recent X-ray structure determination confirmed the existence of H-bonded dimers of the pyridine-2-thione tautomer in the crystal.¹³ A neutron diffraction study, reported by the same authors, located the mobile proton firmly on the nitrogen atom which is, in turn, H-bonded to a sulphur atom on another molecule (N-H---S = 3.289(2) Å). Bond lengths and angles for the two determinations are given in Figure 1.3. The authors

also noted that the structure complied with the general rule for pyridine derivatives which states that where the ring nitrogen atom is protonated, the C–N–C angle is greater than 120° ,¹⁴ the angle at the N atom of the ring in this case being $124.6(2)^\circ$. Evidence for the existence of the H-bonded dimer in the solid state also comes from infrared data ($\nu(\text{NH}) = 2870 \text{ cm}^{-1}$).¹⁵

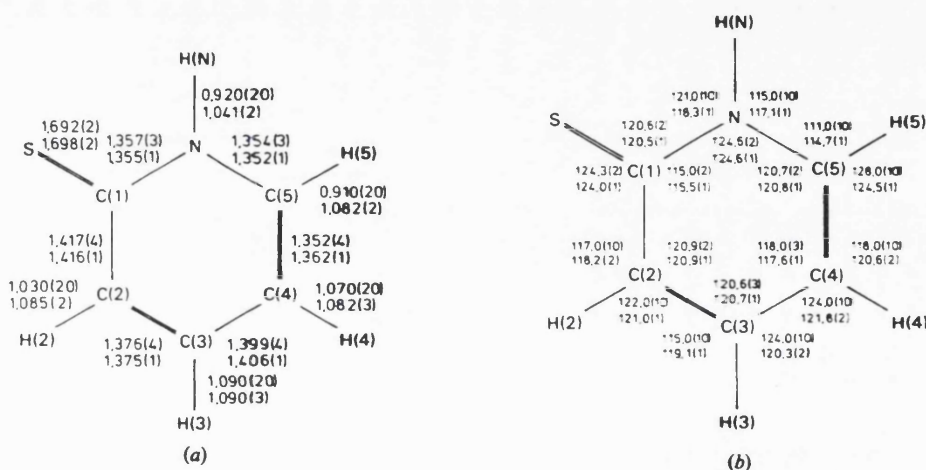


Figure 1.3 (a) Bond lengths (Å) and (b) bond angles ($^\circ$) in pyridine-2-thione. The upper values refer to the X-ray investigation, the lower values to the neutron investigation.

The ^1H NMR spectra of pyridines¹⁶ and substituted pyridines,¹⁶⁻¹⁸ and tautomeric systems in particular,¹⁷⁻¹⁹ have been the subject of intensive investigation. The various factors that influence spectral parameters can be divided grossly into substituent and solvent effects. The chemical shifts of α -protons in pyridine and its derivatives are at lower field than those of the other protons in the ring,¹⁸ which is due to the magnetic anisotropy of the ring nitrogen. One characteristic feature of pyridine spectra and of many nitrogen-containing hetero-aromatic compounds, is the broadening of the signals for the α -protons, which has been shown to be due to coupling with the nitrogen

atom by heteronuclear decoupling techniques.²⁰ These α -proton resonances are observed to sharpen up on coordination of the nitrogen lone-pair.²¹ The NH resonance in free pyridine-2-thione is observed as a sharp singlet at $\delta = 13.48$ ppm in CDCl_3 and fast exchange of this proton has the result that no vicinal coupling to the α -protons is observed. When the neutral ligand is in a monodentate mode of coordination *via* the sulphur atom, this singlet tends to broaden, *i.e.* slow exchange. In some complexes there is no exchange process occurring at room temperature, evident from the H^6 proton of the coordinated pySH ligand showing clear coupling to the NH proton.²⁵⁹ When the coordinated ligand is deprotonated (pyS), or under conditions of fast chemical exchange for the NH proton (in the coordinated or free ligand pySH), the ring protons represent an asymmetric four-spin system characterised by four chemical shifts and six coupling constants. The NMR spectrum of pyridine-2-thione has been analysed as an ABCD system and the calculated spectrum was found to correlate well with the observed spectrum.¹⁷ ^1H NMR data for pyridine-2-thione¹⁸ and pyridine¹⁶ are given in Table 1.1.

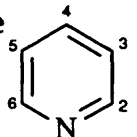
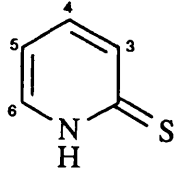
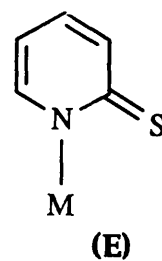
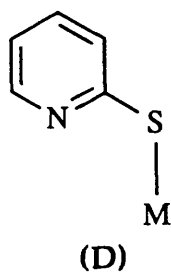
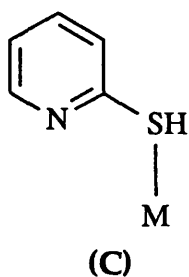
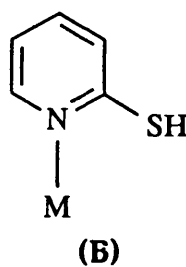
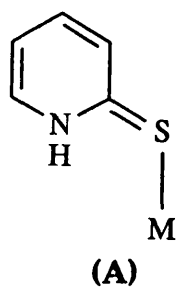
Compound	Chemical Shifts δ	Coupling Constants J/Hz
Pyridine 	8.60 (H^2) 7.25 (H^3) 7.64 (H^4)	$J_{23}=4.93$ $J_{34}=7.66$ $J_{24}=1.80$ $J_{35}=1.44$ $J_{25}=1.00$ $J_{26}=-0.03$
Pyridine-2-thione 	7.68 (H^6) 6.82 (H^5) 7.42 (H^4) 7.55 (H^3) 13.48 (<u>NH</u>)	$J_{56}=6.25$ $J_{45}=7.13$ $J_{34}=8.72$ $J_{46}=1.83$ $J_{35}=1.20$ $J_{36}=0.83$

Table 1.1 ^1H NMR data for pyridine and pyridine-2-thione (recorded in CDCl_3 at 60 MHz).

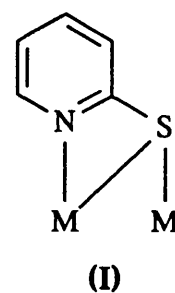
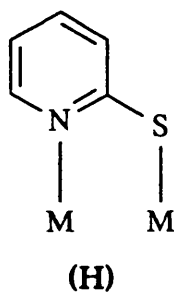
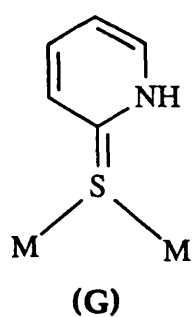
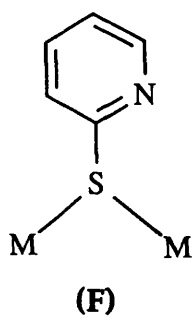
Figure 1.4 Possible modes of coordination for pySH and pyS ligands.

Monodentate



Monodentate doubly bridging

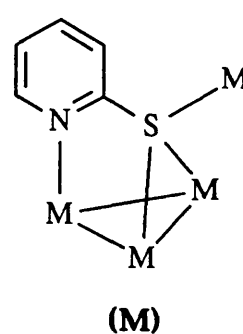
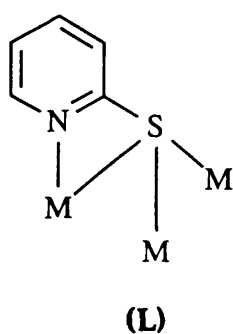
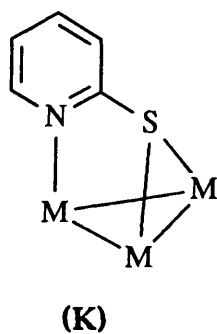
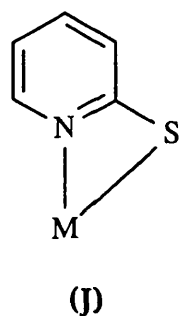
Bidentate doubly bridging



Bidentate chelating

Bidentate triply bridging

Bidentate quadruply bridging



1.3 Transition metal complexes of pyridine-2-thione and pyridine-2-thionato ligands.

Pyridine-2-thione can coordinate to metal centres either as the neutral ligand (pySH) or the conjugate base (pyS⁻) depending on the reaction conditions. The potential modes of coordination that might be considered are shown in Figure 1.4, modes A to C and G involving the neutral ligand and modes D to F and H to M for the anionic ligand. Sulphur is less electronegative and more polarisable than nitrogen²² which would suggest a greater affinity towards class (b) metals such as the later and heavier transition metals and this has been confirmed in a number of cases.²³ It is conceivable that in the presence of class (a) metals the tautomeric equilibrium may be shifted to the thiol form and thus enable coordination through the harder base, nitrogen,²⁴ however there is no evidence for this occurring. Indeed, in complexes with metals such as molybdenum³⁵ or zinc²⁷ which are considered to belong to class (a),²⁵ it has been shown that the pySH ligand coordinates through the sulphur rather than the nitrogen atom. All other available evidence suggests that neutral pyridine-2-thione coordinates through the sulphur atom alone whereas the conjugate anion coordinates through both the sulphur and nitrogen atoms.²⁶⁻²⁸ A total of ten of the thirteen possible coordination modes have been observed in transition metal complexes containing pyridine-2-thione or its conjugate base and these can be divided into five general categories as follows:

- (i) Monodentate coordination through the sulphur atom (modes A and D).

- (ii) Chelation through the nitrogen and sulphur atoms (mode J).
- (iii) Doubly-bridging coordination, either through the sulphur atom alone (modes F and G) or through both nitrogen and sulphur atoms (modes H and I).
- (iv) Triply-bridging coordination with the sulphur atom bridging two metal atoms (mode K and L).
- (v) Quadruply-bridging coordination with the sulphur atom bridging three metal atoms (mode M).

In some complexes containing more than one pySH or pyS ligand, more than one mode of coordination is observed in the molecule.^{28-29,76}

1.4 Complexes containing monodentate pySH or pyS ligands.

As discussed previously pyridine-2-thione exists predominantly as the thione tautomer and is found to coordinate to metal atoms in this form. It forms monodentate sulphur-bonded complexes with a number of transition metals. Known complexes with iron,³⁰ cobalt,²⁶⁻²⁷ nickel,^{27,30} and the three elements of the zinc group,²⁷ include species with the common formula $[MCl_2(pySH)_2]$, amongst others. In addition to mononuclear complexes such as $[Cu(pySH)_3][NO_3]$ which has trigonal planar geometry,³¹ copper is known to form at least two kinds of dimeric species, $[Cu_2(pySH)_2Cl_2]^{30}$ and $[Cu_2(pySH)_6]Cl_2$,³² the latter compound also containing a rare example of doubly-bridging neutral pySH ligands (mode G). Many complexes of the second and third row transition metals containing a monodentate pySH ligand have been reported, such as $[Pt(pySH)_4]Cl_2$,²⁷ the analogous palladium and

silver compounds³⁰ and $[\text{Au}(\text{pySH})_2][\text{ClO}_4]$,³³ but, in general, mixed-ligand compounds such as $[\text{RuHCl}(\text{pySH})(\text{CO})(\text{PPh}_3)]$,²³ $[\text{W}(\text{CO})_5(\text{pySH})]$ ³⁴ and $[\text{MBr}(\text{NNH}_2)(\text{pySH})(\text{PMe}_2\text{Ph})_3]\text{Br}$ ($\text{M} = \text{Mo}, \text{W}$)³⁵ as well as a range of gold³³ complexes are more prevalent in the literature.

Complexes containing the deprotonated ligand (pyS) in a monodentate mode of coordination are less well-known, primarily because chelation, using the lone-pair of electrons on the nitrogen atom, is preferred. For instance, a chloroform-hexane solution of the complex $[\text{Ru}(\text{pyS})_2(\text{CO})_2(\text{PPh}_3)]$, which contains one chelating and one non-chelating pyS ligand, will lose CO on standing for several days at room temperature to give the monocarbonyl species $[\text{Ru}(\text{pyS})_2(\text{CO})(\text{PPh}_3)]$, which contains two chelating pyS ligands.²³ Monodentate pyS ligands have been observed in the gold(I) complexes $[\text{Au}(\text{pyS})_2][\text{PPN}]$ ³⁶ and $[\text{Au}(\text{PPh}_3)(\text{pyS})]$,³⁷ two-coordinate geometry being prevalent for the metal in this oxidation state although tetrahedral geometry is known.³⁸ Several other stable complexes containing this mode of coordination have been reported such as $[\text{RuCl}_2(\text{CO})_2(\text{pyS})_2]$,³⁹ but more commonly these compounds contain other pyS or pySH ligands in a variety of coordination modes. These include $[\text{Rh}(\text{pyS})_3(\text{pySH})]$ which contains monodentate pyS and pySH ligands and two chelating pyS ligands,⁴⁰ and $[\text{Rh}(\text{pyS})_3(\text{PMe}_2\text{Ph})_2]$, which has one chelating and two monodentate pyS ligands.⁴¹

Since the discovery of *cis*-platin,⁴² there have been many studies to develop new, more effective and less toxic platinum complexes.⁴³ One such study involved monodentate pyridine-2-thionato ligands and the complexes $[\text{Pt}(\text{NH}_3)(\text{H}_2\text{O})(\text{pyS})_2]$ and $[\text{Pt}(\text{NH}_3)(\text{H}_2\text{O})_2(\text{pyS})][\text{NO}_3]$ have shown high anti-

tumour activity.⁴⁴

1.5 Complexes containing chelating pyS ligands.

In addition to the complexes mentioned above which contain chelating pyS ligands, there are numerous other examples. The first metal pyridine-2-thionato complex $[\text{Ru}(\text{pyS})_2(\text{PPh}_3)_2]$,⁴⁵ synthesised by Wilkinson *et al.*, was formulated as containing two chelating pyS ligands and this was confirmed by an X-ray diffraction study.⁴⁶ The triphenylphosphine groups are *cis*, with the sulphur atoms of the pyS ligand mutually *trans*. Recently, Robinson *et al.* have shown that, in solution, this complex and its osmium analogue adopt a configuration such that the phosphine ligands are *trans* with the two chelating pyS ligands in the same plane as each other.⁴⁷ Rhodium,⁴⁰ cobalt⁴⁸ and antimony⁴⁹ all form tris-chelate complexes with the general formula $[\text{M}(\text{pyS})_3]$, as does iron⁵⁰ but this is an anionic species since the metal is in an oxidation state of +2. The chelating pyS ligand, which is a three-electron donor, has a short 'bite' and formation of these four-membered chelate rings gives rise to distortion in the geometry around the metal, and also produces considerable strain in the ligand framework. For instance, the N-Fe-S angles in $[\text{Fe}(\text{pyS})_3]^-$ are around 66°, while the Fe-N-C and N-C-S angles are distorted from 120°, the expected values for sp^2 hybridised atoms, to 102.5 and 114.5° respectively. In this iron complex the average C-S bond length is 1.73 Å compared with 1.68(2) Å in the free ligand, and the C-C bond lengths in the ring are very similar which has been taken as evidence that the chelating pyS ligand is coordinated in the thiolate form with very little contribution from the

tautomeric thione form. This is a general feature in complexes containing the chelating pyS ligand. Chelating pyridine-2-thionato complexes are also known for titanium,⁵¹ molybdenum,⁵²⁻⁵³ tungsten,⁵³⁻⁵⁴ ruthenium,⁵⁵ osmium,⁵⁶ iridium,⁵⁷ nickel,⁵⁸ gold,³³ tin,⁵⁹ zinc,⁶⁰ and cadmium.⁶¹ An interesting aside concerns the related tris(2-mercapto-ethylamine) cobalt(III) complex, $[\text{Co}(\text{NH}_2\text{CH}_2\text{CH}_2\text{S})_3]$, which has the ability to function as a tridentate ligand to a variety of metal atoms to form tri- or tetranuclear products.⁶² The lone-pairs of electrons on the sulphur atoms are being utilised to form bonds to other metal atoms, and this has also been observed as a feature of coordinated pyS ligands which will be described in Section 1.8.

Complexes of the type $[\text{Ru}(\text{pyS})_2\text{L}]$ (L = cycloocta-1,5-diene and norbornadiene),⁶³⁻⁶⁴ contain two chelating pyS ligands and have been used as intermediates in the synthesis of other pyridine-2-thionato ruthenium compounds because of the lability of the ligand L.⁶⁴ The related carbonyl species $[\text{Ru}(\text{pyS})_2(\text{CO})_2]$ ⁶⁵ has also been used as a source of pre-metallated pyS, in reactions with, for example, $[\text{Ru}_3(\text{CO})_{12}]$, both in this work and elsewhere.⁶⁶

1.6 *Complexes containing doubly-bridging pyS ligands.*

The pyridine-2-thionato ligand displays an unusual flexibility since, in addition to monodentate (modes A and D) and chelating (mode J) coordination modes, it has been found to adopt four types of doubly-bridging coordination modes, through the S atom alone (modes F and G), or through both N and S atoms (modes H and I).

Type H is fairly common and in this case the bidentate pyS ligand acts

as a three-electron donor. Examples include $[\text{Rh}_2\text{Cl}_2(\mu\text{-pyS})_2(\text{pySH})(\text{CO})_2]$, in which the two bridging pyS ligands span the metal-metal bond,²⁸ and $[\text{Pt}_2(\mu\text{-pyS})_2(\text{en})_2]\text{Cl}_2$, which has no Pt–Pt bond, the metal centres being held together by the two bridging pyS ligands.⁶⁷⁻⁶⁸ The dirhodium compound also contains two monodentate pySH ligands which form pseudochelate rings through N–H---Cl hydrogen bonds. The compound $[\text{Pd}_2(\text{pyS})_4]$ contains four $\mu\text{-pyS}$ ligands in a cage-like arrangement, and, on reaction with iodine, gives the complex $[\text{Pd}_4(\text{pyS})_6\text{I}_2]$ in which four of the pyS ligands are doubly-bridging and two are triply-bridging.⁶⁹ Doubly-bridging pyS ligands have also been found in some mixed-ligand rhodium⁷⁰ and palladium⁷¹ compounds and in a range of gold dinuclear species.³³ Also known is $[\text{Os}_3\text{H}(\text{CO})_{10}(\mu\text{-pyS})]^{72}$ and its ruthenium analogue,⁷³ although this has only been reported as the [PPN]⁺ salt of $[\text{Ru}_3(\text{CO})_{10}(\mu\text{-pyS})]^-$.

When the ligand adopts the doubly-bridging mode I, an extra M–S bond is formed and the ligand is now acting as a five-electron donor. This coordination mode is rare and was first observed in the complex $[\text{Re}_2(\mu\text{-pyS})_2(\text{CO})_6]$, which contains no metal-metal bond, the structure of the 6-methyl analogue having been determined by X-ray crystallography.⁷⁴ Subsequent reaction with $[\text{Ru}_3(\text{CO})_{12}]$ produces a range of mixed-metal tetranuclear compounds in which pyS ligands adopt the same coordination mode as that found in the parent, as well as other modes, and are bound to both rhenium and ruthenium centres.⁷⁵⁻⁷⁶

The coordination modes F and G, in which the ligand is monodentate and bridges two metal atoms through the sulphur atom alone, is also rarely observed. It appears that the only example of the neutral ligand in a doubly-

bridging mode (G) is in the complex $[\text{Cu}_2(\text{pySH})_6]\text{Cl}_2$, which also contains four terminal monodentate pySH ligands (mode A).³² Examples of the analogous coordination mode with the deprotonated ligand (mode F) are restricted to the dirhodium complexes $[\text{Rh}_2(\mu\text{-pyS})_2\text{L}_2]$ (L = tetrafluorobenzobicyclooctatriene⁷⁰ and tetrafluorobenzobarrelene⁷⁷), in which both pyS ligands are doubly-bridging, one through both N and S atoms (mode H) and the other through the S atom alone (mode F).

1.7 Complexes containing triply-bridging pyS ligands.

Until recently, there had been few studies involving the pyS ligand in triply-bridging modes of coordination (modes K and L), and while there are several instances of the ligand adopting mode K, there seems to be only one example of mode L. This is given by the heterocubane cluster $[\text{Cu}_4(\text{pyS})_4]$,^{32,78} in which one M–N bond and three M–S bonds are formed, the ligand donating seven electrons to the cluster. Mode K is more common and differs from mode L in that only two M–S bonds are formed and the ligand is a five-electron donor. The first example of this type of coordination was found in the triosmium cluster compound $[\text{Os}_3\text{H}(\text{CO})_9(\mu_3\text{-pyS})]$,⁷² and its ruthenium congener is now also known.⁷⁹ Soon afterwards, $[\text{Rh}_3(\mu_3\text{-pyS})_2(\text{CO})_6][\text{ClO}_4]$ was reported,⁷⁷ in which each ligand is bonded to one metal atom through the nitrogen and to the other two through the sulphur atom, as in the triosmium compound, the main difference being that there are no metal-metal bonds in the trirhodium species. Other compounds featuring the pyS ligand in this mode include the tripalladium complex $[\text{Pd}_3(\text{dmp})_3(\text{pyS})_2][\text{BF}_4]$ (dmp = 2-

(dimethylaminomethyl)phenyl),⁷¹ and a mixed rhodium-palladium species,⁸⁰ $[\text{Rh}(\text{pyS})_4\{\text{Pd}(\eta^3\text{-C}_4\text{H}_7)\}_2][\text{BF}_4]$, in which two pyS ligands are chelating at rhodium and the other two form μ_3 -bridges between the three metal atoms. New compounds containing pyS in this bonding mode are described in Chapter Five.

1.8 Complexes containing quadruply-bridging pyS ligands.

In the triply-bridging mode K, there is still a lone-pair of electrons on the sulphur atom, giving the potential for the ligand to behave as a seven-electron donor by bridging four metal atoms. Previous attempts in these laboratories to achieve this situation of maximum electron donation led to alternative C–S bond cleavage which will be discussed in Section 1.9. The only reported complex in which the pyS ligand adopts this coordination mode (mode M) is the nonaruthenium cluster $[\{\text{Ru}_3\text{H}(\text{CO})_7(\mu_4\text{-pyS})\}_3]$, which is formed by double decarbonylation and trimerisation of $[\text{Ru}_3\text{H}(\text{CO})_9(\mu_3\text{-pyS})]$.⁷⁹ In the course of the reaction, the μ_3 -pyS ligand makes a new M–S bond and in doing so links trinuclear clusters through μ_4 -bridges. The attempts at extending our knowledge of this novel coordination mode are discussed in Chapter Five.

1.9 Cleavage of the C-S bond in the pyS ligand.

Another important facet of the behaviour of pyS ligands in reactions with transition metals is its ability for C–S cleavage. In this way, the original

pyS ligand can donate a total of nine electrons, even without using the π -electrons of the heterocyclic ring, as the separated μ_4 -S and μ -2-pyridyl ligands, both fragments usually being retained in the final molecule. Several mixed rhenium-ruthenium clusters,⁷⁶ the formation of which depends on this process, have been recently reported and are described in Chapter Two. This behaviour is a common theme throughout this thesis and will be discussed in greater depth in subsequent chapters.

1.10 Physical properties of pyridine.

Pyridine is a hygroscopic colourless liquid (b.p. 116 °C) and is miscible with water which is due to the lone-pair of electrons on the nitrogen atom readily forming hydrogen bonds with water. The use of pyridine and its derivatives in industry is widespread, for example, catalysts containing $[\text{Ru}_3(\text{CO})_{12}]$ and pyridine are used in the selective preparation of linear aldehydes.⁸¹ Pyridine is known from electron diffraction experiments and microwave spectroscopy to be a flat molecule, with bond angles that vary slightly, but which approximate to 120°, as in benzene. These data point to sp^2 hybridisation of the nitrogen orbitals, the lone-pair occupying a σ -orbital in the plane of the ring. Because of this, pyridine is a weak base ($pK_a = 5.2$), far weaker than piperidine and aliphatic amines since the lone-pair of an aliphatic nitrogen atom is in an sp^3 -hybridised orbital, *i.e.* has less s-component and is therefore more available for donation to suitable acceptor molecules.⁸²

1.11 Transition metal complexes of pyridine.

In comparison to the pyridine-2-thione ligand, the range of possible coordination modes available to pyridine is rather limited, which is due to the absence of any exocyclic functionality. Five different types of coordination have been observed in transition metal complexes containing pyridine (C_5H_5N) or pyridyl (C_5H_4N) ligands and these are as follows:

- (i) Monodentate coordination through the nitrogen atom.
- (ii) Monodentate coordination through a carbon atom.
- (iii) Bidentate bridging coordination through both the nitrogen atom and the adjacent carbon atom (ortho-metallation).
- (iv) Chelation through the nitrogen and adjacent carbon atom.
- (v) Hexahapto coordination through the π -electron ring system.

The most common coordination mode of pyridine is *via* the nitrogen atom alone and complexes in which this mode occurs are too numerous to mention here. Pyridine is known to adopt this type of coordination in complexes with most transition metals, as well as many of the s- and p-block metals.⁸³ Considerable attention has been paid to transition metal complexes of pyridines, and in particular, complexes of 2,2'-bipyridine, because of their interesting properties and applications in, for example, solar energy conversion and storage.⁸⁴⁻⁸⁵ Compounds containing pyridine ligands coordinated through the nitrogen atom alone have been observed in this work and are described in Chapter Four.

Coordination through the carbon atom alone is less common and is

most often observed in complexes of nickel, palladium and platinum of the type $[\text{MX}(\text{C}_5\text{H}_4\text{N})\text{L}_2]$ ($\text{X} = \text{Cl}, \text{Br}$; $\text{L} =$ tertiary phosphine), which are usually prepared by oxidative addition of the halopyridine to $[\text{ML}_4]$.⁸⁶⁻⁸⁹ The position of metallation depends on the halide position in the original pyridine, for example, C^2 , C^3 and C^4 carbon-bonded pyridyl complexes have been obtained from 2-, 3- and 4-bromopyridine.⁸⁸⁻⁸⁹ In such complexes, the nitrogen atom is markedly nucleophilic, for example, $[\text{PtCl}(\text{C}_5\text{H}_4\text{N})(\text{PPh}_3)_2]$ is slowly *N*-alkylated in dichloromethane solution to give $[\text{PtCl}\{(1\text{-CH}_2\text{Cl})\text{C}_5\text{H}_4\text{N}\}(\text{PPh}_3)_2]\text{Cl}$.⁸⁶ The binuclear derivatives of these complexes, $[\{\text{MX}(\mu\text{-C}_5\text{H}_4\text{N})(\text{PPh}_3)\}_2]$ ($\text{M} = \text{Ni}$,⁹⁰ Pd ⁹¹ and Pt ,⁸⁶ $\text{X} = \text{Cl}, \text{Br}$), are also known and contain bridging 2-pyridyl ligands. Carbon-bonded pyridyl compounds of other metals, including cobalt,⁹² gold⁹³ and some carbonyl complexes of iron, manganese and rhenium have also been isolated.⁹⁴

Ortho-metallation of pyridine is well known and in this mode the ligand can span a wide range of metal-metal distances. In $[\text{Ru}_5\text{H}(\text{C})(\mu\text{-C}_5\text{H}_4\text{N})(\text{CO})_{14}]$, for example, the 2-pyridyl ligand spans a distance of 3.59 Å across a non-bonded edge,⁹⁵ while in $[\text{Ru}_6\text{S}_2(\text{C}_5\text{H}_4\text{N})_2(\text{CO})_{18}]$, the 2-pyridyl-bridged Ru–Ru bond is 2.713(2) Å.⁶⁶ Ortho-metallated 2-pyridyl ligands are also found in a number of other carbonyl clusters of iron,⁹⁶ ruthenium,⁹⁷⁻⁹⁹ osmium¹⁰⁰ and rhenium.¹⁰¹ In addition to ortho-metallated pyridyl ligands, some of these complexes also contain a monodentate pyridine ligand, bound through the nitrogen only.¹⁰⁰⁻¹ The aforementioned dimers $[\{\text{MX}(\mu\text{-C}_5\text{H}_4\text{N})(\text{PPh}_3)\}_2]$ ($\text{M} = \text{Ni}$,⁹⁰ Pd ⁹¹ and Pt ,⁸⁶ $\text{X} = \text{Cl}, \text{Br}$) all contain 2-pyridyl bridges, the structure of the palladium congener, $[\{\text{PdBr}(\mu\text{-C}_5\text{H}_4\text{N})(\text{PPh}_3)\}_2]$, having been confirmed by X-ray diffraction which showed that there was no metal-metal bonding

(Pd–Pd = 3.194 Å). Also known is a gold complex, $[\{\text{Au}(\mu\text{-C}_5\text{H}_4\text{N})\}_3]$, the structure of which is thought to involve three 2-pyridyl bridges, with linear geometry for each gold atom.⁹³ Ortho-metallated pyridyl ligands are prevalent throughout this thesis and new compounds containing this mode of coordination are described in Chapters Two, Three and Four.

Complexes containing a chelating pyridyl ligand are even rarer. This coordination mode was first postulated for the 2-substituted pyridyl ligand in $[(\text{cp})_2\text{Ti}(\text{C}_5\text{H}_3\text{NR})]$ (R = methyl, phenyl or vinyl group; cp = cyclopentadienyl ($\eta^5\text{-C}_5\text{H}_5$)).¹⁰² Structural analyses have since been performed on lutetium and scandium complexes of similar stoichiometry, $[(\text{cp}^*)_2\text{M}(\text{C}_5\text{H}_4\text{N})]$ (M = Lu,¹⁰³ Sc;¹⁰⁴ cp* = pentamethylcyclopentadienyl ($\eta^5\text{-C}_5\text{Me}_5$)), and the tantalum complex, $[(\text{silox})_3\text{Ta}(\text{C}_5\text{H}_5\text{N})]$ (silox = $t\text{-Bu}_3\text{SiO}^-$),²⁶⁰ which all contain 3-membered metallocycles formed by the chelating pyridyl or pyridine ligand.

There are several examples of pyridines acting as η^6 -ligands in complexes with transition metals,²⁶¹⁻⁵ the first π -complex with pyridine itself being $[\text{Cr}(\eta^6\text{-C}_5\text{H}_5\text{N})(\text{PF}_3)_3]$.²⁶⁶ Usually, π -complexes are synthesised from pyridines with ortho-substituents, most commonly 2,6-dimethylpyridine, in order to inhibit coordination through the nitrogen atom, and compounds including the 'sandwich' complexes $[\text{M}(\text{Me}_2\text{C}_5\text{H}_3\text{N})_2]$ (M = Ti, V, Mo, Cr)²⁶⁷⁻⁸ have now been structurally characterised.

There have been several studies concerning the adsorption of pyridine onto metal surfaces. Unlike benzene, which interacts almost exclusively via the π -electrons with the substrate surface and consequently adopts a parallel or near-parallel adsorption geometry, pyridine can involve both π and N lone-pair electrons in the surface chemical bond. As a result, different orientations

of the pyridine ring plane with respect to the surface plane are conceivable: parallel, perpendicular or tilted, and indeed all three adsorption geometries have been reported.¹⁰⁵ For the perpendicularly orientated pyridine moieties adsorbed on Pt(111) and Ir(111), α -pyridyl species have been proposed, *i.e.* ortho-metallation through the nitrogen and an adjacent carbon atom.¹⁰⁶

CHAPTER TWO

Mixed Tetranuclear Rhenium-Ruthenium Compounds

2.1 Introduction

The chemistry of metal cluster complexes is a topic of much current interest, one reason being that a study of the reactions of small molecules coordinated to metal clusters will show chemistry unique to clusters resulting from the concerted effects of several metal atoms,¹⁰⁷ and the expectation that they will find uses in catalysis, directly in the form of novel homogeneous catalysts (or catalyst precursors) and indirectly by serving as models for chemisorption processes in heterogeneous catalysis.¹⁰⁸ Studies in this area have produced many intrinsically interesting molecules, whose unusual and intriguing structures have prompted many theoretical developments which are now leading to a greater understanding of these systems. Organic ligands may be activated by polynuclear metal sites and this has received a great deal of attention. Thus, on reaction with clusters, C-H, C-C, C-N and other bonds in reacting molecules may be cleaved leaving the fragments in bridging sites in clusters. It has been shown that C-S bonds can be activated in different ways. Thus when the compounds $[\text{Os}_3\text{H}(\mu_3\text{-SCH=NAr})(\text{CO})_9]$ ($\text{Ar} = \text{C}_6\text{H}_5$, *p*- $\text{C}_6\text{H}_4\text{Me}$, *p*- $\text{C}_6\text{H}_4\text{F}$) are heated at 125 °C, the C-S bonds in the N-aryltioformamido ligands are cleaved and the cluster $[\text{Os}_3\text{H}(\mu_3\text{-S})(\mu\text{-HC=NAr})]$ is formed.¹⁰⁹ It is unlikely that the initial coordination of the sulphur atom to two osmium atoms weakens the C-S bond but certainly cleavage of this bond allows the S atom to slot into a μ_4 -site with very little reorganisation and to make new Os to ligand bonds which are strong enough to compensate energetically for the broken bond.

Sulphur-containing ligands can be used as the precursors for the

synthesis of big clusters or mixed-metal clusters. This is partly because of the strength of the metal to sulphur bonds but also because of the availability of electrons. For example, triply-bridging S can donate four electrons and quadruply-bridging S can donate four or six electrons depending on geometric circumstances. This idea has led many chemists to react complexes containing sulphur ligands with other metal centres to generate metal clusters or cages. Some recently reported pyS-containing cages or clusters are the tripalladium species $[\text{Pd}_3(\text{dmp})_3(\text{pyS})_2][\text{BF}_4]$, (dmp = 2-(dimethylaminomethyl)phenyl),⁷¹ the mixed-metal compound $[\text{Rh}(\text{pyS})_4\{\text{Pd}(\text{C}_4\text{H}_7)\}_2][\text{BF}_4]$ (C_4H_7 = 2-methylallyl),⁸⁰ and the tetranuclear complex $[\text{Pd}_4(\text{pyS})_6\text{I}_2]$.⁶⁹ In each of these complexes the sulphur atoms use their lone-pairs of electrons to form bonds to at least two metal atoms and hence cages are formed. There have been many studies,¹¹⁰ particularly by Adams *et al.*, that have focused on sulphido ligands and their ability for promoting the agglomeration of metal-containing groups and for stabilising the cluster products. It is believed that the lone-pair of electrons on the sulphido ligand can serve as the site for initial attachment of a metal-containing moiety to a sulphur-bridged cluster complex. Much of this work has centred on osmium, but recently the approach has been utilised for the synthesis of mixed-metal complexes such as $[\text{Os}_3\text{W}(\text{CO})_{12}(\text{PMe}_2\text{Ph})(\mu_3\text{-S})_2]$.¹¹¹ Also known are a series of ruthenium-molybdenum species with nuclearities as high as seven, derived from $[\text{Ru}(\text{CO})_5]$ and $[\text{Mo}_2\text{Ru}(\text{CO})_7(\text{cp})_2(\mu_3\text{-S})]$, containing bridging sulphido and carbonyl ligands.¹¹²

Clusters in which bonds are formed between different types of metal atom have been known for some time and their structures are similar to those containing only one type of metallic element.¹¹³ Some of the earliest of these

heterometallic species were synthesised *via* the displacement reaction of a metal carbonyl anion with a metal halide compound.¹¹⁴ Other methods involving either the copyrolysis of different homometallic carbonyl units¹¹⁴⁻⁵ or the combination of a metal carbonyl anion and a neutral metal carbonyl¹¹⁶⁻⁷ have also been used but frequently afford a mixture of products. One of the most versatile approaches involves substitution of labile ligands such as acetonitrile, THF, cyclo-octadiene or phosphines,¹¹⁸ and many compounds have been synthesised in this way. The process of addition of a metal-containing species to a closed cluster of n metal atoms, leading to a new closed cluster of $n+1$ metal atoms, presumably involves the stepwise formation of metal-metal bonds. An illustration of this process is provided by a series of rhenium-osmium species¹¹⁹ derived from $[\text{ReH}(\text{CO})_5]$ and $[\text{Os}_3(\text{CO})_{12-n}(\text{MeCN})_n]$, such as the metalloligated cluster $[\text{Os}_3\text{Re}(\mu\text{-H})(\text{CO})_{15}(\text{MeCN})]$ which can be induced to close to the tetrahedral compound $[\text{Os}_3\text{Re}(\mu\text{-H})_5(\text{CO})_{12}]$.

The reactivity of mixed-metal clusters has been of interest for many years.¹²⁰ Research has been stimulated by the belief that the combination of metals having very different chemical properties within one compound may induce unique chemical transformations. In addition, there have been numerous investigations¹²¹ into the homogeneous catalytic activity of metal clusters. Little is known about their mode of reaction, but it has been demonstrated that clusters can add substrates reversibly with opening of metal-metal bonds.¹²² Addition of a substrate molecule with cleavage of a metal-metal bond, and elimination of the modified substrate with formation of a metal-metal bond, could therefore be the first and last steps of a catalytic cycle with cluster participation. In the hydroformylation reaction of pentenes,

clusters have been used as catalysts and there is evidence to suggest that fragmentation into catalytically active mononuclear fragments can be ruled out.¹²³ However, although there are some strong indications of catalysis by metal clusters, definitive proof that these are the active species has been very difficult to obtain.¹⁰⁸

Several mixed-metal complexes derived from $[\text{Ru}_3(\text{CO})_{12}]$ are known. However, there is a much greater tendency for triruthenium clusters, as opposed to triosmium clusters, to undergo cluster fragmentation. For instance, when the mononuclear acetylide complex $[(\text{cp})\text{W}(\text{CO})_3\text{C}\equiv\text{CR}]$ is treated with $[\text{Os}_3(\text{CO})_{10}(\text{MeCN})_2]$, a tetranuclear complex, $[(\text{cp})\text{Os}_3\text{W}(\text{CO})_{11}\text{C}\equiv\text{CR}]$,¹²⁴ is formed in addition to the trinuclear compound $[(\text{cp})\text{WOs}_2(\text{CO})_8\text{C}\equiv\text{CR}]$, whereas in the analogous reaction with $[\text{Ru}_3(\text{CO})_{12}]$, the only product is the trinuclear $[(\text{cp})\text{WRu}_2(\text{CO})_8\text{C}\equiv\text{CR}]$.¹²⁵ This behaviour is due to the greater M–M bond strength for the heavier metal; the M–M bond enthalpies of $[\text{Ru}_3(\text{CO})_{12}]$ and $[\text{Os}_3(\text{CO})_{12}]$ are 78 and 94 kJ mol⁻¹ respectively.¹²⁶ To overcome the problem of cluster fragmentation, capping ligands have been used as 'protecting groups' to hold the metal atoms together. For example, treatment of the imido complex $[\text{Ru}_3(\text{CO})_{10}(\mu_3\text{-NPh})]$ ¹²⁷ with the aforementioned tungsten acetylide species generates the butterfly cluster $[(\text{cp})\text{WRu}_3(\text{CO})_9(\mu\text{-NPh})(\text{C}\equiv\text{CPh})]$.¹²⁸ Hydrogenation of this compound induces CO loss and framework reorganisation, giving a dihydrido-vinyl complex with a tetrahedral geometry. This is unusual since, in general, hydrogenation of acetylide cluster complexes transfers both hydrogen atoms to the β -carbon to give an alkylidyne fragment ($\mu_3\text{-CCH}_2\text{R}$).^{124,129} Phosphido ligands also have been used to inhibit fragmentation during studies of the reactivity and catalytic properties of

clusters.¹²²⁻³ For instance, the compound $[\text{Ru}_3\text{H}(\text{CO})_9(\mu_3\text{-PPh})]^-$ has been reacted with a variety of mononuclear metal complexes to produce a range of tetra- and pentanuclear mixed-metal species containing an intact triruthenium unit such as the tetrahedral compound $[\text{Ru}_3\text{ReH}(\text{CO})_{11}(\mu_3\text{-PPh})(\text{MeCN})]$.¹¹⁸ It should be noted that phosphido ligands are probably superior to imido ligands in this protecting capacity, since $[\text{Ru}_3(\text{CO})_{10}(\mu_3\text{-NPh})]$ will react with $[(\text{cp})\text{WH}(\text{CO})_3]$ with the result of breakdown of the Ru_3 trimeric unit to give $[(\text{cp})\text{WRu}_2(\mu\text{-H})(\text{CO})_8(\mu_3\text{-NPh})]$,¹³⁰ whereas when the phosphido species $[\text{Ru}_3\text{H}(\text{CO})_{10}(\mu\text{-PPh}_2)]$ is treated with $[(\text{cp})\text{WH}(\text{CO})_3]$, the analogous trinuclear compound is formed together with the tetranuclear complex $[(\text{cp})\text{WRu}_3(\mu_3\text{-H})(\text{CO})_{10}(\mu_3\text{-PPh})]$.¹³¹ The extra stability of the phosphido bridge is probably due to the effect of synergic π back-donation from metal d_π orbitals to vacant $3d_\pi$ orbitals on the phosphorus atom. It is not surprising that when the phosphido ligand is only doubly-bridging, such as in $[\text{Ru}_3(\text{CO})_9(\mu\text{-PPh}_2)(\mu_3\text{-}\eta^2\text{-C}\equiv\text{CPr}^i)]$,¹³² fragmentation of the trimeric unit occurs in reactions with other metal-containing species, the acetylide ligand being either too reactive or too weakly bound to prevent fragmentation. For example, when treated with $[(\eta\text{-C}_5\text{H}_5)\text{Ni}(\text{CO})_2]_2$, the latter ruthenium compound forms the pentanuclear complex $[\text{NiRu}_4(\text{CO})_9(\mu\text{-PPh}_2)_2(\mu_4\text{-C}\equiv\text{CPr}^i)_2]$,¹³³ the structure of which consists of a nickel atom bridging the wing-tips of an Ru_4 butterfly. It is interesting to note that the phosphido-bridged dinuclear ruthenium unit has remained intact during the reaction, again illustrating the effectiveness of bridging phosphido ligands as protecting groups against fragmentation. This behaviour is also observed in the formation of $[(\text{cp})\text{WRu}_2(\mu\text{-H})(\text{CO})_8(\mu_3\text{-PPh})]$, from $[\text{Ru}_3\text{H}(\text{CO})_{10}(\mu\text{-PPh}_2)]$ and $[(\text{cp})\text{WH}(\text{CO})_3]$ discussed above.¹³¹

The heteroatoms of the pyridine-2-thionato radical (pyS) have potentially seven non-bonding electrons for metal-ligand bonding and in known compounds it has been shown to make use of three or five of these electrons by bridging. However, oxidative addition with C-S cleavage would give the strongly-bridging S atom and 2-pyridyl group which together could donate as many as nine electrons through the heteroatoms even without using π -bonding of the heterocyclic ring. This high capacity for supplying electrons gives scope for the synthesis of clusters in which metal atoms, with or without metal-metal bonds between them, are bridged by these S and 2-pyridyl ligands. The pySH may be introduced either directly or, alternatively, already bound to metal atoms. For example, the compound $[\text{Ru}(\text{pyS})_2(\text{CO})_2]$, in which the pyS ligands are chelating, has been used in reactions with $[\text{Ru}_3(\text{CO})_{12}]$ to provide S and 2-pyridyl groups in order to generate larger clusters such as the pentanuclear compound $[\text{Ru}_5(\mu_4\text{-S})_2(\mu\text{-C}_5\text{H}_4\text{N})_2(\text{CO})_{11}]$ ⁶⁶ and work with this system is discussed in Chapter Three. The dimer $[\text{Re}_2(\text{pyS})_2(\text{CO})_6]$ can also be used as a source of pyS and S and 2-pyridyl fragments. It can be prepared, in good yields, by direct reaction of $[\text{Re}_2(\text{CO})_{10}]$ with pyridine-2-thione in refluxing xylene.⁷⁴ The pyS ligands bridge as five-electron donors and the pyridine rings are on the same side of the Re_2S_2 ring. This compound is cleaved by various monodentate ligands L to give $[\text{Re}(\text{pyS})(\text{CO})_3\text{L}]$ containing pyS as a chelating ligand. Solutions containing a mixture of $[\text{Re}_2(\text{pyS})_2(\text{CO})_6]$ and the analogous 6-methylpyridine-2-thionato (mpyS) complex reach an equilibrium over several days at room temperature involving the mixed-ligand compound $[\text{Re}_2(\text{pyS})(\text{mpyS})(\text{CO})_6]$. These three species may be separated by TLC but a solution of the mixed ligand

compound regenerates the three-component mixture over days at room temperature. It is believed that this scrambling process occurs via a 16-electron mononuclear species $[\text{Re}(\text{pyS})(\text{CO})_3]$ or the corresponding 18-electron species with a coordinated solvent ligand. We considered that these transient monomers might be precursors to heterometallic compounds and with this in mind we treated $[\text{Re}_2(\text{pyS})_2(\text{CO})_6]$ with $[\text{Ru}_3(\text{CO})_{12}]$ with the initial intention of generating $[\text{ReRu}(\text{pyS})(\text{CO})_x]$ ($x = 7$ or 8). Instead, a series of tetranuclear compounds were obtained,⁷⁵⁻⁶ each containing μ_4 -sulphido and μ -2-pyridyl ligands formed by cleavage of a C-S bond of a pyS ligand.

The reaction is carried out in refluxing *m*-xylene over 30 mins using equimolar amounts of $[\text{Re}_2(\text{pyS})_2(\text{CO})_6]$ and $[\text{Ru}_3(\text{CO})_{12}]$. Separation by successive TLC treatment yielded the compounds $[\text{ReRu}_3\text{S}(\text{C}_5\text{H}_4\text{N})(\text{CO})_{14}]$ **1**, $[\text{Re}_2\text{Ru}_2\text{S}(\text{C}_5\text{H}_4\text{N})(\text{pyS})(\text{CO})_{13}]$ **2** and $[\text{Re}_3\text{RuS}(\text{C}_5\text{H}_4\text{N})(\text{pyS})_2(\text{CO})_{11}]$ **3** as shown in Scheme 2.1. These compounds all exhibit complexity in the carbonyl-stretching region of the infrared spectrum and each exists in two isomeric forms, evident from ^1H NMR spectra and X-ray structure determinations.

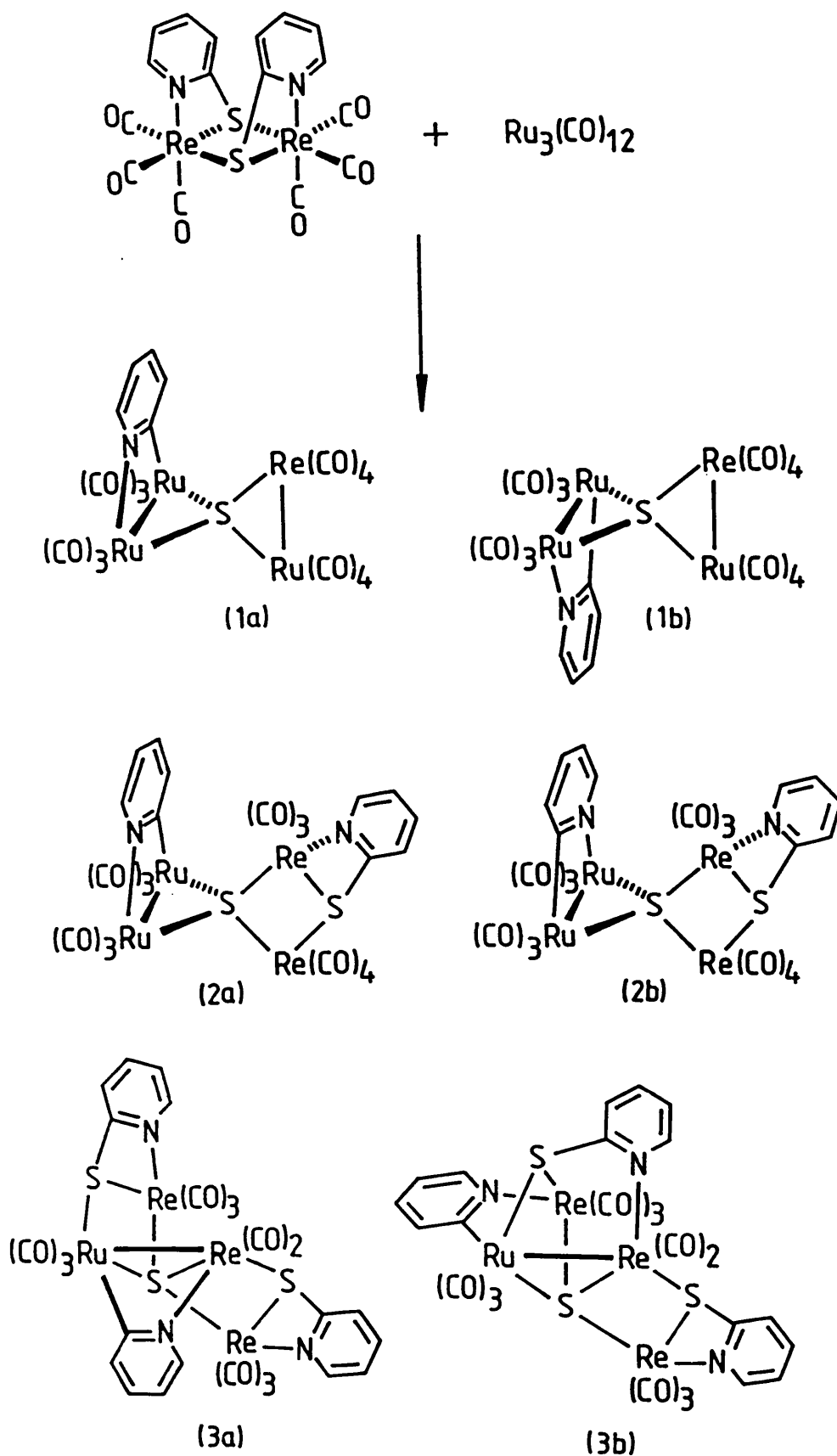
Scheme 2.1 Reaction of $[\text{Ru}_3(\text{CO})_{12}]$ with $[\text{Re}_2(\text{pyS})_2(\text{CO})_6]$.

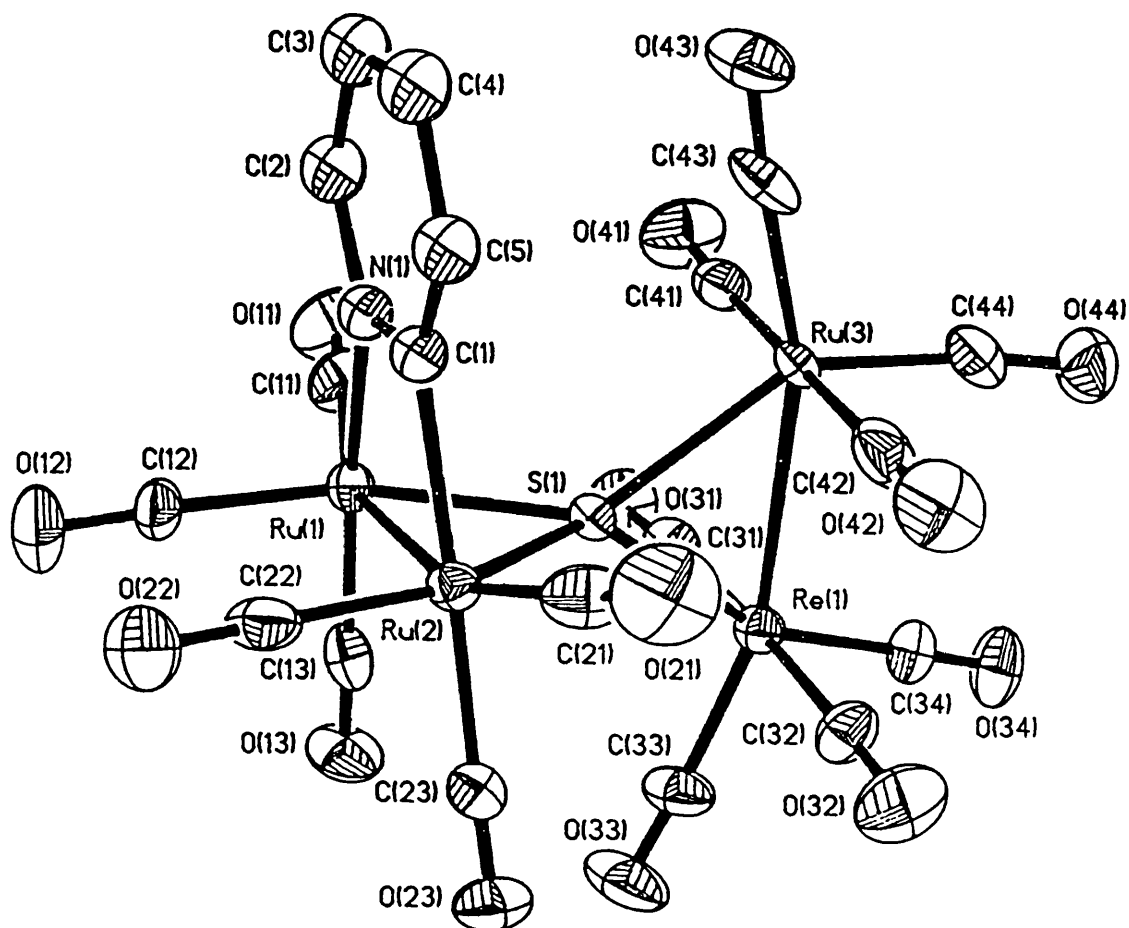
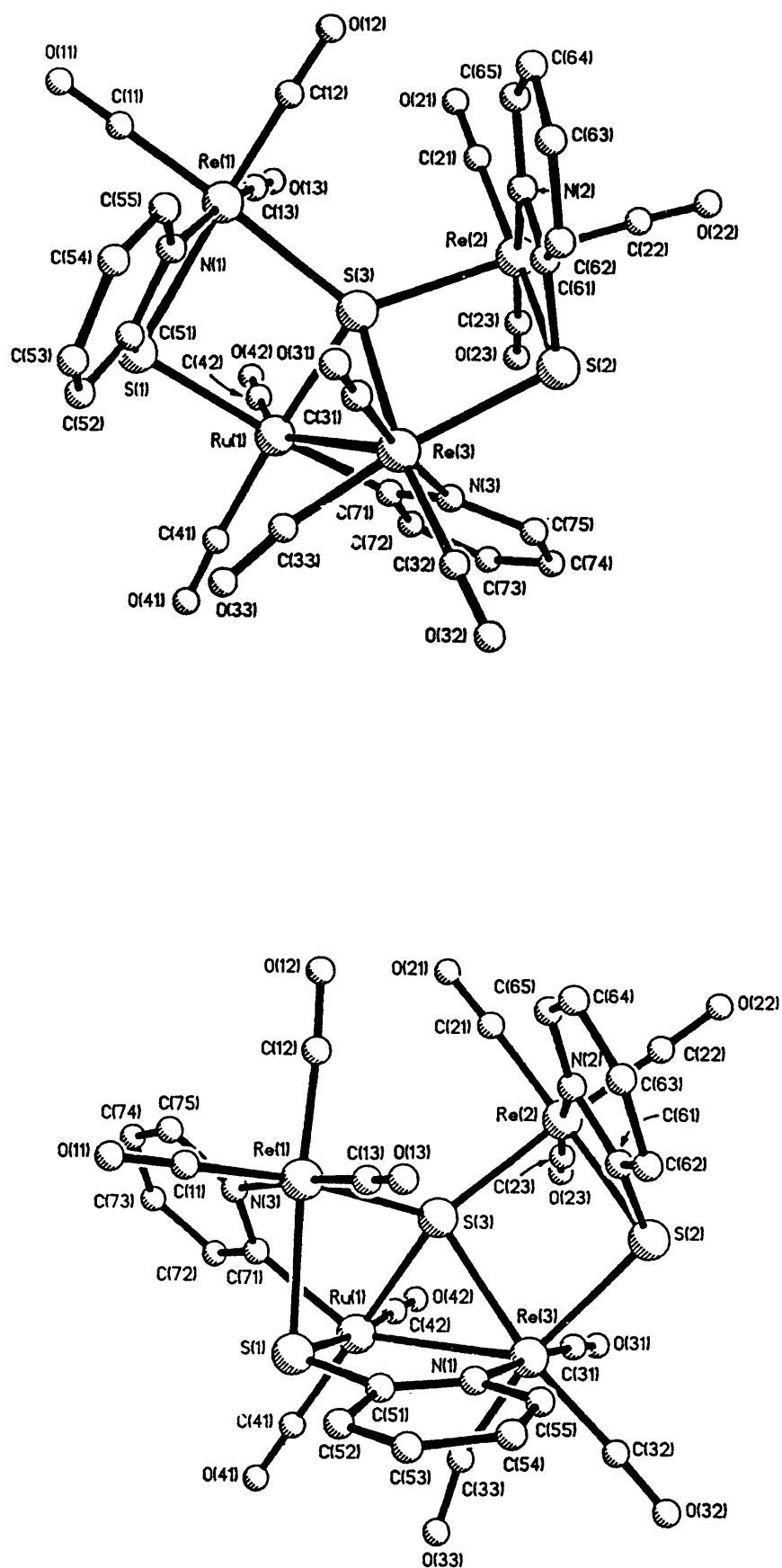
Figure 2.1 Structure of $[\text{ReRu}_3\text{S}(\text{C}_5\text{H}_4\text{N})(\text{CO})_{14}]$.

Figure 2.2 Structures of the two isomers of $[\text{Re}_3\text{RuS}(\text{C}_5\text{H}_4\text{N})(\text{pyS})_2(\text{CO})_{11}]$.

There are two equal-intensity sets of 2-pyridyl resonances in the ^1H NMR spectrum for compound 1, corresponding to two equally abundant isomers in solution which are not interconverting. These two isomers could not be separated chromatographically. The crystal structure of one of the isomers is shown in Figure 2.1, crystallisation having led to a diastereomerically pure crystal.

The isomers of compound 3 are separable by TLC, the ^1H NMR spectra of each showing three types of pyS or $\text{C}_5\text{H}_4\text{N}$ groups, although it is not easy to determine from the ^1H NMR spectra whether cleavage of C-S bonds has occurred. The crystal structures of both have been determined and are shown in Figure 2.2.

The work on compound 2, $[\text{Re}_2\text{Ru}_2\text{S}(\text{C}_5\text{H}_4\text{N})(\text{pyS})(\text{CO})_{13}]$, is described in this chapter.

2.2 Isomers of $[\text{Re}_2\text{Ru}_2\text{S}(\text{C}_5\text{H}_4\text{N})(\text{pyS})(\text{CO})_{13}]$

Before separation of the isomers, the ^1H NMR spectrum of this compound showed four sets of 2-pyridyl resonances in the intensity ratio 2:3:2:3. Treatment by TLC allowed us to obtain separated samples of isomers A and B, each of which contained two non-equivalent rings. The separated isomers show no tendency to interconvert at room temperature, either in the solid or solution. We could not discriminate unequivocally between a 2-pyridyl and a pyS ligand from NMR spectra, so that proper characterisation of these isomers depended upon X-ray structure determinations. The structure of isomer A was solved by Professor K. I. Hardcastle at the California State

University, Northridge, while the structure of isomer **B** was solved by myself.

The molecular structures of compounds **A** and **B** · 0.5CH₂Cl₂ are shown in Figures 2.3 and 2.4 respectively. Selected bond lengths and angles are in Table 2.1. Superficially, *i.e.* ignoring the orientations of the 2-pyridyl bridges, these molecular structures appear to be completely identical and bond lengths and angles are not significantly different in the two compounds. The only difference between the isomers arises from the orientations of the 2-pyridyl ligand and to establish these properly we needed to examine carefully the refinement of the carbon and nitrogen atoms bound to ruthenium. Reversing these atoms in each isomer and re-refining the structure gave unsatisfactory thermal parameters for these atoms which is illustrated pictorially in Figure 2.5 by the size of the thermal ellipsoids. Thermal parameters (U_{eq} or U_{11} if the atom is refined isotropically) that appear too large indicate that there is too much electron density at this site in the model, *i.e.* a lighter atom is required. Similarly, if U_{eq} is too small, then a heavier atom is required at this site. The correct orientation of the 2-pyridyl ligand also leads to a lower *R* value for the refinement, and although *R* differs only by a fraction of a per-cent between orientations, this too can be a guide to the correct ligand orientation. Allowing the populations of nitrogen and carbon atoms at these sites to be refined gave populations in each isomer consistent with the arrangements in Figures 2.3 and 2.4. This was not surprising since the crystals were obtained from diastereomerically pure samples which do not interconvert and any disorder involving 2-pyridyl orientation would have required the presence of different diastereomers.

In considering the possible isomers of this compound, there are four

possible sites of attachment of the N atom associated with the μ -pyS ligand if the $\text{Re}(\text{CO})_3$ group is to remain facial. The N atom could be attached at either side of either Re atom. The two observed isomers, those with the pyS ligand on the opposite side of the Ru_2S plane to the 2-pyridyl ring, correspond to two of the four possibilities but we have not found evidence for any others. We are fairly sure that chromatography would have provided these if they were present in anything but very low quantities. It is possible that those isomers with the 2-pyridyl and pyS ligands on the same side of the Ru_2S plane as each other are not produced due to steric unfavourability.

Figure 2.3 Molecular structure of $[\text{Re}_2\text{Ru}_2\text{S}(\text{C}_5\text{H}_4\text{N})(\text{pyS})(\text{CO})_{13}]$ Isomer A showing one of the two independent molecules in the unit cell.

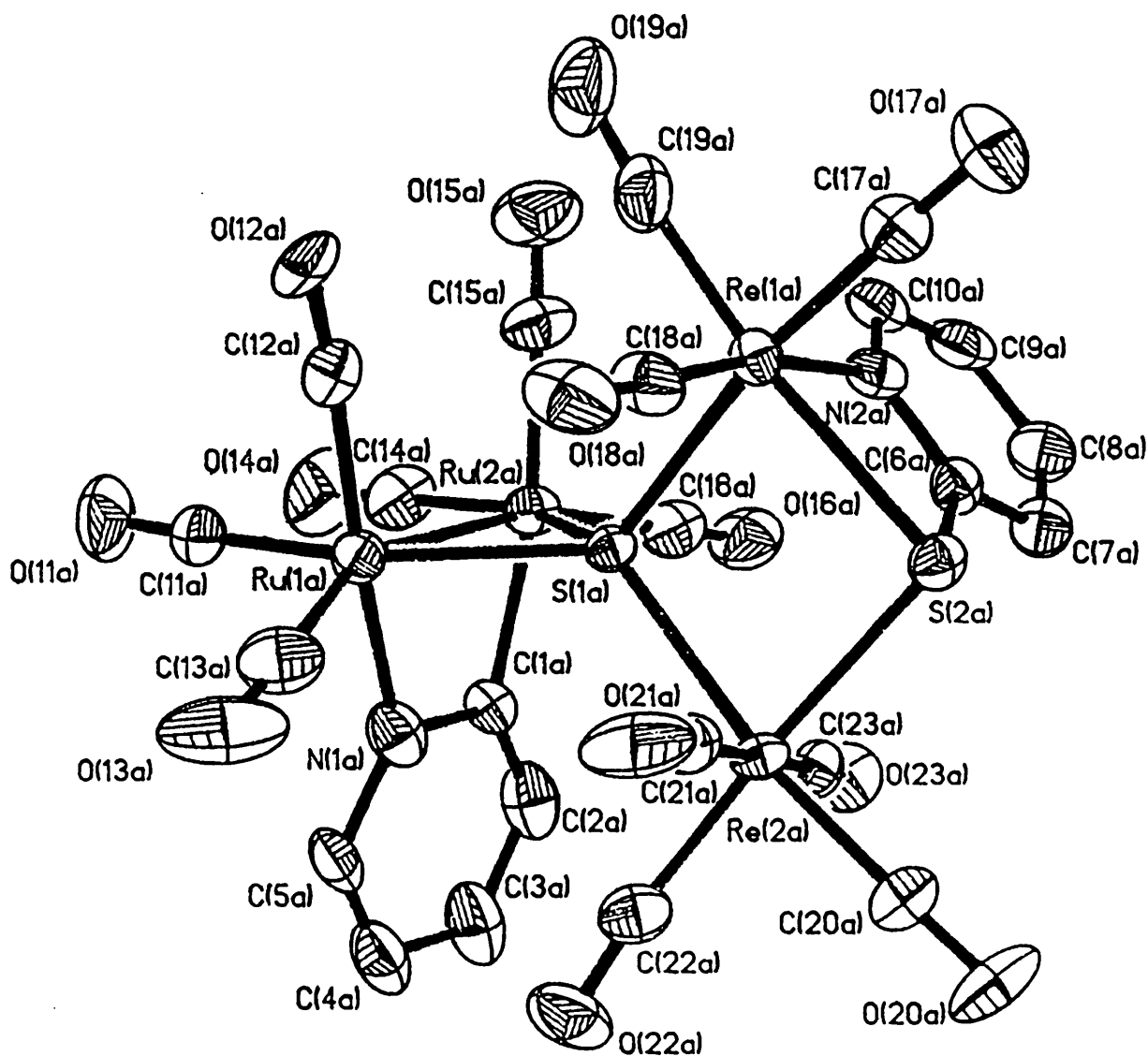


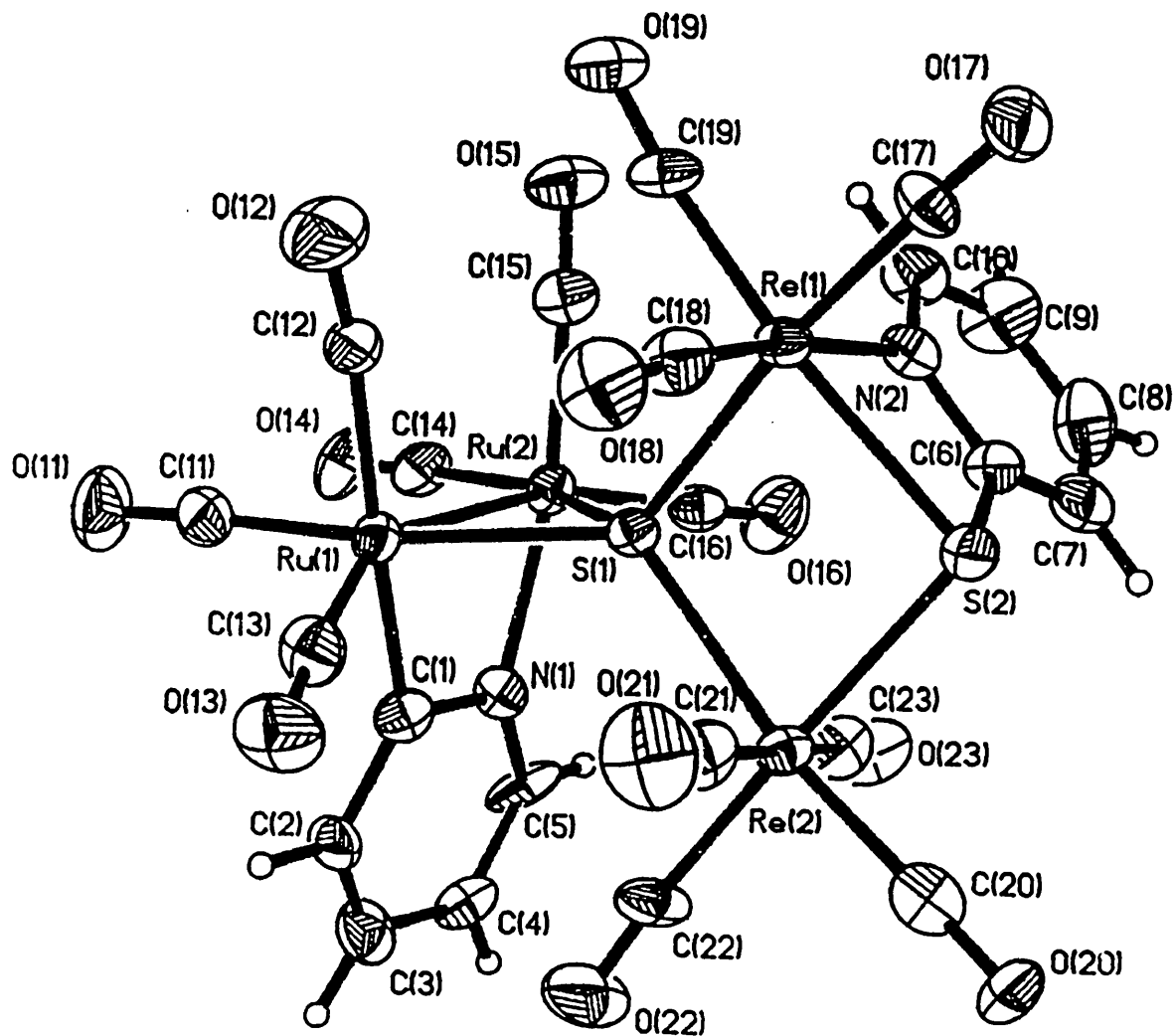
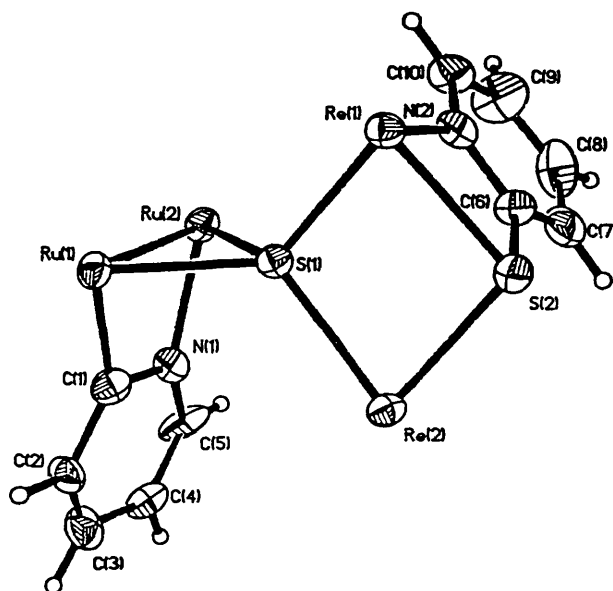
Figure 2.4 Molecular structure of $[\text{Re}_2\text{Ru}_2\text{S}(\text{C}_5\text{H}_4\text{N})(\text{pyS})(\text{CO})_{13}]$ Isomer B

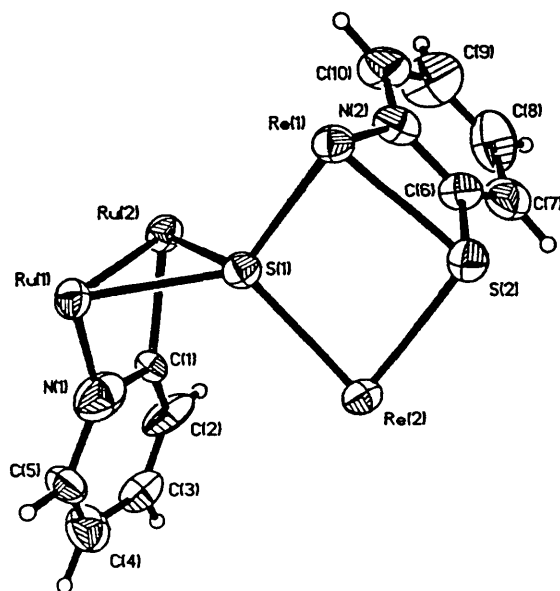
Figure 2.5 Molecular structures of $[\text{Re}_2\text{Ru}_2\text{S}(\text{C}_5\text{H}_4\text{N})(\text{pyS})(\text{CO})_{13}]$ Isomer B with carbonyl ligands removed, showing correct (a) and incorrect (b) 2-pyridyl orientations. The thermal parameters U_{eq} of the atoms N(1) and C(1) are given.



(a) Correct 2-pyridyl orientation.

$$U_{\text{eq}}(\text{N1}) = 0.04623$$

$$U_{\text{eq}}(\text{C1}) = 0.04553$$



(b) Incorrect 2-pyridyl orientation.

$$U_{\text{eq}}(\text{N1}) = 0.06647$$

$$U_{\text{eq}}(\text{C1}) = 0.02920$$

Table 2.1 Selected bond lengths (Å) and angles (°) for the two isomers of $[\text{Re}_2\text{Ru}_2\text{S}(\text{C}_5\text{H}_4\text{N})(\text{pyS})(\text{CO})_{13}]$.

	Isomer A		Isomer B
	Molecule A	Molecule B	
Ru(1)-Ru(2)	2.706(1)	2.701(1)	2.715(2)
Ru(1)-S(1)	2.412(2)	2.409(2)	2.417(4)
Ru(2)-S(1)	2.416(2)	2.419(2)	2.412(5)
Re(1)-S(1)	2.543(2)	2.553(2)	2.532(4)
Re(2)-S(1)	2.541(2)	2.545(2)	2.527(4)
Re(1)-S(2)	2.533(2)	2.547(2)	2.542(4)
Re(2)-S(2)	2.514(2)	2.508(2)	2.512(4)
Ru(1)-N(1)	2.114(8)	2.124(9)	-
Ru(1)-C(1)	-	-	2.07(1)
Ru(2)-N(1)	-	-	2.11(1)
Ru(2)-C(1)	2.076(8)	2.102(9)	-
Re(1)-N(2)	2.181(7)	2.170(6)	2.19(2)
N(1)-C(1)	1.35(1)	1.33(1)	1.36(2)
C(1)-C(2)	1.38(1)	1.39(1)	1.41(2)
C(2)-C(3)	1.41(2)	1.43(2)	1.33(3)
C(3)-C(4)	1.37(2)	1.37(2)	1.40(3)
C(4)-C(5)	1.41(2)	1.39(2)	1.33(3)
C(5)-N(1)	1.38(1)	1.39(1)	1.37(2)
S(2)-C(6)	1.768(9)	1.762(8)	1.76(2)
N(2)-C(6)	1.35(1)	1.35(1)	1.36(2)

Table 2.1 (cont.)

	Isomer A		Isomer B
	Molecule A	Molecule B	
C(6)-C(7)	1.38(1)	1.39(1)	1.38(3)
C(7)-C(8)	1.41(2)	1.39(1)	1.39(4)
C(8)-C(9)	1.40(2)	1.38(1)	1.37(4)
C(9)-C(10)	1.39(2)	1.40(1)	1.40(3)
C(10)-N(2)	1.36(1)	1.35(1)	1.31(3)

Averages

	Isomer A		Isomer B	All
	Molecule A	Molecule B		molecules
M-CO	1.927	1.928	1.932	1.929
Re-CO	1.936	1.938	1.940	1.938
Ru-CO	1.915	1.916	1.922	1.918
M-CO trans to S	1.902	1.907	1.907	1.905
M-CO trans to CO	1.997	2.000	1.995	1.997

Table 2.1 (cont.)

Bond angles (°)

	Isomer A		Isomer B
	Molecule A	Molecule B	
Ru(1)-S(1)-Ru(2)	68.18(6)	68.05(6)	68.4(1)
Ru(1)-S(1)-Re(1)	124.91(8)	123.23(8)	124.8(2)
Ru(1)-S(1)-Re(2)	122.37(8)	124.42(8)	122.8(2)
Ru(2)-S(1)-Re(1)	120.99(8)	123.14(8)	121.2(2)
Ru(2)-S(1)-Re(2)	125.63(8)	123.09(8)	124.4(2)
Re(1)-S(1)-Re(2)	96.52(7)	96.56(6)	96.8(2)
Re(1)-S(2)-Re(2)	97.46(7)	97.70(7)	98.9(2)
Ru(1)-Ru(2)-S(1)	55.83(5)	55.79(5)	55.9(1)
Ru(2)-Ru(1)-S(1)	55.99(5)	56.15(5)	55.7(1)
S(1)-Re(1)-S(2)	79.62(7)	79.23(7)	80.1(1)
S(1)-Re(2)-S(2)	80.00(7)	80.12(7)	80.8(1)
S(1)-Ru(1)-N(1)	84.9(2)	84.7(2)	-
S(1)-Ru(2)-C(1)	83.6(2)	84.0(2)	-
S(1)-Ru(1)-C(1)	-	-	87.0(5)
S(1)-Ru(2)-N(1)	-	-	84.6(4)
S(1)-Re(1)-N(2)	83.3(2)	85.5(2)	84.9(4)
S(2)-Re(1)-N(2)	65.5(2)	65.1(2)	65.9(4)
Re(1)-S(2)-C(6)	80.3(3)	80.0(3)	79.5(5)

Isomers **A** and **B** contain only one metal-metal bond each, that between the two ruthenium atoms, and are electron-precise. The μ_4 -S ligand which is surrounded tetrahedrally by four metal atoms is a six-electron donor and the 2-pyridyl ligand is a three-electron donor. The intact pyS ligand, as in $[\text{Re}_2(\text{pyS})_2(\text{CO})_6]$, donates five electrons. It has the same arrangement found in the parent molecule and the Re_2S_2 skeleton is likewise extremely similar with that of the parent. The Re-S distances are in the range 2.512(4) to 2.533(2) Å, in close agreement with those found in $[\text{Re}_2(\text{pyS})_2(\text{CO})_6]$ (2.529(6)-2.556(6) Å).⁷⁴ The Ru-S distances are slightly longer than those found in $[\text{ReRu}_3(\mu_4\text{-S})(\mu\text{-C}_5\text{H}_4\text{N})(\text{CO})_{14}]$.⁷⁶ The Ru-Ru distance of 2.706(1) Å is much shorter than that of 2.8515(4) Å in $[\text{Ru}_3(\text{CO})_{12}]$ ¹³⁴ but is similar to that of 2.719(1) Å found in $[\text{ReRu}_3(\mu_4\text{-S})(\mu\text{-C}_5\text{H}_4\text{N})(\text{CO})_{14}]$.⁷⁶ The shorter Ru-Ru bond lengths of these mixed-metal species, in relation to $[\text{Ru}_3(\text{CO})_{12}]$, are probably due to the requirements of the bridging S and $\text{C}_5\text{H}_4\text{N}$ groups in terms of optimum metal-ligand orbital overlap.

The formation of these isomers could be easily rationalised by the addition of a CO to $[\text{Re}_2(\text{pyS})_2(\text{CO})_6]$ to give $[\text{Re}_2(\text{pyS})_2(\text{CO})_7]$ in which the pyS ligands are three- and five-electron donors respectively. The three-electron donor could bridge just through the S atom leaving the pyridine ring free and oxidative addition of this ligand to an $\text{Ru}_2(\text{CO})_6$ unit would give $[\text{Re}_2\text{Ru}_2(\mu_4\text{-S})(\mu\text{-C}_5\text{H}_4\text{N})(\mu\text{-pyS})(\text{CO})_{13}]$. This may not be the actual mechanism since the formation of the other products from the reaction requires the fragmentation of $[\text{Re}_2(\text{pyS})_2(\text{CO})_6]$, as has been shown to occur readily under the action of ligands, so there is no reason to believe that this does not occur generally. Note that both pyS ligands of the parent compound remain in the final cluster.

Cleavage of the pyS ligand leaves a S atom and a C₅H₄N group, both of which are strongly bound to the metal atoms and are not lost. The cleaved pyS ligand donates nine electrons in the final compound and this is probably the driving force for C–S cleavage. The creation of four strong M–S, one M–N and one M–C bond for this cleaved pyS ligand makes the formation of the compound energetically favourable and C–S bond cleavage under these circumstances is not a problem energetically.

The formal addition of one Ru₂(CO)₆ unit to a pyS ligand of [Re₂(pyS)₂(CO)₇] to give the two isomers of [Re₂Ru₂S(C₅H₄N)(pyS)(CO)₁₃], as described above, could be envisaged as being followed by a similar addition of another Ru₂(CO)₆ unit to the remaining bridge to give the hypothetical compound [Re₂Ru₄(μ₄-S)₂(μ-C₅H₄N)₂(CO)₁₉]. However, we have no evidence for this as a product and the reactions of [Re₂Ru₂S(C₅H₄N)(pyS)(CO)₁₃] with [Ru₃(CO)₁₂] gave products of a different nature as described in Section 2.4.

Attempts at separating the two isomers of compound 1, [ReRu₃(μ₄-S)(μ-C₅H₄N)(CO)₁₄], using similar methods to those used for [Re₂Ru₂(μ₄-S)(μ-C₅H₄N)(μ-pyS)(CO)₁₃] were unsuccessful. Even sectioning off the lower and upper portions of the TLC band on silica resulted in fractions with identical ¹H NMR spectra. It could be that the isomers interconvert too fast for separation, but too slow to give NMR coalescence. However, on rechromatography we were able to separate a pure mixture of both isomers of [ReRu₃(μ₄-S)(μ-C₅H₄N)(CO)₁₄] from a trace quantity of a compound identified as [Ru₆(μ₄-S)₂(μ-C₅H₄N)₂(CO)₁₈]. Its characterisation and X-ray structure will be reported in Chapter Three.

Several other minor products were obtained from the reaction but none

in sufficient quantity to allow characterisation.

2.3 Effect of altered reaction conditions on product ratios.

In order to attempt to understand this system more fully, the reaction was carried out using solvents of different boiling points and with variable reaction times. It was expected that this would lead to an alteration in the relative yields of compounds 1-3, possibly giving a higher yield of one particular species thereby enabling the chemistry of that compound to be developed further. It was also hoped that some insight into the mechanism could be gained in this way. The results of these experiments are presented in Table 2.2.

Compound	Thermolysis			Photolysis
	<i>m</i> -Xylene		Toluene	Toluene
	½ h	1 h	1 h	27 h
[ReRu ₃ S(C ₅ H ₄ N)(CO) ₁₄]	32	8	12	No Reaction
[Re ₂ Ru ₂ S(C ₅ H ₄ N)(pyS)(CO) ₁₃]	31	20	36	
[Re ₃ RuS(C ₅ H ₄ N)(pyS) ₂ (CO) ₁₁]	18	5	27	

Table 2.2 Percentage yields under different reaction conditions.

(The boiling points of *m*-xylene and toluene are 132 and 111 °C respectively).

Under photolytic conditions, no reaction was observed, possibly because the reactants were only slightly soluble at room temperature. However, even when the two reactants were dissolved separately in warm solvent, mixed and then exposed to UV radiation, there was still no reaction.

When the reaction was carried out in refluxing *m*-xylene with an increased reaction time of 1 h, lower yields were obtained for each of the compounds 1-3 and no new products were observed. This seems to indicate that decomposition of the reaction products has taken place and that the optimum reaction time is probably around 30 mins. When a lower-boiling solvent such as toluene is employed, an increase in the relative yield of compound 3, $[\text{Re}_3\text{RuS}(\text{C}_5\text{H}_4\text{N})(\text{pyS})_2(\text{CO})_{11}]$, is observed. This may indicate that compound 3 is one of the first products formed, which is reasonable, since these species are all derived from $[\text{Re}_2(\text{pyS})_2(\text{CO})_6]$ and its formation would require the least number of Re-S and Re-N bond cleavages.

It is interesting to note that the product ratio observed when a 30 minute reaction time in refluxing *m*-xylene is employed, is consistent with a ratio which would arise from a binomial distribution of $[\text{Re}(\text{CO})_3(\text{pyS})]$ and $[\text{Ru}(\text{CO})_3 \text{ or } 4]$ fragments. This is calculated on the basis that equimolar amounts of starting materials, $[\text{Re}_2(\text{pyS})_2(\text{CO})_6]$ and $[\text{Ru}_3(\text{CO})_{12}]$, were used, giving a relative abundance of 2/5 for a $[\text{Re}(\text{CO})_3(\text{pyS})]$ fragment and 3/5 for a $[\text{Ru}(\text{CO})_3 \text{ or } 4]$ fragment. Assuming there is no preference in fragment combination, then the probability distribution shown in Table 2.3 would result.

Only three of these compounds have been isolated from this reaction but the presence of the tetraruthenium compound in trace amounts seems likely in view of the isolation of $[\text{Ru}_6(\mu_4\text{-S})_2(\mu\text{-C}_5\text{H}_4\text{N})_2(\text{CO})_{18}]$ from this reaction. In fact, $[\text{Ru}_4(\mu_4\text{-S})(\mu\text{-C}_5\text{H}_4\text{N})_2(\text{CO})_{12}]$ has been synthesised, and by a more direct route, which will be discussed in Chapter Three. One possible reason why the distribution seems to fit the product ratio observed for the reaction in *m*-xylene, but not toluene, is that at the lower temperature there is

insufficient energy for the cleavage of all necessary metal-metal or metal-ligand bonds and the product ratio is governed by kinetic stability.

Compound	Probability	Yields in <i>m</i> -Xylene
$[\text{Ru}_4\text{S}(\text{C}_5\text{H}_4\text{N})_2(\text{CO})_{12}]$	$1(3/5)^4 = 0.1296$	-
$[\text{ReRu}_3\text{S}(\text{C}_5\text{H}_4\text{N})(\text{CO})_{14}]$	$4(2/5)(3/5)^3 = 0.3456$	32 %
$[\text{Re}_2\text{Ru}_2\text{S}(\text{C}_5\text{H}_4\text{N})(\text{pyS})(\text{CO})_{13}]$	$6(2/5)^2(3/5)^2 = 0.3456$	31 %
$[\text{Re}_3\text{RuS}(\text{C}_5\text{H}_4\text{N})(\text{pyS})_2(\text{CO})_{11}]$	$4(2/5)^3(3/5) = 0.1536$	18 %
$[\text{Re}_4\text{S}(\text{C}_5\text{H}_4\text{N})_x(\text{pyS})_y(\text{CO})_z]$	$1(2/5)^4 = 0.0256$	-

Table 2.3 Binomial Probability Distribution and Observed Yields in *m*-Xylene.

It should also be possible to control the distribution of products by varying the ratio of reagents. For example, an excess of $[\text{Ru}_3(\text{CO})_{12}]$ should lead to a build-up of the $[\text{ReRu}_3\text{S}(\text{C}_5\text{H}_4\text{N})(\text{CO})_{14}]$ species. However, there is a problem since $[\text{Ru}_3(\text{CO})_{12}]$ is known to react with arenes such as *m*-xylene to give the hexanuclear carbido species $[\text{Ru}_6\text{C}(\textit{m}\text{-xylene})(\text{CO})_{14}]^{135}$ so any excess $[\text{Ru}_3(\text{CO})_{12}]$ will react with the solvent.

2.4 Reaction of $[\text{Re}_2\text{Ru}_2\text{S}(\text{C}_5\text{H}_4\text{N})(\text{pyS})(\text{CO})_{13}]$ (2) with $[\text{Ru}_3(\text{CO})_{12}]$.

In the compound $[\text{Re}_2\text{Ru}_2\text{S}(\text{C}_5\text{H}_4\text{N})(\text{pyS})(\text{CO})_{13}]$, the pyS ligand is already a five-electron donor but there is still a lone-pair of electrons on the sulphur atom, giving rise to the possibility of further coordination to metal atoms. Because of this, and in light of the isolation of the compound $[\text{Ru}_6(\mu_4\text{-S})_2(\mu\text{-C}_5\text{H}_4\text{N})_2(\text{CO})_{18}]$, which contains two quadruply-bridging sulphur atoms and

indicates that clusters with higher nuclearities could be formed, we decided to react $[\text{Re}_2\text{Ru}_2(\mu_4\text{-S})(\mu\text{-C}_5\text{H}_4\text{N})(\mu\text{-pyS})(\text{CO})_{13}]$ with more $[\text{Ru}_3(\text{CO})_{12}]$. We predicted that products might be formed in two different ways. Firstly, there was the possibility of pyS cleavage at the C–S bond and an increase in the chain length to form the hypothetical compound $[\text{Re}_2\text{Ru}_4(\text{S})_2(\text{C}_5\text{H}_4\text{N})_2(\text{CO})_{19}]$ containing two $\mu_4\text{-S}$ ligands joining three dinuclear metal units, which seemed likely considering the isolation of the $[\text{Ru}_6(\text{S})_2(\text{C}_5\text{H}_4\text{N})_2(\text{CO})_{18}]$. The second possibility was addition of an intact trinuclear Ru_3 unit to the original compound through the available lone-pair on the S atom.

When the reaction was performed, however, neither of the above two routes were followed. The reaction was carried out at 150 °C in a sealed tube and several products were isolated, the only one of which we have been able to characterise is $[\text{Re}_2\text{Ru}_2(\mu_4\text{-S})(\mu\text{-H})(\mu\text{-C}_5\text{H}_4\text{N})(\text{CO})_{14}]$ **4**. The compound is electron-precise and gives a peak of $m/e = 1079$ in the mass spectrum corresponding to the molecular ion $[\text{Re}_2\text{Ru}_2\text{S}(\text{H})(\text{C}_5\text{H}_4\text{N})(\text{CO})_{14}]^+$. An X-ray diffraction structure determination was performed and a view of the molecule is shown in Figure 2.6. Selected bond lengths and angles are in Table 2.4. The tetrahedral $\mu_4\text{-S}$ atom and the $\mu\text{-2-pyridyl}$ ligand are six- and three-electron donors respectively, as in the starting material. However, the pyS ligand has been lost from the original molecule and has been replaced by an extra CO ligand, a hydride and an Re–Re bond. Compound **4**, like the other mixed tetranuclear rhenium-ruthenium compounds **1-3** which all contain the tetrahedral $\mu_4\text{-S}$ ligand, is chiral. The infrared spectrum of the compound is complex in the carbonyl stretching region but, because of its higher symmetry, there are fewer peaks than in the spectrum of the starting material.

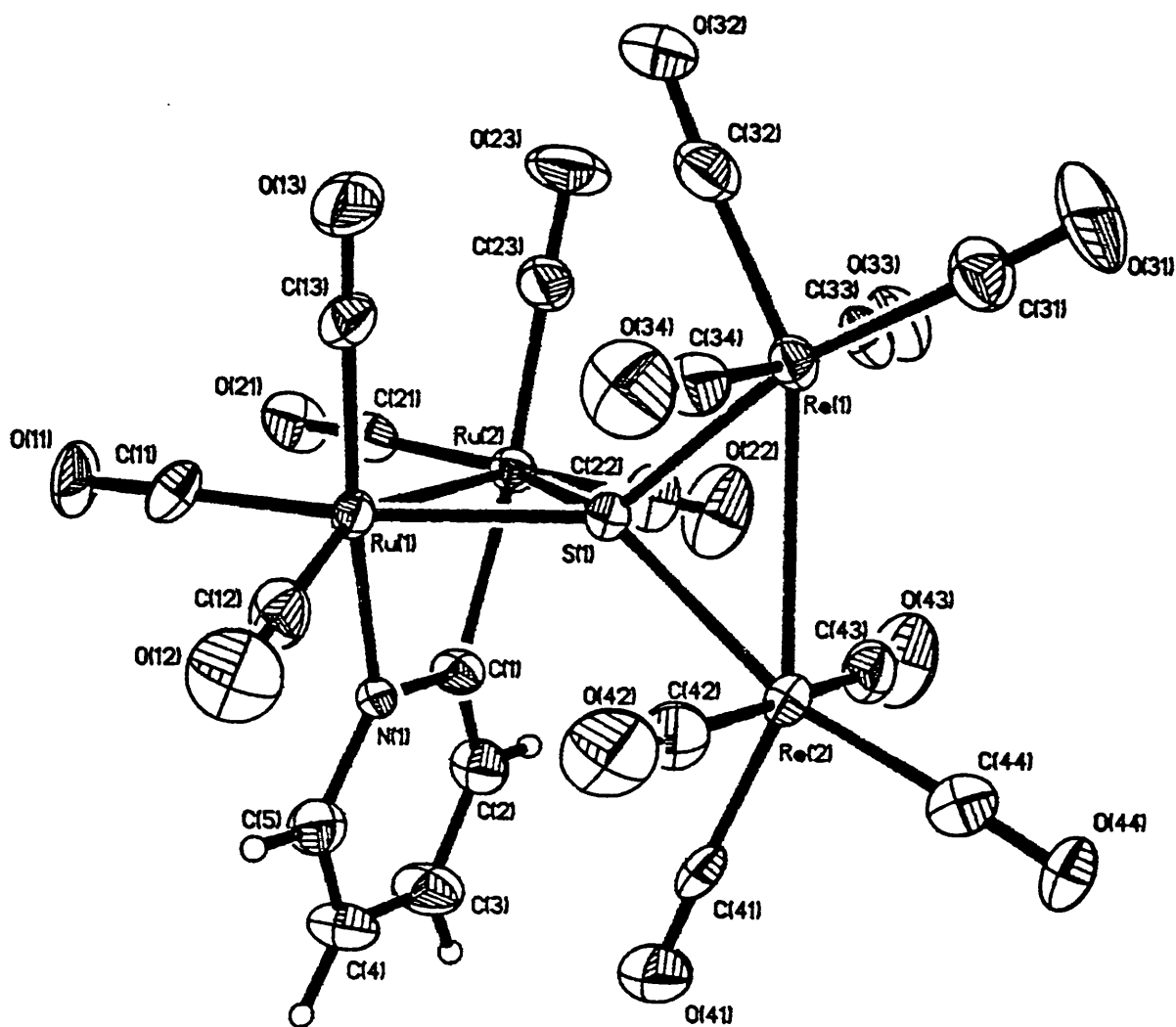
Figure 2.6 Molecular structure of $[\text{Re}_2\text{Ru}_2(\text{S})(\text{H})(\text{C}_5\text{H}_4\text{N})(\text{CO})_{14}]$ 4.

Figure 2.7 Alternative view of $[\text{Re}_2\text{Ru}_2(\text{S})(\text{H})(\text{C}_5\text{H}_4\text{N})(\text{CO})_{14}]$ **4** showing the probable hydride position.

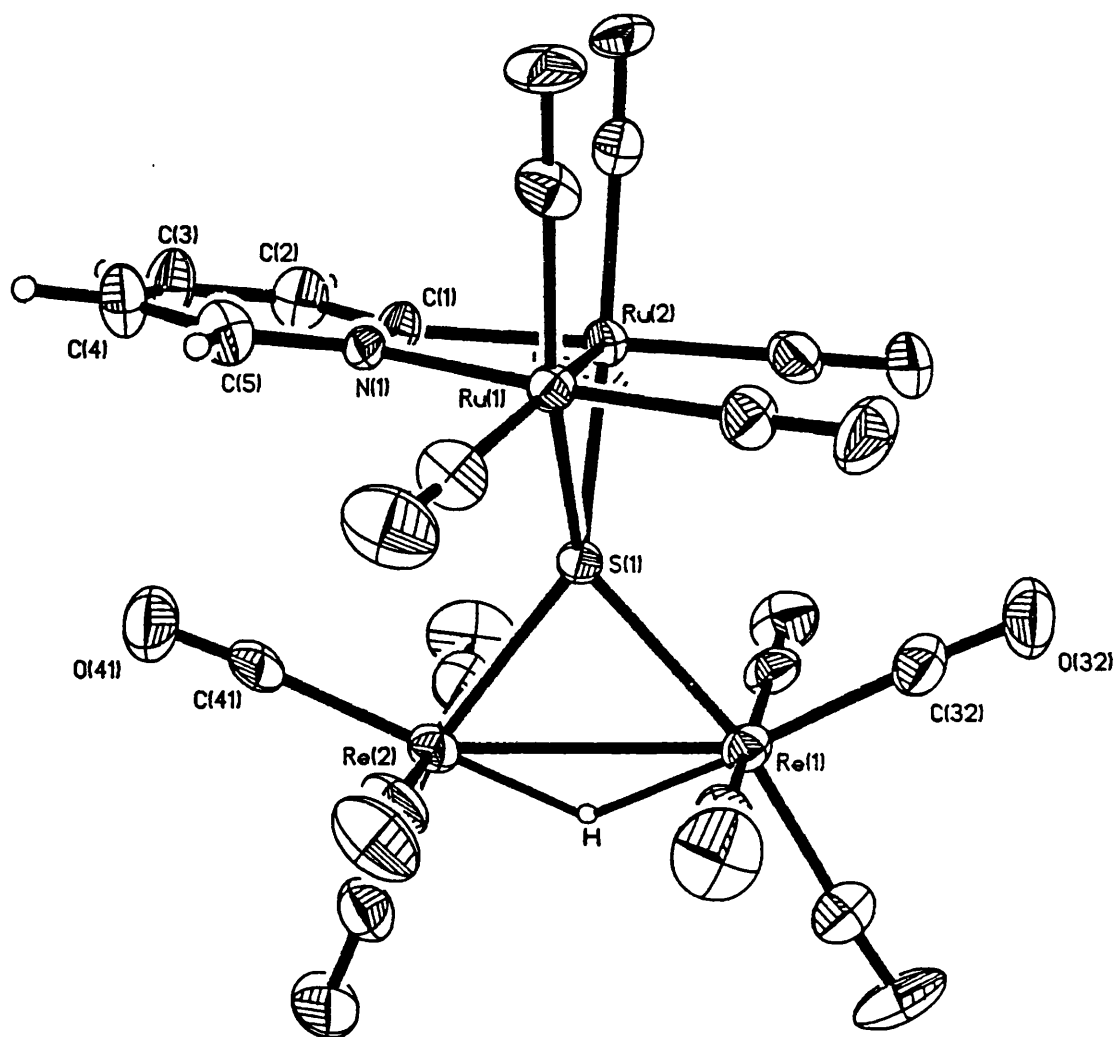


Table 2.4 Selected bond lengths (Å) and angles (°) for
 $[\text{Re}_2\text{Ru}_2(\text{S})(\text{H})(\text{C}_5\text{H}_4\text{N})(\text{CO})_{14}]$ **4**.

Bond lengths (Å)

Ru(1)-Ru(2)	2.728(2)	Re(1)-Re(2)	3.129(2)
Ru(1)-S(1)	2.396(4)	Re(1)-S(1)	2.464(4)
Ru(2)-S(1)	2.390(3)	Re(2)-S(1)	2.472(3)
Ru(1)-N(1)	2.10(1)	Ru(2)-C(1)	2.10(1)
N(1)-C(1)	1.36(1)	C(1)-C(2)	1.37(2)
C(2)-C(3)	1.35(2)	C(3)-C(4)	1.39(2)
C(4)-C(5)	1.40(2)	C(5)-N(1)	1.38(2)

M-CO averages (Å)

Ru-CO	1.934	Re-CO	1.967
-------	-------	-------	-------

Bond Angles (°)

Ru(1)-S(1)-Ru(2)	69.5(1)	Re(1)-S(1)-Re(2)	78.7(1)
Ru(1)-Ru(2)-S(1)	55.4(1)	Re(1)-Re(2)-S(1)	50.6(1)
Ru(2)-Ru(1)-S(1)	55.1(1)	Re(2)-Re(1)-S(1)	50.8(1)
Ru(1)-S(1)-Re(1)	130.6(1)	Ru(1)-S(1)-Re(2)	130.9(1)
Ru(2)-S(1)-Re(1)	125.4(1)	Ru(2)-S(1)-Re(2)	130.8(1)
Ru(1)-Ru(2)-C(1)	71.1(3)	Ru(2)-Ru(1)-N(1)	70.7(3)
Ru(1)-N(1)-C(1)	109.3(8)	Ru(2)-C(1)-N(1)	108.8(8)
S(1)-Ru(1)-N(1)	84.0(3)	S(1)-Ru(2)-C(1)	83.6(3)

Unlike the ^1H NMR spectrum of the starting material $[\text{Re}_2\text{Ru}_2(\mu_4\text{-S})(\mu\text{-C}_5\text{H}_4\text{N})(\mu\text{-pyS})(\text{CO})_{13}]$, which demonstrated that there are two diastereomers present, the ^1H NMR spectrum of $[\text{Re}_2\text{Ru}_2(\mu_4\text{-S})(\mu\text{-H})(\mu\text{-C}_5\text{H}_4\text{N})(\text{CO})_{14}]$ shows only one set of 2-pyridyl resonances, *i.e.* the isomerism present in the parent compound has been removed on loss of the pyS ligand and addition of the hydride and CO ligands. The hydride signal occurs at $\delta = -13.78$, in a high-field region, which is consistent with a bridging mode of bonding. There is the possibility of isomerism but this would depend upon the bridging hydride ligand lying out of the plane created by the Re_2S atoms, leading to two diastereomers which would have opposite 2-pyridyl orientations. Since only one set of resonances is observed in the ^1H NMR spectrum, this must mean that the hydride lies in the Re_2S plane, and symmetrically between the two rhenium atoms. If we consider the projection of the molecule shown in Figure 2.7 there seems to be a place for the hydride opposite the carbonyl ligands C(41)O(41) and C(32)O(32) and this is almost certainly where it lies. The source of the hydride can probably be attributed to abstraction from dichloromethane which was used in the work-up of the reaction. To establish the correct orientation of the 2-pyridyl ligand, the thermal parameters of carbon and nitrogen atoms bound to ruthenium atoms were examined. However, the orientation showed in Figure 2.6 and the reverse 2-pyridyl orientation both gave satisfactory values of U_{eq} . The best refinement of the structure was when orientational disorder was included in the model. Allowing the relative populations of C and N atoms to refine gave a best solution with a fractional population of 0.6(1) for N(1) and C(1) in the positions shown in Figure 2.6, together with a 0.4(1) population of the reverse

orientation of these atoms (N(1a) and C(1a)). This disorder corresponds to an approximately equal distribution of enantiomers throughout the crystal lattice.

The Ru–Ru bond length of 2.728(2) Å is of a similar length to those of 2.701(1)-2.715(2) Å found in the parent molecule $[\text{Re}_2\text{Ru}_2\text{S}(\text{C}_5\text{H}_4\text{N})(\text{pyS})(\text{CO})_{13}]$. There was no Re–Re bond in the starting material but we can compare the metal-metal bond length of 3.129(2) Å with that of 3.041(1) Å found in $[\text{Re}_2(\text{CO})_{10}]$,¹³⁶ and that of 2.946(1) Å found in the sulphido-bridged dimer $[(\text{cp})_2\text{Re}_2(\text{CO})_4(\mu\text{-S})]$.¹³⁷ This is further evidence for the presence of a bridging hydride ligand in this position since previous observations suggest that $\mu\text{-H}$ ligands produce significant lengthening effects on metal-metal bonds.¹³⁸ A slightly longer H-bridged Re–Re bond (3.1956(5) Å) is observed in $[\text{Re}_2(\mu\text{-H})(\text{CO})_8(\mu\text{-C}_5\text{H}_4\text{N})]$.¹⁰¹ Increases of 0.080 - 0.134 Å have been observed for the hydride-bridged Os–Os bonds in $[\text{Os}_6\text{H}_4(\text{CO})_{15}(\mu_4\text{-S})(\mu_3\text{-S})(\mu\text{-HC=NPh})_2]$ ¹³⁹ in relation to the unbridged bonds in $[\text{Os}_3(\text{CO})_{12}]$.¹⁴⁰ The Ru–S distances of 2.390(3) - 2.396(3) Å in compound 4 are slightly shorter than those in the parent molecule (av. 2.415 Å), whereas the Re–S distances of 2.464(4) - 2.472(3) Å are appreciably shorter than those in $[\text{Re}_2\text{Ru}_2\text{S}(\text{C}_5\text{H}_4\text{N})(\text{pyS})(\text{CO})_{13}]$ (av. 2.540 Å). Similarly, the Ru–S–Ru bite angles are approximately similar in the two molecules (*ca.* 69°), whereas the Re–S–Re angle in 4 is smaller (78.7(1)°) than that in $[\text{Re}_2\text{Ru}_2\text{S}(\text{C}_5\text{H}_4\text{N})(\text{pyS})(\text{CO})_{13}]$ (av. 96.3°), which is to be expected since there is an Re–Re bond in compound 4. This Re–S–Re angle is similar to that of 76.4(1)° found in $[(\text{cp})_2\text{Re}_2(\text{CO})_4(\mu\text{-S})]$ ¹³⁷ in which there is also a sulphido-bridged Re–Re bond.

There has not been any increase in nuclearity of the molecule during the course of the reaction, the role of $[\text{Ru}_3(\text{CO})_{12}]$ in the formation of this product

being to abstract pyS and to add a carbonyl ligand although other products to support this idea were not obtained. If this was the only process occurring, then it might have been expected that $[\text{Ru}_3\text{H}(\text{pyS})(\text{CO})_9]^{79}$ would have been observed in the product mixture. This was not the case so presumably any $[\text{Ru}_3\text{H}(\text{pyS})(\text{CO})_9]$ formed has reacted further which is quite likely since other, unidentified products were isolated from the reaction.

Table 2.5 ^1H NMR data for the new compounds.

Compound	^1H NMR data (δ) ^{a,b}
[Re ₂ Ru ₂ S(C ₅ H ₄ N)(pyS)(CO) ₁₃] (Isomer A)	8.54 (ddd, J = 5.4, 0.8 Hz, H ^{6y}), 7.91 (ddd, J = 7.9, 7.9, 1.6 Hz, H ^{4y}), 7.76 (ddd, J = 5.5, 0.9 Hz, H ^{6x}), 7.55 (ddd, J = 7.7, 5.6, 1.1 Hz, H ^{5y}), 7.21 (ddd, J = 7.6 Hz, H ^{3y}), 7.11 (ddd, J = 7.5, 7.5, 1.6 Hz, H ^{4x}), 6.97 (ddd, J = 7.5, 1.1 Hz, H ^{3x}), 6.72 (ddd, J = 6.6, 5.7, 1.8 Hz, H ^{5x}).
[Re ₂ Ru ₂ S(C ₅ H ₄ N)(pyS)(CO) ₁₃] (Isomer B)	8.47 (ddd, J = 5.5, 0.8 Hz, H ^{6y}), 7.94 (ddd, J = 7.9, 7.9, 1.7 Hz, H ^{4y}), 7.58 (ddd, J = 5.6, 1.2 Hz, H ^{6x}), 7.51 (ddd, J = 7.7, 5.5, 1.2 Hz, H ^{5y}), 7.23 (ddd, J = 7.0 Hz, H ^{3y}), 7.19 (ddd, H ^{3x}), 7.06 (ddd, J = 7.5, 7.5, 1.7 Hz, H ^{4x}), 6.74 (ddd, J = 7.3, 5.6, 1.7 Hz, H ^{5x}).
[Re ₂ Ru ₂ (S)(H)(C ₅ H ₄ N)(CO) ₁₄] ^c	7.82 (ddd, J = 5.3, 1.2 Hz, H ⁶), 7.29 (ddd, J = 7.5, 7.5, 1.6 Hz, H ⁴), 7.25 (ddd, H ³), 6.92 (ddd, J = 7.3, 5.6, 1.7 Hz, H ⁵), -13.78 (s, hydride).

a. Recorded in CDCl₃ at 200 MHz at room temperature unless otherwise stated

b. The superscripts x and y refer to the 2-pyridyl and pyS groups respectively

c. Recorded in CDCl₃ at 400 MHz at room temperature

Table 2.6 Infrared spectroscopic data for the new compounds.

Compound	$\nu(\text{CO})^a/\text{cm}^{-1}$
[Re ₂ Ru ₂ S(C ₅ H ₄ N)(pyS)(CO) ₁₃] (Isomer A)	2102m, 2075s, 2045vs, 2027s, 2010s, 2006s, 2002s, 1994s, 1986m, 1971m, 1954s, 1950s, 1930s, 1921s, 1915m.
[Re ₂ Ru ₂ S(C ₅ H ₄ N)(pyS)(CO) ₁₃] (Isomer B)	2102m, 2075s, 2045vs, 2027s, 2011s, 2007s, 1990s, 1982m, 1973w, 1953s, 1932s, 1921s, 1915w.
[Re ₂ Ru ₂ (S)(H)(C ₅ H ₄ N)(CO) ₁₄]	2110w, 2087m, 2084m, 2075s, 2065s, 2053sh, 2050s, 2046s, 2011vs, 1994sh, 1992s, 1975m, 1967s.

a. Recorded in cyclohexane solution.

2.5 Experimental

Reaction of $[\text{Re}_2(\text{pyS})_2(\text{CO})_6]$ with $[\text{Ru}_3(\text{CO})_{12}]$.

A solution of $[\text{Re}_2(\text{pyS})_2(\text{CO})_6]$ (0.238 g, 0.313 mmol) and $[\text{Ru}_3(\text{CO})_{12}]$ (0.220 g, 0.313 mmol) in *m*-xylene (50 cm³) was heated under reflux under nitrogen for 30 mins. The solvent was removed under reduced pressure and the deep yellow solid residue separated by TLC [SiO_2 , light petroleum (b.p. <40 °C)-dichloromethane (7:3 v/v)] to give several broad bands which were collected in three fractions corresponding to the major concentrations of material on the plates. These three bands yielded $[\text{ReRu}_3(\mu_4\text{-S})(\mu\text{-C}_5\text{H}_4\text{N})(\text{CO})_{14}]$ (0.100 g, 32%) as yellow crystals from slow evaporation of a dichloromethane-hexane solution, $[\text{Re}_2\text{Ru}_2(\mu_4\text{-S})(\mu\text{-C}_5\text{H}_4\text{N})(\mu\text{-pyS})(\text{CO})_{13}]$ (0.114 g, 31%) as lemon-yellow crystals from a dichloromethane-methanol mixture and $[\text{Re}_3\text{Ru}(\mu_4\text{-S})(\mu\text{-C}_5\text{H}_4\text{N})(\mu\text{-pyS})_2(\text{CO})_{11}]$ (0.070 g, 18%) as orange crystals.

Separation of isomers

(i) $[\text{Re}_2\text{Ru}_2(\mu_4\text{-S})(\mu\text{-C}_5\text{H}_4\text{N})(\mu\text{-pyS})(\text{CO})_{13}]$. The band containing this material was rechromatographed by TLC [SiO_2 , light petroleum (b.p. <40 °C)-dichloromethane-toluene (15:2:1 v/v)]. The slowly moving material separated into two bands giving the pure isomers A and B. Crystals of each were obtained by adding a layer of methanol to a dichloromethane solution and allowing slow diffusion to occur.

(ii) $[\text{ReRu}_3(\mu_4\text{-S})(\mu\text{-C}_5\text{H}_4\text{N})(\text{CO})_{14}]$. All attempts to separate the isomers by careful TLC were unsuccessful, although rechromatography separated a pure

mixture of both isomers of this compound from a trace quantity of a compound characterised as $[\text{Ru}_6(\mu_4\text{-S})_2(\mu\text{-C}_5\text{H}_4\text{N})_2(\text{CO})_{18}]$. The characterisation of this trace material will be reported in Chapter Three.

Reaction of $[\text{Re}_2(\text{pyS})_2(\text{CO})_6]$ with $[\text{Ru}_3(\text{CO})_{12}]$ in toluene.

A solution of $[\text{Re}_2(\text{pyS})_2(\text{CO})_6]$ (0.095 g, 0.125 mmol) and $[\text{Ru}_3(\text{CO})_{12}]$ (0.080 g, 0.125 mmol) in toluene (40 cm³) was heated under reflux under nitrogen for 1 h. The products were isolated using conditions identical to those used for the reaction in *m*-xylene, and resulted in the following yields: $[\text{ReRu}_3\text{S}(\text{C}_5\text{H}_4\text{N})(\text{CO})_{14}]$ (0.015 g, 12%), $[\text{Re}_2\text{Ru}_2\text{S}(\text{C}_5\text{H}_4\text{N})(\text{pyS})(\text{CO})_{13}]$ (0.045 g, 31%) and $[\text{Re}_3\text{RuS}(\text{C}_5\text{H}_4\text{N})(\text{pyS})_2(\text{CO})_{11}]$ (0.043 g, 27%), identified by their infrared spectra.

Photolysis reaction of $[\text{Re}_2(\text{pyS})_2(\text{CO})_6]$ with $[\text{Ru}_3(\text{CO})_{12}]$.

A suspension of $[\text{Re}_2(\text{pyS})_2(\text{CO})_6]$ (0.095 g, 0.125 mmol) and $[\text{Ru}_3(\text{CO})_{12}]$ (0.080 g, 0.125 mmol) in toluene (30 cm³) was irradiated with UV light at room temperature for 24 h. The reaction was monitored by infrared spectroscopy and no change was observed.

Reaction of $[\text{Re}_2\text{Ru}_2\text{S}(\text{C}_5\text{H}_4\text{N})(\text{pyS})(\text{CO})_{13}]$ with $[\text{Ru}_3(\text{CO})_{12}]$.

A solution of $[\text{Re}_2\text{Ru}_2\text{S}(\text{C}_5\text{H}_4\text{N})(\text{pyS})(\text{CO})_{13}]$ (0.078 g, 0.067 mmol) and $[\text{Ru}_3(\text{CO})_{12}]$ (0.029 g, 0.045 mmol) in petroleum spirit (b.p. 120-160 °C) (35 cm³) were placed in a Carius tube which was then evacuated and sealed under vacuum. This was heated at 150 °C for 3 h. This treatment produced an orange suspension. After cooling to room temperature, the tube was opened

and the contents transferred to a flask. The tube was washed with dichloromethane and the washings were added to the product mixture. The solvent was removed under reduced pressure to give a deep yellow solid residue. The mixture was separated by TLC [SiO_2 , light petroleum (b.p. <40 °C)-dichloromethane (7:3 v/v)]. Several bands were collected, only one of which was obtained in sufficient quantity for characterisation. Yellow crystals of $[\text{Re}_2\text{Ru}_2(\mu_4\text{-S})(\mu\text{-H})(\mu\text{-C}_5\text{H}_4\text{N})(\text{CO})_{14}]$ (0.010 g, 15%) were obtained by layering methanol on a yellow solution of the compound in dichloromethane and allowing slow diffusion of the two layers to occur.

X-ray structure determination for $[\text{Re}_2\text{Ru}_2\text{S}(\text{C}_5\text{H}_4\text{N})(\text{pyS})(\text{CO})_{13}]$ (Isomer B).

Crystals were obtained by adding a layer of methanol to a dichloromethane solution and allowing slow diffusion to occur.

A yellow crystal of the compound $[\text{Re}_2\text{Ru}_2(\mu_4\text{-S})(\mu\text{-C}_5\text{H}_4\text{N})(\mu\text{-pyS})(\text{CO})_{13}] \cdot 0.5\text{CH}_2\text{Cl}_2$ with dimensions $0.20 \times 0.18 \times 0.10 \text{ mm}^3$ was mounted on a thin glass fibre on a Nicolet R3v/m automatic four-circle diffractometer. A monoclinic cell, $a = 10.470(2)$, $b = 18.805(3)$, $c = 17.064(5) \text{ \AA}$, $\beta = 107.07(2)^\circ$, $U = 3211(1) \text{ \AA}^3$, was determined by auto-indexing and least-squares fitting of 30 orientation reflections in the range $6 \leq 2\theta \leq 24^\circ$, selected from a rotation photograph. The cell parameters and crystal system were confirmed by taking axial photographs. A total of 5620 unique intensity data were collected at room temperature using graphite-monochromated Mo- K_α radiation ($\lambda = 0.71073 \text{ \AA}$) with the diffractometer operating in the ω - 2θ scan mode between the limits $5 \leq 2\theta \leq 50^\circ$. The reflection intensities were corrected for Lorentz and polarisation effects and for decay by fitting the data to a curve calculated from

three standard reflections collected periodically throughout the experiment. The data were finally corrected for absorption using the asimuthal scan method, $\mu(\text{Mo-K}\alpha) = 88.0 \text{ cm}^{-1}$.

The structure was solved by routine application of direct methods, in the space group $P2_1/c$, $Z = 4$, $F(000) = 2220$, $D_c = 2.40 \text{ g cm}^{-3}$. The model, with 410 parameters, was refined to $R = 0.0559$, $R_w = 0.0504$,* using 3742 intensity data with $F_o \geq 3\sigma(F_o)$ by alternating cycles of full-matrix least-squares and by difference Fourier synthesis. The largest shift-to-error ratio in the final least-squares cycle was 0.011. All non-hydrogen atoms, except those of the CH_2Cl_2 molecules, were refined anisotropically and H atoms for the 2-pyridyl ligands were included in the model in idealised positions with C–H distances fixed at 0.96 Å and isotropic thermal parameter $U = 0.08 \text{ Å}^2$ but their positions were not allowed to refine. The largest peak in the final difference Fourier map was 1.1 e/Å^3 , found close to Re(2). The CH_2Cl_2 molecule refined best with a site occupancy of 0.5 which resulted in the stoichiometry $[\text{Re}_2\text{Ru}_2(\mu_4\text{-S})(\mu\text{-C}_5\text{H}_4\text{N})(\mu\text{-pyS})(\text{CO})_{13}] \cdot 0.5\text{CH}_2\text{Cl}_2$. The C–Cl bond length in the solvent molecule was fixed at 1.772(5) Å, which is the distance in free dichloromethane. The best orientations of the 2-pyridyl rings were established by monitoring the thermal parameters of the Ru-bonded carbon and nitrogen atoms when these were interchanged.

Fractional atomic coordinates for $[\text{Re}_2\text{Ru}_2\text{S}(\text{C}_5\text{H}_4\text{N})(\text{pyS})(\text{CO})_{13}]$ are given in Table A1 found in the appendix. All calculations were performed on a MicroVax II computer running SHELXTL PLUS.¹⁴¹

$$* R = \Sigma [|F_o| - |F_c|] / \Sigma |F_o|$$

$$R_w = [\Sigma w(|F_o| - |F_c|)^2 / \Sigma w|F_o|^2]^{1/2}$$

$$w = 1/[\sigma^2(F_o) + 0.0005F_o^2]$$

X-ray structure determination for [Re₂Ru₂(S)(H)(C₅H₄N)(CO)₁₄]

Crystals were obtained by adding a layer of methanol on to a dichloromethane solution and allowing slow diffusion to occur at room temperature.

A yellow crystal of the compound [Re₂Ru₂(S)(H)(C₅H₄N)(CO)₁₄] with dimensions 0.65 x 0.15 x 0.08 mm³ was mounted on a thin glass fibre on a Nicolet R3v/m automatic four-circle diffractometer. A monoclinic cell, $a = 10.015(4)$, $b = 17.073(9)$, $c = 10.198(4)$ Å, $\beta = 94.30(2)^\circ$, $U = 2762(2)$ Å³, was determined by auto-indexing and least-squares fitting of 24 orientation reflections in the range $11 \leq 2\theta \leq 28^\circ$, selected from a rotation photograph. The cell parameters and crystal system were confirmed by taking axial photographs. A total of 4816 unique intensity data were collected at room temperature using graphite-monochromated Mo-K α radiation ($\lambda = 0.71073$ Å) with the diffractometer operating in the ω - 2θ scan mode between the limits $5 \leq 2\theta \leq 50^\circ$. The reflection intensities were corrected for Lorentz and polarisation effects and for decay by fitting the data to a curve calculated from three standard reflections collected periodically throughout the experiment. The data were finally corrected for absorption using the asimuthal scan method, $\mu(\text{Mo-K}\alpha) = 100.5 \text{ cm}^{-1}$.

The structure was solved by routine application of direct methods, in the space group $P2_1/c$, $Z = 4$, $F(000) = 1968$, $D_c = 2.59 \text{ g cm}^{-3}$. The model, with 353 parameters, was refined to $R = 0.0516$, $R_w = 0.0490$,* using 3710 intensity

data with $F_0 \geq 3\sigma(F_0)$ by alternating cycles of full-matrix least-squares and by difference Fourier synthesis. The largest shift-to-error ratio in the final least-squares cycle was 0.008. All non-hydrogen atoms were refined anisotropically and H atoms for the 2-pyridyl ligands were included in the model in idealised positions with C–H distances fixed at 0.96 Å and isotropic thermal parameter $U = 0.08 \text{ \AA}^2$ but their positions were not allowed to refine. The largest peak in the final difference Fourier map was 1.9 e/\AA^3 , found close to Re(2). The populations of the different orientations of the 2-pyridyl ring were established by allowing the ring atoms bonded to ruthenium to have partial populations of N and C atoms. The dominant orientation is that shown in Figure 2.6 (population 0.6 ± 0.1) while the alternative orientation has atoms C(1a) and N(1a) replacing N(1) and C(1) (population 0.4 ± 0.1). Refinements with the 2-pyridyl ligands fixed in one or the other orientation were poorer, although because of the similar relative populations, the thermal parameters of the C and N atoms were realistic and approximately equal in both orientations. The hydride position was not determined from diffraction data nor calculated.

Fractional atomic coordinates for $[\text{Re}_2\text{Ru}_2(\text{S})(\text{H})(\text{C}_5\text{H}_4\text{N})(\text{CO})_{14}]$ are given in Table A2 found in the appendix. All calculations were performed on a MicroVax II computer running SHELXTL PLUS.¹⁴¹

$$R = \frac{\sum [|F_o| - |F_c|]}{\sum |F_o|}$$

$$R_w = [\frac{\sum w(|F_o| - |F_c|)^2}{\sum w|F_o|^2}]^{1/2}$$

$$w = 1/[\sigma^2(F_o) + 0.0005F_o^2]$$

CHAPTER THREE

Higher Nuclearity Ruthenium Carbonyl Complexes Derived From $[\text{Ru}(\text{pyS})_2(\text{CO})_2]$ and $[\text{Ru}_3(\text{CO})_{12}]$

3.1 Introduction

Polynuclear ruthenium carbonyl clusters have been known for some time.¹⁴² In many cases a non-metallic element is involved in the cluster expansion process and often stabilises unusual cluster geometries with carbon, sulphur and phosphorus atoms and donor ligands most typically employed. The hexanuclear carbido complexes $[\text{Ru}_6\text{C}(\text{CO})_{17}]$ and $[\text{Ru}_6\text{C}(\text{CO})_{14}(\text{arene})]$ ¹³⁵ were some of the earliest of such compounds isolated, together with the tetranuclear hydrido carbonyl complexes $[\text{Ru}_4\text{H}_4(\text{CO})_{12}]$ and $[\text{Ru}_4\text{H}_2(\text{CO})_{13}]$ ¹⁴² of which the osmium analogues are also known.¹⁴³ A series of hexanuclear hydrido carbonyl species are also known for these two metals.¹⁴⁴ These compounds are part of a much larger class of transition metal hydridocarbonyl or carbidocarbonyl clusters,¹⁴⁵ which are isolated as either neutral or anionic species. One of the most often used synthetic methods for the formation of high nuclearity metal carbonyl clusters involves thermolysis of lower nuclearity species to induce ligand loss and framework reorganisation.¹⁴⁶⁻⁸ Although generally unpredictable as to the nuclearity and composition of the final product, many important compounds have been made by this procedure and often in high yields.¹⁴⁹ No neutral binary carbonyl clusters containing more than three ruthenium atoms are known although a considerable number of high nuclearity ruthenium carbonyl clusters containing other ligands have been isolated and bridging ligands appear to play an important role in their formation.¹⁸⁴ The occurrence of stable neutral binary carbonyls is restricted to the central area of the d-block, where there are low-lying vacant metal orbitals to accept σ -donated lone-pairs and also filled d-orbitals for π back-donation.

Outside this area carbonyl compounds are either very unstable (e.g. Ag^{151}), or anionic, or require additional ligands besides CO for stabilisation. In addition, nuclearity tends to increase down the triad due to stronger metal-metal bonding, which is evident in the isolation of high nuclearity binary carbonyl clusters of osmium such as $[\text{Os}_6(\text{CO})_{18}]$, $[\text{Os}_7(\text{CO})_{21}]$ and $[\text{Os}_8(\text{CO})_{23}]$.¹⁴⁷

More recently, the structure of the $[\text{Ru}_{10}\text{C}_2(\text{CO})_{24}]^{2-}$ dianion has been elucidated,¹⁵² which was the first reported cluster containing more than six ruthenium atoms. The structure of this decanuclear complex consists of two octahedral polyhedra fused at a common equatorial edge. The monocarbido osmium analogue is known,¹⁵³ although its structure is very different, a carbido-centred Os_6 octahedron capped on four faces by $\text{Os}(\text{CO})_3$ groups. These polynuclear carbido species can also be made to react further. For instance, the cluster $[\text{Ru}_6\text{C}(\text{CO})_{16}(\text{AuPR}_3)_2]$ can be synthesised¹⁵⁴ from $[\text{Ru}_6\text{C}(\text{CO})_{16}]^{2-}$. A considerable number of rhodium complexes of a similar nature have also been reported with nuclearities as high as seventeen,¹⁵⁵ and with a variety of encapsulated heteroatoms.¹⁵⁶ These studies of high nuclearity carbonyl cluster compounds have shown that the metal atoms possess a marked tendency to assume arrangements which are fragments of metallic lattices.¹⁵⁷ Different, less compact geometries are usually related to the presence of interstitial main-group elements which require large interstitial holes as, for instance, in the trianion $[\text{Rh}_{17}\text{S}_2(\text{CO})_{32}]$.¹⁵⁸ There are many further examples of very large heteronuclear metal carbonyl clusters with novel geometries¹⁵⁹⁻¹⁶⁵ too numerous to mention here, emphasising the diversity of chemistry in this area.

There has been much interest in the synthesis of ruthenium carbonyl

clusters involving phosphorus-donor ligands,¹⁶⁶ often bridging and/or capping monodentate ligands such as diphenylphosphido (PPh_2) or phenylphosphinidene (PPh), the function of these ligands being to stabilise the metal clusters towards fragmentation during the course of the chemical reaction.¹⁶⁷ Clusters with four Ru metal centres, most often adopt a butterfly-type structure typified by $[\text{Ru}_4(\text{CO})_{13}(\mu_3\text{-PPh})]^{168}$ or an approximately square-planar configuration of metal atoms as in $[\text{Ru}_4(\text{CO})_{13}(\mu\text{-PPh}_2)(\mu\text{-}\eta^2\text{-C}_2\text{CMe}_3)]^{169}$. Clusters with five and six ruthenium centres have also been extensively studied^{167,170-3} and often contain triply- or quadruply-bridging phenylphosphinidene ligands such as the square-pyramidal complex $[\text{Ru}_5(\text{CO})_{14}(\mu_4\text{-PPh})]^{173}$. Much less common are clusters with higher nuclearities, although the heptaruthenium cluster $[\text{Ru}_7(\text{CO})_{18}(\mu_4\text{-PPh})_2]^{174}$ has recently been reported which consists of two fused square-pyramidal polyhedra. Although other homoheptanuclear clusters are known,¹⁷⁴ they are still relatively rare, particularly in comparison with penta-, hexa- and octanuclear species. Octaruthenium clusters containing P-donor ligands are known,¹⁷⁵⁻⁶ such as $[\text{Ru}_8(\text{CO})_{21}(\mu_6\text{-P})(\mu_4\text{-PPh})(\mu\text{-PPh}_2)]$, the framework of which consists of a square pyramid of ruthenium atoms fused to an open network of six ruthenium atoms. These types of compound are often prepared by direct reaction of $[\text{Ru}_3(\text{CO})_{12}]$ with the phosphine (for example PPh_2H or PPhH_2), or by thermolysis of species such as $[\text{Ru}_3\text{H}(\text{CO})_{10}(\mu\text{-PPh}_2)]$, the result usually being a complex mixture of products, emphasising the reactivity of $[\text{Ru}_3(\text{CO})_{12}]$ and the ease of formation of this group of compounds.

There is a much smaller body of work concerning ruthenium clusters of nuclearity higher than three with sulphur-donor ligands, although the

tetranuclear species, $[\text{Ru}_4(\text{CO})_{13}(\mu\text{-SMe}_2)]$, and the hydride-substituted form $[\text{Ru}_4\text{H}_2(\text{CO})_{12}(\mu\text{-SMe}_2)]$, which both adopt a butterfly structure, have recently been reported.¹⁷⁷ Treatment of $[\text{Ru}_6\text{C}(\text{CO})_{17}]$ with HSEt results in opening of the cluster to give two hexanuclear products, $[\text{Ru}_6\text{H}_2(\text{CO})_{15}(\text{SEt})_2]$ and $[\text{Ru}_6\text{H}(\text{C})(\text{CO})_{15}(\text{SEt})_3]$.¹⁷⁸ The reaction of $[\text{Ru}_3(\text{CO})_{12}]$ with thioureas has been found to give a large variety of ruthenium clusters containing S-donor ligands such as $[\text{Ru}_6\text{H}(\mu_5\text{-S})(\mu_3\text{-SC}(\text{NHPH})\text{NPh})(\text{CO})_{16}]$.¹⁷⁹ Polynuclear coordination of sulphur-containing molecules to organometallic compounds has recently been investigated in relation to corrosion inhibition¹⁸⁰ and the desulphurisation of organic molecules,^{150,181} the latter reaction being of particular interest in the purification of fossil fuels.¹⁰⁹ There is, however, a relatively large number of compounds containing the sulphido ligand. Due to its ability to serve as a multi-coordinate, multi-electron donor, the bridging sulphido ligand has been of great value in the synthesis of transition metal cluster compounds.⁹⁶ Although there has been an extensive chemistry developed for high nuclearity sulphido-osmium carbonyl cluster compounds,¹¹⁰ it is only recently that comparable ruthenium species have been identified. The development of this chemistry has been facilitated by the discovery of high yield syntheses for the compounds $[\text{Ru}_3(\text{CO})_9(\mu_3\text{-CO})(\mu_3\text{-S})]$ and $[\text{Ru}_3(\text{CO})_9(\mu_3\text{-S})_2]$ ¹⁸² which have been found to be useful precursors for the preparation of higher nuclearity sulphido-ruthenium carbonyl clusters,¹⁸²⁻⁵ in addition to some mixed tungsten-ruthenium complexes.¹⁸⁶ Clusters containing up to eight ruthenium atoms have been synthesised in this way and usually contain quadruply-bridging sulphido ligands, for example $[\text{Ru}_8(\text{CO})_{17}(\eta\text{-toluene})(\mu_4\text{-S})_2]$,¹⁸³ the structure of which consists of two fused square pyramids in which the square bases are

bridged by the sulphido ligands. A series of pentanuclear sulphido carbonyl clusters, $[\text{Ru}_5(\text{CO})_{14}(\mu_4\text{-S})]^{2-}$, $[\text{Ru}_5(\mu\text{-H})(\text{CO})_{14}(\mu_4\text{-S})]^-$ and $[\text{Ru}_5(\mu\text{-H})_2(\text{CO})_{14}(\mu_4\text{-S})]$ has been prepared by the reaction of $[\text{Ru}_3(\text{CO})_{12}]$ with $\text{SC}(\text{NMe}_2)_2$ under pressure.¹⁸⁷ When an excess of $\text{SC}(\text{NMe}_2)_2$ is used under similar conditions, an anionic hexa-ruthenium complex, $[\text{Ru}_6\text{H}(\mu_3\text{-S})_3(\text{CO})_{15}]^-$, is produced, which adopts a 'raft' structure with three capping sulphido ligands.¹⁷⁹

Other interesting high nuclearity ruthenium clusters include the raft^{161,188} complex $[\text{Ru}_6\text{H}_2(\text{CO})_{16}(\text{C}_6\text{H}_4\text{O})]^{189}$ and the anionic cluster $[\text{Ru}_6\text{H}(\text{CO})_{18}(\text{O}=\text{CNMe}_2)]^-$ which contains a cyclical array of ruthenium atoms.¹⁹⁰

The chemistry of triruthenium clusters with N-donor ligands is well-documented.¹⁹¹ The retention of the trimeric unit is due in some part to the milder reaction conditions employed using activated triruthenium precursors such as $[\text{Ru}_3(\text{CO})_{12-n}(\text{MeCN})_n]$ ($n = 1-2$).^{97,192-3} Recently, however, there has been an increase in the number of higher nuclearity ruthenium clusters reported with N-donor ligands. Tetra-ruthenium species that adopt a butterfly structure for example, include $[\text{Ru}_4(\mu_4\text{-N}_2\text{Et}_2)(\text{CO})_{12}]^{194}$ and $[\text{Ru}_4(\mu\text{-H})(\text{CO})_{12}(\mu_4\text{-}\eta^2\text{-CNMe}_2)]^{195}$ which reacts further with $[\text{Ru}(\text{CO})_5]$ to form penta- and heptanuclear complexes.¹⁹⁶ There are also several imido,^{149,197} nitrido^{191,198} and nitrosyl^{191,199} clusters known with nuclearities of four, five, six and seven including several hexanuclear clusters derived from $[\text{Ru}_6\text{C}(\text{CO})_{17}]^{200-1}$ and one in which two trimeric units are joined by a quadruply-bridging mercury atom.²⁰² Polynuclear complexes with N-containing heterocycles include the complex $[\text{Ru}_5\text{H}(\text{C})(\text{CO})_{14}(\mu\text{-C}_5\text{H}_4\text{N})]^{95}$ its osmium analogue,¹⁵³ and $[\text{Ru}_5(\mu_4\text{-S})_2(\mu\text{-C}_5\text{H}_4\text{N})_2(\text{CO})_{11}]^{66}$ which all adopt a pentagonal bipyramidal or 'bridged butterfly' metal framework, the former with an interstitial carbon atom.

The mononuclear compound $[\text{Ru}(\text{pyS})_2(\text{CO})_2]$ which can be synthesised in high yields from either $[\text{Ru}_3(\text{CO})_{12}]$ or $[\text{RuCl}_3 \cdot 3\text{H}_2\text{O}]$,⁶⁵ is a *cis*-dicarbonyl octahedral ruthenium(II) species with equivalent chelating pyS ligands, analogous to the osmium complex for which the structure is known.⁵⁶ Each of the sulphur atoms in the complex has four non-bonding electrons capable of further coordination giving scope for reaction with binary metal carbonyl complexes to generate larger molecules with pyS bridges. The complex can be used as a source of pyS in which the ligand is already bound to a metal centre, giving an alternative to direct reaction with the free ligand pySH and hence a diversity of product. In addition, the use of this compound, in controlled stoichiometric amounts, as a source of ruthenium atoms gives a degree of control over the nuclearity and nature of products formed in reaction with existing clusters, which is not possible with, for example, $[\text{Ru}_3(\text{CO})_{12}]$. This is evident in the formation of the compound $[\text{Ru}_6(\mu_4\text{-S})_2(\mu\text{-C}_5\text{H}_4\text{N})_2(\text{CO})_{18}]$ which is discussed in this Chapter. This hexanuclear compound was first isolated in trace amounts from the reaction between $[\text{Ru}_3(\text{CO})_{12}]$ and $[\text{Re}_2(\text{pyS})_2(\text{CO})_6]$, the majority of products being mixed tetranuclear ruthenium-rhenium species as described in Chapter Two. We believed that by controlling the stoichiometry of the reaction between $[\text{Ru}_3(\text{CO})_{12}]$ and $[\text{Ru}(\text{pyS})_2(\text{CO})_2]$ we could synthesise $[\text{Ru}_6(\mu_4\text{-S})_2(\mu\text{-C}_5\text{H}_4\text{N})_2(\text{CO})_{18}]$ by a more direct route. Using a molar ratio of 5 : 3 of the above reactants gave the desired hexaruthenium product. Also formed was a tetranuclear species, $[\text{Ru}_4(\mu_4\text{-S})(\mu\text{-C}_5\text{H}_4\text{N})_2(\text{CO})_{12}]$. Each complex contains μ_4 -sulphido and μ -2-pyridyl ligands formed by cleavage of a C-S bond of a pyS ligand. In these ruthenium cluster compounds there is the possibility of isomerism arising from the orientation

of the 2-pyridyl ligands with respect to the metal framework and this is indeed observed for both the tetra- and hexaruthenium species. These compounds are the subject of this chapter.

3.2 Results and Discussion.

3.2.1 Syntheses.

The monomeric compound $[\text{Ru}(\text{pyS})_2(\text{CO})_2]$ and $[\text{Ru}_3(\text{CO})_{12}]$ were heated in petroleum spirit (b.p. 120-160 °C) at 150 °C for 18 hours in an evacuated sealed tube. The resulting mixture was separated by successive TLC treatment into two major components: yellow crystals of $[\text{Ru}_6(\mu_4\text{-S})_2(\mu\text{-C}_5\text{H}_4\text{N})_2(\text{CO})_{18}]$ **1** in 38% yield, and yellow crystals of $[\text{Ru}_4(\mu_4\text{-S})(\mu\text{-C}_5\text{H}_4\text{N})_2(\text{CO})_{12}]$ **2** in 23% yield. These samples were characterised by elemental analysis, infrared, mass, ^1H and ^{13}C NMR spectroscopy and in the case of compound **1** by X-ray diffraction.

3.2.2 Characterisation.

Generally ^1H NMR spectra of this ligand system are easily analysed since four well-separated multiplets are usually observed for each $\text{C}_5\text{H}_4\text{N}$ ligand, the most easily assigned feature being the H^6 signal at highest δ value. This resonance normally appears as a fairly narrow doublet [$J(\text{H}^5\text{H}^6) = \text{ca. } 5.5 \text{ Hz}$] with further small couplings to the H^4 and H^3 protons and its chemical shift is most sensitive to the environment of the ligand. It is possible

to distinguish between the H⁴ and H⁵ protons by analysis of the coupling constants associated with these signals. The two three-bond coupling constants of the H⁴ resonance are usually very similar (*ca.* 7.5 Hz), while the values for the H⁵ resonance differ by about 2 Hz (*ca.* 7.5 and 5.5 Hz). In addition, the H⁵ signal is invariably observed at lower chemical shift than the H⁴ signal.

The ¹H NMR spectrum (Table 3.4) of compound 1 [Ru₆(μ₄-S)₂(μ-C₅H₄N)₂(CO)₁₈] showed a complicated set of overlapping multiplets for protons H³, H⁴ and H⁵. However the signals for the H⁶ protons were well resolved and indicated a mixture of three isomers in an approximate ratio of 8:3:2. Careful thin layer chromatography, collecting the upper and lower extremes of the yellow band separately gave no evidence for even a partial separation. HPLC was also applied but no separation was observed. Complexity in the carbonyl-stretching region of the infrared spectrum (data in Table 3.3) is indicative of a metal cluster compound. The parent molecular ion (*m/e* = 1333) corresponding to [Ru₆(μ₄-S)₂(μ-C₅H₄N)₂(CO)₁₈]⁺ was observed in the mass spectrum and analytical data were also consistent with this formulation.

A single-crystal X-ray structure of compound 1 was determined for a crystal selected from those grown by slow evaporation of a layered dichloromethane-methanol solution. The molecular structure is shown in Figures 3.1 and 3.2, and selected bond lengths and angles are in Table 3.1.

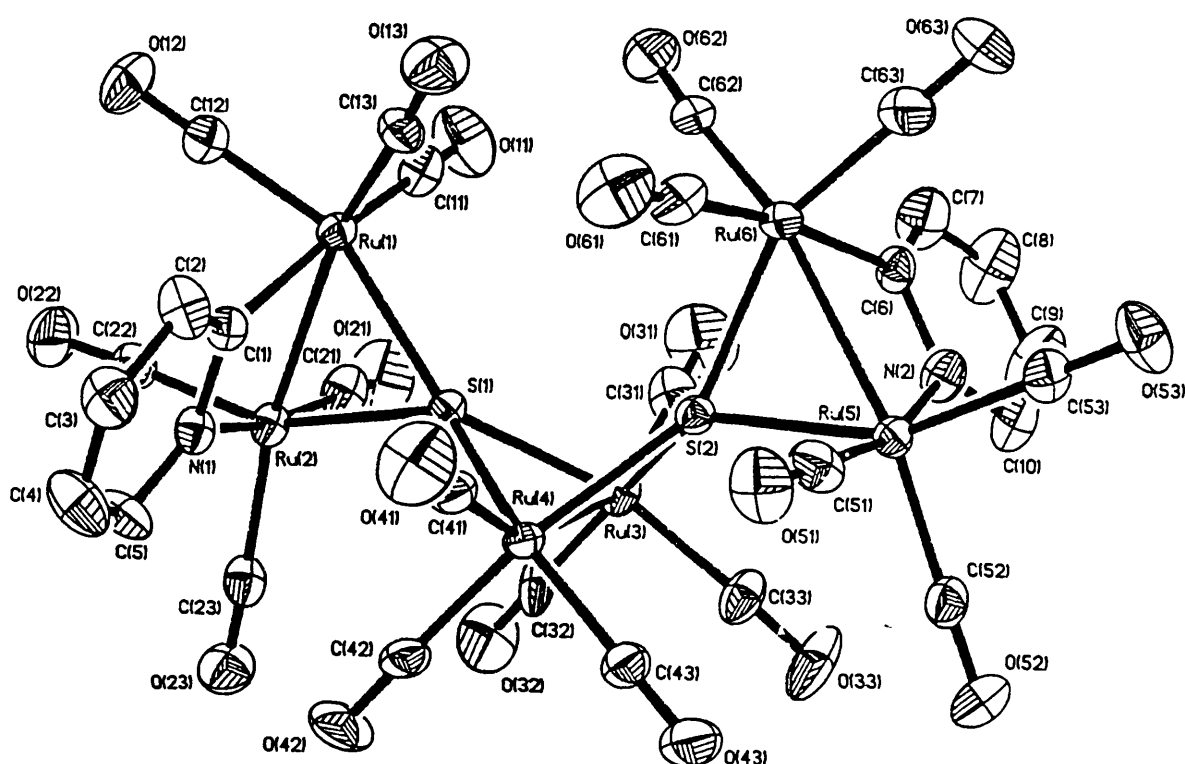


Figure 3.1 Molecular structure of $[\text{Ru}_6(\mu_4\text{-S})_2(\mu\text{-C}_5\text{H}_4\text{N})_2(\text{CO})_{18}]$ **1** showing the predominant orientations of the 2-pyridyl ligands (0.7 ± 0.1). Replacing N(1), C(1), N(2) and C(6) by C(1a), N(1a), C(6a) and N(2a) respectively generates the minor orientational isomer (0.3 ± 0.1).

Figure 3.2 Alternative views of $[\text{Ru}_6(\mu_4\text{-S})_2(\mu\text{-C}_5\text{H}_4\text{N})_2(\text{CO})_{18}]$ 1 with the carbonyl ligands omitted.

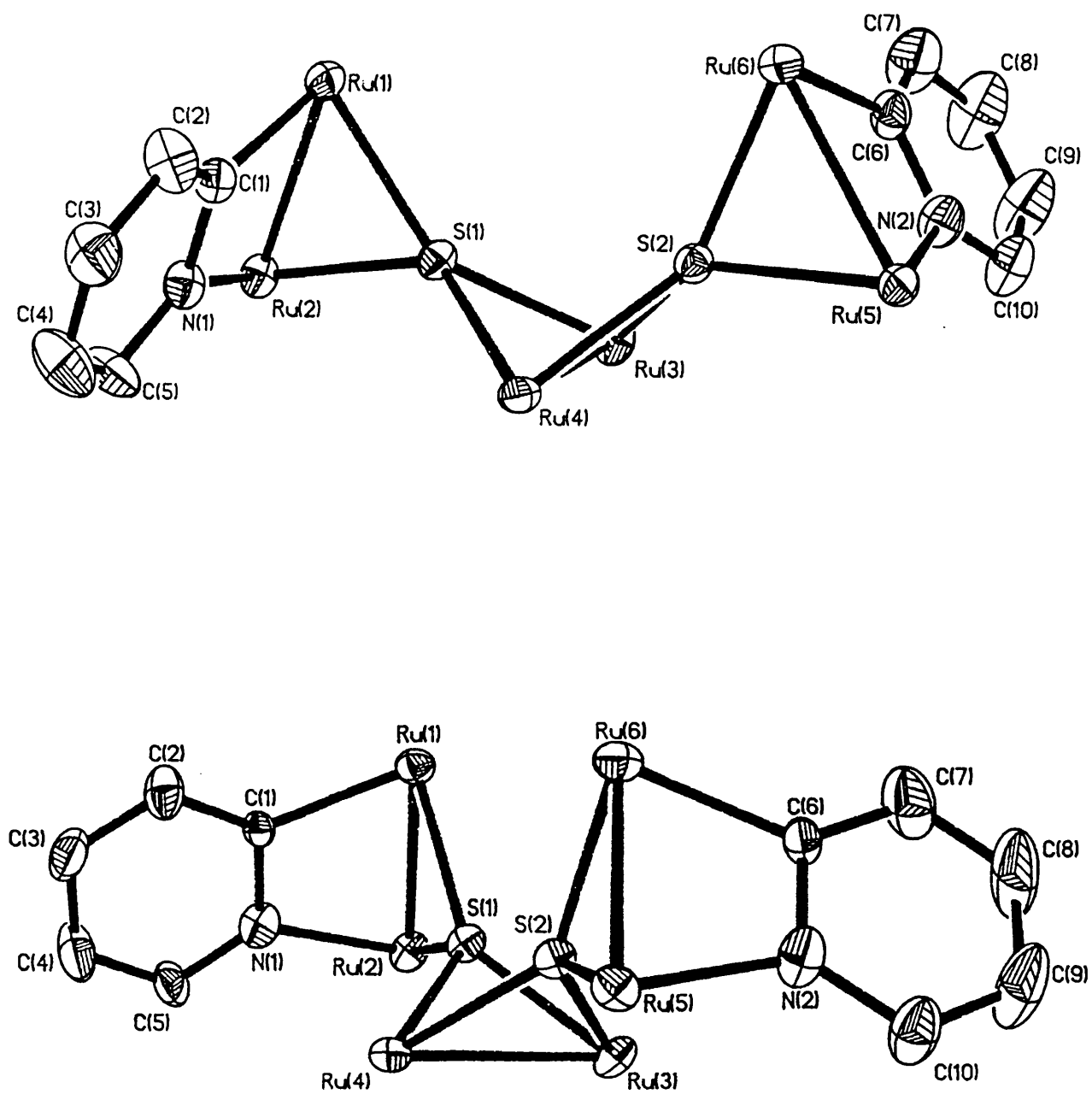


Figure 3.3 Isomers of $[\text{Ru}_6(\mu_4\text{-S})_2(\mu\text{-C}_5\text{H}_4\text{N})_2(\text{CO})_{18}]$ **1** showing all possible orientations of the 2-pyridyl ligands (CO ligands are omitted).

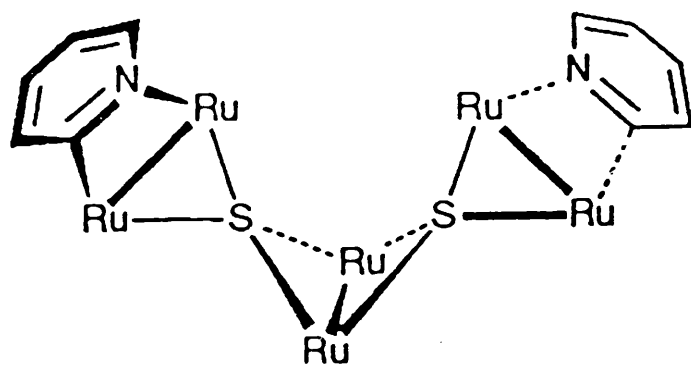
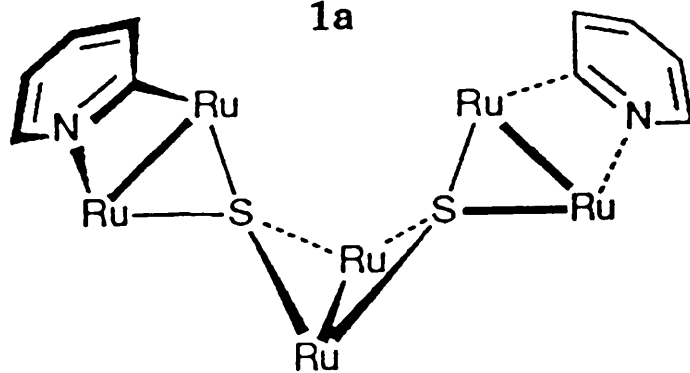
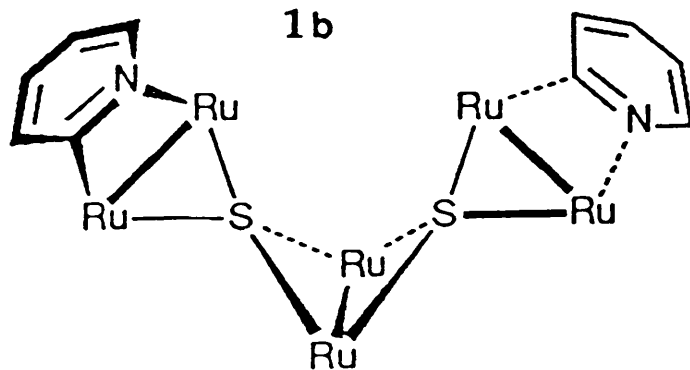
**1a****1b****1c**

Table 3.1 Selected bond lengths (Å) and angles (°) for
 $[\text{Ru}_6(\mu_4\text{-S})_2(\mu\text{-C}_5\text{H}_4\text{N})_2(\text{CO})_{18}]$ 1.

Ru(2)-Ru(1)	2.722(1)	Ru(4)-Ru(3)	2.714(1)
Ru(5)-Ru(6)	2.713(2)	Ru(2)-S(1)	2.398(3)
Ru(1)-S(1)	2.409(3)	Ru(3)-S(1)	2.407(3)
Ru(4)-S(1)	2.403(3)	Ru(4)-S(2)	2.406(3)
Ru(3)-S(2)	2.382(3)	Ru(5)-S(2)	2.387(3)
Ru(6)-S(2)	2.390(3)	Ru(2)-N(1)	2.09(1)
Ru(1)-C(1)	2.097(9)	Ru(5)-N(2)	2.09(1)
Ru(6)-C(6)	2.12(1)		
Ru(1)-S(1)-Ru(2)	69.0(1)	Ru(3)-S(1)-Ru(4)	68.7(1)
Ru(3)-S(2)-Ru(4)	69.1(1)	Ru(5)-S(2)-Ru(6)	69.2(3)
Ru(1)-S(1)-Ru(3)	146.0(1)	Ru(1)-S(1)-Ru(4)	130.2(1)
Ru(2)-S(1)-Ru(3)	126.8(1)	Ru(2)-S(1)-Ru(4)	126.8(1)
Ru(3)-S(2)-Ru(5)	131.1(1)	Ru(3)-S(2)-Ru(6)	132.79(1)
Ru(4)-S(2)-Ru(5)	124.0(1)	Ru(4)-S(2)-Ru(6)	142.4(1)
Ru(1)-Ru(2)-S(1)	55.7(1)	Ru(2)-Ru(1)-S(1)	55.3(1)
Ru(3)-Ru(4)-S(1)	55.7(1)	Ru(4)-Ru(3)-S(1)	55.6(1)
Ru(3)-Ru(4)-S(2)	55.1(1)	Ru(4)-Ru(3)-S(2)	55.9(1)
Ru(5)-Ru(6)-S(2)	55.3(1)	Ru(6)-Ru(5)-S(2)	55.5(1)
Ru(1)-Ru(2)-N(1)	71.2(2)	Ru(2)-Ru(1)-C(1)	71.3(3)
Ru(1)-C(1)-N(1)	108.4(7)	Ru(2)-N(1)-C(1)	109.0(7)
Ru(6)-Ru(5)-N(2)	71.0(3)	Ru(5)-Ru(6)-C(6)	71.2(3)
Ru(6)-C(6)-N(2)	107.5(7)	Ru(5)-N(2)-C(6)	110.2(7)

Compound 1 is electron-precise with three Ru–Ru bonds. The two μ_4 -S atoms are approximately tetrahedral and act as six-electron donors linking the three metal-metal bonded Ru_2 units. The metal-metal bond length in the central Ru_2 unit, which is bridged by the two tetrahedral sulphido ligands, is 2.714(1) Å and is only slightly shorter than the sulphido-bridged Ru–Ru bond distances of 2.749(1)–2.787(1) Å in, for example, $[\text{Ru}_5(\mu_4\text{-S})(\text{CO})_{15}]$,¹⁸⁵ although in this compound the μ_4 -S ligands are pyramidal and the Ru–Ru bonds are also bridged by a CO ligand, which probably contributes to the slight lengthening. The metal-metal distances in the 2-pyridyl-bridged Ru_2 units are 2.713(2) and 2.722(1) Å which are similar to that of 2.715(2) Å found in the dinuclear complex $[\text{Ru}_2(\mu\text{-C}_5\text{H}_4\text{N})(\mu\text{-C}_{10}\text{H}_7\text{N}_2)(\text{CO})_5]$.²⁰³ However, these lengths are significantly shorter than those of the pyridyl-bridged Ru–Ru bonds (2.838(1)–2.920(1) Å) found in the compound $[\text{Ru}_5(\mu_4\text{-S})_2(\mu\text{-C}_5\text{H}_4\text{N})_2(\text{CO})_{11}]$ 3.⁶⁶ This difference probably arises because the pyridyl-bridged Ru–Ru bonds in compound 3 are also bridged by two pyramidal sulphido ligands or further Ru atoms which want to attain configurations as close as possible to octahedral geometry within the pentagonal bipyramidal structure, leading to a relative increase in Ru–Ru bond lengths. In other words, the Ru–Ru distance is not primarily controlled by the presence of a 2-pyridyl bridge but also results from the total coordination of the Ru atoms which are considerably different. It is interesting to note that the 2-pyridyl ligand in $[\text{Ru}_5\text{H}(\text{C})(\mu\text{-C}_5\text{H}_4\text{N})(\text{CO})_{14}]$ ⁹⁵ spans a distance of 3.59 Å across a non-bonded edge, indicating the considerable range of metal-metal distances over which this ligand can bridge. The eight Ru–S bond distances in compound 1 are not significantly different and span the small range 2.382(3) Å to 2.409(3) Å. These distances are similar

to the Ru–S distances (2.348–2.584 Å) observed for quadruply-bridging pyramidal sulphido ligands in a variety of polynuclear ruthenium cluster complexes.^{66,182-5} The Ru–S–Ru bond angles are acute, 68.7(1)–69.2(3)°, where the metal atoms are bonded, and are fairly large, 124.0(1)–146.0(1)°, when they are not. Because the tricarbonyl units are facial, the Ru₂CN and Ru₂S rings are close to orthogonal and the Ru₂SRu₂SRu₂ chain is therefore twisted. The local environment of each sulphido ligand deviates slightly from *D*_{2d} symmetry since the dihedral angles between the planes Ru(1)–Ru(2)–S(1) and Ru(3)–Ru(4)–S(1) and the planes Ru(3)–Ru(4)–S(2) and Ru(5)–Ru(6)–S(2) are 82.7° and 80.7°, respectively.

An obvious source of disorder in the structure is the orientations of the 2-pyridyl ligands. Figure 3.3 shows three possible isomers based on this crystal structure and differing only in C₅H₄N orientations. Isomer 1a has both nitrogen atoms (N1, N2) in the 'up' position, in isomer 1b both nitrogen atoms are in the 'down' position and in 1c one nitrogen atom is 'up' and the other 'down'. Isomers 1a and 1b are of C₂ symmetry and have equivalent ligands related by the two-fold axis whereas 1c is of C₁ symmetry with non-equivalent ligands. Experimentally, a knowledge of the orientation of the C₅H₄N ligands in the crystal depends upon the relative positioning of the C and N atoms bonded to ruthenium. The best refinement of the structure was when orientational disorder of the 2-pyridyl ligands was included in the model. Allowing the relative populations of C and N atoms to refine gave a best solution with a fractional population of 0.7(1) for N(1) and C(1) in the positions illustrated in Figure 3.1, together with a 0.3(1) population of the reverse orientation of these atoms, labelled as N(1a) and C(1a) when reversed.

There is a closely similar situation for the other pyridyl ring, for which the best refinement gave atoms N(2) and C(2) with a fractional population of 0.7(1) and the reversely orientated atoms N(2a) and C(2a) having a population of 0.3(1). Overall then, there is an approximately 70% preference for the N atoms to be in the positions occupied by N(1) and N(2) in Figure 3.1. This observed crystallographic disorder could be rationalised as resulting from an unequal distribution of all three isomers **1a-1c** (Figure 3.3) throughout the crystal lattice. A completely statistical distribution of 2-pyridyl orientations would, of course, lead to an isomer ratio of 1:1:2 for the isomers **1a:1b:1c** and fractional populations of 0.5 for both C and N atoms in each of the metal-bound sites. However, the determined populations of the disordered 2-pyridyl ligands in the crystal indicates isomer **1b** is favoured over **1a** and **1c**, the relative ratios being 1:5:4 for **1a:1b:1c**. It is these isomers that account for the observed ^1H NMR spectrum. The H^6 protons in each of isomers **1a** and **1b** are identical, but there exist two different environments for this proton in **1c**, giving a total of four H^6 environments, two of which correspond to 'up' pyridyl orientations and two to 'down' orientations. However, in the ^1H NMR spectrum of **1** only three H^6 signals are observed and these have a ratio of 8:3:2. Since the diffraction structure showed that the 'down' position of the pyridyl nitrogen atoms was the most populated, we have assigned the most intense signal at $\delta = 7.85$ to an accidental coincidence of the two H^6 signals of the 'down' pyridyl ligands of **1b** and **1c**. The resonances at $\delta = 7.77$ and 7.75 correspond to the two H^6 protons of the 'up' pyridyl ligands of **1a** and **1c**. Furthermore, since the fractional population of 'down' and 'up' nitrogen atoms in the crystal was found to be 0.7(1) and 0.3(1) respectively, then we can calculate that the

four different H⁶ environments would have a population ratio of 5:2:2:1. Taking into account the accidental coincidence then this ratio becomes 7:2:1 which is reasonably close to the 8:3:2 ratio observed in the ¹H NMR spectrum, implying that the isomeric distribution in the bulk sample is similar to that in the crystal.

There is another potential source of isomerism in which both pyridyl ligands are orientated on the same side of the molecule in an eclipsed arrangement, which would lead to isomers corresponding to those shown in Figure 3.3 but with both 2-pyridyl rings coming forward. It is likely that these isomers would be chromatographically separable from the other isomers because of the structural differences, but since no such separation was observed we can assume that they are not formed. It appears then that the favoured conformation is such that the 2-pyridyl ligands are orientated on opposite sides of the molecule to each other.

Isomers resulting from the orientation of 2-pyridyl ligands have been seen previously. Head-to-head and head-to-tail isomers of the 2-pyridyl complex $[\text{Os}_2(\mu\text{-C}_5\text{H}_4\text{N})_2(\text{CO})_6]$ have been separated¹⁰⁰ and the X-ray structures of the 4-methylpyridine analogues will be described in Chapter Four. More recently, isomeric forms of the cluster $[\text{Ru}_5\text{H}(\text{C})(\text{C}_5\text{H}_4\text{N})(\text{CO})_{14}]$ containing different orientations of this ligand have been separated and structurally characterised.⁹⁵ Enantiomers of $[\text{Os}_3\text{H}(\mu\text{-C}_5\text{H}_4\text{N})(\text{CO})_{10}]$ differ only in the 2-pyridyl orientation and these have been resolved.²⁰⁴ There is apparently a very large barrier to the reorientation of μ -2-pyridyl bridges in all observed cases.

A structure directly analogous to that of compound 1 is observed for the compound $[\text{Os}_6(\mu_4\text{-S})_2(\mu\text{-HC=NPh})_2(\text{CO})_{18}]$.⁹⁶ Again there are six metal atoms

arranged into three metal-metal bonded dinuclear units which are linked by tetrahedral μ_4 -S atoms as in compound 1, although the presence of orientational isomers was not reported. Tetrahedral geometry of bridging sulphido ligands has been seen in a number of other osmium and iron systems.^{96,205-7}

It should be noted that the colour of compound 1 is yellow while the colours of related polynuclear sulphido ruthenium complexes tend to deepen with increasing nuclearity (Table 3.2).

Compound	Colour	No. of M-M bonds	Ref.
$[\text{Ru}_3(\mu_4\text{-S})(\text{CO})_{10}]$	Yellow	3	182
$[\text{Ru}_4(\mu_4\text{-S})_2(\text{CO})_{11}]$	Orange	4	182
$[\text{Ru}_5(\mu_4\text{-S})_2(\text{CO})_{14}]$	Green	6	184
$[\text{Ru}_5(\mu_4\text{-S})(\text{CO})_{15}]$	Light Brown	8	185
$[\text{Ru}_6(\mu_4\text{-S})_2(\text{CO})_{17}]$	Brown	9	184
$[\text{Ru}_6(\mu_4\text{-S})(\text{CO})_{18}]$	Dark Brown	10	185
$[\text{Ru}_7(\mu_4\text{-S})_2(\text{CO})_{20}]$	Dark Brown	11	184
$[\text{Ru}_7(\mu_4\text{-S})(\text{CO})_{21}]$	Violet solution (Black crystals)	12	185
$[\text{Ru}_8(\mu_4\text{-S})_2(\eta\text{-tol})(\text{CO})_{17}]$	Dark Brown	14	183

Table 3.2 Colours of some polynuclear sulphido ruthenium carbonyl clusters.

However, the important factor is the way in which the metal atoms are connected and the number of metal-metal bonds in the cluster. As this increases and the metal cluster expands, the energy gap between the HOMO and LUMO decreases and the d-d electronic transitions are shifted to longer wavelengths. Hence, the observed colour deepens as longer wavelengths are being absorbed from the incident white light. So, even though $[\text{Ru}_6(\mu_4\text{-S})_2(\mu\text{-$

$\text{C}_5\text{H}_4\text{N})_2(\text{CO})_{18}]$ contains six metal atoms, because it has only three unconnected metal-metal bonds, the compound is yellow. This a general feature of cluster compounds and occurs, for example, in the analogous osmium systems¹¹⁰ and the phosphido complexes discussed in Section 3.1. A nice example of this behaviour is provided by the two isomeric forms of $[\text{Os}_6(\mu\text{-H})_2(\mu_4\text{-S})(\mu_3\text{-S})(\text{CO})_{17}]$.²⁰⁸ The red isomer contains six Os–Os bonds, while the green isomer contains eight.

The structure that we assigned to $[\text{Ru}_4(\mu_4\text{-S})(\mu\text{-C}_5\text{H}_4\text{N})_2(\text{CO})_{12}]$ **2** was based on spectroscopic results and analogy with the structure of compound **1**. Compound **2** also exhibits isomerism arising from the orientation of the 2-pyridyl ligands with respect to each other but, again, attempts to resolve these isomers by TLC and HPLC were unsuccessful. Three isomers of the complex can be envisaged, **2a-c** (Figure 3.4), all of which are chiral. Isomer **2a** has C_1 symmetry but isomers **2b** and **2c** possess C_2 axes of symmetry relating the two $\text{C}_5\text{H}_4\text{N}$ ligands.

Analysis of the H^6 proton signals in the ^1H NMR spectrum (Figure 3.5 and Tables 3.4 and 3.5) indicates that all three isomers are present. The unsymmetrical isomer **2a** contains two different environments for the H^6 proton giving two signals of equal intensity as indicated in Figure 3.5. In each of the symmetrical isomers **2b** and **2c** there is only one pyridyl environment resulting in one H^6 signal for each isomer. This should lead to four H^6 signals in total, exactly as observed in the spectrum. For a purely statistical distribution of these isomers, we would expect a relative population of 2 : 1 : 1 for **2a**, **2b** and **2c**. However, there is an observed distribution of

approximately 2.5 : 0.8 : 1 (as measured from ^1H NMR integrations) indicating a small preference for the unsymmetrical isomer **2a** over the symmetrical isomers. The reason for this very small favourability is uncertain.

We can assign the H^6 signals at $\delta = 7.80$ and 7.55 to the unsymmetrical isomer **2a** because they are of equal intensity to each other and of different intensity to the other two H^6 signals. Each of the weaker signals can be assigned to one of the symmetric isomers. We can tentatively assign the signal at higher field ($\delta = 7.58$) to **2b** since each H^6 proton experiences an upfield shift (relative to those in **2c**) due to the diamagnetic anisotropy of the adjacent pyridyl ring. In isomer **2c** there is no such effect since each H^6 proton is on the opposite side of the molecule and well away from the other pyridyl ring. Hence, the H^6 signal at $\delta = 7.82$ can be assigned to isomer **2c**. It should be noted that for **2a** one H^6 signal is at high δ and the other at low δ . A similar argument can be used to assign the H^3 signals which are also separated by approximately 0.2 ppm. The ^1H NMR spectrum of the isomeric mixture was also obtained using d^6 -acetone as the solvent (Figure 3.5 and Table 3.5) and this spectrum showed a more complete separation of the H^3 signals from the H^4 and H^5 signals in relation to the spectrum obtained using CDCl_3 . However, because of overlap, no new information regarding the H^4 and H^5 signals could be obtained. The ^{13}C NMR spectrum of compound **2** (data in Table 3.6) confirmed the presence of three isomers. Signals corresponding to the CO carbon atoms and the ortho-metallated carbon atom of the 2-pyridyl ligands were observed in the region $\delta = 185$ - 205 . Resonances between $\delta = 120$ and 155 were assigned to the remaining carbon atoms of the pyridyl ring by reference to the ^{13}C NMR spectrum of pyridine.²⁰⁹ Assignments were assisted by the use

of double resonance techniques, irradiating at the frequencies observed for the H⁶, H⁴ and H³ protons in the ¹H NMR spectrum. Four sets of resonances corresponding to each of the carbon atoms C³-C⁶ were observed. Each of these sets should, of course, be split into four further signals corresponding to the four different pyridyl environments. However, fifteen instead of sixteen of these signals were observed due to an accidental coincidence in the set of resonances we assigned to the C⁵ carbon atom. Assignment of signals to individual isomers was not attempted.

A correlated two-dimensional ¹H NMR spectrum of compound 2 was obtained in an attempt to assign each signal in the spectrum to the appropriate isomer and is shown in Figure 3.6. The signals on the diagonal running from bottom-left to top-right correspond to the one-dimensional spectrum shown at the top of the diagram, and the off-diagonal peaks give information about the three-bond couplings between the protons. Although it was possible to assign unambiguously each set of resonances to the protons H⁶-H³, the resolution was not sufficient to give information that could be used to assign the H⁵ and H⁴ signals to individual isomers.

A mass spectrum of compound 2 has been obtained using the fast atom bombardment (FAB) technique. The highest-mass ion is observed at $m/e = 873$ which corresponds to loss of two CO ligands from the complex to give $[\text{Ru}_4(\mu_4\text{-S})(\mu\text{-C}_5\text{H}_4\text{N})_2(\text{CO})_{10}]^+$. Calculated isotopic abundance patterns for this species are entirely consistent with the observed isotopic patterns. Complexity in the carbonyl-stretching region of the infrared spectrum (data in Table 3.3) and analytical data are all consistent with the formulation of $[\text{Ru}_4(\mu_4\text{-S})(\mu\text{-C}_5\text{H}_4\text{N})_2(\text{CO})_{12}]$.

Compounds **2a,2b** and **2c** contain two metal-metal bonds each and are electron-precise. The μ_4 -S atom is acting as a six-electron donor as in compound **1** and links the two dinuclear $[\text{Ru}_2(\text{C}_5\text{H}_4\text{N})(\text{CO})_6]$ units.

Figure 3.4 Isomers of $[\text{Ru}_4(\mu_4\text{-S})(\mu\text{-C}_5\text{H}_4\text{N})_2(\text{CO})_{12}]$ 2 showing all possible orientations of the 2-pyridyl ligands (CO ligands are omitted).

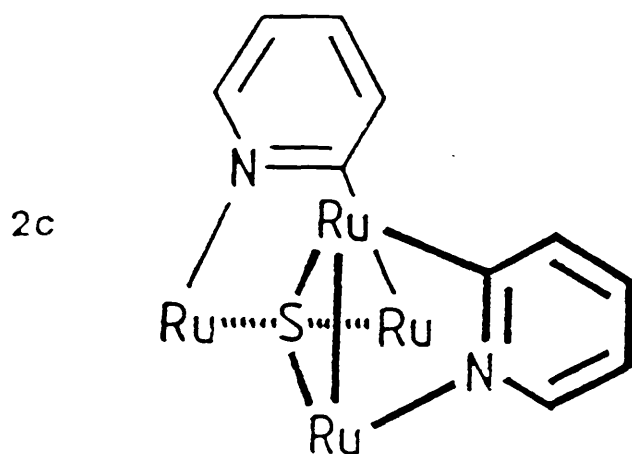
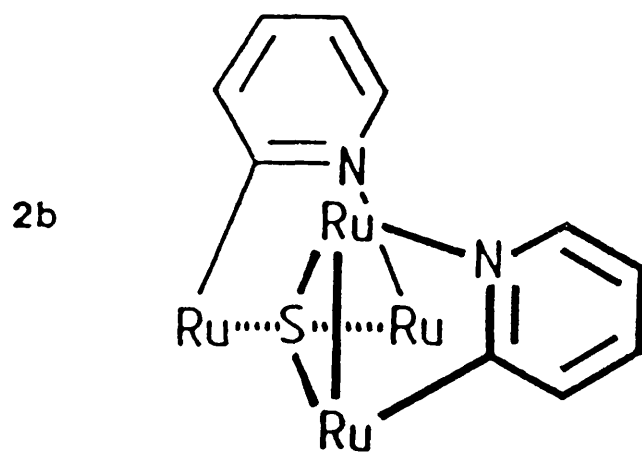
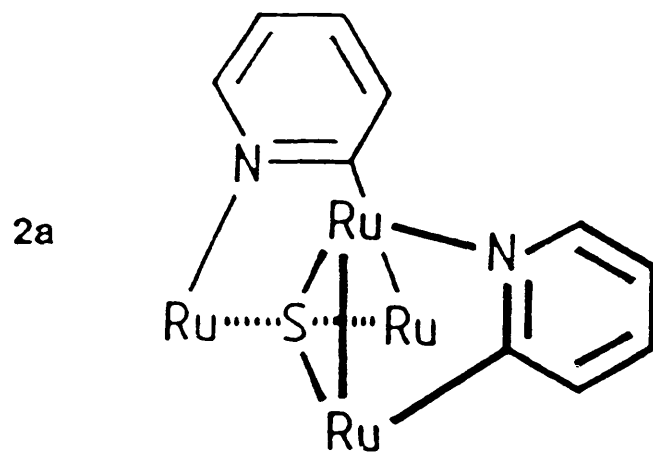
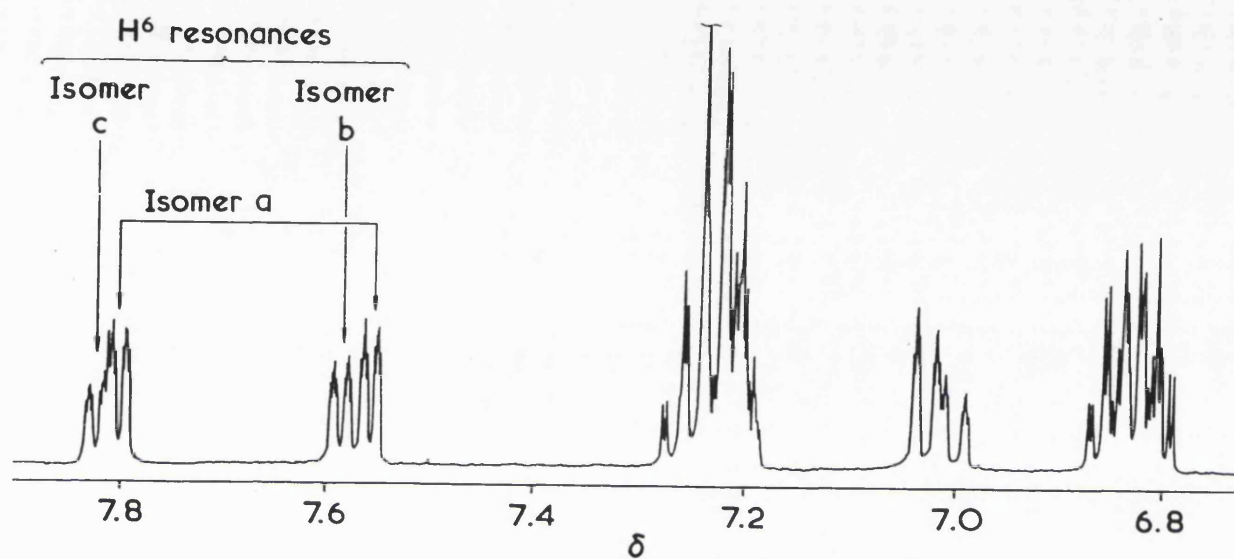
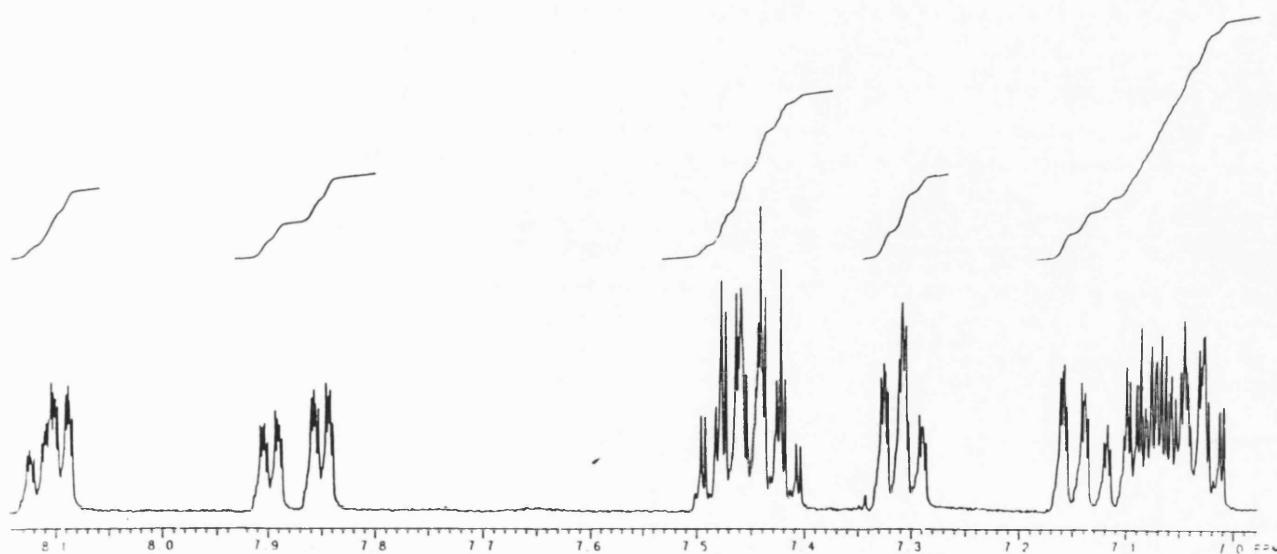


Figure 3.5 ^1H NMR spectra of the isomeric mixture of $[\text{Ru}_4(\mu_4\text{-S})(\mu\text{-C}_5\text{H}_4\text{N})_2(\text{CO})_{12}] \cdot 2$.

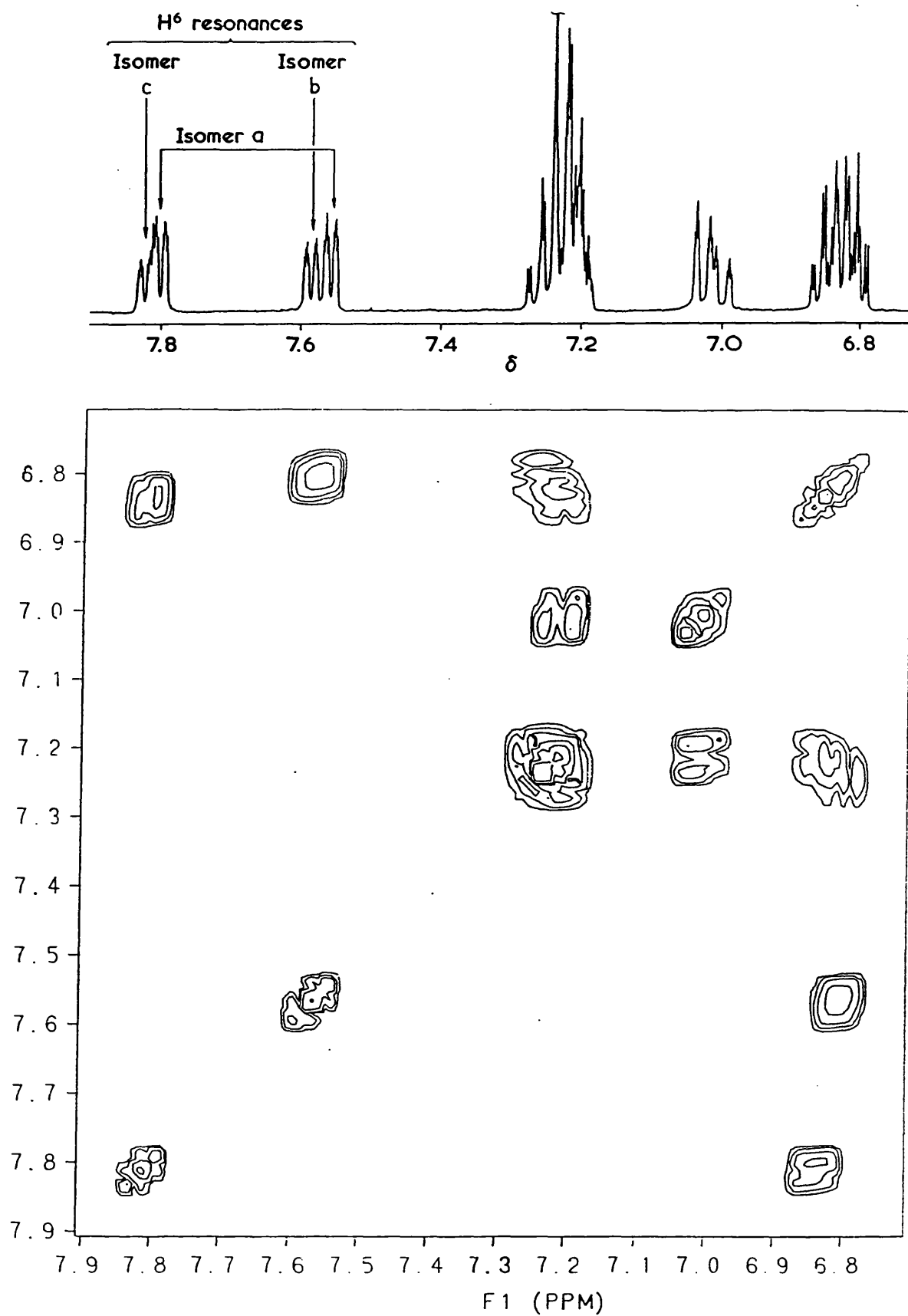


a. recorded in CDCl_3 at 20°C at 400 MHz.



b. recorded in d^6 -acetone at 20°C at 400 MHz.

Figure 3.6 Two-dimensional ^1H NMR spectrum of an isomeric mixture of $[\text{Ru}_4(\mu_4\text{-S})(\mu\text{-C}_5\text{H}_4\text{N})_2(\text{CO})_{12}]$ **2** recorded in CDCl_3 at 20°C at 400 MHz.



A similar metal-sulphur framework has been observed in a number of tetra-iron species, including $[\text{Fe}_4(\mu_4\text{-S})(\mu\text{-SMe})_2(\text{CO})_{12}]$,²⁰⁵ and a compound closely related to **2**, $[\text{Fe}_4(\mu_4\text{-S})(\mu\text{-C}_5\text{H}_4\text{N})(\mu\text{-SC}_5\text{H}_4\text{N})(\text{CO})_{12}]$ **4**.^{96a} Since the ligands in compound **2** are derived from the pyS moiety, it is likely that the ruthenium analogue of **4** is formed as an intermediate during the reaction between $[\text{Ru}_3(\text{CO})_{12}]$ and $[\text{Ru}(\text{pyS})_2(\text{CO})_2]$, the fairly harsh conditions employed leading to S–C cleavage and removal of a sulphur atom to give $[\text{Ru}_4(\mu_4\text{-S})(\mu\text{-C}_5\text{H}_4\text{N})_2(\text{CO})_{12}]$.

The formation of compounds **1** and **2** can be envisaged to occur by addition of an $[\text{Ru}(\text{CO})_4]$ unit to $[\text{Ru}(\text{pyS})_2(\text{CO})_2]$ to give $[\text{Ru}_2(\text{pyS})_2(\text{CO})_6]$, which would contain bridging pyS ligands. The analogous osmium complex, $[\text{Os}_2(\mu\text{-pyS})_2(\text{CO})_6]$,²¹⁰ has recently been isolated and so we know that $[\text{Ru}_2(\text{pyS})_2(\text{CO})_6]$ is a viable intermediate, but is probably not observed here because of the long reaction time employed. The next stage would involve cleavage of an Ru–N bond to give an intermediate containing a monodentate pyS ligand bound through the S atom only. S–C cleavage within this pyS ligand together with the formation of bonds between the sulphur atom and $[\text{Ru}(\text{CO})_3]$ or $[\text{Ru}(\text{CO})_4]$ units would result in $[\text{Ru}_4\text{S}(\text{C}_5\text{H}_4\text{N})(\text{pyS})(\text{CO})_{12}]$, analogous to the aforementioned iron complex **4**, which could follow one of two pathways. A repetition of the process would result in compound **1**, while the formation of compound **2** would require cleavage of pyS and subsequent loss of a sulphur atom. It is conceivable that long chains of Ru_2 units linked by $\mu_4\text{-S}$ atoms could be built up by this mechanism but as yet we have no evidence for compounds containing more than six ruthenium atoms.

It should be noted that recently the pentanuclear compound, $[\text{Ru}_5(\mu_4\text{-$

$S)_2(\mu_2-C_5H_4N)_2(CO)_{11}]$,⁶⁶ was isolated in fairly low yield from a reaction using the same starting materials as those used in the synthesis of compounds 1 and 2, but carried out in an open vessel. The lower CO:Ru ratio of the pentanuclear compound is probably the result of allowing any CO evolved to escape from the system. Another consequence of this is the likelihood of excessive decarbonylation of the starting materials and any intermediates, which would result in polymer formation and hence the lower product yield. Compounds 1 and 2 were isolated from a reaction carried out in an evacuated sealed tube. Thus, any CO liberated is retained in the system and available for further reaction. These conditions explain the higher CO:Ru ratio and the higher yields of compounds 1 and 2.

The pentanuclear compound adopts a structure that is described as an Ru_4 butterfly with the fifth metal atom bridging the wing-tip atoms or alternatively, considering the Ru_5S_2 system as a whole, a pentagonal bipyramid. The quadruply-bridging sulphido ligands in this molecule donate four electrons and are pyramidal with a lone-pair pointing radially away from the centre of the cage. It is interesting to note that only the one isomer of $[Ru_5(\mu_4-S)_2(\mu_2-C_5H_4N)_2(CO)_{11}]$ has been observed. However, theoretically there are several possible isomers, obtained by changing the orientations of the 2-pyridyl ligands. All possible isomers were observed for compound 2, $[Ru_4(\mu_4-S)(\mu_2-C_5H_4N)_2(CO)_{12}]$, which contains four equivalent ruthenium atoms, and for compound 1, $[Ru_6(\mu_4-S)_2(\mu_2-C_5H_4N)_2(CO)_{18}]$, which has two equivalent $[Ru_2(\mu_2-C_5H_4N)_2(CO)_6]$ end-units. However, in $[Ru_5(\mu_4-S)_2(\mu_2-C_5H_4N)_2(CO)_{11}]$ there are five non-equivalent ruthenium atoms, the C_5H_4N ligands bridging Ru atoms that are in very different environments, and the observation of only one isomer

probably indicates that one C_5H_4N orientation is much preferred energetically over the other. Both pyS ligands of the mononuclear starting material, $[Ru(pyS)_2(CO)_2]$, remain in the final cluster as in the formation of compound 1. Cleavage of a pyS ligand leaves an S atom and a C_5H_4N group both of which bind strongly to the metal atoms and neither is lost. This was also found for some mixed Re-Ru compounds described in Chapter Two and the tetra-iron compound 4 described above and seems to be a common feature with this ligand system. However, an exception is compound 2, $[Ru_4(\mu_4-S)(\mu-C_5H_4N)_2(CO)_{12}]$, in which one of the sulphur atoms is lost and only the C_5H_4N group is retained in the final molecule. Note that the components of a single pyS ligand donate seven electrons in the pentanuclear compound and nine electrons in compounds 1 and 2. The strength and number of bonds formed between metal atoms and S and C_5H_4N groups and the high number of electrons donated by these ligands are the driving force of C-S bond cleavage in these systems.

Table 3.3 Infrared spectroscopic data.

Compound	$\nu(\text{CO})^{\text{a}}/\text{cm}^{-1}$
$[\text{Ru}_6(\text{S})_2(\text{C}_5\text{H}_4\text{N})_2(\text{CO})_{18}]^{\text{b}}$	2076s, 2066s, 2051s, 2046s, 2013s, 2007s, 1997s, 1990s, 1975m, 1956w.
$[\text{Ru}_4\text{S}(\text{C}_5\text{H}_4\text{N})_2(\text{CO})_{12}]^{\text{b}}$	2083s, 2065s, 2046s, 2009s, 1993br, 1976w.

a. Recorded in cyclohexane solution.

b. Mixture of isomers.

Table 3.4 ^1H NMR spectroscopic data recorded in CDCl_3 .

Compound	Chemical Shifts (δ) ^a
[Ru ₄ S(C ₅ H ₄ N) ₂ (CO) ₁₂] (Isomer 2a)	7.80 (ddd, J = 5.5, 1.6, 0.9 Hz, H ⁶), 7.55 (ddd, J = 5.5, 1.6, 0.9 Hz, H ^{6'}), 7.28-7.19 (m, 2H ⁴ , H ³), 7.03 (ddd, J = 7.7, 1.5, 0.9 Hz, H ³), 6.87-6.79 (m, 2H ⁵).
[Ru ₄ S(C ₅ H ₄ N) ₂ (CO) ₁₂] (Isomer 2b)	7.58 (ddd, J = 5.5 Hz, H ⁶), 7.28-7.19 (m, H ⁴ , H ³), 6.87-6.79 (m, H ⁵).
[Ru ₄ S(C ₅ H ₄ N) ₂ (CO) ₁₂] (Isomer 2c)	7.82 (ddd, J = 5.5 Hz, H ⁶), 7.28-7.19 (m, H ⁴), 7.00 (ddd, J = 7.7 Hz, H ³), 6.87-6.79 (m, H ⁵).
[Ru ₆ (S) ₂ (C ₅ H ₄ N) ₂ (CO) ₁₈] (All three isomers)	7.85 (ddd, J = 5.5, 2.5, 1.6 Hz, H ⁶), 7.77 (ddd, J = 5.5 Hz, H ^{6'}), 7.75 (ddd, J = 5.6 Hz, H ^{6''}), 7.30-7.18 (m, 3H ⁴ , 3H ³), 6.89-6.83 (m, 3H ⁵).

a. Recorded at 400 MHz at room temperature.

Table 3.5 ^1H NMR spectroscopic data recorded in d^6 -acetone.

Compound	Chemical Shifts (δ) ^a
[Ru ₄ S(C ₅ H ₄ N) ₂ (CO) ₁₂] (Isomer 2a)	8.09 (ddd, J = 5.5, 1.6, 0.9 Hz, H ⁶), 7.85 (ddd, J = 5.5, 1.6, 0.9 Hz, H ^{6'}), 7.50-7.40 (m, 2H ⁴), 7.32 (ddd, J = 6.7, 1.5, 1.0 Hz, H ^{3'}), 7.15 (ddd, J = 7.7, 1.5, 0.9 Hz, H ³), 7.10-7.01 (m, 2H ⁵).
[Ru ₄ S(C ₅ H ₄ N) ₂ (CO) ₁₂] (Isomer 2b)	7.90 (ddd, J = 5.5, 1.6, 1.0 Hz, H ⁶), 7.50-7.40 (m, H ⁴), 7.30 (ddd, J = 6.6, 1.2, 0.9 Hz, H ³), 7.10-7.01 (m, H ⁵).
[Ru ₄ S(C ₅ H ₄ N) ₂ (CO) ₁₂] (Isomer 2c)	8.12 (ddd, J = 5.6, 1.6, 1.0 Hz, H ⁶), 7.50-7.40 (m, H ⁴), 7.11 (ddd, J = 7.7, 1.5, 1.0 Hz, H ³), 7.10-7.01 (m, H ⁵).

a. Recorded at 400 MHz at room temperature.

Table 3.6 ^{13}C NMR spectroscopic data recorded in CDCl_3 .

Compound	Chemical Shifts (δ) ^a	Assignment
[Ru ₄ S(C ₅ H ₄ N) ₂ (CO) ₁₂] ^b	120.3, 120.3, 120.6	C ⁵
	133.8, 133.8, 134.2, 134.2	C ⁴
	138.2, 138.3, 138.4, 138.5	C ³
	153.6, 153.7, 153.8, 153.8	C ⁶
	186-201 (24 resonances in total) ^c	<u>C</u> -O, <u>C</u> -Ru
[Ru ₆ (S) ₂ (C ₅ H ₄ N) ₂ (CO) ₁₈] ^b	120.5, 120.5, 120.8	C ⁵
	134.0, 134.5	C ⁴
	138.6, 138.6	C ³
	153.9, 154.0, 154.1	C ⁶
	185-201 (45 resonances in total) ^c	<u>C</u> -O, <u>C</u> -Ru

a. Recorded in CDCl_3 at 20 °C at 400 MHz

b. Mixture of isomers

c. Total number of resonances is approximate due to accidental coincidence and the poor signal:noise ratio

3.3 Experimental

Reaction of [Ru(pyS)₂(CO)₂] with [Ru₃(CO)₁₂] in petroleum spirit (b.p. 120-160 °C) at 150 °C for 18 hours.

[Ru(pyS)₂(CO)₂] (0.1732 g, 0.459 mmol) and [Ru₃(CO)₁₂] (0.4905 g, 0.767 mmol) were introduced into the bottom of a Carius tube and petroleum spirit (b.p. 120-160 °C) (30 cm³) was added. Three freeze-pump-thaw cycles were performed using liquid nitrogen in order to evacuate the tube which was then sealed under vacuum. The sealed tube and contents were then heated at 150 °C for 18 hours. The solvent was removed under reduced pressure and the residue separated by TLC [silica; light petroleum (b.p. < 40 °C) and dichloromethane (5:1 v/v)] to give three fractions. The middle yellow band (major) was re-chromatographed by TLC [conditions as above] to give [Ru₆(S)₂(C₅H₄N)₂(CO)₁₈] (0.233 g, 38%) as a yellow solid formed by slow evaporation of a dichloromethane solution. (Found: C, 25.45; H, 0.65; N, 2.12; S, 4.64 %. C₂₈H₈N₂S₂O₁₈Ru₆ requires: C, 25.27; H, 0.61; N, 2.10; S, 4.82 %) and [Ru₄S(C₅H₄N)₂(CO)₁₂] (0.096 g, 23%) as a yellow solid formed by slow evaporation of a dichloromethane solution. (Found: C, 28.41; H, 0.98; N, 3.01; S, 3.31 %. C₂₂H₈N₂SO₁₂Ru₄ requires: C, 28.44; H, 0.97; N, 3.00; S, 3.45 %). One green (0.012 g) and one yellow (0.027 g) fraction remain unidentified.

X-ray structure determination for [Ru₆(S)₂(C₅H₄N)₂(CO)₁₈].

Crystals were obtained by slow diffusion of methanol into a dichloromethane solution of [Ru₆(S)₂(C₅H₄N)₂(CO)₁₈].

A yellow crystal of the compound [Ru₆(S)₂(C₅H₄N)₂(CO)₁₈], *M* = 1330.92

g mol^{-1} , with dimensions $0.25 \times 0.22 \times 0.05 \text{ nm}^3$ was mounted on a thin glass fibre on a Nicolet R3v/m automatic four-circle diffractometer. A monoclinic cell, $a = 10.329(3)$, $b = 16.256(5)$, $c = 24.126(7) \text{ \AA}$, $\beta = 90.73(2)^\circ$, $U = 4050(2) \text{ \AA}^3$, was determined by auto-indexing and least-squares fitting of 30 orientation reflections in the range $6 \leq 2\theta \leq 24^\circ$, selected from a rotation photograph. The cell parameters and crystal system were confirmed by taking axial photographs. A total of 6113 unique intensity data were collected at room temperature using graphite-monochromated Mo- K_α radiation ($\lambda = 0.71073 \text{ \AA}$) with the diffractometer operating in the ω - 2θ scan mode between the limits $5 \leq 2\theta \leq 50^\circ$. The reflection intensities were corrected for Lorentz and polarisation effects and for decay by fitting the data to a curve calculated from three standard reflections collected periodically throughout the experiment. The data were finally corrected for absorption using the asimuthal scan method, $\mu(\text{Mo-}K_\alpha) = 23.1 \text{ cm}^{-1}$.

The structure was solved by routine application of direct methods, in the space group Cc , $Z = 4$, $F(000) = 2520$, $D_c = 2.18 \text{ g cm}^{-3}$. The model, with 505 parameters, was refined to $R = 0.0420$, $R_w = 0.0366$,* using 5346 intensity data with $F_0 \geq 3\sigma(F_0)$ by alternating cycles of full-matrix least-squares and by difference Fourier synthesis. The largest shift-to-error ratio in the final least-squares cycle was 0.001. All non-hydrogen atoms were refined anisotropically and H atoms for the 2-pyridyl ligands were included in the final model in idealised positions with C-H distances fixed at 0.96 \AA and isotropic thermal parameter $U = 0.08 \text{ \AA}^2$ but their positions were not allowed to refine. The largest peak in the final difference Fourier map was 0.9 e/\AA^3 , found close to Ru(4). The populations of the different orientations of the $\text{C}_5\text{H}_4\text{N}$ ligands were

refined by allowing the ring atoms bonded to ruthenium to have partial populations of N and C atoms. The dominant orientation is that shown in Figure 3.1 (population 0.7 ± 0.1) while the alternative minor orientation has atoms C(1a) and N(1a) replacing N(1) and C(1) in one ring and C(6a) and N(2a) replacing N(2) and C(6) in the other respectively (population 0.3 ± 0.1). Refinements with C_5H_4N ligands fixed in one or other orientation were poorer and the thermal parameters of the ruthenium-bonded atoms were less realistic.

The fractional atomic coordinates for $[Ru_6(S)_2(C_5H_4N)_2(CO)_{18}]$ can be found in Table A3 in the appendix. All calculations were performed on a MicroVax II computer running SHELXTL PLUS.¹⁴¹

$$^* R = \Sigma [|F_o| - |F_c|] / \Sigma |F_o|$$

$$R_w = [\Sigma w (|F_o| - |F_c|)^2 / \Sigma w |F_o|^2]^{1/2}$$

$$w = 1 / [\sigma^2(F_o) + 0.000245 F_o^2]$$

CHAPTER FOUR

Ruthenium and Osmium Carbonyl Complexes

Derived from Pyridine and

4-Methylpyridine

4.1 Introduction

The use of controlled synthetic methods in osmium carbonyl cluster chemistry is well established. The preparation of stable intermediates, such as the cyclohexadiene complex $[\text{Os}_3(\text{CO})_{10}(\text{C}_6\text{H}_8)]^{211}$ and the acetonitrile complexes $[\text{Os}_3(\text{CO})_{11}(\text{MeCN})]$ and $[\text{Os}_3(\text{CO})_{10}(\text{MeCN})_2]^{212}$ allows the displacement of ligand groups under relatively mild conditions, thus avoiding the extreme thermal conditions normally required for direct substitution of carbonyl groups. The higher reactivity and the greater tendency towards cluster fragmentation of $[\text{Ru}_3(\text{CO})_{12}]$ has resulted in a smaller amount of comparable cluster chemistry. It was only fairly recently that the analogous acetonitrile complexes of ruthenium were synthesised.⁹⁷ Up to this point, although many examples of cyclometallated complexes of osmium incorporating a heterocyclic donor were known,^{72,100,213} there were no analogous ruthenium cluster compounds of this nature. The preparation of these important acetonitrile compounds has provided a pathway for the synthesis of ruthenium cluster compounds using mild reaction conditions with less likelihood of fragmentation and, as a result, there now exist a number of cyclometallated complexes of ruthenium clusters with heterocyclic donor ligands. For example, the ortho-metallated clusters $[\text{Ru}_3\text{H}(\text{CO})_{10}(\text{L})]$ are produced when $[\text{Ru}_3(\text{CO})_{10}(\text{MeCN})_2]$ is treated with ligands such as pyridine,⁹⁷ methyl-substituted pyridines, quinoline, isoquinoline, diazines¹⁹⁴ and pyrazoles⁹⁸ amongst others.²¹⁴ In some cases the products are different from those obtained from $[\text{Ru}_3(\text{CO})_{12}]$ under thermal conditions. Thus, 2,2'-bipyridine gives $[\text{Ru}_3(\text{CO})_{10}(\mu\text{-C}_{10}\text{H}_8\text{N}_2)]$ from $[\text{Ru}_3(\text{CO})_{10}(\text{MeCN})_2]^{194}$ whereas with $[\text{Ru}_3(\text{CO})_{12}]$ it gives $[\text{Ru}_3(\mu\text{-CO})_2(\text{CO})_8(\text{C}_{10}\text{H}_8\text{N}_2)]$ in which the bipy ligand is

chelating.^{98,215} The complex $[\text{Ru}_3(\mu\text{-H})(\text{CO})_{10}(\mu\text{-C}_5\text{H}_4\text{N})]$ has also been obtained directly from $[\text{Ru}_3(\text{CO})_{12}]$ and pyridine, but in lower yield.⁹⁸ The reaction is believed to occur by way of $[\text{Ru}_3(\text{CO})_{11}(\text{py})]$, but this intermediate was not detected either here or in reactions of pyridine with $[\text{Ru}_3(\text{CO})_{12-n}(\text{MeCN})_n]$ ($n = 1-2$).⁹⁷ Reaction with excess pyridine gives the bis-ortho-metallated complex $[\text{Ru}_3(\mu\text{-H})_2(\text{CO})_8(\mu\text{-C}_5\text{H}_4\text{N})_2]$.⁹⁸⁻⁹⁹ By contrast, in the analogous osmium system, it is possible to isolate the compound $[\text{Os}_3(\mu\text{-H})(\text{CO})_9(\mu\text{-C}_5\text{H}_4\text{N})(\text{C}_5\text{H}_5\text{N})]$, which has two isomeric forms, in addition to the mono- and bis-ortho-metallated pyridyl complexes. Under harsh reaction conditions, cluster fragmentation occurs, and it is possible to isolate the diosmium species $[\text{Os}_2(\text{CO})_6(\mu\text{-C}_5\text{H}_4\text{N})_2]$ from the reaction between pyridine and $[\text{Os}_3(\text{CO})_{12}]$, which is also formed in thermolysis of $[\text{Os}_3\text{H}_2(\text{CO})_8(\text{C}_5\text{H}_4\text{N})_2]$.¹⁰⁰ The 4-methylpyridine ligand gives an analogous series of complexes to those obtained with pyridine, including $[\text{Os}_2(\text{CO})_6(\mu\text{-MeC}_5\text{H}_3\text{N})_2]$. The dimeric species exist as two isomers which only interconvert at high temperatures (180 °C) and then with decomposition. The X-ray diffraction determination of one of these isomers is included in this Chapter. The analogous diruthenium compounds had not been reported, and their synthesis, together with the isolation of some other, more interesting diruthenium complexes, is the main subject of this Chapter.

During the course of our studies on the reactions of pyridine with $[\text{Ru}_3(\text{CO})_{12}]$, we isolated complexes containing the 2,2'-bipyridyl ligand, which had been formed from the coupling of pyridine molecules at ruthenium centres. Coupling of pyridyl ligands coordinated to metal atoms is not unknown and has been observed in both mono- and dinuclear compounds, although in these cases the newly-formed 2,2'-bipyridyl ligands do not remain coordinated to the metal centres. Pyrolysis of 2-pyridyl gold(I), in which the

pyridyl ligand is C-bonded, quantitatively produces metallic gold and 2,2'-bipyridine.⁹³ Similar reductive elimination reactions are observed for $\text{Na}_3[\text{Co}(\text{CN})_5(\text{C}_5\text{H}_4\text{N})]^{92}$ and an acac-bridged dinuclear nickel complex,⁸⁹ which also contain C-bonded pyridyl ligands. 2,2'-Bipyridine is a common ligand in mononuclear metal complexes,²¹⁵ but is rarely used in cluster chemistry, which is largely due to its propensity for adopting chelating as opposed to bridging coordination modes. However, some cluster complexes of bipy are known, including $[\text{M}_3\text{H}(\text{CO})_9(\mu\text{-C}_{10}\text{H}_7\text{N}_2)]$ ($\text{M} = \text{Ru},^{194} \text{Os}^{216}$) which contain an ortho-metallated bipy ligand, $[\text{Rh}_6(\text{CO})_{14}(\text{bipy})_2]^{217}$ and $[\text{Ru}_3(\text{CO})_{10}(\mu\text{-C}_{10}\text{H}_8\text{N}_2)]^{98,215}$ in which it is chelating. In addition, the $[\text{Ru}_3(\text{CO})_{12}]$ -bipyridine mixture acts as a catalyst precursor for the reduction of nitrobenzene to aniline with good conversion,²¹⁸ but the nature of the catalytically active species is not known. One of the most studied bipy complexes is $[\text{Ru}(\text{bipy})_3]^{2+}$ which has interesting photocatalytic properties, and numerous applications of $[\text{Ru}(\text{bipy})_3]^{2+}$ and related compounds in catalytic systems are known.⁸⁴⁻⁵

4.2 Results and discussion

4.2.1 Crystal structures of the two isomers of $[\text{Os}_2(\text{CO})_6(4\text{-MeC}_5\text{H}_3\text{N})_2]$ 1.

Separation of the two isomers was achieved by careful TLC on silica using several slow elutions with light petroleum (b.p. 30-40 °C). Evaporation of a hot hexane solution yielded each isomer as colourless crystals which were suitable for X-ray diffraction experiments. Views of the molecules are shown in Figure 4.1 and selected bond lengths and angles are given in Table 4.1. The two isomers are essentially the same, differing only in the orientation of the

ortho-metallated 2-(4-methylpyridyl) ligands. The problem of crystallographically determining the correct ligand orientation, as discussed in previous chapters in relation to the 2-pyridyl ligand, is not present in this ligand system due to the presence of the methyl group in the 4-position of the ring, making full crystallographic characterisation much more straightforward. The arrangement of the 4-methylpyridyl ligands in the head-to-head isomer **1a** is such that both nitrogen atoms are attached to the same osmium centre giving an unsymmetrical dimer, while in the head-to-tail isomer **1b** the two nitrogen atoms are bonded to different osmium atoms and both ends of the molecule are identical. In both isomers these two ligands adopt a *cis*-configuration with respect to each other and are *trans* to carbonyl ligands. The Os–Os bond lengths of 2.762(1) Å for **1a** and 2.741(1) Å for **1b** are similar to the formimidoyl-bridged Os–Os bond lengths of 2.752(1) Å and 2.756(1) Å in $[\text{Os}_6(\mu_4\text{-S})_2(\mu\text{-HC=NPh})_2(\text{CO})_{18}]$, the structure of which consists of dinuclear Os_2 units linked by sulphido bridges.⁹⁶ These lengths are considerably shorter than that of 2.877(3) Å found in $[\text{Os}_3(\text{CO})_{12}]$,¹⁴⁰ and those of 2.936(1) and 2.940(1) Å observed for the 2-pyridyl-bridged Os–Os bonds in $[\text{Os}_3\text{H}_2(\text{CO})_8(\mu\text{-C}_5\text{H}_4\text{N})_2]$,²¹⁹ although in this compound there is an extra bond-lengthening effect due to the presence of bridging hydride ligands.¹³⁸ It can be seen from Figure 4.1 that ortho-metallation of two 4-methylpyridyl ligands has the effect of tilting the coordination planes perpendicular to the M–M axis towards each other such that the axial CO ligands are pulled up towards the organic ligands, the average Os–Os–CO^{axial} angle being 161°, and the average Os–Os–CO^{equatorial} angle being 96°.

Figure 4.1 Molecular structures of the two isomers of $[\text{Os}_2(\text{CO})_6(\text{MeC}_5\text{H}_3\text{N})_2]$ (1a and 1b).

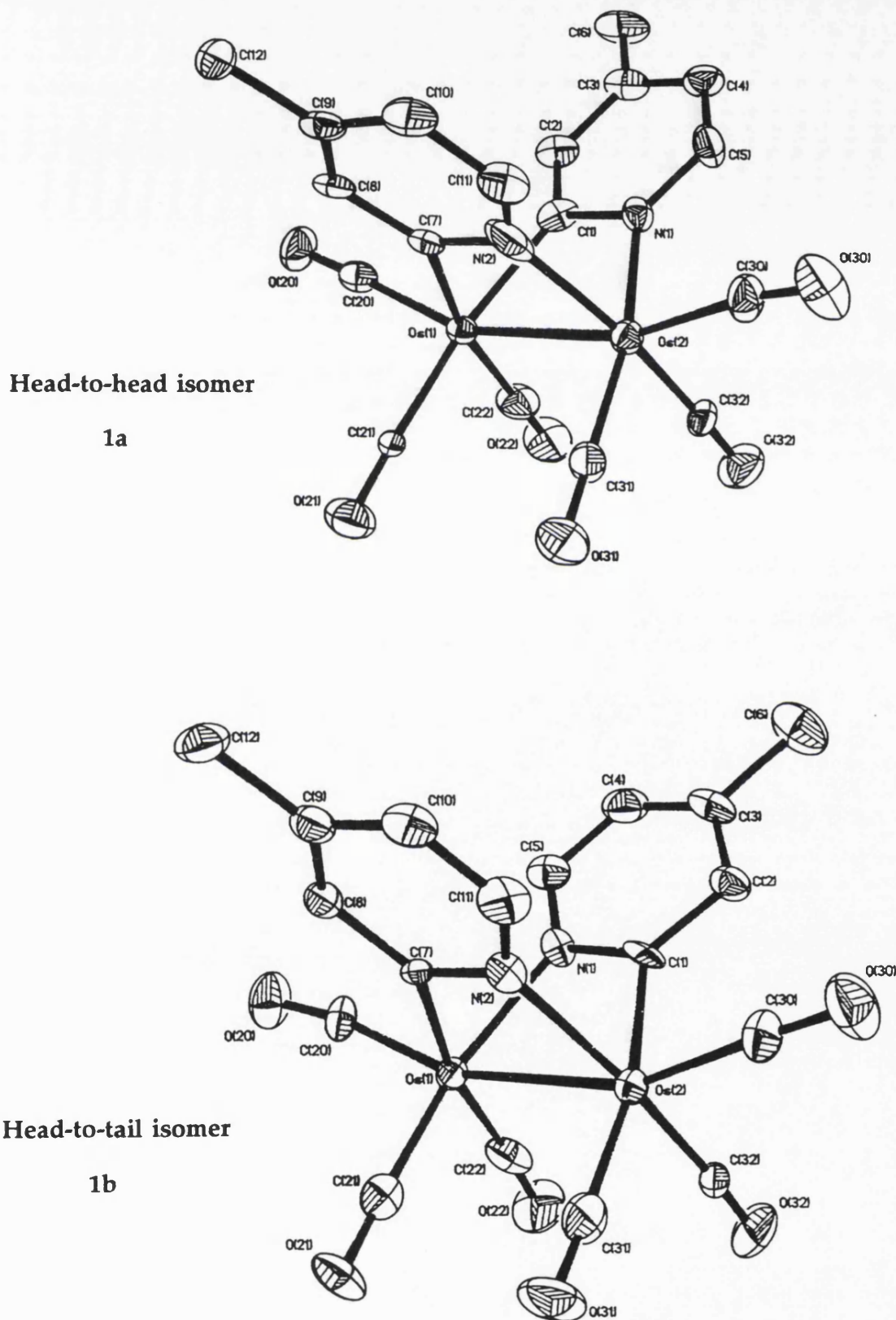


Table 4.1 Selected bond lengths (Å) and angles (°) for the two isomers of $[\text{Os}_2(\text{CO})_6(\text{MeC}_5\text{H}_3\text{N})_2]$ (**1b** and **1a**).

Bond lengths (Å)

	Head-to-head isomer 1a	Head-to-tail isomer 1b
Os(1)-Os(2)	2.762(5)	2.741(1)
Os(1)-N(1)	-	2.11(1)
Os(2)-N(2)	2.110(8)	2.12(2)
Os(2)-N(1)	2.111(8)	-
Os(1)-C(1)	2.117(8)	-
Os(2)-C(1)	-	2.11(1)
Os(1)-C(7)	2.114(9)	2.09(1)
N(1)-C(1)	1.36(1)	1.33(2)
C(1)-C(2)	1.40(1)	1.40(2)
C(2)-C(3)	1.40(1)	1.40(2)
C(3)-C(4)	1.37(1)	1.34(2)
C(3)-C(6)	1.53(1)	1.56(2)
C(4)-C(5)	1.37(1)	1.35(2)
C(5)-N(1)	1.36(1)	1.37(2)
N(2)-C(7)	1.36(1)	1.35(2)
C(7)-C(8)	1.37(1)	1.42(2)
C(8)-C(9)	1.40(1)	1.40(2)
C(9)-C(10)	1.38(2)	1.44(2)
C(9)-C(12)	1.48(1)	1.48(2)
C(10)-C(11)	1.40(2)	1.32(2)
C(11)-N(2)	1.35(1)	1.35(2)

Table 4.1 (cont.)

Bond angles (°)

	Head-to-head isomer 1a	Head-to-tail isomer 1b
Os(1)-Os(2)-C(1)	-	69.6(3)
Os(2)-Os(1)-N(1)	-	71.1(3)
Os(1)-N(1)-C(1)	-	108.2(8)
Os(2)-C(1)-N(1)	-	111.0(8)
Os(1)-Os(2)-N(1)	71.28(2)	-
Os(2)-Os(1)-C(1)	69.89(3)	-
Os(1)-C(1)-N(1)	110.59(7)	-
Os(2)-N(1)-C(1)	108.20(6)	-
Os(1)-Os(2)-N(2)	70.70(2)	70.8(4)
Os(2)-Os(1)-C(7)	70.52(2)	70.7(3)
Os(1)-C(7)-N(2)	109.43(6)	110(1)
Os(2)-N(2)-C(7)	109.35(6)	108(1)
N(1)-Os(1)-C(7)	-	81.7(5)
N(2)-Os(2)-C(1)	-	82.6(5)
C(1)-Os(1)-C(7)	83.69(3)	-
N(1)-Os(2)-N(2)	83.14(3)	-
Os(2)-Os(1)-C(20)	158.13(5)	161.7(5)
Os(1)-Os(2)-C(30)	163.85(3)	160.1(5)
Os(2)-Os(1)-C(21)	98.67(4)	92.2(5)
Os(2)-Os(1)-C(22)	97.30(3)	98.0(6)
Os(1)-Os(2)-C(31)	97.08(3)	98.1(6)
Os(1)-Os(2)-C(32)	94.38(3)	96.0(5)

4.2.2 The ruthenium dimers $[\text{Ru}_2(\text{CO})_6(\text{C}_5\text{H}_4\text{N})_2]$ 2.

An isomeric mixture of the dimeric compound $[\text{Ru}_2(\text{CO})_6(\text{C}_5\text{H}_4\text{N})_2]$ 2 was obtained in highest yield by heating $[\text{Ru}_3(\text{CO})_{12}]$ and pyridine in a molar ratio of 1:6 in n-heptane in an evacuated, sealed glass Carius tube at 120 °C for 72 hours. Treatment by TLC yielded compound 2 as a white solid in 27% yield. The ^1H NMR spectrum of this product indicated that the dimer exists as a 1:1 mixture of two isomers. Careful TLC on silica eluting with light petroleum spirit (b.p. 30-40 °C) allowed total separation of the mixture of head-to-head 2a and head-to-tail 2b isomers which are shown in Figure 4.2.

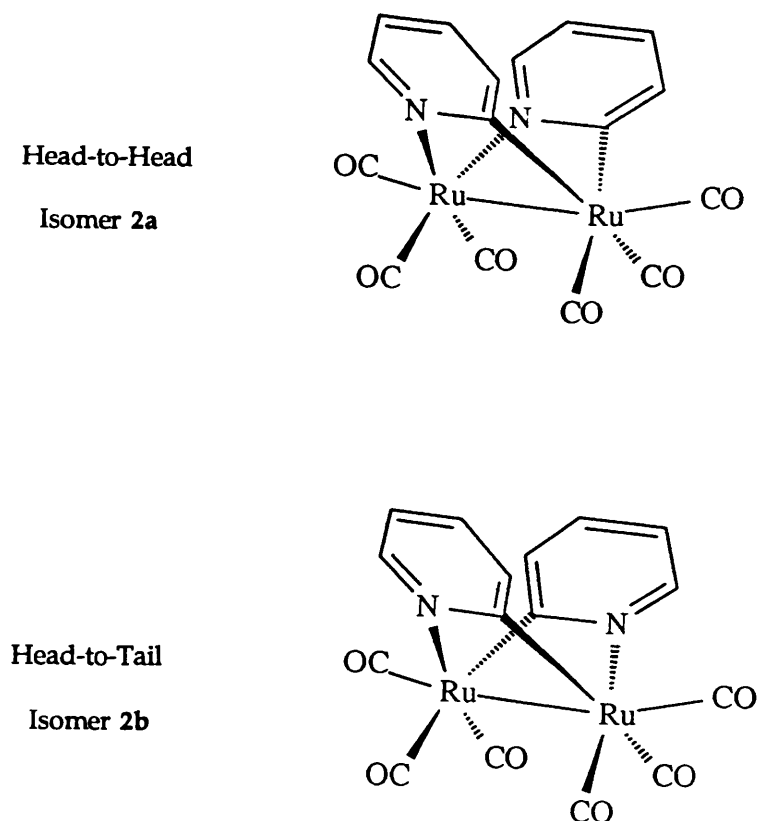


Figure 4.2 The two isomers of $[\text{Ru}_2(\text{CO})_6(\text{C}_5\text{H}_4\text{N})_2]$.

The infrared spectra of each isomer (data in Table 4.7) are very similar in the carbonyl stretching region to those of the corresponding osmium species $[\text{Os}_2(\text{CO})_6(\text{C}_5\text{H}_4\text{N})_2]$ and the 4-methylpyridine osmium analogues **1a** and **1b** for which the crystal structures have been determined and so we can assume that the ligand arrangements are the same. We have also been able to assign each isomer from their ^{13}C NMR spectra. For both isomers, aromatic resonances are observed in the region 119-155 ppm, corresponding to the four aromatic $\underline{\text{C}}\text{H}$ carbon atoms of the pyridyl ring. In the free ligand these resonances occur at 124, 136 and 150 ppm for the meta, para and ortho positions respectively.²²⁰ In addition, weaker quarternary carbon signals can be seen in the region 183-205 ppm which we can assign to the carbonyl ligands and the metallated carbon atom of the pyridyl ligand. The head-to-tail isomer (**2b**) contains three unique carbonyl ligands and one metallated carbon atom producing four signals in this region. In the head-to-head isomer there are four unique carbonyl ligands which, combined with the metallated pyridyl carbon atom, gives five resonances in total. We have not been able to differentiate between a carbonyl carbon atom and the metallated carbon of the pyridyl ring, although by comparison of the two spectra we can tentatively assign the resonance at 190.2 ppm in compound **2a** to the metallated pyridyl carbon atom. In compound **2b** this resonance occurs at either 185.9 or 196.1 ppm.

Working from the assumption that the H^6 proton would give a signal furthest downfield because of its proximity to the nitrogen atom, we can assign each resonance in the ^1H NMR spectra using {H-H} decoupling techniques. Furthermore, double-resonance techniques were used to assign each of the pyridyl $\underline{\text{C}}\text{H}$ resonances in the ^{13}C NMR spectra. Irradiating at the

resonance frequency of a particular proton while running the ^{13}C NMR spectrum causes signal enhancement of the carbon atom to which that proton is bonded and, to a lesser extent, signal enhancement of the adjacent carbon atom. It is interesting to compare the chemical shifts of these $\underline{\text{C}}\text{H}$ resonances with the corresponding values in the ^{13}C NMR spectrum of free pyridine²²⁰ (Table 4.2).

Free Pyridine		$[\text{Ru}_2(\text{CO})_6(\text{C}_5\text{H}_4\text{N})_2]$	
Position	Chemical Shift δ/ppm	Position	Chemical Shift δ/ppm
<i>ortho</i>	150	C^6	155
<i>meta</i>	124	C^5	120
<i>para</i>	136	C^4	133
<i>meta</i>	124	C^3	139
<i>ortho</i>	150	$\underline{\text{C}}\text{-Ru}$	190

Table 4.2 Comparison of the ^{13}C NMR chemical shifts of free pyridine and compound 2.

The large difference in chemical shift for the ortho-metallated carbon atom can be rationalised in that the net effect (σ and π bond contributions) of the Ru atom is to withdraw electron density from the carbon atom giving a large downfield shift (higher δ). It should be noted that the C^3 and C^6 positions both show a positive $\Delta\delta$ in relation to the corresponding signals in pyridine, while the C^4 and C^5 resonances show a small negative $\Delta\delta$, and this type of behaviour has been observed before for β - and γ -carbon atoms

respectively, of alkyl groups bound to transition metals.²²¹ In addition, the C³ position shows a relatively large change (15 ppm) compared to the C⁶ signal (5 ppm), which is probably due to a combination of ring current effects, the presence of the metal atoms and position relative to the nitrogen atom. Once identified, infrared spectroscopy can, of course, be used to distinguish the two isomers.

There are other examples of ruthenium dimeric species that exhibit a similar type of isomerism to that observed in compound 2. The compound $[\text{Ru}_2(\text{CO})_6(\mu\text{-pz})_2]$ (pz = pyrazolato, $\text{C}_3\text{H}_3\text{N}_2$), together with the 3- and 4-methyl analogues, have recently been reported.²²² In contrast to the pyridyl ligand, which bridges through nitrogen and carbon atoms, the pyrazole ligand bridges the Ru–Ru bond by bonding through the two nitrogen atoms and so no isomerism is observed for the pyrazole or 4-methylpyrazole ligand systems. However, when the ligand is substituted in the 3 position, then head-to-head and head-to-tail isomers of $[\text{Ru}_2(\text{CO})_6(\mu\text{-3-Mepz})_2]$ are observed. There is also the possibility of orientational isomerism in the bisoximato-bridged dinuclear complex $[\text{Ru}_2(\text{CO})_4(\mu\text{-ONCMe}_2)_2(\text{HONCMe}_2)_2]$,²²³ in which the bridging ligands are *cis* to each other, as in compound 2. However, only the isomer in which the nitrogen atoms of the bridging ligands are bound to different Ru centres is observed, *i.e.* the head-to-tail isomer. One possible explanation for this is that the head-to-head isomer would probably be sterically unfavourable because of interaction between the methyl groups. In addition, there are two O–H---O hydrogen-bonding interactions between the monodentate and bridging oxime ligands in the head-to-tail arrangement which would not be present in the opposite orientation. Steric interaction also probably accounts

for the observation of only one isomer of $[\text{Ru}_2(\text{CO})_4(\mu\text{-ONCR}_2)_2(\text{PPh}_3)_2]$ ($\text{R} = \text{H}, \text{Ph}$) and $[\text{Ru}_2(\text{CO})_4(\mu\text{-ONCR}_2)_2(\text{S}(\text{CH}_2\text{Ph})_2)_2]$.²²³ In general, the head-to-tail isomer of these types of complexes seems to be the most favourable. Polymeric chains of $[\{\text{Ru}_2(\text{CO})_4(\mu\text{-HNOCR})_2\}_n]$ contain a similar head-to-tail arrangement of carbamoylato ligands, which form three-atom bridges. The chains are held together by two Ru–O bonds between adjacent molecules and the extra stability this confers is probably the reason for the observed ligand orientation. The triphenylphosphine and acetonitrile derivatives have been isolated as discrete dinuclear units $[\text{Ru}_2(\text{CO})_4(\mu\text{-HNOCR})_2\text{L}_2]$.²²⁴

4.2.3 *The reaction of $[\text{Ru}_3(\text{CO})_{12}]$ with pyridine and 4-methylpyridine under more forcing conditions.*

Attempting to improve the yields of **2a** and **2b**, we carried out a reaction under the same conditions that had previously been used for the analogous osmium system. Heating $[\text{Ru}_3(\text{CO})_{12}]$ in neat pyridine in an evacuated, sealed tube at 180 °C for 6 hours and subsequent treatment by TLC gave red crystals of $[\text{Ru}_2(\text{CO})_5(\mu\text{-C}_5\text{H}_4\text{N})(\mu\text{-C}_{10}\text{H}_7\text{N}_2)]$ **3** in low yield (12%). The reaction of $[\text{Ru}_3(\text{CO})_{12}]$ in γ -picoline (4-methylpyridine) under similar conditions gave $[\text{Ru}_2(\text{CO})_5(\mu\text{-MeC}_5\text{H}_3\text{N})(\mu\text{-Me}_2\text{C}_{10}\text{H}_5\text{N}_2)]$ **4**, analogous to **3**, in similar yield (16%). A mass spectrum of compound **3** has been obtained using the electron impact technique (EI). The highest-mass ion is at $m/e = 519$ which corresponds to the loss of two CO ligands from the parent complex to give $[\text{Ru}_2(\text{CO})_3(\text{C}_5\text{H}_4\text{N})(\text{C}_{10}\text{H}_7\text{N}_2)]^+$. The ^1H NMR spectrum of compound **3** (Figure 4.4 and Table 4.5) contains 11 equal intensity multiplets and thus four

H atoms have been lost from three pyridine rings in the formation of **3**. An analysis of the couplings observed in the spectrum was consistent with two 2-pyridyl rings and a third ring containing just three adjacent H-substituents. A single-crystal X-ray diffraction experiment was performed on a suitable crystal of **3** selected from those grown by slow diffusion of a layer of methanol into a dichloromethane solution. Figure 4.3 shows an ORTEP diagram of the complex and selected bond lengths and angles are in Table 4.3. The compound contains two organic ligands: pyridyl and 2,2'-bipyridyl ligands both ortho-metallated at sites adjacent to nitrogen atoms. The intramolecular Ru–Ru distance is 2.716(2) Å, which corresponds to a single bond and is of a similar length to those we have seen previously for 2-pyridyl-bridged Ru–Ru units. For example, the metal-metal bonds are in the range 2.713(2)-2.722(1) Å in $[\text{Ru}_6(\mu_4\text{-S})_2(\mu\text{-C}_5\text{H}_4\text{N})_2(\text{CO})_{18}]$ and 2.701(1)-2.728(2) Å in the mixed rhenium-ruthenium complexes described in Chapter Two. These bond distances are all shorter than that of 2.8515(4) Å found in $[\text{Ru}_3(\text{CO})_{12}]$.¹³⁴ The ortho-metallated bipy ligand is the same as that found in the cluster $[\text{Os}_3\text{H}(\text{CO})_9(\mu\text{-C}_{10}\text{H}_7\text{N}_2)]$,²¹⁶ *i.e.* both nitrogen atoms of the ligand are bound to one metal atom with an ortho-metallated carbon atom bound at the other, although in this case the cluster was formed directly from bipy and not through the coupling of 2-pyridyl units as in the formation of **3** and **4**. The corresponding ruthenium compound $[\text{Ru}_3\text{H}(\text{CO})_9(\mu\text{-C}_{10}\text{H}_7\text{N}_2)]$ has also been reported,¹⁹³ and its structure is probably like that of its osmium analogue although this has not been established by diffraction methods.

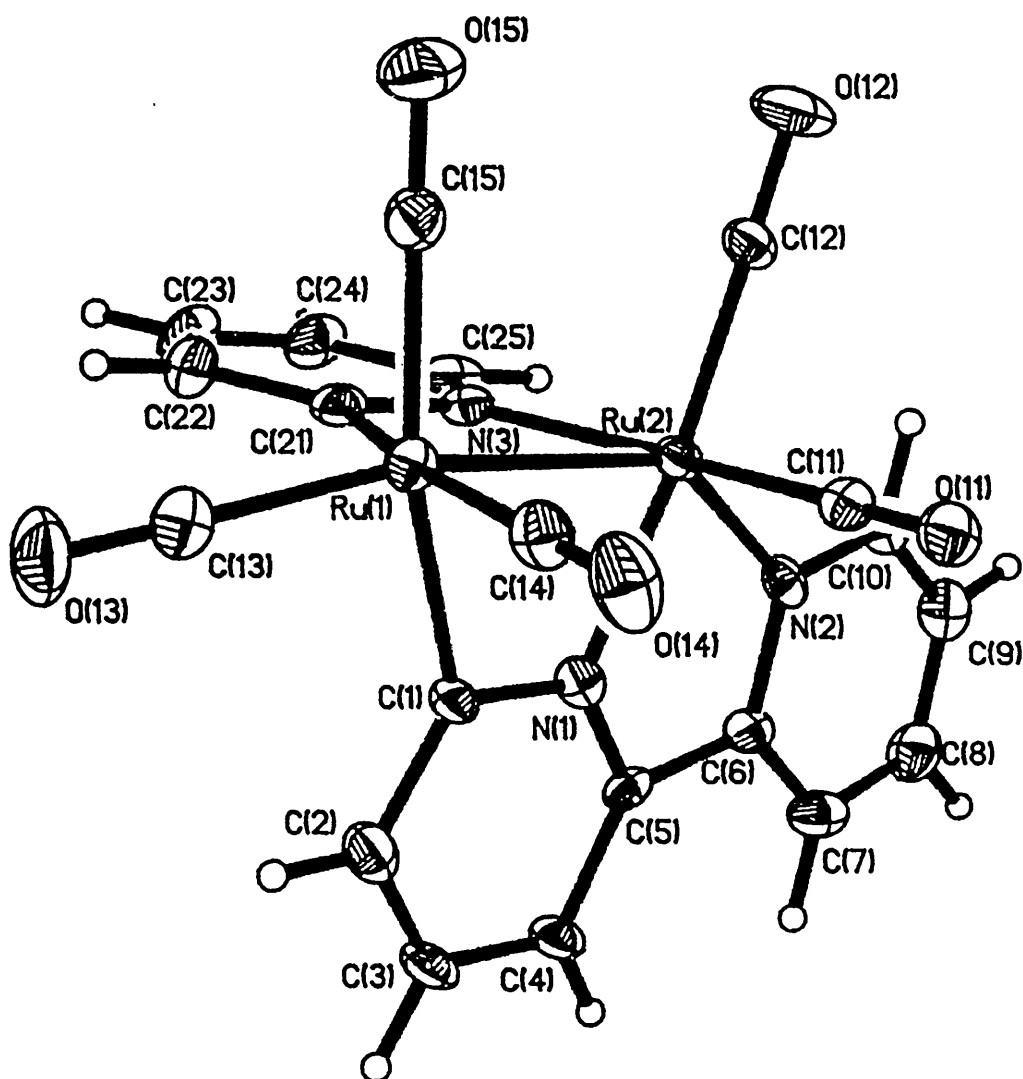
Figure 4.3 Molecular structure of $[\text{Ru}_2(\text{CO})_5(\text{C}_5\text{H}_4\text{N})(\text{C}_{10}\text{H}_7\text{N}_2)]$ 3.

Table 4.3 Selected bond lengths (Å) and angles (°) for
 $[\text{Ru}_2(\text{CO})_5(\text{C}_5\text{H}_4\text{N})(\text{C}_{10}\text{H}_7\text{N}_2)]$ **3**.

Bond lengths (Å)

Ru(1)-Ru(2)	2.715(2)	Ru(2)-N(1)	2.04(1)
Ru(2)-N(2)	2.23(1)	Ru(1)-C(1)	2.11(1)
Ru(2)-N(3)	2.13(1)	Ru(1)-C(21)	2.12(1)
N(1)-C(1)	1.33(2)	C(1)-C(2)	1.42(2)
C(2)-C(3)	1.35(2)	C(3)-C(4)	1.38(2)
C(4)-C(5)	1.41(2)	C(5)-N(1)	1.35(2)
C(5)-C(6)	1.45(2)	C(6)-C(7)	1.41(2)
C(7)-C(8)	1.34(2)	C(8)-C(9)	1.37(2)
C(9)-C(10)	1.38(2)	C(10)-N(2)	1.31(2)
N(2)-C(6)	1.37(2)	N(3)-C(21)	1.32(2)
C(21)-C(22)	1.40(2)	C(22)-C(23)	1.40(2)
C(23)-C(24)	1.31(2)	C(24)-C(25)	1.38(2)
C(25)-N(3)	1.35(2)		

M-CO averages (Å)

Ru-CO	1.88	RuC-O	1.15
-------	------	-------	------

Bond Angles (°)

Ru(1)-Ru(2)-N(1)	70.3(3)	Ru(2)-Ru(1)-C(1)	70.5(4)
Ru(1)-C(1)-N(1)	106.5(9)	Ru(2)-N(1)-C(1)	112.5(9)
Ru(2)-N(1)-C(5)	122.2(9)	N(1)-C(5)-C(6)	113(1)

Table 4.3 (cont.)

C(5)-C(6)-N(2)	116(1)	C(6)-N(2)-Ru(2)	113.0(8)
N(2)-Ru(2)-N(1)	74.6(4)	Ru(1)-Ru(2)-N(3)	71.1(3)
Ru(2)-Ru(1)-C(21)	70.6(4)	Ru(1)-C(21)-N(3)	110.3(9)
Ru(2)-N(3)-C(21)	108.0(8)	N(1)-Ru(2)-N(3)	82.5(4)
N(2)-Ru(2)-N(3)	94.3(4)	C(1)-Ru(1)-C(21)	84.2(5)

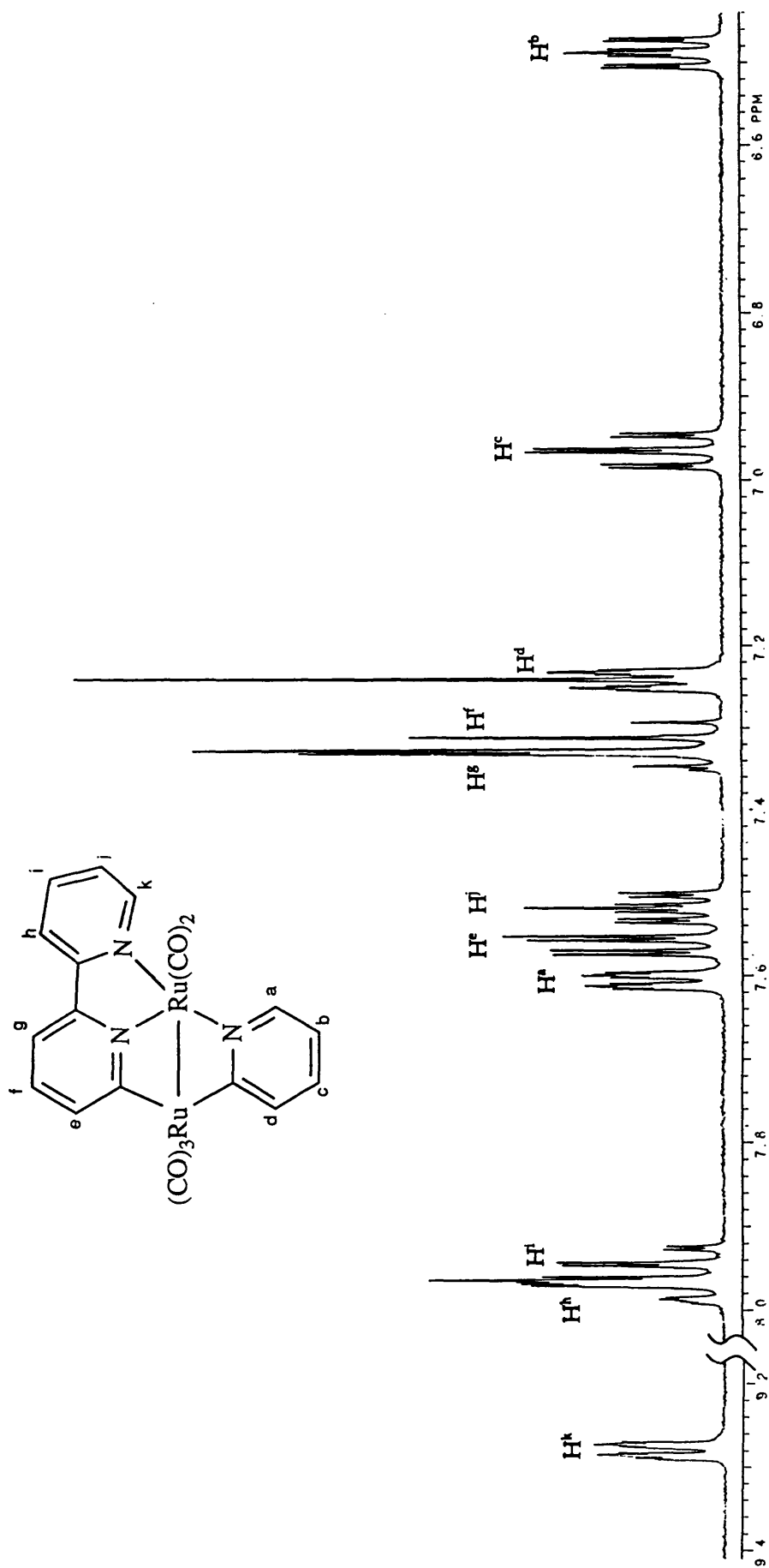


Figure 4.4 ^1H NMR spectrum of $[\text{Ru}_2(\text{CO})_5(\text{C}_5\text{H}_4\text{N})(\text{C}_{10}\text{H}_7\text{N}_2)]$ 3.

Coupling between two 2-pyridyl ligands at metal centres to give a 2,2'-bipyridyl ligand is not unknown, and has been observed in dinuclear nickel,⁸⁹ and mononuclear cobalt⁹² and gold⁹³ complexes as discussed in Section 4.1. In these cases, however, the original pyridyl ligand was coordinated in a monodentate mode through the carbon atom and the newly-formed 2,2'-bipyridyl ligand was eliminated from the metal complex. The main difference in this dinuclear ruthenium system is that the 2,2'-bipyridyl ligand is retained in the final molecule. In addition, assuming that compound 3 is derived from the dimer $[\text{Ru}_2(\mu\text{-C}_5\text{H}_4\text{N})_2(\text{CO})_6]$, then the original pyridyl ligands were ortho-metallated as opposed to monodentate, which may explain the retention of the bipy ligand. There are parallels to this behaviour in the reactions of the bisbenzoyl dinuclear iron complex $[\text{Fe}_2(\mu\text{-OCC}_6\text{H}_5)_2(\text{CO})_6]$,²²⁵ in which both acyl groups bridge the Fe-Fe bond. Treatment with triphenylphosphine results in cleavage of the metal-metal bond and C-C bond formation between the two benzoyl groups to give a PhC(O)-C(O)Ph ligand.²²⁶ This remains bonded to one of the iron atoms in the mononuclear complex, $[\text{Fe}(\text{CO})_2\{\text{PhC(O)-C(O)Ph}\}(\text{PPh}_3)]$, presumably through the oxygen atoms.

There is the possibility of isomerism arising from the orientation of the 2-pyridyl ligand relative to that of the bipyridyl ligand. However, unlike compounds 1 and 2, it is clear from NMR data that $[\text{Ru}_2(\text{CO})_5(\mu\text{-C}_5\text{H}_4\text{N})(\mu\text{-C}_{10}\text{H}_7\text{N}_2)]$ exists as a single isomer, as does the 4-methylpyridine analogue. The X-ray structure refines best with all three nitrogen atoms bound to the same ruthenium atom as in Figure 4.3. The isomer in which the orientation of the 2-pyridyl ligand is reversed has not been observed for either compounds 3 or 4. In addition, the two ligands are arranged *cis* with respect

to each other, the same configuration as observed for the dimeric compounds 1 and 2. The 2-pyridyl ligand does not easily re-orientate,^{75-76,95} for example, enantiomers of $[\text{Os}_3\text{H}(\text{CO})_{10}(\mu\text{-C}_5\text{H}_4\text{N})]$ have been resolved and do not interconvert.²⁰⁴ Although compound 3 may be the kinetically-controlled isomer with the 2-pyridyl ligand locked in that particular orientation, it is more likely that the most thermodynamically stable product is obtained at the elevated temperatures used in the preparation.

Generally, in ^1H NMR spectra of this ligand system, it is the H^6 proton that lies at lowest field and this signal usually occurs in the range 7.3-8.7 ppm. However, an unusually high δ value of 9.28 ppm is observed for one of the H^6 protons in this molecule. With reference to Figure 4.3, it can be seen that in this particular arrangement of ligands the H^6 proton of the bipyridyl ligand is situated in the plane of the pyridyl ligand and is therefore subject to the diamagnetic anisotropy of the ring. The ring current induced in the pyridyl ligand has the effect of increasing the local magnetic field at this proton causing resonance at a higher frequency and a further downfield shift is experienced in addition to that caused by the adjacent nitrogen atom. We have assigned this proton at lowest field as H^k in the labelling scheme (see Figure 4.4). Using this argument in conjunction with information gained from {H-H} decoupling experiments it is possible to assign each proton in the ^1H NMR spectra of both complexes 3 and 4.

Interestingly, the reaction of 4-methylpyridine with $[\text{Ru}_3(\text{CO})_{12}]$ gave rise to two extra products, analogues of which were not produced, or not produced in large enough quantities to be observed, in the analogous reaction with

pyridine. The only one which we have been able to characterise so far is an orange solid, formulated as $[\text{Ru}_2\text{HCl}(\text{CO})_3(\mu\text{-MeC}_5\text{H}_3\text{N})_2(\text{Me}_2\text{C}_{10}\text{H}_6\text{N}_2)]$ **5**, which was isolated in 12% yield. A mass spectrum of the compound has been obtained using the fast atom bombardment technique (FAB) and the parent molecular ion is at $m/e = 692$ which corresponds to $[\text{Ru}_2\text{HCl}(\text{CO})_3(\mu\text{-MeC}_5\text{H}_3\text{N})_2(\text{Me}_2\text{C}_{10}\text{H}_6\text{N}_2)]^+$. Lower mass peaks correspond to loss of one chloride or carbonyl ligand, with a preference for chloride, followed by loss of one 4-methylpyridyl ligand and then loss of the remaining carbonyl ligands. There are three absorptions in the carbonyl-stretching region of the infrared spectrum (data in Table 4.7) and these are at frequencies that correspond to terminal CO ligands. The ^1H NMR spectrum of **5** (Figure 4.8a and Table 4.5) shows six multiplets of equal intensity in the aromatic region of the spectrum and two singlets in the aliphatic region, which correspond to two types of 4-methylpyridyl environment. In addition there is a singlet at -17.43 ppm which is consistent with the presence of a hydride ligand in a bridging mode of coordination. From this spectroscopic information, we have postulated the structure shown in Figure 4.5 for compound **5**, although this has not been confirmed by diffraction methods. Considering the two ortho-metallated 4-methylpyridyl ligands as three-electron donors, the bi(4-Mepy) ligand as a four-electron donor and the chloride and hydride ligands as one-electron donors, an electron count would require the presence of an Ru-Ru single bond. This molecule has C_s symmetry, the plane of symmetry passing through the Ru-Ru axis, bisecting the bi(4-Mepy) ligand. The two ortho-metallated 4-methylpyridyl ligands are then equivalent, giving rise to three signals in the ^1H NMR spectrum. The remaining three signals can be assigned to the

2,2'-bi(4-methylpyridyl) ligand, the two rings of which are equivalent. The formulation was aided by the isolation and crystal structure determination of the compound $[\text{Ru}_2\text{HCl}(\text{CO})_3(\mu\text{-MeC}_5\text{H}_3\text{N})_2(\text{C}_{10}\text{H}_8\text{N}_2)]\cdot\text{H}_2\text{O}$ **8**, which gives very similar absorptions in the carbonyl-stretching region of the infrared spectrum to that of **5**. This compound will be discussed in Section 4.2.5. The only difference between these two complexes is that **5** contains a bi(4-methylpyridyl) ligand whereas **8** contains a bipyridyl ligand. There is a set of resonances in the ^1H NMR spectrum of **5** which has chemical shifts very close to those of the 4-methylpyridyl ligands in **8** and so we have tentatively assigned these signals to the corresponding ligands in **5** and the remaining three signals to the bi(4-Mepy) ligand. Two-dimensional ^1H NMR spectroscopy (Figure 4.9) confirms that these three signals belong to the same ring. Presumably, the chloride ion has been abstracted from dichloromethane used during the work-up of the reaction.

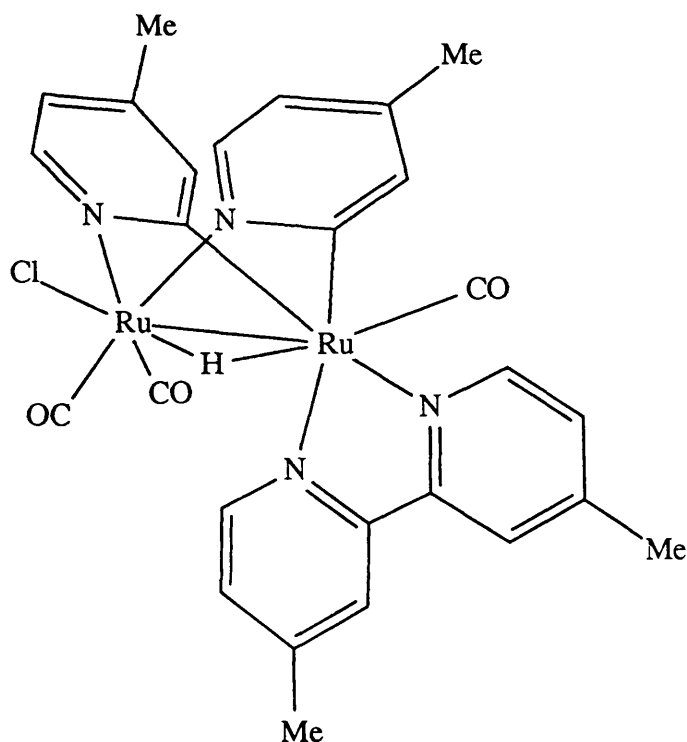


Figure 4.5 Probable structure of $[\text{Ru}_2\text{HCl}(\text{CO})_3(\mu\text{-MeC}_5\text{H}_3\text{N})_2(\text{Me}_2\text{C}_{10}\text{H}_8\text{N}_2)]$ **5**.

The formation of compounds 3-5 can be thought of as successive addition of pyridine or 4-methylpyridine to molecules of $[\text{Ru}_2(\text{CO})_6(\mu\text{-C}_5\text{H}_4\text{N})_2]$ **2** or its 4-methylpyridyl analogue. After initial attachment of the incoming ligand, the process could follow one of two general mechanistic pathways: ortho-metallation of the incoming pyridine ring and coupling of this ring to one of the existing pyridyl ligands, or the two existing pyridyl rings could be coupled and the incoming pyridine group could form the μ -2-pyridyl bridge. Loss of H_2 must also occur at some stage. Both routes would lead to two ortho-metallated ligands, one pyridyl and one bipyridyl (compounds **3** and **4**). We shall see in Section 4.2.5 that it is, in fact, the pre-coordinated pyridyl ligands which couple to produce the bipy ligand. The addition of a fourth pyridyl group to $[\text{Ru}_2(\text{CO})_5(\mu\text{-C}_5\text{H}_4\text{N})(\mu\text{-C}_{10}\text{H}_7\text{N}_2)]$ could form products in similar ways. The first route would involve coupling of the incoming pyridine group to the existing 2-pyridyl ligand to form the hypothetical molecule $[\text{Ru}_2(\text{CO})_4(\mu\text{-C}_{10}\text{H}_7\text{N}_2)_2]$, but this is not produced, which is consistent with the observation (Section 4.2.5) that it is the existing ligands that couple rather than the incoming pyridyl group. The second route would involve coupling of the existing ortho-metallated pyridyl and bipyridyl ligands to form an ortho-metallated terpyridyl ligand coordinated through one carbon and three nitrogen atoms, while the incoming pyridine group would form an ortho-metallated 2-pyridyl ligand to give the hypothetical product $[\text{Ru}_2(\text{CO})_4(\mu\text{-C}_5\text{H}_4\text{N})(\mu\text{-C}_{15}\text{H}_{10}\text{N}_3)]$. The alternative product, and the one that has been observed (compound **5**), is that formed by coordination and ortho-metallation of a 2-pyridyl group, forcing the coordination of the bipy ligand to change from a bridging to a chelating mode. We might speculate that another

possible explanation for not observing the hypothetical bisbipyridyl species is that this complex would probably have a head-to-tail arrangement of the two bipy ligands for steric reasons, each ruthenium atom being coordinated to the two nitrogen atoms of one ligand. Indeed, previous work does suggest that dinuclear ruthenium complexes of ligands containing two ring systems, such as benzotriazole, adopt a head-to-tail arrangement.²¹⁴ $[\text{Ru}_2(\text{CO})_4(\mu\text{-C}_{10}\text{H}_7\text{N}_2)_2]$ could not then be formed from $[\text{Ru}_2(\text{CO})_5(\mu\text{-C}_5\text{H}_4\text{N})(\mu\text{-C}_{10}\text{H}_7\text{N}_2)]$ **3** since all three nitrogen atoms in compound **3** are coordinated to the same metal atom, which is the wrong arrangement for formation of the head-to-tail isomer of the bisbipyridyl species.

4.2.4 The reaction between $[\text{Ru}_3(\text{CO})_{12}]$ and pyridine under very forcing conditions.

Attempting to induce further coupling of 2-pyridyl units *via* C–C bond formation, with a view to producing the hypothetical compound $[\text{Ru}_2(\text{CO})_4(\mu\text{-C}_{10}\text{H}_7\text{N}_2)_2]$ or possibly compounds containing higher oligomers of pyridine such as terpyridine, even more forcing conditions for the reaction between $[\text{Ru}_3(\text{CO})_{12}]$ and pyridine were used. Heating $[\text{Ru}_3(\text{CO})_{12}]$ in neat pyridine at 180 °C for 49 hours in an evacuated, sealed tube led to a very reactive mixture. Opening of the reaction tube, removal of the pyridine under reduced pressure and extraction into dichloromethane before TLC separation gave a series of yellow fractions. The major fractions were identified as the known mononuclear complexes $[\text{RuCl}_2(\text{CO})_2(\text{py})_2]$ ^{39,227} (8%) **6** and $[\text{RuCl}_2(\text{CO})(\text{py})_3]$ ²²⁸ (69%) **7**, characterised by microanalysis together with infrared, ¹H and ¹³C NMR and mass spectroscopy. In the ¹H NMR spectra of these complexes, one or two sets of resonances are observed, each consisting of three signals in a 2:2:1 ratio. This is consistent with pyridine ligands coordinated to the metal through the nitrogen atom alone, as opposed to ortho-metallated or bound through one of the carbon atoms. The only spectroscopic data reported for **6** and **7** are infrared carbonyl stretching frequencies, so our spectral data for these compounds are given in Tables 4.8 and 4.9.

There are several possible isomers of compound **6** and these can be distinguished spectroscopically. Only one set of pyridine resonances is observed in the ¹H NMR spectrum of **6**, indicating that the pyridine ligands are equivalent. In the carbonyl stretching region of the infrared spectrum there are two bands of similar intensity, at 2067 and 2004 cm⁻¹, which is

indicative of a *cis*-dicarbonyl species,²²⁹ a *trans* arrangement would usually give only one infrared band in this region. We have also examined the far infrared region and there is only one band in the region where Ru–Cl vibrations would be expected to occur, implying the chloride ligands are mutually *trans*.²³⁰ There have been several investigations into the dependence of $\nu(\text{M–Cl})$ upon the nature of the ligand L *trans* to chloride, the most important factor being the electronegativity of L. The relatively high value of 333 cm^{-1} for $\nu(\text{Ru–Cl})$, also suggests *trans* chloride ligands, rather than chlorides *trans* to CO ligands.²³⁰ This can be compared with $\nu(\text{Ru–Cl})$ in $[\text{RuCl}_6]^{2-}$ which lies between 332 and 346 cm^{-1} depending on the counter-ion.²²⁹ From this data we have postulated the structure shown in Figure 4.6 for compound 6.

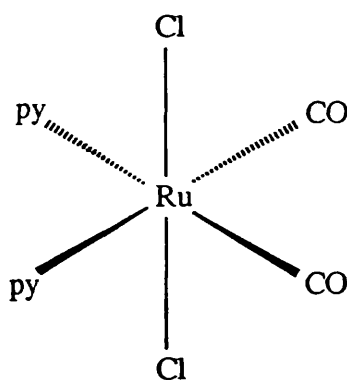


Figure 4.6 Probable Structure of $[\text{RuCl}_2(\text{CO})_2(\text{py})_2]$ 6.

Compound 7 was reported to be found in one isomeric form although the stereochemistry was not specified. However, we obtained two isomers 7a (58%) and 7b (11%) that were separable by TLC. Of the three possible structures of the tris-pyridine complex, one has a facial arrangement of py ligands while the other two are meridional isomers, as shown in Figure 4.7.

Each of these structures would give two sets of pyridine resonances in an intensity ratio of 2:1 in the ^1H NMR spectrum, and one band in the carbonyl stretching region of the infrared spectrum, as was observed for both **7a** and **7b**. The observation of a single band at 335 cm^{-1} , which we have assigned to $\nu(\text{Ru}-\text{Cl})$, in the far infrared spectrum of **7a** suggests mutually *trans* chloride ligands, *i.e.* the meridional structure (iii) for compound **7a**.

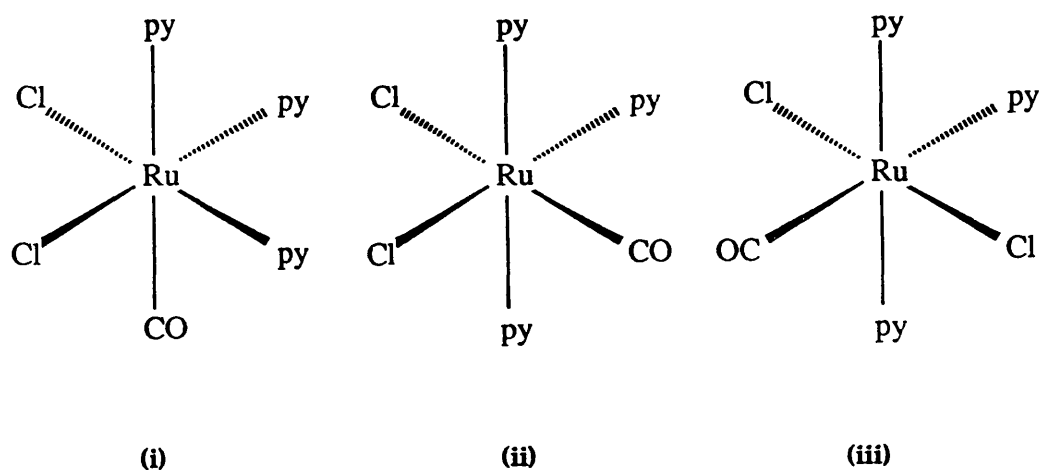


Figure 4.7 Possible Isomers of $[\text{RuCl}_2(\text{CO})(\text{py})_3]$ **7**.

Compound **7b** must then have structure (i) or (ii) but both are *cis*-dichloride species and so are indistinguishable by the number of Ru-Cl stretches in the far infrared spectrum. We have assigned the bands at 317 and 250 cm^{-1} in the far infrared spectrum of **7b** to the symmetric and asymmetric Ru-Cl stretches respectively. The lower value of 317 cm^{-1} for the symmetric stretch, in relation to those observed for **6** and **7a**, reflects that the *trans* ligand is now CO or pyridine rather than chloride. We can tentatively propose the meridional structure (ii) for compound **7b** for the following reasons. Firstly, the carbonyl ligand in **7a** is *trans* to a pyridine ligand and gives an absorption

at 1956 cm^{-1} in the infrared spectrum. In **7b**, the carbonyl stretch occurs at 1942 cm^{-1} , *i.e.* there is increased electron density in the π^* -orbital of the CO ligand. In complexes where there are competing π -acceptor ligands *trans* to CO, there is less π -donation from the metal to the CO ligand which is reflected in a higher $\nu(\text{CO})$. Chloride ligands have effectively zero π -acceptor properties, while pyridine is known to be a poor π -acceptor. Hence, the stretching frequency for a carbonyl ligand *trans* to pyridine would be expected to be higher than that observed for a carbonyl ligand *trans* to chloride, *i.e.* the CO ligand in **7b** is *trans* to a chloride as opposed to a pyridine ligand. Secondly, the signals corresponding to the two equivalent pyridine ligands in the ^1H NMR spectrum of **7b** have similar chemical shifts to the two equivalent, mutually *trans* py ligands of **7a**. This might suggest that compound **7b** also contains mutually *trans* pyridine ligands, *i.e.* the meridional structure (ii). In summary, the two isomers we have observed for $[\text{RuCl}_2(\text{CO})(\text{py})_3]$ are the two meridional isomers, one with *cis*-chloride ligands (**7b**) and one with *trans*-chloride ligands (**7a**).

The chloride ions in these compounds are almost certainly derived from dichloromethane which was used in the work-up of the reaction. It appears that the high temperature and the absence of aerial oxidation during the course of the reaction, has led to very reactive species in low oxidation states which will readily abstract chloride from dichloromethane. This has also been observed in the formation of the diruthenium compounds **5** and **8**.

4.2.5 Reaction of the dimer $[\text{Ru}_2(\text{CO})_6(\mu\text{-C}_5\text{H}_4\text{N})_2]$ with 4-methylpyridine.

To attempt some investigation into the mechanism of the formation of $[\text{Ru}_2(\text{CO})_5(\text{C}_5\text{H}_4\text{N})(\text{C}_{10}\text{H}_7\text{N}_2)]$, we decided to react $[\text{Ru}_2(\text{CO})_6(\mu\text{-C}_5\text{H}_4\text{N})_2]$ with 4-methylpyridine in order to determine whether it is the existing 2-pyridyl ligands that couple to give a bipy ligand or whether the incoming pyridine groups take part in the coupling process. Furthermore, we were interested in the difference in reaction path, if any, between the two isomers of $[\text{Ru}_2(\text{CO})_6(\mu\text{-C}_5\text{H}_4\text{N})_2]$, **2a** and **2b**. Each isomer was dissolved separately in 4-methylpyridine and heated in an evacuated, sealed tube at 180 °C for 3 hours, the resulting mixture being separated by TLC treatment. It would be expected that the head-to-head isomer **2a** would lead to products similar to compounds **3-5**, since the two nitrogen atoms are already coordinated to the same ruthenium atom. However, this is not what is observed. Compounds similar to **5**, as well as compound **5** itself, are indeed produced, but the reaction time is sufficiently long for the reaction path to pass through the formation of compounds like **3** and **4**, if indeed these were intermediates. However, these products were obtained from the head-to-tail isomer **2b**, the reaction with the head-to-head isomer **2a** resulted in cleavage of the Ru–Ru bond to give monoruthenium species.

(i) Reaction of the head-to-tail isomer of $[\text{Ru}_2(\text{CO})_6(\mu\text{-C}_5\text{H}_4\text{N})_2]$ **2b** with 4-methylpyridine.

The two compounds that we have been able to characterise from this

reaction are $[\text{Ru}_2\text{HCl}(\text{CO})_3(\mu\text{-MeC}_5\text{H}_3\text{N})_2(\text{Me}_2\text{C}_{10}\text{H}_6\text{N}_2)]$ **5**, which was also formed in the reaction between $[\text{Ru}_3(\text{CO})_{12}]$ and 4-methylpyridine (Section 4.2.3), and a new compound $[\text{Ru}_2\text{HCl}(\text{CO})_3(\mu\text{-MeC}_5\text{H}_3\text{N})_2(\text{C}_{10}\text{H}_8\text{N}_2)]$ **8**. There are seven resonances in the aromatic region of the ^1H NMR spectrum of **8** (Figure 4.8b and Table 4.5), which correspond to one type of pyridyl environment and one type of 4-methylpyridyl environment. The two sets are easily distinguishable because of the more extensive coupling between the protons of the pyridyl group. A two-dimensional ^1H NMR spectrum (Figure 4.9) confirmed the assignments. In addition, a singlet is observed at -17.82 ppm which is indicative of a bridging hydride ligand. We were not able to ascertain the nature of the coordination for the two types of ligand by spectroscopic methods alone and this was only determined by X-ray crystallography. It should be noted that because of their similarity, compounds **5** and **8** could not be separated by TLC and a small amount of a pure sample of **8** was only obtained by fractional crystallisation. Consequentially, the one and two-dimensional ^1H NMR spectra presented in Figures 4.8b and 4.9 are of the bulk sample, *i.e.* a mixture of compounds **5** and **8**. The ^1H NMR spectrum of three single crystals of **8**, including the crystal from which the diffraction structure was obtained, confirms the assignments. The infrared data for compound **8** given in Table 4.7 is also that of the single crystals and is extremely similar to that of compound **5**.

The molecular structure of **8** is shown in Figure 4.10 and selected bond lengths and angles are given in Table 4.4.

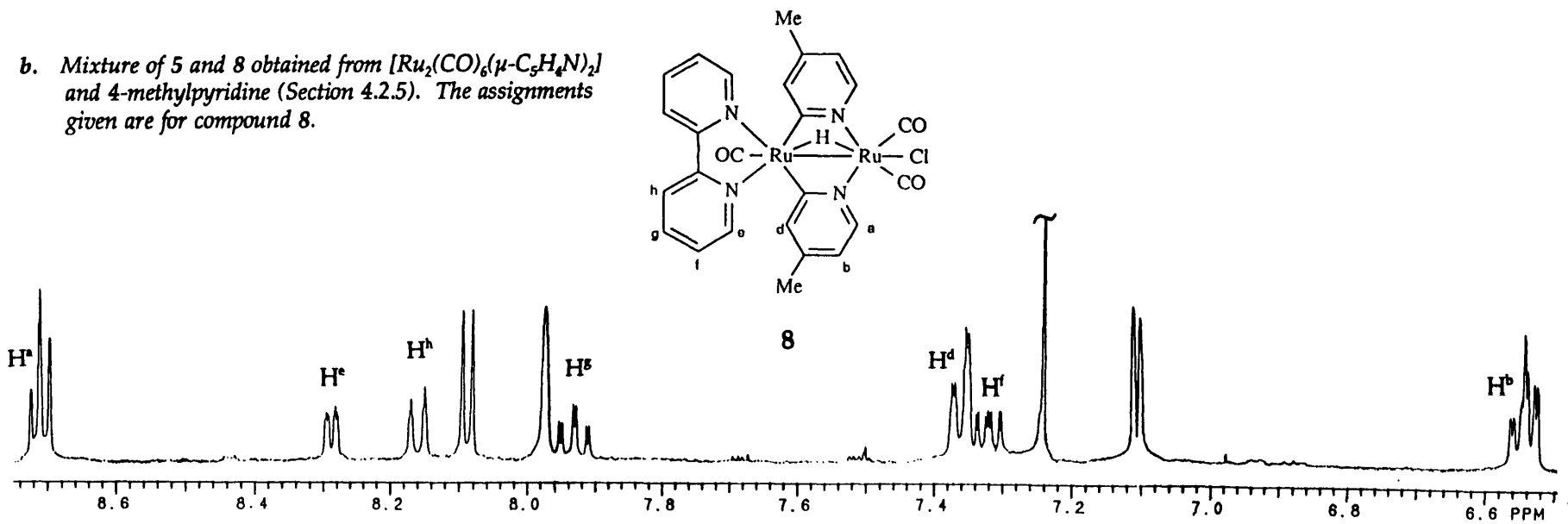
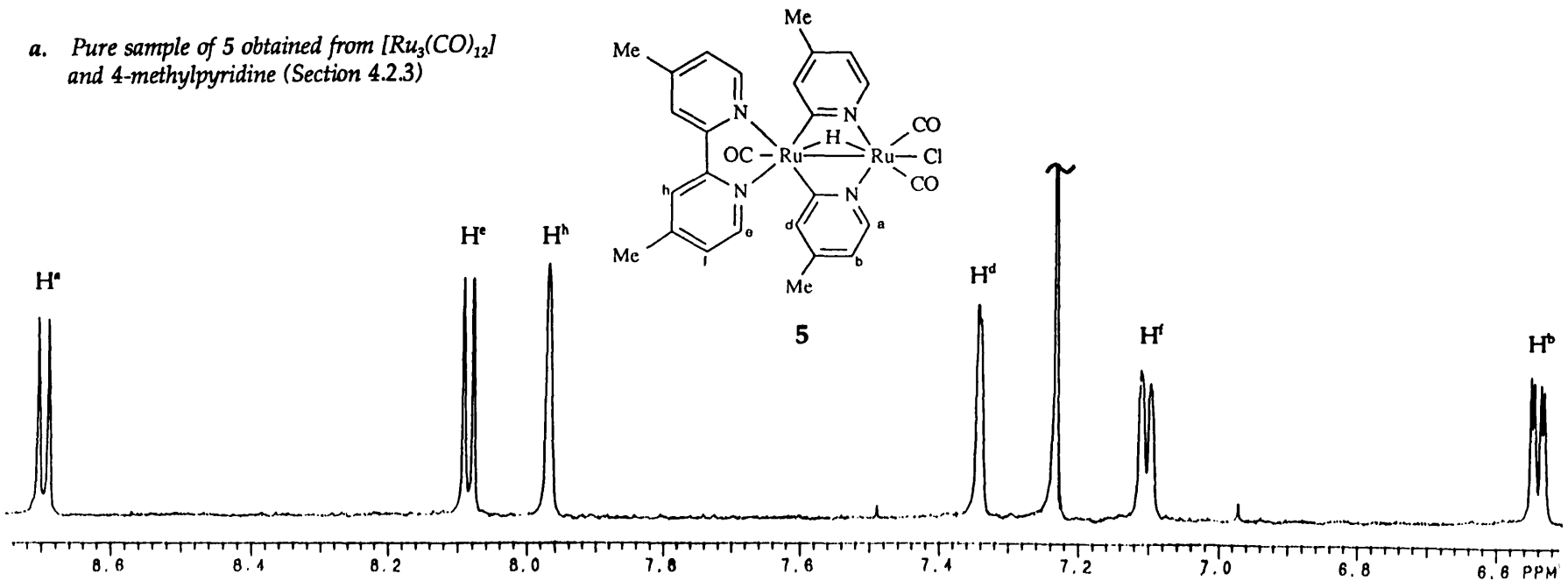
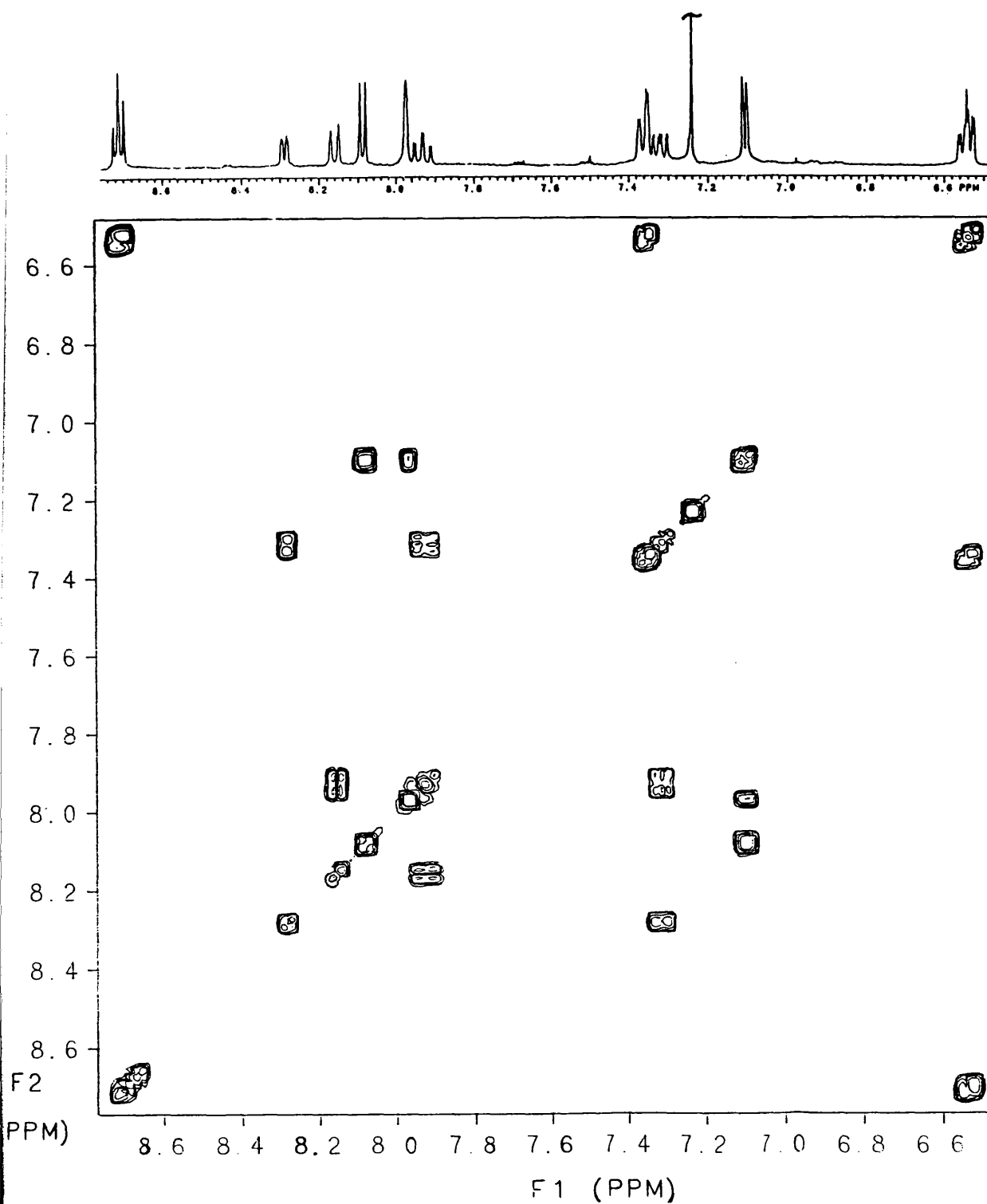
Figure 4.8 ^1H NMR spectra of $[\text{Ru}_2\text{HCl}(\text{CO})_3(\text{MeC}_5\text{H}_4\text{N})_2(\text{Me}_2\text{C}_{10}\text{H}_8\text{N}_2)]$ 5 and $[\text{Ru}_2\text{HCl}(\text{CO})_3(\text{MeC}_5\text{H}_4\text{N})_2(\text{C}_{10}\text{H}_8\text{N}_2)]$ 8.

Figure 4.9 2-D ^1H NMR spectrum of $[\text{Ru}_2\text{HCl}(\text{CO})_3(\text{MeC}_5\text{H}_3\text{N})_2(\text{Me}_2\text{C}_{10}\text{H}_6\text{N}_2)]$ **5** and $[\text{Ru}_2\text{HCl}(\text{CO})_3(\text{MeC}_5\text{H}_3\text{N})_2(\text{C}_{10}\text{H}_8\text{N}_2)]$ **8**.^{a,b}



a. Recorded in CDCl_3 at 400 MHz at room temperature.

b. See Figure 4.8 for assignments of resonances in compounds **5** (major component in the mixture) and **8** (minor component).

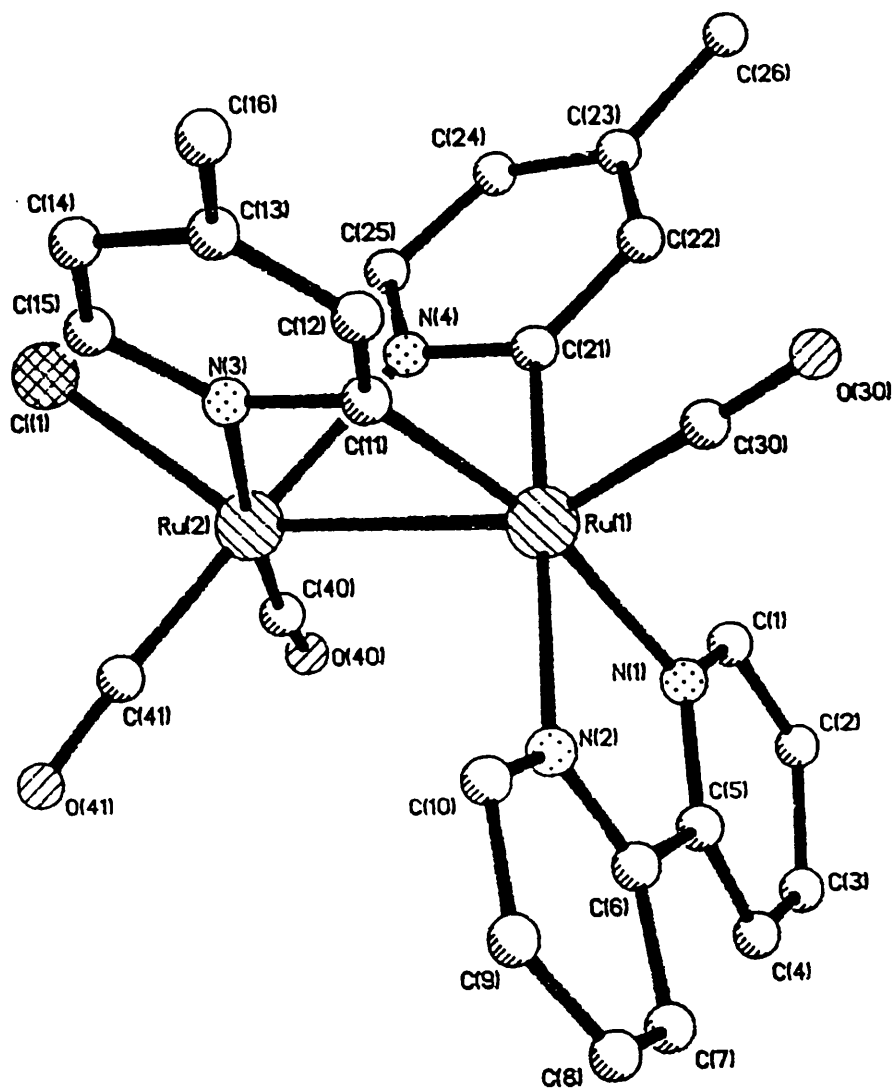
Figure 4.10 Molecular structure of $[\text{Ru}_2\text{HCl}(\text{CO})_3(\text{MeC}_5\text{H}_3\text{N})_2(\text{C}_{10}\text{H}_8\text{N}_2)]$ 8.

Figure 4.11 Molecular structure of $[\text{Ru}_2\text{HCl}(\text{CO})_3(\text{MeC}_5\text{H}_3\text{N})_2(\text{C}_{10}\text{H}_8\text{N}_2)]$ **8** showing probable hydride position.

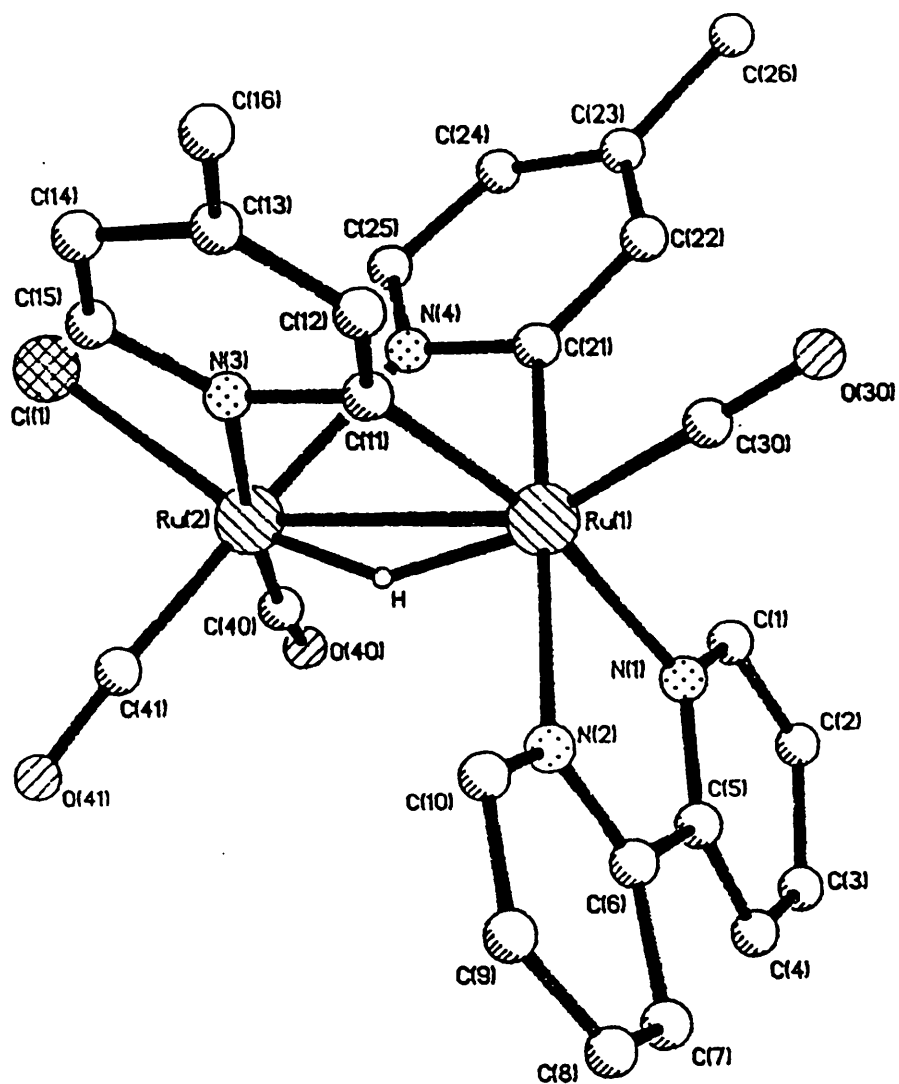


Table 4.4 Selected bond lengths (Å) and angles (°) for
 $[\text{Ru}_2\text{HCl}(\text{CO})_3(\text{MeC}_5\text{H}_3\text{N})_2(\text{C}_{10}\text{H}_8\text{N}_2)]$ **8**.

Bond lengths (Å)

Ru(1)-Ru(2)	2.949(3)	Ru(2)-Cl(1)	2.445(5)
Ru(1)-N(1)	2.20(1)	Ru(1)-N(2)	2.18(1)
Ru(2)-N(3)	2.09(1)	Ru(2)-N(4)	2.12(1)
Ru(1)-C(11)	2.00(1)	Ru(1)-C(21)	2.05(1)
N(1)-C(1)	1.31(2)	C(1)-C(2)	1.40(3)
C(2)-C(3)	1.37(3)	C(3)-C(4)	1.32(3)
C(4)-C(5)	1.42(3)	C(5)-N(1)	1.37(2)
C(5)-C(6)	1.44(2)	C(6)-C(7)	1.43(3)
C(7)-C(8)	1.38(3)	C(8)-C(9)	1.33(3)
C(9)-C(10)	1.42(3)	C(10)-N(2)	1.31(2)
N(2)-C(6)	1.34(2)	N(3)-C(11)	1.36(2)
C(11)-C(12)	1.43(3)	C(12)-C(13)	1.34(3)
C(13)-C(14)	1.37(3)	C(13)-C(16)	1.48(3)
C(14)-C(15)	1.35(3)	C(15)-N(3)	1.34(2)
N(4)-C(21)	1.34(2)	C(21)-C(22)	1.37(2)
C(22)-C(23)	1.36(2)	C(23)-C(24)	1.39(3)
C(23)-C(26)	1.51(3)	C(24)-C(25)	1.41(3)
C(25)-N(4)	1.35(2)		

M-CO averages (Å)

Ru-CO	1.797	RuC-O	1.185
-------	-------	-------	-------

Table 4.4 (cont.)

Bond Angles (Å)

Ru(1)-Ru(2)-Cl(1)	145.4(1)	Ru(2)-Ru(1)-C(30)	154.0(6)
Ru(2)-Ru(1)-N(1)	104.4(4)	Ru(2)-Ru(1)-N(2)	106.6(4)
Ru(1)-Ru(2)-C(40)	111.6(6)	Ru(1)-Ru(2)-C(41)	109.8(8)
Ru(1)-Ru(2)-N(3)	65.3(4)	Ru(2)-Ru(1)-C(11)	69.2(5)
Ru(1)-C(11)-N(3)	111(1)	Ru(2)-N(3)-C(11)	114(1)
Ru(1)-Ru(2)-N(4)	65.3(3)	Ru(2)-Ru(1)-C(21)	69.2(4)
Ru(1)-C(21)-N(4)	111(1)	Ru(2)-N(4)-C(21)	114(1)
Ru(1)-N(1)-C(5)	114(1)	N(1)-C(5)-C(6)	117(1)
Ru(1)-N(2)-C(6)	115(1)	N(2)-C(6)-C(5)	118(1)
N(3)-Ru(2)-N(4)	85.0(5)	C(11)-Ru(1)-C(21)	87.8(6)
N(1)-Ru(1)-C(21)	96.0(5)	N(2)-Ru(1)-C(11)	99.3(6)
N(1)-Ru(1)-C(11)	167.9(6)	N(2)-Ru(1)-C(21)	170.0(5)
N(1)-Ru(1)-N(2)	75.7(5)		

We detected the presence of a solvent molecule in the crystal lattice and we believe that it is a molecule of water, for the following reasons: firstly, the best refinement of the structure was when the atom at this site was designated as oxygen and secondly, taking into account the solvents and reagents used during the reaction, there seems to be no other likely alternative for its identity. It is most probable that the H₂O molecule originated from water present in the solvents used in the course of the reaction or work-up. The water molecule is situated in such a position that the formation of two O-H---Cl hydrogen-bonds seems possible. However, one of the criteria used for the existence of hydrogen-bonding is that the total bond length R(A---B) must be less than or equal to the sum of the van der Waals radii of atoms A and B.²³¹ For oxygen and chlorine atoms, the sum of the van der Waals radii is 3.20 Å and since the O-Cl distance in this crystal is 3.32 Å, it is unlikely that there is any significant intermolecular interaction. The diiridium complex [Ir₂(CO)₂(μ-OH · Cl)(Ph₂PCH₂PPh₂)₂]²³² contains a bridging hydroxide ligand having a chloride anion hydrogen-bonded to it, with an O---Cl distance of 3.10(2) Å. The position of the hydrogen atom of the OH group was clearly defined on a difference Fourier map, enabling an O-H-Cl bond angle of 163° to be estimated. This was not possible for our diruthenium complex, but the Cl-O-Cl angle is 73° which, if the hydrogen atoms were aligned towards the two chloride ligands and taking the H-O-H angle to be 104.5°, would give an O-H---Cl angle of *ca.* 164°. Even though there is no formal hydrogen-bond in the crystal it is possible that there is a weak electrostatic attraction which causes the observed orientation of two molecules of **8** in relation to the water molecule.

Considering the two ortho-metallated 4-methylpyridyl ligands as three-electron donors, the bipy ligand as a four-electron donor and the chloride and hydride ligands as one-electron donors, then an electron count would require the presence of a metal-metal bond. The Ru–Ru bond length of 2.949(3) Å is longer by *ca.* 0.2 Å than we have seen for other pyridyl-bridged Ru–Ru bonds and also longer than the Ru–Ru bonds in [Ru₃(CO)₁₂] (2.8515(4) Å),¹³⁴ which can be attributed to the presence of the bridging hydride ligand. It can be compared with the Ru–Ru bond bridged by a hydride and a pyrazole ligand in [Ru₃H(μ-N₂C₃HR₂)(CO)₁₀] (R = CF₃),⁹⁸ which is 2.902(1) Å. Increases in the length of metal-metal bonds which are bridged by hydride ligands is a well-documented effect,¹³⁸ as discussed in Chapter Two. The bond angles Ru(2)–Ru(1)–Cl and Ru(1)–Ru(2)–C(30) are 145.4(1)° and 154.0(6)° respectively, which are significant deviations from linearity. It was observed that for both isomers of compound 1, [Os₂(CO)₆(MeC₅H₃N)₂], ortho-metallation of two 4-methylpyridyl ligands has the effect of tilting the coordination planes perpendicular to the M–M axis towards each other such that the axial CO ligands are pulled up towards the organic ligands, the average Os–Os–CO^{axial} and Os–Os–CO^{equatorial} angles being 161° and 96° respectively. The steric requirements of the hydride ligand in 8 enhances this effect, pushing apart the two metal atoms and further displacing the axial ligands away from the Ru–Ru axis. This is also reflected in the positions of the equatorial carbonyl ligands in this molecule, which are at angles of 111.6(6)° and 109.8(8)° to the Ru–Ru bond, and the position of the bipy ligand: Ru(2)–Ru(1)–N(1) and Ru(2)–Ru(1)–N(2) are 101.4(4)° and 106.6(4)° respectively. The probable position for the hydride ligand is shown in Figure 4.11. The compound

contains three organic ligands: two ortho-metallated 4-methylpyridyl ligands and a 2,2'-bipyridyl ligand in a chelating mode of coordination. The two 4-methylpyridyl ligands are arranged in a head-to-head arrangement with respect to each other, *i.e.* both nitrogen atoms are bound to the same ruthenium atom. The bipy ligand is coordinated *via* its two nitrogen atoms to the other ruthenium centre. The two 4-methylpyridyl ligands are arranged *cis* with respect to each other, as in compounds 1-4, and the carbon atoms of these ligands are *trans* to the nitrogen atoms of the bipy ligand. One of the carbonyl ligands and the chloride ligand occupy the two axial sites. There is a similarly coordinated bipy ligand in $[\text{Ru}_3(\text{CO})_{10}(\text{bipy})]$,²¹⁵ although in this complex the chelating bipy ligand was derived directly from 2,2'-bipyridine. The bipy ligand in **8** is derived from coupling of the two 2-pyridyl ligands present in the original molecule **2b** (the head-to-tail isomer of $[\text{Ru}_2(\text{CO})_6(\mu\text{-C}_5\text{H}_4\text{N})_2]$). However, in **2b** the two nitrogen atoms were coordinated to different ruthenium atoms, whereas in compound **8** the nitrogen atoms of the bipy ligand are bound to the same ruthenium atom, implying migration of the pyridyl ligand across the Ru-Ru bond to the adjacent metal centre. There has apparently been a rearrangement involving the cleavage of an Ru-N bond and two Ru-C bonds, followed by C-C and Ru-N bond formation. In the final molecule, the 4-methylpyridyl ligands are in positions that were occupied by the ortho-metallated pyridyl ligands in the original molecule **2b**, and these pyridyl ligands have become coupled to give a chelating bipy ligand. With reference to the possible mechanisms discussed previously, it seems then, that it is the existing ligands rather than the incoming ligands that take part in the coupling process to produce the bipyridyl group, since there is no evidence for

coupling between 4-methylpyridine and the pyridyl ligands in this reaction. It is then understandable that we observe compounds **5** and **8** as opposed to a complex of the type $[\text{Ru}_2(\text{CO})_4(\mu\text{-C}_{10}\text{H}_7\text{N}_2)_2]$ as the next stage after formation of $[\text{Ru}_2(\text{CO})_5(\text{C}_5\text{H}_4\text{N})(\text{C}_{10}\text{H}_7\text{N}_2)]$ **3**. It is conceivable that the two ligands in compound **3** could couple to give a terpyridine ligand after attachment of further pyridyl groups, but this was not observed. It would have been interesting to treat **3** with 4-methylpyridine to establish whether this reaction would produce compounds similar to **5** and **8**, but due to low yields of **3** this was not possible.

The compounds **5** and **8** are related structurally, although the rings in **5** are derived entirely from 4-methylpyridine while those in **8** are derived from 4-methylpyridine and pyridine. It is evident that **8** is formed before compound **5** in this reaction, and is possibly an intermediate in the formation of **5**. The processes involved in the formation of **8** have repeated themselves in the formation of **5**, the difference being that in the second 'cycle' there is already a bipy ligand together with two 4-methylpyridyl ligands present in the complex. Attachment of two further 4-Mepy ligands to **8** forces the two existing ortho-metallated 4-methylpyridyl ligands to couple giving a bi(4-Mepy) ligand, resulting in the original bipy ligand being lost from the molecule.

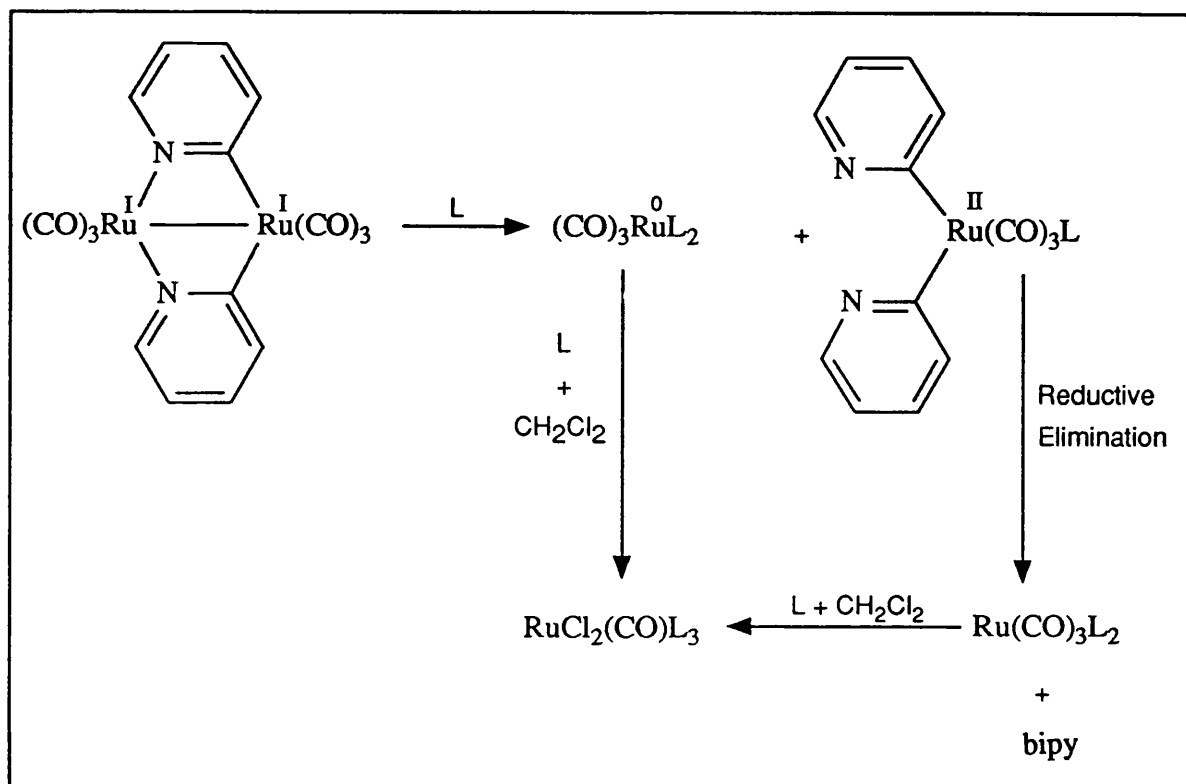
(ii) *Reaction of the head-to-head isomer of $[Ru_2(CO)_6(\mu-C_5H_4N)_2]$ 2a with 4-methylpyridine.*

The reaction of the head-to-head isomer 2a with 4-methylpyridine gave a monomeric species that we have tentatively characterised as $[RuCl_2(CO)(Mepy)_3]$ 9 from spectroscopic data. There is a single absorption in the carbonyl stretching region of the infrared spectrum of 9, and this is at the same frequency (1956 cm^{-1}) as that observed for the analogous pyridine complex $[RuCl_2(CO)(py)_3]$ (7a). In the aromatic region of the 1H NMR spectrum of 9, there are two sets of signals in a 2:1 ratio. Each set of signals consists of two resonances that are consistent with coordination of the 4-methylpyridine ligand through the nitrogen atom alone, as opposed to ortho-metallation which would give three resonances. In addition, these resonances have chemical shifts similar to those observed for the corresponding protons in the analogous pyridine complex 7a. There is a similar 2:1 pattern of singlets in the aliphatic region of the spectrum corresponding to the hydrogen atoms of the methyl group. Due to low yields of this compound, micro-analytical data was unobtainable, but the spectroscopic data does seem to imply a monoruthenium species. Apparently then, Ru–Ru cleavage has occurred in the reaction between 4-methylpyridine and the head-to-head isomer of $[Ru_2(CO)_6(\mu-C_5H_4N)_2]$, whereas in the reaction of the head-to-tail isomer, under identical conditions, the Ru–Ru bond remains intact and the products are dinuclear. The reasons for this are uncertain, but the way in which the pyridyl groups couple probably plays a significant role in the overall mechanism of the reaction. It does seem unusual that when the starting compound is the head-

to-tail isomer, then the product (compound 8) contains the two nitrogen atoms of the newly-formed bipy ligand coordinated to the same ruthenium atom and yet there is no comparable product in the corresponding reaction with the head-to-head isomer. Surely the head-to-head isomer would be the more likely to form products such as 5 or 8 since the nitrogen atoms are already coordinated to the same Ru atom and less ligand rearrangement would be required? One explanation is that the head-to-head isomer more readily breaks up as illustrated in Figure 4.12. The unsymmetrical cleavage of the ruthenium dimer may not be possible with the head-to-tail isomer.

Another possible explanation is that products such as 5 and 8 are indeed formed in the course of the reaction with the head-to-head isomer, but under these reaction conditions a subsequent step has occurred, *i.e.* Ru–Ru cleavage to give monomeric products. It would have been interesting to perform additional experiments employing a shorter reaction time for the reaction of the head-to-head isomer with 4-methylpyridine, to see if dimeric species are produced. Furthermore, the reaction time for the reaction of the head-to-tail isomer could have been increased to investigate whether monomeric species result. Unfortunately, as with much of this work, low yields, especially of the dimers $[\text{Ru}_2(\text{CO})_6(\mu\text{-C}_5\text{H}_4\text{N})_2]$, have frustrated our efforts to understand this system more fully.

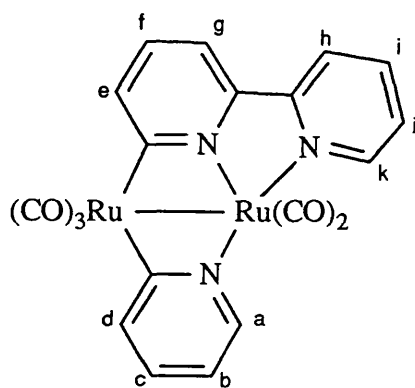
Figure 4.12 Possible Mechanism for Ru–Ru cleavage.



L = 4-methylpyridine

Table 4.5 ^1H NMR spectroscopic data for the new compounds.

Compound	^1H NMR data (δ) ^a
$[\text{Ru}_2(\text{CO})_6(\text{C}_5\text{H}_4\text{N})_2]$ (Isomer 2a)	7.94 (ddd, $J = 5.5, 1.6, 0.9$ Hz, H^6), 7.32 (ddd, $J = 7.4, 1.2, 1.2$ Hz, H^3), 7.13 (ddd, $J = 7.6, 7.6, 1.7$ Hz, H^4), 6.71 (ddd, $J = 7.3, 5.6, 1.5$ Hz, H^5).
$[\text{Ru}_2(\text{CO})_6(\text{C}_5\text{H}_4\text{N})_2]$ (Isomer 2b)	7.87 (ddd, $J = 5.5, 1.6, 0.9$ Hz, H^6), 7.38 (ddd, $J = 7.4, 1.2, 1.2$ Hz, H^3), 7.17 (ddd, $J = 7.5, 7.5, 1.7$ Hz, H^4), 6.73 (ddd, $J = 7.3, 5.6, 1.5$ Hz, H^5).
$[\text{Ru}_2(\text{CO})_5(\text{C}_5\text{H}_4\text{N})(\text{C}_{10}\text{H}_7\text{N}_2)]$ 3	9.28 (ddd, $J = 5.4, 1.6, 0.9$ Hz, H^k), 7.98 (ddd, $J = 8.1, 1.9$ Hz, H^h), 7.94 (ddd, $J = 8.0, 8.0, 1.6$ Hz, H^i), 7.61 (ddd, $J = 5.4, 1.7, 1.0$ Hz, H^a), 7.56 (dd, $J = 6.6, 2.0$ Hz, H^e), 7.52 (ddd, $J = 6.1, 5.2, 1.8$ Hz, H^f), 7.34 (dd, $J = 7.6, 1.9$ Hz, H^g), 7.31 (dd, $J = 7.5$ Hz, H^f), 7.24 (ddd, $J = 7.5, 1.2$ Hz, H^d), 6.96 (ddd, $J = 7.5, 7.5, 1.7$ Hz, H^c), 6.49 (ddd, $J = 7.3, 5.6, 1.4$ Hz, H^b).



a. Recorded in CDCl_3 at 400 MHz at room temperature.

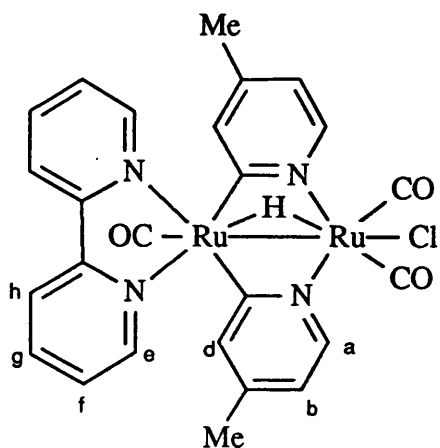
Table 4.5 (cont.)

Compound	^1H NMR data (δ) ^a
$[\text{Ru}_2(\text{CO})_5(\text{MeC}_5\text{H}_3\text{N})(\text{Me}_2\text{C}_{10}\text{H}_5\text{N}_2)]$ 4	9.08 (d, $J = 5.3$ Hz, H^{k}), 7.75 (d, $J = 0.8$ Hz, H^{h}), 7.43 (d, $J = 5.6$ Hz, H^{a}), 7.37 (d, $J = 0.8$ Hz, H^{e}), 7.29 (dd, $J = 5.4, 0.7$ Hz, H^{i}), 7.13 (d, $J = 0.8$ Hz, H^{g}), 7.05 (dd, $J = 1.9$ Hz, H^{d}), 6.29 (dd, $J = 5.6, 2.0$ Hz, H^{b}), 2.51 (s, Me), 2.27 (s, Me), 2.04 (s, Me).
$[\text{Ru}_2\text{HCl}(\text{CO})_3(\text{MeC}_5\text{H}_3\text{N})_2(\text{Me}_2\text{C}_{10}\text{H}_6\text{N}_2)]$ 5	8.71 (d, $J = 5.7$ Hz, H^{a}), 8.09 (d, $J = 5.6$ Hz, H^{e}), 7.97 (s, H^{h}), 7.35 (dd, $J = 2.0, 0.8$ Hz, H^{d}), 7.11 (dd, $J = 5.5, 0.9$ Hz, H^{f}), 6.54 (dd, $J = 5.9, 2.0$ Hz, H^{b}), 2.52 (s, Me), 2.19 (s, Me), -17.43 (s, hydride).

a. Recorded in CDCl_3 at 400 MHz at room temperature.

Table 4.5 (cont.)

Compound	^1H NMR data (δ) ^a
$[\text{Ru}_2\text{HCl}(\text{CO})_3(\text{MeC}_5\text{H}_3\text{N})_2(\text{C}_{10}\text{H}_8\text{N}_2)]$ 8	8.72 (d, $J = 5.1$ Hz, H^{a}), 8.29 (ddd, $J = 5.3, 0.9$ Hz, H^{e}), 8.16 (ddd, $J = 8.1$ Hz, H^{h}), 7.93 (ddd, $J = 7.9, 7.9,$ 1.7 Hz, H^{g}), 7.37 (dd, $J = 2.0, 0.8$ Hz, H^{d}), 7.32 (ddd, $J = 7.6, 5.3,$ 1.2 Hz, H^{f}), 6.56 (dd, H^{b}), 2.20 (s, Me). -17.82 (s, hydride).
$[\text{RuCl}_2(\text{CO})(\text{MeC}_5\text{H}_4\text{N})_3]$ 9	8.71 (dd, $J = 5.1, 1.5$ Hz, H^2), 8.50 (dd, $J = 5.3, 1.4$ Hz, 2H^2), 7.15 (d, $J = 6.2$ Hz, H^3), 6.94 (d, $J = 6.0$ Hz, 2H^3), 2.41 (s, Me), 2.33 (s, 2Me).



a. Recorded in CDCl_3 at 400 MHz at room temperature.

Table 4.6 ^{13}C NMR spectroscopic data for the two isomers of $[\text{Ru}_2(\text{CO})_6(\text{C}_5\text{H}_4\text{N})_2]$.

Compound	^{13}C NMR data (δ) ^a
$[\text{Ru}_2(\text{CO})_6(\text{C}_5\text{H}_4\text{N})_2]$ (Isomer 2a)	204.6, 201.7, 183.3, 196.1 or 185.9 (CO ligands) 196.1 or 185.9 ($\underline{\text{C}}$ -Ru), 154.5 (C^6), 139.1 (C^3), 132.9 (C^4), 119.4 (C^5).
$[\text{Ru}_2(\text{CO})_6(\text{C}_5\text{H}_4\text{N})_2]$ (Isomer 2b)	204.3, 202.0, 183.7 (CO ligands) 190.2, ($\underline{\text{C}}$ -Ru), 154.8 (C^6), 138.7 (C^3), 133.0 (C^4), 120.1 (C^5).

a. Recorded in CDCl_3 at 400 MHz at room temperature.

Table 4.7 Infrared spectroscopic data for the new compounds.

Compound	$\nu(\text{CO})^a/\text{cm}^{-1}$
$[\text{Ru}_2(\text{CO})_6(\text{C}_5\text{H}_4\text{N})_2]$ (Isomer 2a)	2071s, 2033vs, 2004vs, 1985m, 1967s
$[\text{Ru}_2(\text{CO})_6(\text{C}_5\text{H}_4\text{N})_2]$ (Isomer 2b)	2071s, 2034vs, 2003vs, 1985m, 1974s, 1968s.
$[\text{Ru}_2(\text{CO})_5(\text{C}_5\text{H}_4\text{N})(\text{C}_{10}\text{H}_7\text{N}_2)]$ 3	2051m, 1996s, 1981vs, 1958m, 1926m.
$[\text{Ru}_2(\text{CO})_5(\text{MeC}_5\text{H}_3\text{N})(\text{Me}_2\text{C}_{10}\text{H}_5\text{N}_2)]$ 4	2050s, 2001s, 1992s, 1978s, 1954m, 1922m.
$[\text{Ru}_2\text{HCl}(\text{CO})_3(\text{MeC}_5\text{H}_3\text{N})_2(\text{Me}_2\text{C}_{10}\text{H}_6\text{N}_2)]$ 5	2037s, 1968s, 1918m,br. ^b
$[\text{Ru}_2\text{HCl}(\text{CO})_3(\text{MeC}_5\text{H}_3\text{N})_2(\text{C}_{10}\text{H}_8\text{N}_2)]$ 8	2038s, 1968s, 1918m,br. ^b
$[\text{RuCl}_2(\text{CO})(\text{MeC}_5\text{H}_4\text{N})_3]$ 9	1956s. ^b

a. Recorded in cyclohexane solution unless stated otherwise.

b. Recorded in dichloromethane solution.

Table 4.8 Infrared, Mass and ^{13}C NMR Spectroscopic Data for $[\text{RuCl}_2(\text{CO})_2(\text{py})_2]$ and $[\text{RuCl}_2(\text{CO})(\text{py})_3]$.

Compound	MS ^a	Infrared		^{13}C NMR ^{d,e}
		$\nu(\text{CO})^b$	$\nu(\text{Ru-Cl})^c$	
$[\text{RuCl}_2(\text{CO})_2(\text{py})_2]$ 6	386	2067, 2004	333	194.8 (<u>C</u> O), 152.6 (2C ²), 138.8 (C ⁴), 125.2 (2C ³).
$[\text{RuCl}_2(\text{CO})(\text{py})_3]$ 7a	437	1956	335	203.9 (<u>C</u> O), 156.3 (4C ²), 152.7 (2C ²), 137.9 (C ⁴), 136.6 (2C ⁴), 124.6 (2C ³), 124.0 (4C ³).
$[\text{RuCl}_2(\text{CO})(\text{py})_3]$ 7b	437	1942	317, 250	156.5 (4C ²), 156.4 (2C ²), 137.4 (C ⁴), 137.2 (2C ⁴), 125.2 (2C ³), 124.5 (4C ³).

- Mass Spectrum obtained by Fast Atom Bombardment Technique; the parent molecular ion was observed for each compound.
- Recorded in dichloromethane solution.
- Recorded as a CsI disc.
- Recorded in CDCl_3 at 400 MHz at room temperature.
- The CO resonance in the ^{13}C NMR spectrum of **7b** was not observed, which is probably due to the low concentration of sample and poor signal-to-noise ratio of the spectrum.

Table 4.9 ^1H NMR Spectroscopic Data for $[\text{RuCl}_2(\text{CO})_2(\text{py})_2]$ and $[\text{RuCl}_2(\text{CO})(\text{py})_3]$.

Compound	^1H NMR data (δ) ^a
$[\text{RuCl}_2(\text{CO})_2(\text{py})_2]$ 6	8.86 (ddd, $J = 5.0, 1.5, 1.5$ Hz, 2H^2), 7.87 (tt, $J = 7.6, 1.6$ Hz, H^4), 7.40 (ddd, $J = 7.6, 5.1, 1.5$ Hz, 2H^3).
$[\text{RuCl}_2(\text{CO})(\text{py})_3]$ 7a	8.90 (ddd, $J = 5.0, 1.5, 1.5$ Hz, 2H^2), 8.70 (ddd, $J = 5.1, 1.5, 1.5$ Hz, 4H^2), 7.87 (tt, $J = 7.6, 1.6$ Hz, H^4), 7.65 (tt, $J = 7.6, 1.5$ Hz, 2H^4), 7.37 (ddd, $J = 7.6, 5.0, 1.4$ Hz, 2H^3), 7.14 (ddd, $J = 7.6, 5.3, 1.3$ Hz, 4H^3).
$[\text{RuCl}_2(\text{CO})(\text{py})_3]$ 7b	8.79 (ddd, $J = 5.1, 1.4, 1.4$ Hz, 4H^2), 8.55 (ddd, $J = 5.1, 1.5, 1.5$ Hz, 2H^2), 7.74 (tt, $J = 7.6, 1.5$ Hz, H^4), 7.69 (tt, $J = 7.6, 1.5$ Hz, 2H^4), 7.21 (m, $2\text{H}^3 + 4\text{H}^3$).

a. Recorded in CDCl_3 at 400 MHz at room temperature.

4.3 Experimental

Synthesis of $[\text{Ru}_2(\text{CO})_6(\text{C}_5\text{H}_4\text{N})_2]$.

A suspension of $[\text{Ru}_3(\text{CO})_{12}]$ (0.219 g, 0.342 mmol) and pyridine [0.2230 g, 2.819 mmol; 8 mol/mol $\text{Ru}_3(\text{CO})_{12}$] in n-heptane (30 cm³) was placed in a Carius tube which was then evacuated and sealed under vacuum. The tube and contents were heated at 120 °C for 72 h to give a red solution. After cooling to room temperature, the tube was opened and the solvent was removed under reduced pressure to give a deep orange-brown solid residue. The mixture was separated by TLC [SiO_2 , light petroleum (b.p. <40 °C)-dichloromethane (7:3 v/v)] and several bands collected. The top two yellow bands were identified as $[\text{Ru}_3(\text{CO})_{12}]$ (0.029 g, 13%) and the known compound $[\text{Ru}_3\text{H}(\text{CO})_{10}(\text{C}_5\text{H}_4\text{N})]$ (0.030 g, 14%) from their infrared spectra. The third colourless band was characterised as $[\text{Ru}_2(\text{CO})_6(\text{C}_5\text{H}_4\text{N})_2]$ (0.045 g, 25%). (Found: C, 36.71; H, 1.58; N, 5.19 %. Calc. for $\text{C}_{16}\text{H}_8\text{N}_2\text{O}_6\text{Ru}_2$: C, 36.51; H, 1.53; N, 5.32 %). This band was re-chromatographed by TLC [SiO_2 , light petroleum (b.p. <40 °C), six elutions] to give the separated head-to-head and head-to-tail isomers of $[\text{Ru}_2(\text{CO})_6(\text{C}_5\text{H}_4\text{N})_2]$ in an approximately 1:1 ratio. The fourth red band remains unidentified.

Alternative Synthesis of $[\text{Ru}_2(\text{CO})_6(\text{C}_5\text{H}_4\text{N})_2]$.

A suspension of $[\text{Ru}_3(\text{CO})_{12}]$ (0.258 g, 0.404 mmol) in pyridine (30 cm³) was placed in a Carius tube which was then evacuated and sealed under vacuum. The tube and contents were heated at 150 °C for 23 h to give a deep red solution. After cooling to room temperature, the tube was opened and the

solvent was removed under reduced pressure to give a deep red-brown solid residue. The mixture was separated by TLC [SiO_2 , light petroleum (b.p. <40 °C)-dichloromethane (1:1 v/v)]. The top colourless band was identified as $[\text{Ru}_2(\text{CO})_6(\text{C}_5\text{H}_4\text{N})_2]$ (0.038 g, 18%) from its infrared spectrum. Separation of the two isomers was achieved as above. Most of the reaction product, however, did not move from the baseline and this material remains unidentified.

Synthesis of $[\text{Os}_2(\text{CO})_6(\text{C}_5\text{H}_4\text{N})_2]$.

A suspension of $[\text{Os}_3(\text{CO})_{12}]$ (0.108 g, 0.119 mmol) in pyridine (30 cm³) was placed in a Carius tube which was then evacuated and sealed under vacuum. The tube and contents were heated at 220 °C for 7 days to give a clear yellow solution. After cooling to room temperature, the tube was opened and the solvent was removed under reduced pressure to give a yellow solid residue. The mixture was separated by TLC [SiO_2 , light petroleum (b.p. <40 °C)-dichloromethane (7:3 v/v)] and several bands collected. The two major colourless bands were identified as the known compounds $[\text{Os}_2(\text{CO})_6(\text{C}_5\text{H}_4\text{N})_2]$ (0.113 g, 90%) and $[\text{Os}_3\text{H}_2(\text{CO})_8(\text{C}_5\text{H}_4\text{N})_2]$ (0.013 g, 5%) from their infrared spectra.

Synthesis and isomeric separation of $[\text{Os}_2(\text{CO})_6(\text{MeC}_5\text{H}_3\text{N})_2]$.

A suspension of $[\text{Os}_3(\text{CO})_{12}]$ (0.175 g, 0.193 mmol) in γ -picoline (20 cm³) was placed in a Carius tube which was then evacuated and sealed under vacuum. The tube and contents were heated at 180 °C for 72 h to give a clear yellow solution. After cooling to room temperature, the tube was opened and

the solvent was removed under reduced pressure to give a yellow solid residue. The mixture was separated by TLC [SiO_2 , light petroleum (b.p. $<40\text{ }^\circ\text{C}$), five elutions] to give the separated head-to-head and head-to-tail isomers of the known compound $[\text{Os}_2(\text{CO})_6(\text{MeC}_5\text{H}_3\text{N})_2]$ (0.021 g, 15%), identified by their infrared spectra. Both isomers were recrystallised by dissolving in hot hexane and allowing the solution to evaporate.

Synthesis of $[\text{Ru}_2(\text{CO})_5(\text{C}_5\text{H}_4\text{N})(\text{C}_{10}\text{H}_7\text{N}_2)]$.

A suspension of $[\text{Ru}_3(\text{CO})_{12}]$ (0.225 g, 0.342 mmol) in pyridine (20 cm^3) was placed in a Carius tube which was then evacuated and sealed under vacuum. The tube and contents were heated at $180\text{ }^\circ\text{C}$ for 6 h to give a red solution. After cooling to room temperature, the tube was opened and the contents transferred to a flask. The tube was washed with dichloromethane to collect as much product as possible and the washings were added to the main solution. The solvent was removed under reduced pressure to give a deep red-brown solid residue and the mixture separated by TLC [SiO_2 , light petroleum (b.p. $<40\text{ }^\circ\text{C}$)-dichloromethane (3:1 v/v and then 1:1 v/v)] to give a major orange band and two minor yellow bands. The orange band was characterised as $[\text{Ru}_2(\text{CO})_5(\text{C}_5\text{H}_4\text{N})(\text{C}_{10}\text{H}_7\text{N}_2)]$ (0.025 g, 12%). (Found: C, 41.53; H, 1.91; N, 6.78 %. Calc. for $\text{C}_{20}\text{H}_{11}\text{N}_3\text{O}_5\text{Ru}_2$: C, 41.74; H, 1.93; N, 7.30 %).

Synthesis of $[\text{Ru}_2(\text{CO})_5(\text{MeC}_5\text{H}_3\text{N})(\text{Me}_2\text{C}_{10}\text{H}_7\text{N}_2)]$.

A suspension of $[\text{Ru}_3(\text{CO})_{12}]$ (0.227 g, 0.342 mmol) in γ -picoline (20 cm^3) was placed in a Carius tube which was then evacuated and sealed under

vacuum. The tube and contents were heated at 180 °C for 6 h to give a red solution. After cooling to room temperature, the tube was opened and the contents transferred to a flask. The tube was washed with dichloromethane to collect as much product as possible and the washings were added to the main solution. The solvent was removed under reduced pressure to give a deep red-brown solid residue and the mixture separated by TLC [SiO_2 , light petroleum (b.p. <40 °C)-dichloromethane (1:1 v/v)] to give a major yellow band, a minor yellow band which was not collected, and an orange band. The yellow band was characterised as $[\text{Ru}_2(\text{CO})_5(\text{MeC}_5\text{H}_3\text{N})(\text{Me}_2\text{C}_{10}\text{H}_5\text{N}_2)]$ (0.035 g, 16%). (Found: C, 43.73; H, 2.91; N, 6.88 %. Calc. for $\text{C}_{22}\text{H}_{17}\text{N}_3\text{O}_5\text{Ru}_2$: C, 43.64; H, 2.83; N, 6.94 %). The orange band was separated by further TLC [SiO_2 , light petroleum (b.p. <40 °C)-dichloromethane (1:4 v/v)] into an orange band which we have formulated as $[\text{Ru}_2\text{HCl}(\text{CO})_3(\mu\text{-MeC}_5\text{H}_3\text{N})_2(\text{Me}_2\text{C}_{10}\text{H}_6\text{N}_2)]$ (0.030 g, 12%), and a colourless band (0.008 g) which has not been identified.

Reaction of $[\text{Ru}_3(\text{CO})_{12}]$ with pyridine under forcing conditions.

A suspension of $[\text{Ru}_3(\text{CO})_{12}]$ (0.243 g, 0.380 mmol) in pyridine (30 cm^3) was placed in a Carius tube which was then evacuated and sealed under vacuum. The tube and contents were heated at 180 °C for 49 h to give a brown solution. After cooling to room temperature, the tube was opened and the residue extracted into dichloromethane. The solvent was removed under reduced pressure to give a brown solid residue and the mixture separated by TLC [SiO_2 , light petroleum (b.p. <40 °C)-dichloromethane (7:3 v/v followed by 1:4 v/v)] to give several bands, three of which have been characterised by their ^1H NMR and infrared spectra and by micro-analysis. The top yellow

band was identified as the known compound $[\text{RuCl}_2(\text{CO})_2(\text{C}_5\text{H}_5\text{N})_2]$ (0.035 g, 8%). (Found: C, 37.38; H, 2.81; N, 6.69; Cl, 18.61 %. Calc. for $\text{C}_{12}\text{H}_{10}\text{N}_2\text{O}_2\text{Cl}_2\text{Ru}$: C, 37.32; H, 2.60; N, 7.25; Cl, 18.36 %). The second and third yellow bands were identified as two isomers of the known compound $[\text{RuCl}_2(\text{CO})(\text{C}_5\text{H}_5\text{N})_3]$ (0.287 g, 58% for isomer A and 0.057 g, 12% for isomer B). (Found for isomer A: C, 43.64; H, 3.28; N, 9.31; Cl, 18.75 %. Found for isomer B: C, 44.32; H, 3.60; N, 8.82; Cl, 17.61 %. Calc. for $\text{C}_{16}\text{H}_{15}\text{N}_3\text{OCl}_2\text{Ru}$: C, 43.95; H, 3.46; N, 9.61; Cl, 16.21 %). Three other minor colourless bands were also observed but not characterised due to low yields.

Reaction of $[\text{Ru}_2(\text{CO})_6(\text{C}_5\text{H}_4\text{N})_2]$ (head-to-tail isomer 2b) with 4-methylpyridine.

A faint yellow solution of $[\text{Ru}_2(\text{CO})_6(\text{C}_5\text{H}_4\text{N})_2]$ (0.095 g, 0.180 mmol) in γ -picoline (8 cm³) was placed in a Carius tube which was then evacuated and sealed under vacuum. The tube and contents were heated at 180 °C for 3 h to give an orange solution. After cooling to room temperature, the tube was opened and the contents transferred to a flask. The tube was washed with dichloromethane to collect as much product as possible and the washings were added to the main solution. The solvent was removed under reduced pressure to give an orange-brown solid residue and the mixture separated by TLC [SiO_2 , light petroleum (b.p. <40 °C)-dichloromethane (1:1 v/v and then 1:2 v/v)] to give an orange band (0.009 g) and three minor colourless or yellow bands which were discarded. The orange band was itself a three-component mixture from which orange crystals of $[\text{Ru}_2\text{HCl}(\text{CO})_3(\text{MeC}_5\text{H}_3\text{N})_2(\text{C}_{10}\text{H}_8\text{N}_2)] \cdot \text{H}_2\text{O}$ were isolated by adding a layer of

methanol on to a dichloromethane solution and allowing slow diffusion to occur below freezing-point. The ^1H NMR spectra of the remaining two compounds in this mixture were identical to those observed for two of the compounds produced in the reaction between $[\text{Ru}_3(\text{CO})_{12}]$ and γ -picoline, one of which we have formulated as $[\text{Ru}_2\text{HCl}(\text{CO})_3(\text{MeC}_5\text{H}_3\text{N})_2(\text{Me}_2\text{C}_{10}\text{H}_6\text{N}_2)]$ and the other is unknown.

Reaction of $[\text{Ru}_2(\text{CO})_6(\text{C}_5\text{H}_4\text{N})_2]$ (head-to-head isomer 2a) with 4-methylpyridine.

A faint yellow solution of $[\text{Ru}_2(\text{CO})_6(\text{C}_5\text{H}_4\text{N})_2]$ (0.024 g, 0.046 mmol) in γ -picoline (4 cm³) was placed in a Carius tube which was then evacuated and sealed under vacuum. The tube and contents were heated at 180 °C for 2 h to give an orange solution. After cooling to room temperature, the tube was opened and the contents transferred to a flask. The tube was washed with dichloromethane to collect as much product as possible and the washings were added to the main solution. The solvent was removed under reduced pressure to give an orange-brown solid residue and the mixture separated by TLC [SiO_2 , light petroleum (b.p. <40 °C)-dichloromethane (1:1 v/v)] to give a major yellow band (0.007 g) and a minor yellow band which was discarded. Infrared and ^1H NMR spectra are consistent with the formulation of $[\text{RuCl}_2(\text{CO})(\text{MeC}_5\text{H}_4\text{N})_3]$ for this species, and are similar to the analogous pyridine compounds, although because of low yields and the absence of micro-analytical data, the formulation is uncertain.

X-ray structure determination for [Ru₂(CO)₅(C₅H₄N)(C₁₀H₇N₂)].

Crystals were obtained by adding a layer of methanol to a dichloromethane solution and allowing slow diffusion to occur.

A red crystal of the compound [Ru₂(CO)₅(μ -C₅H₄N)(μ -C₁₀H₇N₂)], $M = 575.48 \text{ gmol}^{-1}$, with dimensions $0.28 \times 0.16 \times 0.06 \text{ mm}^3$ was mounted on a thin glass fibre on a Nicolet R3v/m automatic four-circle diffractometer. The crystal did not diffract strongly, probably because of its small size. A monoclinic cell, $a = 24.456(9)$, $b = 11.791(5)$, $c = 14.113(4) \text{ \AA}$, $\beta = 100.65(3)^\circ$, $U = 3999(2) \text{ \AA}^3$, was determined by auto-indexing and least-squares fitting of 23 orientation reflections in the range $9 \leq 2\theta \leq 22^\circ$, selected from a rotation photograph. The cell parameters and crystal system were confirmed by taking axial photographs. A total of 3471 unique intensity data were collected at room temperature using graphite-monochromated Mo-K α radiation ($\lambda = 0.71073 \text{ \AA}$) with the diffractometer operating in the ω scan mode between the limits $5 \leq 2\theta \leq 50^\circ$. The reflection intensities were corrected for Lorentz and polarisation effects and for decay by fitting the data to a curve calculated from three standard reflections collected periodically throughout the experiment. The data were finally corrected for absorption using the asimuthal scan method, $\mu(\text{Mo-K}\alpha) = 15.17 \text{ cm}^{-1}$.

The structure was solved by routine application of direct methods, in the space group $C2/c$ (assigned as $C2/c$ or Cc from examination of the systematic absences, the former giving the more satisfactory structure solution and refinement), $Z = 8$, $F(000) = 2240$, $D_c = 1.91 \text{ g cm}^{-3}$. The model, with 131 parameters, was refined to $R = 0.0638$, $R_w = 0.0595$,* using 1843 intensity data with $I_0 \geq 3\sigma(I_0)$ by alternating cycles of full-matrix least-squares and by

difference Fourier synthesis. Only the ruthenium atoms were refined anisotropically and H atoms were included in the final model in idealised positions with C–H distances fixed at 0.96 Å and isotropic thermal parameter $U = 0.08 \text{ \AA}^2$ but their positions were not allowed to refine. The structural problem of the orientation of the $\text{C}_5\text{H}_4\text{N}$ ligand was solved by attempting a refinement with the Ru-bonded atoms reversed. Less realistic thermal parameters for these atoms were calculated for this alternative orientation. The largest shift-to-error ratio in the final least-squares cycle was 0.002 and the largest peak in the final difference Fourier map was 1.21 e/\AA^3 , found close to Ru(2).

Fractional atomic coordinates for $[\text{Ru}_2(\text{CO})_5(\mu\text{-C}_5\text{H}_4\text{N})(\mu\text{-C}_{10}\text{H}_7\text{N}_2)]$ are given in Table A4 in the appendix. All calculations were performed on a MicroVax II computer running SHELXTL PLUS.¹⁴¹

$$^* R = \Sigma [|F_o| - |F_c|] / \Sigma |F_o|$$

$$R_w = [\Sigma w(|F_o| - |F_c|)^2 / \Sigma w|F_o|^2]^{1/2}$$

$$w = 1/[\sigma^2(F_o) + 0.000316F_o^2]$$

X-ray structure determination for $[\text{Ru}_2\text{HCl}(\text{CO})_3(\text{MeC}_5\text{H}_3\text{N})_2(\text{C}_{10}\text{H}_8\text{N}_2)] \cdot \text{H}_2\text{O}$.

Crystals were obtained by adding a layer of methanol on to a dichloromethane solution and allowing slow diffusion to occur below freezing-point.

A red crystal of the compound $[\text{Ru}_2\text{HCl}(\text{CO})_3(\text{MeC}_5\text{H}_3\text{N})_2(\text{C}_{10}\text{H}_8\text{N}_2)] \cdot \text{H}_2\text{O}$, $M = 681.103 \text{ gmol}^{-1}$, with dimensions $0.18 \times 0.16 \times 0.12 \text{ mm}^3$ was mounted on a thin glass fibre on a Nicolet R3v/m automatic four-circle diffractometer. An

orthorhombic cell, $a = 15.854(6)$, $b = 17.361(9)$, $c = 18.96(1)$ Å, $U = 5217(3)$ Å³, was determined by auto-indexing and least-squares fitting of 24 orientation reflections in the range $7 \leq 2\theta \leq 19^\circ$, selected from a rotation photograph. The cell parameters and crystal system were confirmed by taking axial photographs. A total of 4473 unique intensity data were collected at room temperature using graphite-monochromated Mo-K α radiation ($\lambda = 0.71073$ Å) with the diffractometer operating in the ω - 2θ scan mode between the limits $5 \leq 2\theta \leq 50^\circ$. The reflection intensities were corrected for Lorentz and polarisation effects and for decay by fitting the data to a curve calculated from three standard reflections collected periodically throughout the experiment. The data were finally corrected for absorption using the asimuthal scan method, $\mu(\text{Mo-K}\alpha) = 12.71 \text{ cm}^{-1}$.

The structure was solved by routine application of direct methods, in the space group $Pbcn$, $Z = 8$, $F(000) = 2616$, $D_c = 1.69 \text{ g cm}^{-3}$. The model, with 158 parameters, was refined to $R = 0.0621$, $R_w = 0.0617$,* using 1583 intensity data with $I_0 \geq 3\sigma(I_0)$ by alternating cycles of full-matrix least-squares and by difference Fourier synthesis. Only the ruthenium and chlorine atoms were refined anisotropically and H atoms for the 2-pyridyl ligands were included in the model in idealised positions with C-H distances fixed at 0.96 Å and isotropic thermal parameter $U = 0.08 \text{ Å}^2$ but their positions were not allowed to refine. The hydrogen atoms of the water molecule were not included in the model. The largest shift-to-error ratio in the final least-squares cycle was 0.014 and the largest peak in the final difference Fourier map was 0.79 e/Å^3 , found close to O(41).

Fractional atomic coordinates for the compound

$[\text{Ru}_2\text{HCl}(\text{CO})_3(\text{MeC}_5\text{H}_3\text{N})_2(\text{C}_{10}\text{H}_8\text{N}_2)]\cdot\text{H}_2\text{O}$ are given in Table A5 in the appendix. All calculations were performed on a MicroVax II computer running SHELXTL PLUS.¹⁴¹

$$^*R = \Sigma [|F_o| - |F_c|] / \Sigma |F_o|$$

$$R_w = [\Sigma w(|F_o| - |F_c|)^2 / \Sigma w|F_o|^2]^{1/2}$$

$$w = 1/[\sigma^2(F_o) + 0.000872F_o^2]$$

X-ray structure determination for the head-to-tail isomer of $[\text{Os}_2(\text{CO})_6(\text{MeC}_5\text{H}_3\text{N})_2]$.

Crystals were obtained by evaporation from a hot hexane solution of the compound.

A colourless crystal of the compound $[\text{Os}_2(\text{CO})_6(\text{MeC}_5\text{H}_3\text{N})_2]$, $M = 732.72 \text{ gmol}^{-1}$, with dimensions $0.40 \times 0.35 \times 0.30 \text{ mm}^3$ was mounted on a thin glass fibre on a Nicolet R3v/m automatic four-circle diffractometer. A monoclinic cell, $a = 8.526(2)$, $b = 17.585(7)$, $c = 13.689(5) \text{ \AA}$, $\beta = 106.77(2)^\circ$, $U = 1965(1) \text{ \AA}^3$, was determined by auto-indexing and least-squares fitting of 30 orientation reflections in the range $8 \leq 2\theta \leq 26^\circ$, selected from a rotation photograph. The cell parameters and crystal system were confirmed by taking axial photographs. A total of 3448 unique intensity data were collected at room temperature using graphite-monochromated Mo- K_α radiation ($\lambda = 0.71073 \text{ \AA}$) with the diffractometer operating in the ω - 2θ scan mode between the limits $5 \leq 2\theta \leq 50^\circ$. The reflection intensities were corrected for Lorentz and polarisation effects and for decay by fitting the data to a curve calculated from three standard reflections collected periodically throughout the experiment.

The data were finally corrected for absorption using the asimuthal scan method, $\mu(\text{Mo-K}\alpha) = 129.68 \text{ cm}^{-1}$.

The structure was solved by routine application of direct methods, in the space group $P2_1/c$, $Z = 4$, $F(000) = 1336$, $D_c = 2.48 \text{ g cm}^{-3}$. The model, with 253 parameters, was refined to $R = 0.0533$, $R_w = 0.0485$,* using 2782 intensity data with $F_0 \geq 3\sigma(F_0)$ by alternating cycles of full-matrix least-squares and by difference Fourier synthesis. All non-hydrogen atoms were refined anisotropically and H atoms were included in the final model in idealised positions with C–H distances fixed at 0.96 Å and isotropic thermal parameter $U = 0.08 \text{ Å}^2$ but their positions were not allowed to refine. The largest shift-to-error ratio in the final least-squares cycle was 0.001 and the largest peak in the final difference Fourier map was 1.62 e/Å^3 , found close to Os(1).

Fractional atomic coordinates for the head-to-tail isomer of $[\text{Os}_2(\text{CO})_6(\text{MeC}_5\text{H}_3\text{N})_2]$ are given in Table A6 in the appendix. All calculations were performed on a MicroVax II computer running SHELXTL PLUS.¹⁴¹

$$* R = \Sigma [|F_o| - |F_c|] / \Sigma |F_o|$$

$$R_w = [\Sigma w(|F_o| - |F_c|)^2 / \Sigma w|F_o|^2]^{1/2}$$

$$w = 1/[\sigma^2(F_o) + 0.0002F_o^2]$$

CHAPTER FIVE**Higher Nuclearity Ruthenium Carbonyl****Complexes Derived From**

5.1 Introduction.

As stated previously, the pyridine-2-thionato ligand (pyS) is known to bond to metal atoms in a variety of ways. Even in the triply-bridging mode, in which bonds are formed through both heteroatoms and in which form the ligand donates a total of five electrons, there is still a lone-pair of electrons at the S atom, giving the potential to behave as a seven-electron donor by bridging four metal atoms. Previous attempts to achieve this situation of maximum electron donation have led to an alternative C–S bond cleavage as, for example, in the formation of the μ -2-pyridyl compound $[\text{Ru}_3\text{Re}(\mu_4\text{-S})(\mu\text{-C}_5\text{H}_4\text{N})(\text{CO})_{14}]^{76}$ and similar compounds, as described in Chapter Two, in which the original pyS ligand donates nine electrons as the separated $\mu_4\text{-S}$ and μ -2-pyridyl ligands. Recently, however, a novel cluster condensation process has been reported⁷⁹ whereby a μ_3 -pyS ligand makes a new M–S bond and in doing so links trinuclear clusters through μ_4 -bridges. The compound $[\text{Ru}_3(\mu\text{-H})(\mu_3\text{-pyS})(\text{CO})_9]$, which is shown in Figure 5.1, undergoes double decarbonylation and trimerisation to give $[\{\text{Ru}_3(\mu_3\text{-H})(\mu_4\text{-pyS})(\text{CO})_7\}_3]$ (Figure 5.2).

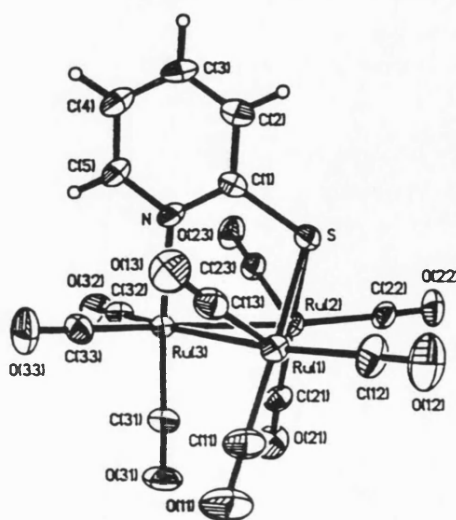
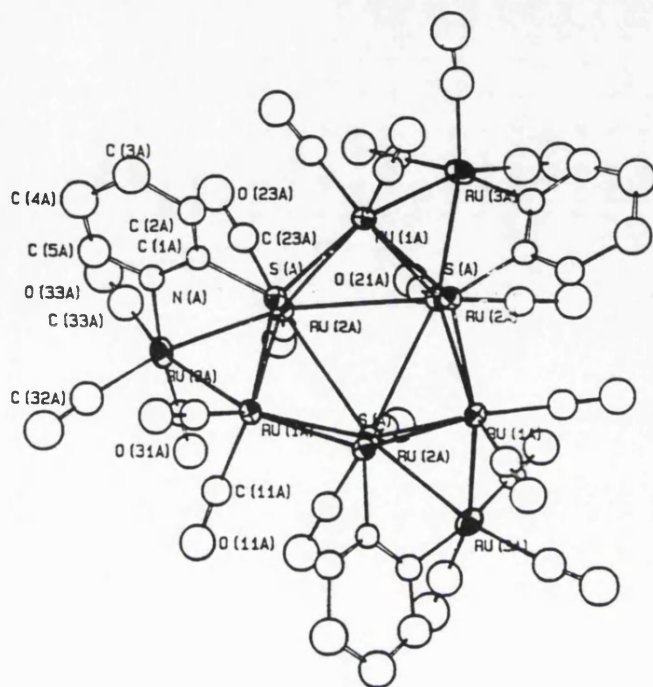
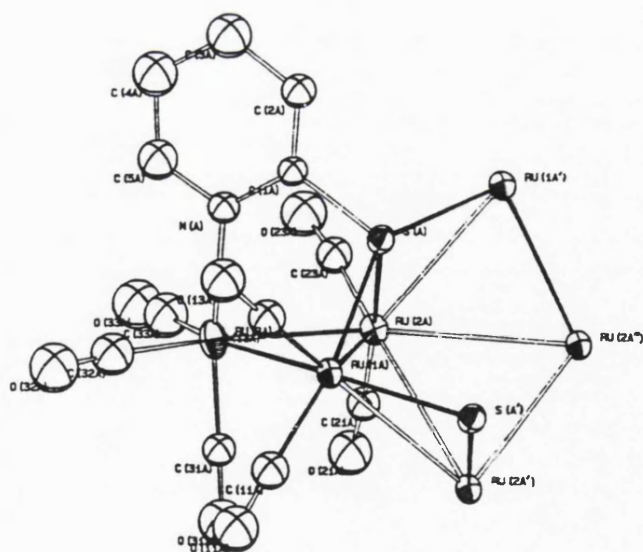


Figure 5.1 Molecular Structure of $[\text{Ru}_3(\mu\text{-H})(\mu_3\text{-pyS})(\text{CO})_9]$.

Figure 5.2 Molecular structure of $[\{\text{Ru}_3(\mu_3\text{-H})(\mu_4\text{-pyS})(\text{CO})_7\}_3]$.



- a. One of the independent molecules in the unit cell.



- b. One Ru_3 component of this molecule, showing the coordination environments of Ru(1) and Ru(2) which are those linked to other Ru_3 units. (The long Ru–Ru contacts are shown as broken lines).

The loss of CO is partially compensated for by the formation of these extra Ru–S bonds which link the Ru₃ units through a six membered RuSRuSRuS ring, but this effect is supplemented by the formation of six long-range Ru–Ru contacts (3.2-3.3 Å) between the clusters. Without these long-range Ru–Ru contacts, the molecule would be unsaturated. A similar process is occurring when the sulphur-capped compound [Ru₃(μ-H)₂(μ₃-S)(CO)₉] is decarbonylated to give [{Ru₃(μ-H)₂(μ₄-S)(CO)₈]₃]. Trimerisation, via the formation of three new Ru–S bonds, occurs in which the three Ru₃ cluster units are linked through μ₄-S bridges to give an analogous six-membered Ru₃S₃ ring in the chair conformation.²⁰⁶ In this case, the Ru₉ system is electron-precise without Ru–Ru bonds between the Ru₃ sub-units.

The synthesis of high nuclearity transition metal cluster compounds is a subject that has received considerable attention,^{146,233} one general method being the fusion of smaller clusters into larger ones as in the formation of [Os₆(CO)₁₈] from [Os₃(CO)₁₂].²³⁴ Frequently, ligands are employed which assist the fusion by acting in the early stages to form bridges between participating clusters and to stabilise the newly-formed large cluster. Sulphido^{96,206-7,235} and phosphido¹⁶⁷⁻⁷⁶ ligands and other sulphur- and phosphorus-containing ligands have commonly been used. Clusters formed *via* linkage of trinuclear osmium or ruthenium carbonyl compounds through bridging ligands have been classified into three types, depending on the nature of the interaction between the linked clusters.²³⁶ Clusters of type A have minimal contact between the M₃ components, while those of type B have completely fused to give an M₆ cluster. There also exists an intermediate situation in which separate clusters persist, but for which there are clear

intercluster metal-metal bonding contacts which control the superstructure of the aggregated system (type C). A variety of bridging ligands have been used to synthesise clusters of type A, including acetylenic acid $\text{HC}_2\text{CO}_2\text{H}$ (carboxylate and alkyne linkages)²³⁷ and ferrocene derivatives such as $[\text{Fe}(\text{C}_5\text{H}_4\text{CHO})_2]$ (acyl linkages)²³⁸ as well as mercury and gold species. These metal atoms can link clusters either *via the* formation of bonds directly to the metal atoms²³³ or by forming bonds to coordinated ligands such as phosphinidene.²³⁹ Complete fusion into new, larger clusters of type B has been achieved in many cases, especially with S- and P-based ligands and some of this work was described in Chapter Three. Adams has developed a rich chemistry based on cluster aggregation using sulphido ligands.¹¹⁰ For instance, two triosmium units are linked by the formation of a $\mu_4\text{-S}$ bridge and an Os–Os bond in the compounds $[\text{Os}_6\text{H}_4(\text{CO})_{15}(\mu_4\text{-S})(\mu_3\text{-S})(\mu\text{-HC=NPh})_2]$ and $[\text{Os}_6\text{H}_6(\text{CO})_{14}(\mu_4\text{-S})(\mu_3\text{-S})(\mu\text{-HC=NPh})_2]$.¹³⁹ Several authors have reported a wide variety of high nuclearity metal clusters with phosphine ligands and some of these contain fused trinuclear clusters.¹⁶⁷⁻⁷⁶ Thermolysis of $[\text{Os}_6\text{H}_2(\text{CO})_{21}(\text{PH})]$, a cluster of type A, in which the two Os_3 groups are linked by a bridging phosphinidene group, results in closure of the metal framework to give $[\text{Os}_6\text{H}(\text{CO})_{18}\text{P}]$, which has a trigonal prismatic structure of type B containing an interstitial phosphorus atom.²⁴⁰ Other examples include the hexaruthenium complexes $[\text{Ru}_6(\text{PPh})_4(\text{CO})_{12}]$ and $[\text{Ru}_6\text{H}_2(\text{PPh})_4(\text{CO})_{12}]$, which are formed from the thermolysis of $[\text{Ru}_3(\text{PPh})_2(\text{CO})_9]$ under H_2 .²⁴¹ These two hexaruthenium compounds have distorted and regular trigonal prismatic geometries respectively.^{167,241} The non-hydride complex can also be formed from direct reaction of PPhH_2 with $[\text{Ru}_3(\text{CO})_{12}]$, which also leads to a related cluster,

$[\text{Ru}_6(\text{PPh})_5(\text{CO})_{12}]$, of similar geometry.¹⁶⁷ The only example of a cluster of type C is $[\{\text{Ru}_3(\mu_3\text{-H})(\mu_4\text{-pyS})(\text{CO})_7\}_3]$, discussed above.⁷⁹ The cluster units remain essentially unperturbed except for the six long-range Ru–Ru bonds formed between them.

We believed that by carrying out the thermolysis of $[\text{Ru}_3(\mu\text{-H})(\mu_3\text{-pyS})(\text{CO})_9]$ under an atmosphere of CO, the formation of the 'trimer of trimers' would be inhibited and that C–S bond cleavage would occur to give a cluster such as $[\text{Ru}_3(\mu\text{-H})(\mu_3\text{-S})(\mu\text{-2-pyridyl})(\text{CO})_9]$. There is a direct precedence for this C–S cleavage in the conversion of $[\text{Os}_3(\mu\text{-H})(\mu_3\text{-RN=CHS})(\text{CO})_9]$ into $[\text{Os}_3(\mu\text{-H})(\mu_3\text{-S})(\mu\text{-RN=CH})(\text{CO})_9]$.¹⁰⁹ We were hoping that this compound too could then be induced to undergo a trimerisation reaction.

This chapter describes the thermolysis reaction of $[\text{Ru}_3(\mu\text{-H})(\mu_3\text{-pyS})(\text{CO})_9]$ in the presence of CO, which led to unexpected products, investigations into other routes to $[\{\text{Ru}_3(\mu_3\text{-H})(\mu_4\text{-pyS})(\text{CO})_7\}_3]$, and also our attempts to synthesise $[\text{Ru}_3(\mu\text{-H})(\mu_3\text{-S})(\mu\text{-2-pyridyl})(\text{CO})_9]$. Investigations on the analogous osmium system are also described.

5.2 Results and Discussion.

A refluxing *n*-decane solution of the cluster $[\text{Ru}_3(\mu\text{-H})(\mu_3\text{-pyS})(\text{CO})_9]$, under an atmosphere of CO, changes from orange to dark green over 1.5 hours and deep green crystals of $[\text{Ru}_6(\mu_4\text{-S})(\mu\text{-SH})(\mu_3\text{-pyS})(\mu\text{-CO})_2(\text{CO})_{15}]$ **1** were isolated by TLC on silica. Other products, together with $[\text{Ru}_3(\text{CO})_{12}]$ and starting material were also recovered from the reaction vessel (Section 5.3). Lower boiling solvents gave little reaction. Longer reaction times in decane gave differing product ratios and increased the amount of decomposition, evident by lower yields. The ^1H NMR spectrum (data in Table 5.3) showed that the hydride ligand had been removed but that the 2-pyridyl group was still present, although we could not tell whether the C–S bond had been cleaved or not. An increase in the complexity in the carbonyl-stretching region of the infrared spectrum (data in Table 5.4) and a highest-mass peak of $m/e = 1258$ in the mass spectrum indicated that simple C–S bond cleavage to give the expected compound, $[\text{Ru}_3\text{H}(\text{S})(\text{C}_5\text{H}_4\text{N})(\text{CO})_9]$, or any other Ru_3 derivative, had not occurred. An X-ray diffraction experiment revealed that a hexaruthenium compound of stoichiometry $[\text{Ru}_6(\mu_4\text{-S})(\mu\text{-SH})(\mu_3\text{-pyS})(\text{CO})_{17}]$ had been formed. The crystal structure is shown in Figure 5.3 and selected bond lengths and angles are in Tables 5.1 and 5.2. Crystals of **1** are monoclinic and there are two independent molecules in the unit cell which are structurally very similar. Each molecule consists of two Ru_3 units joined by a $\mu_4\text{-S}$ atom and two extra metal-metal bonds to give a 'boat' conformation of the six metal atoms. Thus, the compound belongs to type B in the classification system discussed in Section 5.1.

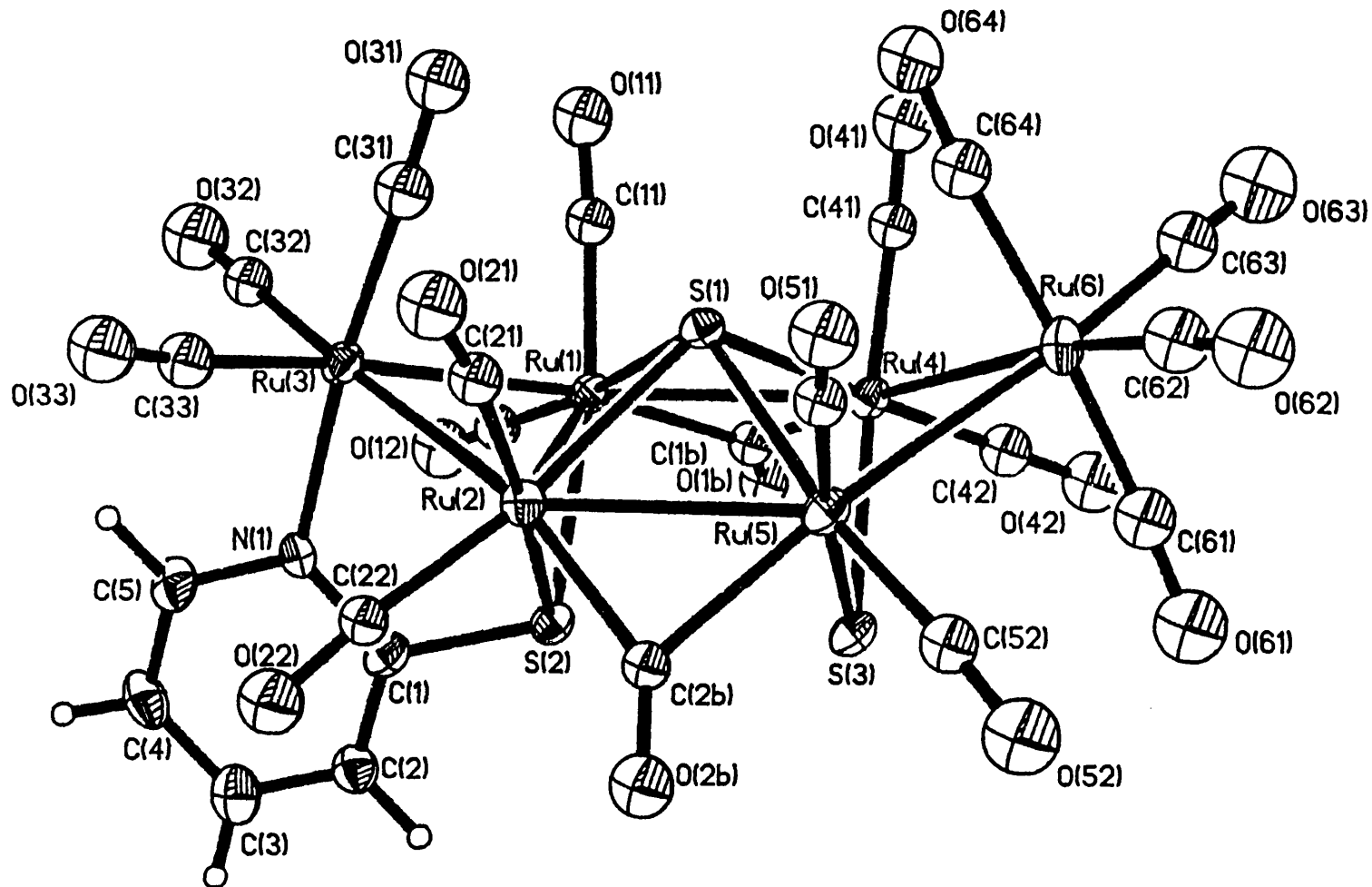


Figure 5.3 Molecular structure of $[\text{Ru}_6(\mu_4\text{-S})(\mu\text{-SH})(\mu_3\text{-pyS})(\text{CO})_{17}]$ showing one of the two independent molecules in the unit cell.

Table 5.1 Selected bond lengths (Å) for $[\text{Ru}_6(\mu_4\text{-S})(\mu\text{-SH})(\mu_3\text{-pyS})(\text{CO})_{17}]$.

	Molecule 1	Molecule 2
Ru(1)-Ru(2)	3.100(1)	3.083(2)
Ru(1)-Ru(3)	2.762(1)	2.770(2)
Ru(2)-Ru(3)	2.775(2)	2.789(2)
Ru(4)-Ru(5)	3.160(2)	3.163(2)
Ru(4)-Ru(6)	2.831(2)	2.837(2)
Ru(5)-Ru(6)	2.830(2)	2.831(2)
Ru(1)-Ru(4)	2.916(1)	2.930(2)
Ru(2)-Ru(5)	2.909(2)	2.926(2)
Ru(1)-S(1)	2.495(3)	2.495(4)
Ru(2)-S(1)	2.488(3)	2.490(3)
Ru(4)-S(1)	2.451(3)	2.453(4)
Ru(5)-S(1)	2.443(3)	2.450(4)
Ru(1)-S(2)	2.452(3)	2.449(3)
Ru(2)-S(2)	2.445(3)	2.443(3)
Ru(4)-S(3)	2.462(4)	2.446(3)
Ru(5)-S(3)	2.467(3)	2.468(3)
Ru(3)-N(1)	2.14(1)	2.18(1)

Table 5.1 (cont.)**Carbonyl ligand averages**

	Molecule 1	Molecule 2
Terminal Ru-CO	1.876	1.872
Bridging Ru-CO	2.132	2.124
Terminal RuC-O	1.154	1.166
Bridging RuC-O	1.152	1.162

Table 5.2 Selected bond angles (°) for $[\text{Ru}_6(\mu_4\text{-S})(\mu\text{-SH})(\mu_3\text{-pyS})(\text{CO})_{17}]$.

	Molecule 1	Molecule 2
Ru(1)-Ru(2)-Ru(3)	55.8(1)	56.0(1)
Ru(1)-Ru(3)-Ru(2)	68.1(1)	67.4(1)
Ru(2)-Ru(1)-Ru(3)	56.2(1)	56.6(1)
Ru(4)-Ru(5)-Ru(6)	56.1(1)	56.2(1)
Ru(4)-Ru(6)-Ru(5)	67.9(1)	67.8(1)
Ru(5)-Ru(4)-Ru(6)	56.1(1)	56.0(1)
Ru(1)-Ru(2)-Ru(5)	90.7(1)	90.6(1)
Ru(2)-Ru(1)-Ru(4)	90.5(1)	91.0(1)
Ru(1)-Ru(4)-Ru(5)	89.4(1)	89.0(1)
Ru(2)-Ru(5)-Ru(4)	89.4(1)	89.5(1)
Ru(1)-Ru(4)-Ru(6)	136.4(1)	138.7(1)
Ru(2)-Ru(5)-Ru(6)	136.5(1)	139.0(1)
Ru(4)-Ru(1)-Ru(3)	141.4(1)	143.3(1)
Ru(5)-Ru(2)-Ru(3)	141.1(1)	142.8(1)
Ru(1)-S(2)-Ru(2)	78.6(1)	78.2(1)
Ru(1)-Ru(2)-S(2)	50.8(1)	51.0(1)
Ru(2)-Ru(1)-S(2)	50.6(1)	50.8(1)
Ru(4)-S(3)-Ru(5)	79.7(1)	80.1(1)
Ru(4)-Ru(5)-S(3)	50.1(1)	49.6(1)
Ru(5)-Ru(4)-S(3)	50.2(1)	50.2(1)
Ru(1)-S(1)-Ru(2)	76.9(1)	76.4(1)
Ru(1)-Ru(2)-S(1)	51.6(1)	51.9(1)

Table 5.2 (cont.)

	Molecule 1	Molecule 2
Ru(2)-Ru(1)-S(1)	51.4(1)	51.7(1)
Ru(4)-S(1)-Ru(5)	80.4(1)	80.3(1)
Ru(4)-Ru(5)-S(1)	49.9(1)	49.9(1)
Ru(5)-Ru(4)-S(1)	49.7(1)	49.8(1)
Ru(1)-S(1)-Ru(4)	72.3(1)	72.6(1)
Ru(1)-Ru(4)-S(1)	54.6(1)	54.4(1)
Ru(4)-Ru(1)-S(1)	53.2(1)	53.0(1)
Ru(2)-S(1)-Ru(5)	72.3(1)	72.6(1)
Ru(2)-Ru(5)-S(1)	54.6(1)	54.3(1)
Ru(5)-Ru(2)-S(1)	53.1(1)	53.1(1)
Ru(1)-S(1)-Ru(5)	120.0(1)	119.5(1)
Ru(2)-S(1)-Ru(4)	119.8(1)	120.4(1)
Ru(1)-S(2)-C(1)	104.4(5)	104.1(4)
Ru(2)-S(2)-C(1)	101.9(4)	103.3(5)
S(2)-C(1)-N(1)	118.2(9)	120.2(9)
Ru(3)-N(1)-C(1)	122.1(8)	120.1(9)
Ru(1)-Ru(3)-N(1)	87.2(3)	87.0(3)
Ru(2)-Ru(3)-N(1)	87.1(3)	88.1(3)

There remains an intact, triply-bridging pyS ligand bonded to one of the trimeric units, as in the starting material (Figure 5.1). However, at the other trimeric unit, C-S bond cleavage and loss of the 2-pyridyl ligand has occurred and all that remains of the original pyS is a μ -SH ligand. We could not locate the SH resonance in the ^1H NMR spectrum which would normally occur in the range -4 to 4 ppm.²⁴² For example, the SH signal in $[\text{Ru}_5(\mu\text{-H})(\mu\text{-SH})\text{C}(\text{CO})_{14}]$ comes at -3.02 ppm.²⁴³ This may have been due to rapid exchange with any residual water in the sample or possibly because of an accidental coincidence with traces of hydrocarbon which were also observed in the spectrum. It is often quite difficult to obtain samples totally free from solvent impurities. However, there is a broad absorption at 2481 cm^{-1} in the infrared spectrum which may be due to the S-H vibration. This can be compared with $\nu(\text{S-H})$ of 2545 cm^{-1} in the compound $[\text{W}(\text{PMe}_3)_4(\text{H})_2(\text{SH})_2]$ in which the SH ligands are terminal,²⁴⁴ while S-H vibrations in organic molecules come at around $2650\text{-}2550\text{ cm}^{-1}$.²⁴⁵ The distances between the μ_4 -S atom and the four ruthenium atoms it bridges range from 2.443(3) to 2.495(4) Å, with an average value of 2.47 Å. This is similar to the average M-S bond length observed for quadruply bridging sulphido ligands in the clusters $[\text{Ru}_5(\text{CO})_{15}(\mu_4\text{-S})]$ (2.42 Å), $[\text{Ru}_6(\text{CO})_{18}(\mu_4\text{-S})]$ (2.43 Å) and $[\text{Ru}_7(\text{CO})_{21}(\mu_4\text{-S})]$ (2.42 Å).¹⁸⁵ The sulphido ligand frequently acts as a quadruply-bridging ligand in the presence of four metal atoms, either in a discrete unit¹¹⁰ or within clusters containing a greater number of metal atoms.^{96,185,207,235,246} If all the metal atoms lie on the same side of a plane that passes through the sulphido ligand, *i.e.* if the S atom is pyramidal, it is regarded as a four-electron donor and it contains a lone-pair of electrons. The ligand then has only three

orbitals for use in bonding to the four metal atoms. Although the bonding is difficult to describe in terms of valence-bond theory, it fits naturally into the framework of the delocalised bonding scheme of the polyhedral skeletal electron pair (PSEP) theory.¹¹⁰

We can compare the Ru–Ru bond lengths within the pyS-bridged trimeric unit with those of the parent compound $[\text{Ru}_3(\mu\text{-H})(\mu_3\text{-pyS})(\text{CO})_9]$.⁷⁹ There are two short Ru–Ru bonds in the range 2.762–2.789 Å, which are similar to those of 2.774–2.790 Å in the parent. However, the Ru–Ru bond bridged by the S atom is significantly longer, at 3.083–3.100 Å, than the analogous bond of 2.841 Å in the parent compound. There is a similar pattern of two short bonds (2.830–2.837 Å) and one long (3.160–3.163 Å) in the other trimeric unit. The Ru–Ru bonds that join the two trimeric units are in the range 2.909–2.930 Å. Counting the pyramidal $\mu_4\text{-S}$ ligand as a four-electron donor and the bridging SH and pyS ligands as three- and five-electron donors respectively, a simple electron count predicts seven metal-metal bonds. However there are a total of eight in the actual molecule, six of which are in the range expected for a normal Ru–Ru single bond (2.7–3.0 Å) and two longer distances (3.083–3.161 Å). Clearly there is some kind of delocalisation effect operating in this electron-rich system, whereby six electrons are shared between the four metal centres that form the square plane linking the two Ru_3 units. Elongation of certain metal-metal bonds within a cluster has been observed previously in the compounds $[\text{Ru}_4(\text{CO})_{13}(\mu\text{-PPh}_2)_2]$ and $[\text{Ru}_4(\text{CO})_{10}(\mu\text{-PPh}_2)_4]$,²⁴⁷ which adopt a butterfly structure, and in several other carbonyl clusters.^{167,248–55} The Ru–Ru bonds bridged by the $\mu\text{-PPh}_2$ ligands show considerable elongation with respect to a normal Ru–Ru single bond, the average length of 3.100 Å

being greater by approximately 0.28 Å than that of 2.8175(6) Å found in the phosphido-bridged ruthenium dimer $[\text{Ru}_2(\text{CO})_6(\mu\text{-PPh}_2)_2]$.²⁴⁷ The remaining, non-bridged Ru–Ru bonds are in the expected range for Ru–Ru single bonds in electron-precise cluster complexes. Both these electron-rich complexes were described as having an additional two electrons placed in an orbital which contains a significant amount of metal-metal anti-bonding character, giving rise to the observed bonding characteristics. There is a direct comparison with the bonding in these Ru_4 clusters and in $[\text{Ru}_6(\mu_4\text{-S})(\mu\text{-SH})(\mu_3\text{-pyS})(\text{CO})_{17}]$. We can consider this hexanuclear molecule as an approximately square-planar Ru_4 unit containing ten CO ligands, bridged by two $\text{Ru}(\text{CO})_4$ units (each being two-electron donors), an SH and an SR ligand (both three-electron donors) and a $\mu_4\text{-S}$ ligand (four-electron donor). This would give a 66-electron species. However, the electron count associated with a square configuration containing 4 M–M bonds is 64 ($4 \times 18 - 4 \times 2$). The two extra electrons are placed in orbitals with significant anti-bonding character, *i.e.* the HOMO is anti-bonding between certain metal atoms of the square. The net anti-bonding effect is manifest in a lengthening of two Ru–Ru bonds within the 66-electron expanded square. In this molecule, the anti-bonding interactions are between Ru(1) and Ru(2) and between Ru(4) and Ru(5) (average bond length = 3.127 Å), while the bonding interactions are between Ru(1) and Ru(4) and between Ru(2) and Ru(5) (av. 2.920 Å).

A very similar ruthenium atom framework has been observed in one of the compounds obtained from the reaction between $[\text{Ru}_3(\text{CO})_{12}]$ and thioureas.¹⁷⁹ $[\text{Ru}_6(\mu_4\text{-S})(\mu_3\text{-EtNCSNHET})(\mu_3\text{-EtNCSNHET})(\text{CO})_{16}]$ **2**, which is shown in Figure 5.4, is pseudo-isoelectronic with compound **1**, the thioureato

ligand corresponding to the pyS ligand in 1. The principal difference between the two compounds is that on C–S cleavage of the thiourea group attached to one of the Ru₃ units in compound 2, the resulting diaminocarbene fragment is retained in the molecule, whereas the 2-pyridyl ligand produced from C–S cleavage of the pyS ligand in 1 is lost and the sulphur atom is retained as a bridging SH ligand. As in 1, the ligands donate a total of 46 electrons to the metal framework and since only 44 are required for a boat-type cluster with eight metal-metal bonds, the system is electron-rich. There is a similar pattern of two short bonds (2.758(3)–2.768(3) Å) and one long (3.081(3) and 3.231(3) Å) within each trimeric unit, while the bonds that link each Ru₃ unit (2.917(3) and 2.930(3) Å) are also of similar lengths to the corresponding distances in 1. Another example of a boat-like cluster, [Ru₆(μ₄-S)(μ-OH)₂(CO)₁₆(μ-CO)₂], has recently been reported by Adams *et al.*²⁵⁶ The basic structure of this cluster is similar to those of 1 and 2, the ligands also donate 46 electrons to the metal framework and the same pattern of bond elongation is observed. The bridging OH ligands are in positions similar to that occupied by the μ-SH ligand in 1.

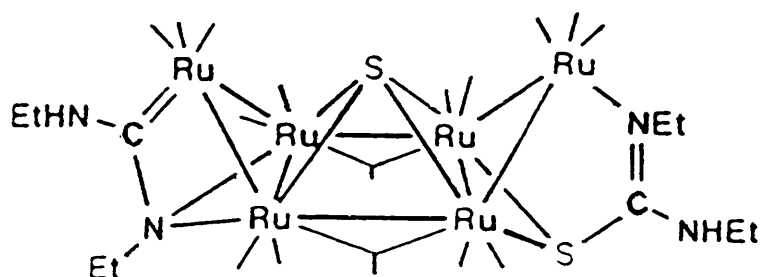


Figure 5.4 Structure of [Ru₆(μ₄-S)(μ₃-EtNCNHEt)(μ₃-EtNCSNHEt)(μ-CO)₂(CO)₁₄]

The dicarbide cobalt carbonyl cluster [Co₆(μ₄-S)(μ₆-C₂)(μ-CO)₆(CO)₈]

also adopts a regular boat configuration, again with a μ_4 -S atom spanning the square-base.²⁵⁷ It is electron-precise and so there is no bond elongation within the cluster. Other hexaruthenium compounds which exhibit elongation of certain metal-metal bonds include the cluster $[\text{Ru}_6(\text{PPh})_5(\text{CO})_{12}]$, which has a trigonal prismatic geometry.¹⁶⁷ The elongated bonds are in similar positions to those in **1**, *i.e.* on opposite sides of the square plane formed by the Ru_3 units, although the bond-lengthening in the phosphinidene compound is much greater, the relevant distances being 3.323(3) Å and 3.509(3) Å.

With the object of establishing whether $[\text{Ru}_6(\mu_4\text{-S})(\mu\text{-SH})(\mu_3\text{-pyS})(\text{CO})_{17}]$ could be oxidised to $[\text{Ru}_6(\mu_4\text{-S})(\mu\text{-SH})(\mu_3\text{-pyS})(\text{CO})_{17}]^{2+}$, its redox chemistry was investigated by cyclic voltammetry (Pt electrode in CH_2Cl_2). However, no oxidation waves were detected.

5.3 Other compounds produced from the thermolysis of $[\text{Ru}_3(\mu\text{-H})(\mu_3\text{-pyS})(\text{CO})_9]$ under an atmosphere of CO.

In addition to compound **1**, the thermolysis reaction of $[\text{Ru}_3(\mu\text{-H})(\mu_3\text{-pyS})(\text{CO})_9]$ under an atmosphere of CO led to a variety of other fractions on work-up using TLC, six of which were distinct and could be separated. The colours of these samples were, in order of elution, red (**i**), green (**ii**), green (**iii**), red (**iv**) and brown (**v**). The ^1H NMR spectrum of the green band (**ii**), showed this to be a mixture of two compounds. Recrystallisation from an ethanol/chloroform solution yielded crystals of the compound $[\text{Ru}_6(\mu_4\text{-S})(\mu\text{-SH})(\mu_3\text{-pyS})(\text{CO})_{17}]$ **1** and a further green complex, (**ii-a**). Apart from **1**, none of these compounds could be isolated in crystalline form and as a consequence

could not be properly characterised. Low yields were also a problem. The spectroscopic data collected on these compounds are displayed in Table 5.5. Data obtained by mass spectroscopy seems to indicate that compounds (i)–(iii) are hexaruthenium species, but since there are many ways in which two M_3 units have been observed to combine to form a new M_6 cluster,^{110,236} we can only speculate on the structure of these compounds. For instance, the ^1H NMR and mass spectra of compound (i) are consistent with a hexaruthenium complex of formula $[\text{Ru}_6(\text{pyS})_2(\text{CO})_{14}]$, or $[\{\text{Ru}_3(\text{pyS})(\text{CO})_7\}_2]$, which might have a structure similar to that found for $[\{\text{Os}_3\text{S}_2(\text{CO})_8\}_2]$ (Figure 5.5).²⁵³ Alternatively, the lone-pair of electrons on the sulphur atom of the pyS ligand may participate in bonding between the two Ru_3 units, as in $[\{\text{Ru}_3\text{H}(\text{pyS})(\text{CO})_7\}_3]$ (Figure 5.2). The spectroscopic data obtained for compound (ii-a), which was inseparable by TLC from $[\text{Ru}_6(\mu_4\text{-S})(\mu\text{-SH})(\mu_3\text{-pyS})(\text{CO})_{17}]$ **1**, is consistent with a formulation of $[\text{Ru}_6(\mu\text{-H})(\text{S})(\text{pyS})(\text{CO})_{16}]$ and might have a structure similar to that found for the thioureato complex $[\text{Ru}_6(\mu\text{-H})(\mu_5\text{-S})(\mu_3\text{-SC}(\text{NPh})\text{NPh})(\text{CO})_{16}]$ (Figure 5.6).¹⁷⁹

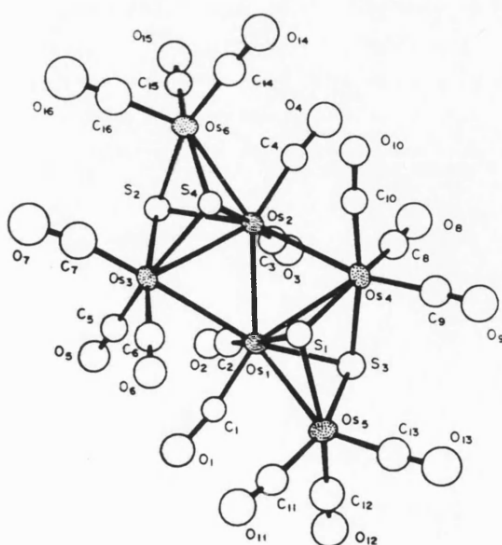


Figure 5.5 Structure of $[\{\text{Os}_3\text{S}_2(\text{CO})_8\}_2]$

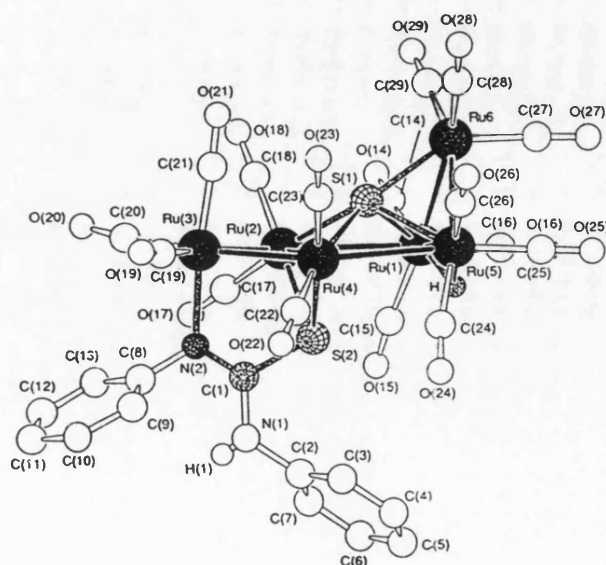


Figure 5.6 Structure of $[Ru_6(\mu-H)(\mu_5-S)(\mu_3-SC(NPh)NPh)(CO)_{16}]$

5.4 Other Reactions

(i) Photolysis of $[Ru_3(\mu-H)(\mu_3-pyS)(CO)_9]$

Initially, we had hoped this work would lead to compounds such as the 'trimer of trimers' and we looked into alternative routes to $[[Ru_3(\mu_3-H)(\mu_4-pyS)(CO)_7]_3]$. Photolysis of $[Os_3(\mu_3-S)_2(CO)_9]$ results in coupling of two trimeric units with loss of a CO ligand to form $[[Os_3(\mu_3-S)_2(CO)_8]_2]$, new Os–Os bonds being formed in the course of the reaction.²⁵³ However, when $[Ru_3(\mu-H)(\mu_3-pyS)(CO)_9]$ is exposed to UV irradiation an intractable black material, probably the result of decomposition or polymerisation, is formed.

(ii) Attempted synthesis of $[M_3(\mu-H)(\mu_3-S)(\mu-2-pyridyl)(CO)_9]$ ($M = Ru, Os$)

The aim of thermolysing $[Ru_3(\mu-H)(\mu_3-pyS)(CO)_9]$ in the presence of CO was to generate a product such as $[Ru_3(\mu-H)(\mu_3-S)(\mu-2-pyridyl)(CO)_9]$

which could then be used to build up molecules like $[\{\text{Ru}_3\text{H}(\text{pyS})(\text{CO})_7\}_3]$. Because this reaction gives rise to the products described in Sections 5.2 and 5.3, the attempted synthesis of this compound was approached in an alternative way. $[\text{Ru}_3(\mu\text{-H})_2(\mu_3\text{-S})(\text{CO})_9]^{258}$ was refluxed in pyridine for 20 mins, during which time the colour of the solution changed from yellow to red and changes were observed in the carbonyl-stretching region of the infrared spectrum. However, on TLC treatment of the resulting mixture, there appeared to be considerable decomposition on the TLC plates and only a small amount of material was recovered. One fraction was identified as starting material by its infrared spectrum, but the other remains unidentified.

A similar reaction was also attempted with the osmium analogue. However, no change in the infrared spectrum was observed after $[\text{Os}_3(\mu\text{-H})_2(\mu_3\text{-S})(\text{CO})_9]^{246}$ and pyridine were refluxed in octane for 6 hours.

(iii) CO Displacement from $[\text{Os}_3\text{H}(\text{pyS})(\text{CO})_9]$ by acetonitrile followed by reflux in cyclohexane

We also considered the possibility of attempting to form an osmium analogue of $[\{\text{Ru}_3(\mu_3\text{-H})(\mu_4\text{-pyS})(\text{CO})_7\}_3]$, which is formed from $[\text{Ru}_3(\mu\text{-H})(\mu_3\text{-pyS})(\text{CO})_9]$ after 3 hours in refluxing cyclohexane. However, $[\text{Os}_3(\mu\text{-H})(\mu_3\text{-pyS})(\text{CO})_9]$ shows no change when refluxed for 6 hours in nonane, *i.e.* there is no directly analogous route. However, when trimethylamine oxide and acetonitrile are used to displace a CO ligand and the resulting product refluxed in cyclohexane for 30 mins under nitrogen, a deep green compound, (vi), was separated by TLC on silica. The ^1H NMR spectrum of this compound shows two equal intensity sets of 2-pyridyl or pyS resonances

indicating that either the compound contains two such ligands or there are two species present, each containing only one of these ligands. There are also two hydride signals at -15.95 and -9.50 ppm. The infrared spectrum shows seven absorptions in the carbonyl-stretching region and is of similar complexity to the starting material. There is a peak at $m/e = 935$ in the mass spectrum which corresponds to the same molecular weight of the starting material. These spectroscopic data are displayed in Table 5.5. It is possible that C-S bond cleavage has occurred and a complex such as $[\text{Os}_3(\mu\text{-H})(\mu_3\text{-S})(\mu\text{-2-pyridyl})(\text{CO})_9]$ has been formed. Alternatively, the product could be of higher nuclearity, the result of some kind of condensation reaction. Unfortunately, the only crystals that it has been possible to grow have been unsuitable for an X-ray diffraction experiment and so the identity of this species remains unknown.

In summary, even though these experiments have proved inconclusive, it is obvious that there is a lot of interesting chemistry related to these systems. The problem is obtaining suitable crystals of these condensation products with high nuclearities, the proper characterisation of which tends to rely rather heavily on X-ray structure determination.

Table 5.3 ^1H NMR data for $[\text{Ru}_6(\mu_4\text{-S})(\mu\text{-SH})(\mu_3\text{-pyS})(\text{CO})_{17}]$

Compound	^1H NMR data (δ) ^a
$[\text{Ru}_6(\text{S})(\text{SH})(\text{pyS})(\text{CO})_{17}]$	8.77 (ddd, $J = 5.7, 0.9$ Hz, H^6), 7.60 (ddd, $J = 7.7, 7.7, 1.6$ Hz, H^4), 7.52 (ddd, $J = 7.7, 1.3$ Hz, H^3), 7.32 (ddd, $J = 7.4, 5.8, 1.6$ Hz, H^5).

a. Recorded in CDCl_3 at 400 MHz at room temperature.

Table 5.4 Infrared spectroscopic data for $[\text{Ru}_6(\mu_4\text{-S})(\mu\text{-SH})(\mu_3\text{-pyS})(\text{CO})_{17}]$.

Compound	$\nu(\text{CO})/\text{cm}^{-1}$
$[\text{Ru}_6(\text{S})(\text{SH})(\text{pyS})(\text{CO})_{17}]$	2103m, 2068s, 2041vs, 2037sh, 2009s, 1984br, 1876br.

a. Recorded in cyclohexane.

Table 5.5 Spectroscopic data for the unidentified compounds.

Compound	¹ H NMR (δ) ^a	IR ν(CO)/cm ⁻¹ ^b	MS ^c m/e
(i) (red)	8.70 ddd, 7.85 ddd, 7.73 ddd, 7.30 ddd.	2090m, 2066s, 2058s, 2044s, 2020m, 2010s, 2006sh, 1990w, 1952br.	1220
(ii-a) (green)	8.76 ddd, 7.61 ddd, 7.56 ddd, 7.32 ddd, -20.98 s.	2114m, 2082s, 2054s, 2033s, 1992br, 1952br.	1201
(iii) (green)	8.71 ddd ^x , 8.63 ddd ^y , 7.77 ddd ^y , 7.44 ddd ^x , 7.39 ddd ^y , 7.27 ddd ^x , 7.19 m ^{x+y} .	2078m, 2065m, 2049s, 2033s, 2024m, 2014w, 2003m, 1999m, 1975br, 1865br.	1280
(iv) (red)	8.59 ddd, 7.97 ddd, 7.66 ddd, 7.20 ddd, -14.60 s.		
(vi) (green)	9.21 ddd, 9.03 ddd, 8.08 ddd, 8.01 ddd, 7.76 ddd, 7.74 ddd, 7.18 ddd, 7.13 ddd, -9.50 s, -15.95 s.	2089m, 2073sh, 2067s, 2021s, 2009m, 2003m, 1964br.	935

- a. Recorded in CDCl₃ at 400 MHz. (The superscripts x and y represent major and minor resonances respectively.)
 b. Recorded in cyclohexane.
 c. Mass spectra obtained by FAB technique.

5.5 Experimental

Reaction of $[\text{Ru}_3\text{H}(\text{pyS})(\text{CO})_9]$ with CO in refluxing decane.

A solution of $[\text{Ru}_3\text{H}(\text{pyS})(\text{CO})_9]$ (0.224 g, 0.336 mmol) in n-decane (100 cm³) was heated under reflux for 1.5 h while CO at atmospheric pressure was bubbled through. The green/brown suspension was reduced to dryness under reduced pressure and the brown residue separated by TLC [SiO_2 , light petroleum (b.p. <40 °C)-dichloromethane (3:1 v/v)] to give several coloured bands, one yellow, two red and two green. The yellow band was identified as starting material by comparison with the infrared spectrum of $[\text{Ru}_3\text{H}(\text{pyS})(\text{CO})_9]$ (0.036 g, 16%). The first green band yielded $[\text{Ru}_6(\mu_4\text{-S})(\mu\text{-SH})(\mu_3\text{-pyS})(\text{CO})_{17}]$ (0.020 g, 5%) as green crystals from an ethanol/chloroform mixture. The two red (0.041 g and 0.014 g) and the other green (0.009 g) band remain unidentified.

Photolysis of $[\text{Ru}_3\text{H}(\text{pyS})(\text{CO})_9]$

$[\text{Ru}_3\text{H}(\text{pyS})(\text{CO})_9]$ (0.050 g, 0.075 mmol) was dissolved in dichloromethane (150 cm³) to form a yellow solution and irradiated with UV light for 19 h, in which time the solution lost its colour and an intractable black material, probably polymeric in nature, was deposited at the bottom of the reaction vessel.

Reaction of $[\text{Ru}_3(\text{H})_2(\text{S})(\text{CO})_9]$ in pyridine

A yellow solution of $[\text{Ru}_3(\text{H})_2(\text{S})(\text{CO})_9]$ (0.100 g, 0.170 mmol) in pyridine (40 cm³) was refluxed under N₂ for 20 mins to give a red solution.

The solvent was removed under reduced pressure and the residue chromatographed by TLC [SiO_2 , light petroleum (b.p. $<40\text{ }^\circ\text{C}$)-dichloromethane (7:3 then 1:4 v/v)]. A small amount of starting material (0.002 g) was recovered together with another very minor yellow band. There appeared to be considerable decomposition on the TLC plate.

Reaction of $[\text{Os}_3(\text{H})_2(\text{S})(\text{CO})_9]$ in pyridine

$[\text{Os}_3(\text{H})_2(\text{S})(\text{CO})_9]$ (0.144 g, 0.169 mmol) and pyridine (2 cm^3 ; approx. 20-fold excess) were dissolved in octane (30 cm^3) and the yellow solution refluxed under N_2 for 17 h. The infrared spectrum showed no change.

CO Displacement from $[\text{Os}_3\text{H}(\text{pyS})(\text{CO})_9]$ by acetonitrile followed by reflux in cyclohexane

$[\text{Os}_3\text{H}(\text{pyS})(\text{CO})_9]$ (0.083 g, 0.089 mmol) was dissolved in acetonitrile (50 cm^3) to form a yellow solution to which a solution of trimethylamine oxide ($\text{Me}_3\text{NO}\cdot 2\text{H}_2\text{O}$, 0.025 g, 0.225 mmol) in acetonitrile (5 cm^3) was added dropwise. After stirring the mixture under N_2 for 15 mins, the slightly darker yellow solution was filtered through a short silica column to remove any excess of Me_3NO . The solvent was removed under reduced pressure and cyclohexane (100 cm^3) added. After refluxing for 30 mins while N_2 was bubbled through, the colour of the solution changed to a clear dark green. The solvent was then removed under reduced pressure and the residue chromatographed by TLC [SiO_2 , light petroleum (b.p. $<40\text{ }^\circ\text{C}$)-dichloromethane (7:3 v/v and then 3:7 v/v)] yielding a green fraction (0.025 g) as well as several very minor fractions. None of these species could be characterised.

X-ray structure determination for [Ru₆(μ₄-S)(μ-SH)(μ₃-pyS)(CO)₁₇]

Crystals were obtained by adding a layer of ethanol to a chloroform solution of [Ru₆(μ₄-S)(μ-SH)(μ₃-pyS)(CO)₁₇] and allowing slow diffusion to occur.

A green crystal of the compound [Ru₆(μ₄-S)(μ-SH)(μ₃-pyS)(CO)₁₇] ($M = 1257.88 \text{ gmol}^{-1}$) with dimensions $0.50 \times 0.40 \times 0.10 \text{ mm}^3$ was mounted on a thin glass fibre on a Nicolet R3v/m automatic four-circle diffractometer. A monoclinic cell, $a = 9.236(1)$, $b = 22.770(4)$, $c = 16.363(3) \text{ \AA}$, $\beta = 98.16(1)^\circ$, $U = 3406(1) \text{ \AA}^3$, was determined by auto-indexing and least-squares fitting of 33 orientation reflections in the range $10 \leq 2\theta \leq 29^\circ$, selected from a rotation photograph. The cell parameters were confirmed by taking axial photographs. A total of 6132 unique intensity data were collected at room temperature using graphite-monochromated Mo-K α radiation ($\lambda = 0.71073 \text{ \AA}$) with the diffractometer operating in the ω scan mode between the limits $5 \leq 2\theta \leq 50^\circ$. The reflection intensities were corrected for Lorentz and polarisation effects and for decay by fitting the data to a curve calculated from three standard reflections collected periodically throughout the experiment. The data were finally corrected for absorption using the asimuthal scan method, $\mu(\text{Mo-K}\alpha) = 27.9 \text{ cm}^{-1}$.

The structure was solved by routine application of direct methods, in the space group $P2_1$, $Z = 4$, $F(000) = 2368$, $D_c = 2.45 \text{ g cm}^{-3}$. The model, with 542 parameters, was refined to $R = 0.0397$, $R_w = 0.0408$,* using 5748 intensity data with $F_0 \geq 3\sigma(F_0)$ by alternating cycles of full-matrix least-squares and by difference Fourier synthesis. The largest shift-to-error ratio in the final least-squares cycle was 0.001. All non-hydrogen atoms, were refined anisotropically

and H atoms for the pyS ligand were included in the model in idealised positions with C–H distances fixed at 0.96 Å and isotropic thermal parameter $U = 0.08 \text{ \AA}^2$ but their positions were not allowed to refine. The largest peak in the final difference Fourier map was 0.9 e/\AA^3 , found close to C(52).

Fractional atomic coordinates for $[\text{Ru}_6(\mu_4\text{-S})(\mu\text{-SH})(\mu_3\text{-pyS})(\text{CO})_{17}]$ are given in Table A7 in the appendix. All calculations were performed on a MicroVax II computer running SHELXTL PLUS.¹⁴¹

$$R = \Sigma [|F_o| - |F_c|] / \Sigma |F_o|$$

$$R_w = [\Sigma w(|F_o| - |F_c|)^2 / \Sigma w|F_o|^2]^{1/2}$$

$$w = 1/[\sigma^2(F_o) + 0.0005F_o^2]$$

APPENDIX

Fractional Atomic Coordinates and Equivalent Isotropic Displacement Parameters for the Crystal Structures

Table A1 Atomic Coordinates ($\times 10^4$) and Equivalent Isotropic Displacement Parameters ($\text{\AA}^2 \times 10^3$) for $[\text{Re}_2\text{Ru}_2\text{S}(\text{C}_5\text{H}_4\text{N})(\text{pyS})(\text{CO})_{13}]$ (Isomer B).

	x	y	z	U(eq)
Re(1)	-5462(1)	-352(1)	-7853(1)	40(1)
Re(2)	-2977(1)	-602(1)	-5757(1)	42(1)
Ru(1)	-3111(1)	-2320(1)	-7479(1)	44(1)
Ru(2)	-1676(1)	-1243(1)	-7863(1)	42(1)
S(1)	-3390(4)	-1080(2)	-7195(2)	38(1)
N(1)	-561(13)	-1683(7)	-6733(8)	46(5)
C(1)	-1255(16)	-2260(9)	-6612(10)	47(7)
C(2)	-569(18)	-2715(9)	-5971(11)	55(7)
C(3)	674(21)	-2593(11)	-5506(13)	69(9)
C(4)	1358(20)	-1988(11)	-5639(12)	62(8)
C(5)	725(16)	-1568(13)	-6256(11)	69(8)
S(2)	-4518(4)	349(2)	-6536(3)	49(2)
N(2)	-4055(14)	484(8)	-7939(9)	52(6)
C(6)	-3700(16)	767(9)	-7173(10)	45(6)
C(7)	-2792(19)	1316(11)	-6992(13)	68(8)
C(8)	-2293(22)	1592(11)	-7602(17)	85(12)
C(9)	-2669(24)	1272(14)	-8358(16)	97(12)
C(10)	-3613(20)	725(10)	-8529(12)	63(8)
C(11)	-2399(23)	-3094(11)	-7931(12)	69(9)
O(11)	-1987(18)	-3578(8)	-8172(10)	98(8)
C(12)	-4739(20)	-2329(10)	-8410(12)	64(8)
O(12)	-5649(17)	-2399(9)	-8942(10)	109(8)
C(13)	-3837(18)	-2804(10)	-6733(13)	60(8)
O(13)	-4212(15)	-3061(8)	-6245(9)	88(7)
C(14)	-606(20)	-1792(11)	-8350(10)	61(8)
O(14)	57(14)	-2160(7)	-8599(8)	73(6)
C(15)	-2843(18)	-1012(10)	-8928(11)	54(8)
O(15)	-3453(15)	-910(9)	-9577(9)	86(7)
C(16)	-652(18)	-357(11)	-7738(10)	50(7)
O(16)	-81(17)	132(9)	-7692(10)	97(8)
C(17)	-6978(18)	276(10)	-8235(12)	55(7)
O(17)	-7827(13)	654(7)	-8444(9)	71(6)
C(18)	-6646(19)	-1050(11)	-7602(12)	62(8)
O(18)	-7250(15)	-1485(8)	-7420(9)	88(7)
C(19)	-5955(16)	-736(10)	-8928(11)	51(7)
O(19)	-6309(13)	-907(8)	-9598(8)	74(6)
C(20)	-2878(16)	-134(11)	-4751(13)	59(8)
O(20)	-2835(14)	121(7)	-4142(8)	66(6)
C(21)	-4515(20)	-1184(11)	-5645(11)	61(8)
O(21)	-5353(17)	-1530(9)	-5595(11)	106(9)
C(22)	-1848(21)	-1323(12)	-5122(11)	71(9)
O(22)	-1144(20)	-1705(10)	-4713(10)	127(10)
C(23)	-1384(16)	-97(10)	-5889(11)	54(7)
O(23)	-472(13)	173(8)	-5930(8)	79(7)
Cl	-321(9)	4331(4)	4600(5)	129(4)
C(30)	-806(44)	4841(21)	5337(21)	85(14)

* Equivalent isotropic U defined as one third of the trace of the orthogonalized U_{ij} tensor

Table A2 Atomic Coordinates ($\times 10^4$) and Equivalent Isotropic DisplacementParameters ($\text{\AA}^2 \times 10^3$) for $[\text{Re}_2\text{Ru}_2(\text{S})(\text{H})(\text{C}_5\text{H}_4\text{N})(\text{CO})_{14}]$.

	x	y	z	U(eq)
Re(1)	2992(1)	1915(1)	3288(1)	44(1)
Re(2)	3764(1)	1051(1)	1689(1)	45(1)
Ru(1)	2489(1)	-641(1)	3546(1)	35(1)
Ru(2)	247(1)	2(1)	2760(1)	37(1)
S(1)	2427(3)	577(2)	2810(2)	34(1)
N(1)	2169(11)	-1133(7)	2360(7)	33(4)
C(1A)	2169(11)	-1133(7)	2360(7)	33(4)
C(1)	1070(11)	-801(7)	1962(7)	42(4)
N(1A)	1070(11)	-801(7)	1962(7)	42(4)
C(2)	648(15)	-1060(10)	1188(10)	59(6)
C(3)	1293(17)	-1630(11)	800(10)	70(7)
C(4)	2411(15)	-1990(11)	1189(10)	63(6)
C(5)	2838(15)	-1727(10)	1983(9)	57(6)
C(11)	1739(14)	-1565(11)	3994(8)	53(5)
O(11)	1261(13)	-2099(7)	4235(7)	77(5)
C(12)	4334(16)	-991(10)	3693(9)	59(6)
O(12)	5387(12)	-1195(10)	3771(9)	103(7)
C(13)	2492(16)	-107(10)	4592(9)	56(6)
O(13)	2458(16)	215(8)	5186(7)	97(6)
C(21)	-995(15)	-803(10)	3078(9)	50(5)
O(21)	-1725(10)	-1256(7)	3223(8)	69(4)
C(22)	-890(14)	526(11)	1874(10)	59(6)
O(22)	-1570(14)	774(10)	1393(10)	114(7)
C(23)	-305(15)	675(10)	3604(11)	59(6)
O(23)	-661(14)	1090(8)	4099(9)	103(6)
C(31)	3536(18)	3031(11)	3404(10)	67(6)
O(31)	3801(15)	3654(8)	3482(10)	110(7)
C(32)	2214(17)	1962(10)	4338(11)	62(6)
O(32)	1770(14)	2011(8)	4974(8)	90(6)
C(33)	1226(15)	2238(9)	2760(10)	55(6)
O(33)	171(12)	2379(7)	2466(8)	79(5)
C(34)	4665(17)	1536(11)	3872(10)	62(6)
O(34)	5590(14)	1308(10)	4254(9)	102(6)
C(41)	3777(17)	154(10)	946(10)	61(6)
O(41)	3835(16)	-353(9)	506(9)	102(6)
C(42)	5412(15)	603(11)	2321(11)	67(7)
O(42)	6299(11)	376(10)	2683(9)	101(6)
C(43)	2078(19)	1384(11)	1077(10)	65(6)
O(43)	1085(15)	1509(10)	723(9)	107(7)
C(44)	4787(19)	1666(12)	971(11)	75(7)
O(44)	5434(15)	2021(8)	553(9)	102(6)

* Equivalent isotropic U defined as one third of the trace of the orthogonalized U_{ij} tensor

Table A3 Atomic Coordinates ($\times 10^4$) and Equivalent Isotropic Displacement

Parameters ($\text{\AA}^2 \times 10^3$) for $[\text{Ru}_6(\text{S})_2(\text{C}_5\text{H}_4\text{N})_2(\text{CO})_{18}]$.				
	x	y	z	U (eq)
Ru(4)	1257	3970(1)	1247	34(1)
Ru(2)	3484(1)	3930(1)	2762(1)	39(1)
Ru(3)	3702(1)	4470(1)	1022(1)	40(1)
Ru(5)	1948(1)	3288(1)	-416(1)	37(1)
Ru(1)	3617(1)	2392(1)	2319(1)	38(1)
Ru(6)	3304(1)	2123(1)	151(1)	40(1)
S(1)	3130(3)	3622(2)	1800(1)	35(1)
S(2)	2597(3)	3401(2)	534(1)	33(1)
N(1)	1679(9)	3364(6)	2837(3)	41(3)
C(1A)	1679(9)	3364(6)	2837(3)	41(3)
C(1)	1745(9)	2580(6)	2622(4)	36(3)
N(1A)	1745(9)	2580(6)	2622(4)	36(3)
C(2)	688(12)	2092(8)	2629(5)	56(4)
C(3)	-492(13)	2374(8)	2823(5)	63(5)
C(4)	-524(13)	3160(9)	3038(6)	73(6)
C(5)	559(11)	3647(8)	3043(6)	58(5)
N(2)	3924(10)	3472(6)	-547(4)	49(4)
C(6)	4620(10)	2876(6)	-290(4)	44(4)
C(7)	5925(14)	2845(11)	-357(6)	84(7)
C(8)	6561(14)	3419(13)	-657(7)	103(8)
C(9)	5914(14)	4010(12)	-907(7)	95(7)
C(10)	4592(13)	4044(9)	-857(5)	67(5)
C(11)	5401(15)	2402(8)	2108(5)	63(5)
O(11)	6488(10)	2451(8)	2011(5)	103(5)
C(12)	3978(12)	1787(8)	2977(5)	51(4)
O(12)	4169(11)	1411(6)	3370(4)	84(4)
C(13)	3103(12)	1452(7)	1880(5)	49(4)
O(13)	2768(11)	884(6)	1647(4)	78(4)
C(21)	5286(16)	4259(9)	2625(5)	67(5)
O(21)	6281(12)	4476(9)	2567(6)	121(6)
C(22)	3885(13)	3614(8)	3504(5)	57(5)
O(22)	4081(12)	3457(6)	3951(4)	88(4)
C(23)	2814(13)	5038(8)	2892(5)	52(4)
O(23)	2467(10)	5669(6)	2991(4)	74(4)
C(31)	5518(16)	4262(9)	899(6)	72(6)
O(31)	6601(11)	4136(9)	836(6)	123(6)
C(32)	3907(15)	5373(8)	1518(5)	67(5)
O(32)	3979(13)	5901(6)	1813(5)	103(5)
C(33)	3421(13)	5199(7)	430(5)	61(5)
O(33)	3204(13)	5642(6)	73(4)	105(5)
C(41)	-52(11)	3122(7)	1389(4)	46(4)
O(41)	-815(11)	2647(7)	1432(5)	97(5)
C(42)	725(13)	4754(8)	1799(5)	56(4)
O(42)	435(11)	5221(6)	2106(4)	86(4)
C(43)	206(12)	4490(7)	695(5)	52(4)
O(43)	-388(10)	4810(6)	370(4)	75(4)
C(51)	262(13)	2932(8)	-184(5)	54(4)
O(51)	-706(9)	2739(7)	-19(4)	75(4)
C(52)	1431(12)	4368(8)	-670(5)	55(4)
O(52)	1108(12)	4995(6)	-831(4)	91(5)
C(53)	1785(10)	2732(7)	-1101(5)	44(4)
O(53)	1662(8)	2396(6)	-1516(4)	71(4)
C(61)	1856(13)	1562(8)	486(5)	55(4)
O(61)	982(11)	1262(6)	672(5)	93(5)
C(62)	4671(14)	1715(7)	648(5)	54(4)
O(62)	5496(10)	1484(6)	904(4)	78(4)
C(63)	3381(14)	1318(8)	-428(6)	67(5)
O(63)	3382(13)	856(6)	-767(4)	99(5)

Table A4 Atomic Coordinates ($\times 10^4$) and Equivalent Isotropic Displacement Parameters ($\text{\AA}^2 \times 10^3$) for $[\text{Ru}_2(\text{CO})_5(\text{C}_5\text{H}_4\text{N})(\text{C}_{10}\text{H}_7\text{N}_2)]$.

	x	y	z	U(eq)
Ru(1)	3952(1)	1663(1)	9150(1)	46(1)
Ru(2)	3432(1)	3708(1)	9007(1)	36(1)
N(1)	4254(4)	3933(9)	8948(7)	44(4)
C(1)	4535(5)	2968(11)	9048(8)	41(5)
C(2)	5104(5)	3013(13)	8982(9)	57(6)
C(3)	5331(5)	4037(13)	8832(9)	55(6)
C(4)	5033(5)	5036(12)	8715(9)	49(5)
C(5)	4467(5)	4939(10)	8759(8)	38(4)
C(6)	4047(5)	5834(11)	8594(8)	43(5)
C(7)	4159(6)	6976(13)	8432(9)	56(6)
C(8)	3740(7)	7746(13)	8241(11)	65(6)
C(9)	3204(6)	7378(13)	8198(9)	61(6)
C(10)	3107(6)	6255(12)	8387(9)	52(5)
N(2)	3507(4)	5504(9)	8553(7)	43(4)
N(3)	3406(4)	3057(9)	7598(7)	40(4)
C(21)	3657(5)	2041(12)	7681(9)	51(5)
C(22)	3674(6)	1407(13)	6858(11)	65(6)
C(23)	3434(7)	1869(16)	5966(11)	79(8)
C(24)	3192(7)	2895(15)	5908(10)	68(7)
C(25)	3179(5)	3493(13)	6726(10)	57(5)
C(11)	3519(5)	3934(10)	10336(10)	42(5)
O(11)	3589(4)	4018(8)	11143(6)	59(4)
C(12)	2680(5)	3390(12)	8990(9)	47(5)
O(12)	2220(4)	3209(11)	8966(7)	90(5)
C(13)	4450(7)	503(14)	8913(13)	78(7)
O(13)	4741(5)	-191(11)	8753(10)	123(7)
C(14)	4168(6)	1677(12)	10551(11)	57(6)
O(14)	4296(5)	1716(10)	11351(7)	87(5)
C(15)	3271(6)	822(12)	9104(11)	59(6)
O(15)	2863(5)	357(10)	9069(9)	94(6)

* Equivalent isotropic U defined as one third of the trace of the orthogonalized U_{ij} tensor

Table A5 Atomic Coordinates ($\times 10^4$) and Equivalent Isotropic DisplacementParameters ($\text{\AA}^2 \times 10^3$) for $[\text{Ru}_2\text{HCl}(\text{CO})_3(\text{MeC}_5\text{H}_3\text{N})_2(\text{C}_{10}\text{H}_8\text{N}_2)] \cdot \text{H}_2\text{O}$.

	x	y	z	U(eq)
Ru(1)	7782(1)	388(1)	5486(1)	44(1)
Ru(2)	6498(1)	-733(1)	5948(1)	49(1)
Cl(1)	6031(3)	-1574(3)	6907(3)	71(2)
N(1)	7006(9)	1224(8)	4907(7)	46(4)
N(2)	8039(9)	143(8)	4377(7)	52(4)
C(1)	6477(12)	1703(10)	5206(10)	59(5)
C(2)	5943(14)	2167(13)	4799(11)	79(7)
C(3)	5899(13)	2042(12)	4086(11)	71(6)
C(4)	6425(13)	1552(11)	3793(11)	67(6)
C(5)	7035(11)	1143(10)	4191(9)	48(5)
C(6)	7618(10)	585(9)	3918(8)	40(4)
C(7)	7788(14)	542(11)	3178(10)	73(5)
C(8)	8428(13)	51(12)	2983(11)	75(6)
C(9)	8811(12)	-430(11)	3422(10)	61(5)
C(10)	8592(13)	-358(11)	4143(10)	68(6)
N(3)	7741(9)	-1060(7)	6149(6)	41(3)
C(11)	8326(10)	-539(9)	5924(9)	47(5)
C(12)	9187(12)	-761(12)	6006(10)	65(5)
C(13)	9430(11)	-1418(11)	6315(9)	53(5)
C(14)	8806(11)	-1908(11)	6534(10)	61(5)
C(15)	7988(12)	-1728(11)	6431(9)	58(5)
C(16)	10334(14)	-1626(14)	6367(13)	101(8)
N(4)	6737(8)	170(7)	6677(7)	42(4)
C(21)	7333(9)	664(9)	6466(8)	34(4)
C(22)	7540(11)	1259(9)	6908(8)	46(5)
C(23)	7119(12)	1387(10)	7520(9)	53(5)
C(24)	6438(12)	925(10)	7700(10)	57(5)
C(25)	6283(11)	280(11)	7269(9)	58(5)
C(26)	7342(13)	2030(11)	8021(10)	79(6)
C(30)	8678(12)	970(11)	5606(10)	62(6)
O(30)	9327(10)	1326(9)	5683(8)	98(5)
C(40)	5429(13)	-367(11)	5811(10)	62(5)
O(40)	4764(10)	-96(9)	5778(7)	89(5)
C(41)	6383(15)	-1479(14)	5292(13)	89(7)
O(41)	6321(10)	-1937(10)	4828(10)	111(6)
O(1)	5000	3119(16)	2500	135(9)

* Equivalent isotropic U defined as one third of the trace of the orthogonalized U_{ij} tensor

Table A6 Atomic Coordinates ($\times 10^4$) and Equivalent Isotropic Displacement Parameters ($\text{\AA}^2 \times 10^3$) for $[\text{Os}_2(\text{CO})_6(\text{MeC}_5\text{H}_3\text{N})_2]$ (Head-to-tail isomer).

	x	y	z	U(eq)
Os(1)	5599(1)	6238(1)	2202(1)	29(1)
Os(2)	3435(1)	7429(1)	1859(1)	35(1)
N(1)	3597(13)	5984(7)	928(8)	31(4)
C(1)	2603(14)	6580(8)	742(10)	32(5)
C(2)	1185(19)	6566(9)	-91(11)	43(5)
C(3)	830(20)	5901(11)	-678(12)	52(6)
C(4)	1842(20)	5305(10)	-437(13)	52(6)
C(5)	3212(21)	5331(9)	359(12)	47(6)
N(2)	2749(15)	6617(7)	2804(9)	41(4)
C(6)	-769(25)	5884(14)	-1585(14)	76(9)
C(7)	3846(15)	6041(7)	2973(10)	26(4)
C(8)	3614(16)	5424(8)	3566(10)	34(5)
C(9)	2317(19)	5406(9)	3998(11)	43(5)
C(10)	1226(18)	6048(10)	3784(13)	47(6)
C(11)	1474(18)	6606(10)	3201(13)	46(6)
C(12)	2100(23)	4751(10)	4631(14)	60(7)
C(20)	6480(19)	5247(9)	2438(11)	40(5)
O(20)	7121(19)	4672(7)	2683(10)	75(6)
C(21)	6990(18)	6709(9)	3339(12)	40(5)
O(21)	7843(15)	7013(8)	4051(10)	67(5)
C(22)	6917(20)	6577(12)	1328(14)	57(7)
O(22)	7707(18)	6793(9)	871(12)	83(7)
C(30)	1415(22)	7970(10)	1507(13)	54(7)
O(30)	222(17)	8303(8)	1246(11)	79(6)
C(31)	4540(26)	8044(10)	3050(15)	64(8)
O(31)	5122(17)	8399(8)	3719(12)	82(6)
C(32)	4419(18)	7989(9)	976(14)	50(6)
O(32)	5027(19)	8272(8)	481(12)	91(7)

* Equivalent isotropic U defined as one third of the trace of the orthogonalized U_{ij} tensor

Table A7 Atomic Coordinates ($\times 10^4$) and Equivalent Isotropic DisplacementParameters ($\text{\AA}^2 \times 10^3$) for $[\text{Ru}_6(\text{S})(\text{SH})(\text{pyS})(\text{CO})_{17}]$.

	x	y	z	U(eq)
Ru(1)	1049(1)	4175	5626(1)	29(1)
Ru(2)	4239(1)	4454(1)	5367(1)	31(1)
Ru(3)	3185(1)	3331(1)	5582(1)	36(1)
Ru(4)	660(1)	5380(1)	6159(1)	31(1)
Ru(5)	3915(1)	5659(1)	5899(1)	39(1)
Ru(6)	2423(1)	6245(1)	7058(1)	43(1)
Ru(7)	1391(1)	9491(1)	10152(1)	37(1)
Ru(8)	2491(1)	9038(1)	8519(1)	38(1)
Ru(9)	2888(2)	8414(1)	10031(1)	50(1)
Ru(10)	1430(1)	10693(1)	9514(1)	39(1)
Ru(11)	2538(1)	10251(1)	7932(1)	35(1)
Ru(12)	2743(1)	11414(1)	8470(1)	43(1)
S(1)	2894(3)	4795(1)	6493(2)	31(1)
S(3)	1628(3)	5737(1)	4923(2)	34(1)
S(2)	2009(3)	4466(1)	4363(2)	33(1)
N(1)	2557(11)	3305(5)	4275(6)	34(3)
C(1)	2158(13)	3798(5)	3826(8)	35(4)
C(2)	1855(15)	3789(6)	2994(8)	42(4)
C(3)	1926(16)	3277(7)	2547(11)	54(5)
C(4)	2294(16)	2776(7)	2998(9)	48(5)
C(5)	2610(15)	2790(7)	3829(10)	50(5)
C(1B)	-721(13)	4778(5)	5433(8)	34(3)
O(1B)	-1885(11)	4778(5)	5071(6)	53(2)
C(2B)	4846(13)	5253(6)	4878(8)	35(3)
O(2B)	5348(13)	5441(5)	4328(7)	64(3)
C(11)	525(16)	3846(6)	6574(9)	45(3)
O(11)	164(13)	3607(6)	7144(8)	69(3)
C(12)	-132(15)	3643(6)	5027(9)	40(3)
O(12)	-912(14)	3297(6)	4637(8)	71(3)
C(21)	5883(15)	4320(6)	6164(8)	41(3)
O(21)	6923(13)	4206(5)	6623(7)	68(3)
C(22)	5196(14)	4091(6)	4577(8)	39(3)
O(22)	5753(13)	3895(5)	4050(7)	66(3)
C(31)	3604(17)	3423(7)	6716(10)	56(4)
O(31)	3893(13)	3465(5)	7444(7)	66(3)
C(32)	2135(15)	2614(6)	5699(9)	44(3)
O(32)	1543(16)	2188(6)	5750(9)	83(4)
C(33)	5079(17)	2977(7)	5565(10)	52(4)
O(33)	6242(14)	2808(5)	5639(7)	71(3)
C(41)	45(14)	5161(6)	7138(8)	41(3)
O(41)	-345(13)	5011(5)	7732(8)	68(3)
C(42)	-831(17)	5930(7)	5956(9)	51(3)
O(42)	-1783(13)	6276(5)	5840(7)	64(3)
C(51)	5544(14)	5659(6)	6664(8)	39(3)
O(51)	6596(13)	5675(5)	7142(7)	65(3)
C(52)	4506(17)	6368(7)	5546(10)	52(4)
O(52)	4943(16)	6802(6)	5294(8)	84(4)
C(61)	1677(19)	6754(8)	6177(11)	60(4)
O(61)	1292(17)	7072(7)	5641(9)	90(4)
C(62)	3961(19)	6770(8)	7458(11)	60(4)
O(62)	4846(17)	7123(7)	7648(9)	89(4)
C(63)	996(19)	6495(8)	7739(11)	60(4)
O(63)	143(19)	6649(8)	8115(11)	105(5)
C(64)	3186(17)	5659(7)	7889(10)	53(4)
O(64)	3618(13)	5358(5)	8412(7)	68(3)

Table A7 (cont.)

	x	y	z	U(eq)
S(4)	3241(4)	9899(2)	9374(2)	38(1)
S(6)	-14(3)	9205(1)	8831(2)	35(1)
S(5)	29(3)	10432(1)	8178(2)	35(1)
N(2)	566(12)	11559(5)	7796(7)	45(4)
C(6)	-398(15)	11118(6)	7692(8)	39(4)
C(7)	-1749(15)	11189(7)	7186(9)	52(5)
C(8)	-2095(17)	11712(7)	6824(10)	55(5)
C(9)	-1119(17)	12175(7)	6953(11)	62(6)
C(10)	163(18)	12088(6)	7440(11)	57(6)
C(3B)	1941(15)	9482(6)	7312(8)	42(3)
O(3B)	1479(12)	9296(5)	6691(7)	56(3)
C(4B)	35(16)	10229(7)	10210(9)	41(3)
O(4B)	-1018(14)	10358(6)	10520(8)	80(4)
C(71)	2620(15)	9632(6)	11121(9)	44(3)
O(71)	3456(14)	9695(5)	11725(8)	69(3)
C(72)	72(17)	9088(7)	10721(9)	51(3)
O(72)	-744(15)	8826(6)	11049(8)	82(4)
C(81)	4401(16)	8885(7)	8427(9)	48(3)
O(81)	5604(17)	8781(7)	8364(10)	96(4)
C(82)	1971(18)	8345(7)	7972(10)	57(4)
O(82)	1683(16)	7893(7)	7633(9)	89(4)
C(91)	4722(18)	8834(7)	10325(10)	55(4)
O(91)	5828(17)	9056(7)	10509(10)	95(4)
C(92)	1015(18)	8082(7)	9635(10)	56(4)
O(92)	-108(15)	7845(6)	9451(8)	80(4)
C(93)	2852(25)	8180(10)	11138(14)	87(6)
O(93)	2876(19)	8019(8)	11815(11)	105(5)
C(94)	3808(24)	7760(10)	9658(14)	84(6)
O(94)	4326(20)	7318(8)	9440(11)	111(5)
C(101)	228(19)	11327(8)	9562(11)	62(4)
O(101)	-603(15)	11725(6)	9584(8)	78(3)
C(102)	2667(19)	10966(8)	10446(11)	60(4)
O(102)	3452(17)	11154(7)	10996(9)	91(4)
C(111)	2130(14)	10619(6)	6916(9)	42(3)
O(111)	1806(12)	10827(5)	6262(7)	61(3)
C(112)	4514(18)	10185(7)	7793(10)	55(4)
O(112)	5724(15)	10157(6)	7706(8)	82(4)
C(121)	4517(18)	11198(7)	9083(10)	58(4)
O(121)	5666(17)	11092(7)	9435(9)	91(4)
C(122)	3702(19)	11723(8)	7628(11)	61(4)
O(122)	4374(17)	11926(7)	7127(9)	89(4)
C(123)	2663(20)	12130(8)	9061(12)	68(5)
O(123)	2702(20)	12567(8)	9410(11)	112(5)

* Equivalent isotropic U defined as one third of the trace of the orthogonalized U_{ij} tensor

GENERAL EXPERIMENTAL

Infrared Spectra

All infrared spectra were recorded on a Perkin-Elmer PE-983 spectrophotometer operated through a data station. The solution spectra were recorded using a cell fitted with calcium fluoride plates. A cell of equal path length filled with pure solvent was placed in the reference beam. The solid state spectra were recorded as caesium iodide discs.

NMR Spectra

All ^1H and ^{13}C NMR spectra were recorded on Varian VXR-400 or XL-200 spectrometers and are referenced to chloroform or acetone.

Mass Spectra

Mass spectra were either recorded on a VG ZAB F-1 high resolution mass spectrometer at the London School of Pharmacy, or on a VG 7070 high-resolution mass spectrometer operated in this department.

Microanalysis

Elemental analyses were performed by the staff in the analytical laboratory, Department of Chemistry, University College London.

Chromatography

Chromatographic separations were performed using preparative thin layer plates (silica gel 60 HF₂₅₄, E.Merck, West Germany) which were prepared as an aqueous slurry and dried at room temperature overnight before being stored in an oven at about 100 °C.

REFERENCES

1. E. S. Raper, *Coord. Chem. Rev.*, 1985, **61**, 115.
2. A. H. Norbury and A. I. P. Sinha, *Quart. Revs. Chem. Soc.*, 1970, **24**, 69.
3. B. Rosenberg, L. VanCamp J. E. Trosko and V. H. Mansour, *Nature*, 1969, **222**, 385.
4. S. J. Lippard, *Acc. Chem. Res.*, 1978, **11**, 211.
5. D. J. Hodgson, *Prog. in Inorg. Chem.*, 1977, **23**, 211.
6. H. L. Yale in *Pyridine and its derivatives.*, Ed. E. Klinsberg, Interscience, 1964, Part IV.
7. A. Albert and G. B. Barlin, *J. Chem. Soc.*, 1959, 2384.
8. A. R. Katritzky and R. A. Jones, *J. Chem. Soc.*, 1958, 3610.
9. P. Beak, J. B. Covington, S. G. Smith, J. M. White and J. M. Zeigler, *J. Org. Chem.*, 1980, **45**, 1354.
10. L. Stefaniak, *Org. Mag. Reson.*, 1979, **12**, 379.
11. a. P. Beak, F. S. Fry Jr., J. Lee and F. Steele, *J. Am. Chem. Soc.*, 1976, **98**, 171.
b. P. Beak, J. B. Covington and S. G. Smith, *J. Am. Chem. Soc.*, 1976, **98**, 8284.
12. B. R. Penfold, *Acta Crystallogr.*, 1953, **6**, 707.
13. U. Ohms, H. Guth, A. Kutoglu and C. Scheringer, *Acta Crystallogr., Sect. B*, 1982, **B38**, 831.
14. A. Kvik and S. S. Booles, *Acta Crystallogr., Sect. B*, 1972, **28**, 3405.
15. A. Lautié and A. Novak, *Chem. Phys. Lett.*, 1980, **71**, 290.
16. T. J. Batterham in *NMR Spectra of simple Heterocycles*, John Wiley, New

York, 1973.

17. P. W. von Ostwalden and J. D. Roberts, *J. Org. Chem.*, 1971, **36**, 3792.
18. D. W. Aksnes and H. Kryvi, *Acta Chem. Scand.*, 1972, **26**, 2255.
19. M. C. Vitorge, M. T. Chenon, C. Coupry and N. Lumbroso Bader, *Org. Magn. Reson.*, 1983, **21**, 20.
20. T. B. Cobb and J. D. Memory, *J. Chem. Phys.*, 1969, **50**, 4262.
21. E. W. Randall and D. G. Gillies, *Prog. in NMR Spectroscopy*, 1969, **6**, pp.125 and references therein.
22. C. G. Kuehn and S. S. Isied, *Prog. in Inorg. Chem.*, 1980, **27**, 153.
23. P. Mura, B. G. Olby and S. D. Robinson, *J. Chem. Soc., Dalton Trans.*, 1985, 2101.
24. R. G. Pearson, *Science*, 1966, **151**, 172.
25. N. N. Greenwood and A. Earnshaw, *Chemistry of the Elements*, Pergamon Press, 1984, pp.1065.
26. E. Binamera-Soriega, M. Lundeen and K. Seff, *Acta Crystallogr. Sect. B*, 1979, **35**, 2875.
27. B. P. Kennedy and A. B. P. Lever, *Can. J. Chem.*, 1972, **50**, 3488.
28. A. J. Deeming, M. N. Meah, H. M. Dawes and M. B. Hursthouse, *J. Organomet. Chem.*, 1986, **299**, C25.
29. P. Mura, B. G. Olby and S. D. Robinson, *Inorg. Chim. Acta*, 1985, **98**, L21.
30. I. P. Evans and G. Wilkinson, *J. Chem. Soc., Dalton Trans.*, 946.
31. S. C. Kokkou, S. Fortier, P. J. Rentzeperis and P. Karagiannidis, *Acta Crystallogr., Sect. C*, 1983, **39**, 178.
32. E. C. Constable and P. R. Raithby, *J. Chem. Soc., Dalton Trans.*, 1987, 2281.

33. R. Usón, A. Laguna, M. Laguna, J. Jiménez, M. P. Gómez, A. Sainz and P. G. Jones, *J. Chem. Soc., Dalton Trans.*, 1990, 3457.
34. J. A. Broomhead, R. Greenwood, W. Pienkowski and M. Sterns, *Aust. J. Chem.*, 1986, **39**, 1895.
35. J. Chatt, A. J. Pearman and R. L. Richards, *J. Chem. Soc., Dalton Trans.*, 1978, 1766.
36. J. Vicente, M.-T. Chicote, I. Saura-Llamas and M.-C. Lagunas, *J. Chem. Soc., Chem. Commun.*, 1992, 915.
37. P. D. Cookson and E. R. T. Tiekink, *J. Chem. Soc., Dalton Trans.*, 1993, 259.
38. N. N. Greenwood and A. Earnshaw, *Chemistry of the Elements*, Pergamon Press, 1984, pp.1389.
39. A. O. Baghlaf, M. Ishaq and A. K. A. Rashed, *Polyhedron*, 1987, **6**, 837.
40. a. A. J. Deeming, K. I. Hardcastle, M. N. Meah, P. A. Bates, H. M. Dawes and M. B. Hursthouse, *J. Chem. Soc., Dalton Trans.*, 1988, 227.
b. A. J. Deeming, M. N. Meah, P. A. Bates and M. B. Hursthouse, *Inorg. Chim. Acta*, 1988, **142**, 37.
41. A. J. Deeming and M. N. Meah, *Inorg. Chim. Acta*, 1988, **142**, 33.
42. B. Rosenberg, L. VanCamp and T. Drigas, *Nature*, 1965, **205**, 698.
43. a. F. K. V. Leh and W. Wolf, *J. Pharm. Sci.*, 1976, **65**, 315.
b. S. Fujieda and T. Osa, *Chem. Ind.*, 1978, **29**, 1145.
44. S. Fujieda, E. Tabata, A. Hatano and T. Osa, *Heterocycles*, 1981, **15**, 743.
45. J. D. Gilbert, D. Rose and G. Wilkinson, *J. Chem. Soc. (A)*, 1970, 2765.
46. S. R. Fletcher and A. C. Skapski, *J. Chem. Soc., Dalton Trans.*, 1972, 635.
47. A. Alteparmakian, B. G. Olby and S. D. Robinson, *Inorg. Chim. Acta*,

- 1985, 104, L5.
48. M. Kita, K. Yamanari and Y. Shimura, *Chem. Lett.*, 1983, 141.
 49. A. P. Bozopoulos, S. C. Kokkou, P. J. Rentzeperis and P. Karagiannidis, *Acta Crystallogr., Sect. C*, 1984, 40, 944.
 50. S. G. Rosenfield, S. A. Swedberg, S. K. Arora and P. K. Mascharak, *Inorg. Chem.*, 1986, 25, 2109.
 51. D. R. Corbin, L. C. Francesconi, D. N. Hendrickson and G. D. Stucky, *Inorg. Chem.*, 1979, 18, 3069.
 52. F. A. Cotton, P. E. Fanwick and J. W. Fitch III, *Inorg. Chem.*, 1978, 17, 3254.
 53. M. A. A. F. De C. T. Carrondo, A. R. Dias, M. H. Garcia, A. Mirpuri, M. F. M. Piedade and M. S. Salema, *Polyhedron*, 1989, 8, 2439.
 54. F. A. Cotton and W. H. Ilsley, *Inorg. Chem.*, 1981, 20, 614.
 55. H. E. Toma, P. S. Santos, M. P. D. Mattioli and L. A. A. Oliveira, *Polyhedron*, 1987, 6, 603.
 56. A. J. Deeming, M. N. Meah, N. P. Randle and K. I. Hardcastle, *J. Chem. Soc., Dalton Trans.*, 1989, 2211.
 57. C. K. Brown, D. Georgiou and G. Wilkinson, *J. Chem. Soc., Dalton Trans.*, 1973, 929.
 58. G. López, G. Sánchez, G. García, J. García, A. Martínez, J. A. Hermoso and M. Martínez-Ripoll, *J. Organomet. Chem.*, 1992, 435, 193.
 59. L. C. Damude, P. A. W. Dean, V. Manivannan, R. S. Srivastava and J. J. Vittal, *Can. J. Chem.*, 1990, 68, 1323.
 60. a. M. Masaki, S. Matsunami, T. Kimura and T. Oshima, *Bull. Chem. Soc. Japan*, 1979, 52, 502.

- b. M. Masaki, S. Matsunami, S. Fujimura and K. Okimoto, *Bull. Chem. Soc. Japan*, 1979, **52**, 536.
61. M. B. Hursthouse, O. F. Z. Khan, M. Mazid, M. Motevalli and P. O'Brien, *Polyhedron*, 1990, **9**, 541.
62. a. D. H. Blinn, P. Butler, K. M. Chapman and S. Harris, *Inorg. Chim. Acta*, 1977, **24**, 139, and references therein.
- b. R. H. Lane, N. S. Pantaleo, J. K. Farr, W. M. Coney and M. G. Newton, *J. Am. Chem. Soc.*, 1978, **100**, 1610.
63. P. Powell, *J. Organomet. Chem.*, 1974, **65**, 89.
64. a. E. C. Constable and J. Lewis, *J. Organomet. Chem.*, 1983, **254**, 105.
- b. E. C. Constable and P. R. Raithby, *Inorg. Chim. Acta*, 1991, **183**, 21.
65. A. J. Deeming and M. Karim, *Polyhedron*, 1991, **10**, 837.
66. K. I. Hardcastle, B. R. Cockerton, A. J. Deeming and M. Karim, *J. Chem. Soc., Dalton Trans.*, 1992, 1607.
67. I. Kinoshita, Y. Yasuba, K. Matsumoto and S. Ooi, *Inorg. Chim. Acta*, 1983, **80**, L13.
68. K. Umakoshi, I. Kinoshita, Y. Fukui-Yasuba, K. Matsumoto, S. Ooi, H. Nakai and M. Shiro, *J. Chem. Soc., Dalton Trans.*, 1989, 815.
69. K. Umakoshi, I. Kinoshita and S. Ooi, *Inorg. Chim. Acta*, 1987, **127**, L41.
70. M. A. Ciriano, F. Viguri, J. J. Perez-Torrente, F. J. Lahoz, L. A. Oro, A. Tiripicchio and M. Tiripicchio-Camellini, *J. Chem. Soc., Dalton Trans.*, 1989, 25.
71. A. J. Deeming, M. N. Meah, P. A. Bates and M. B. Hursthouse, *J. Chem. Soc., Dalton Trans.*, 1988, 2193.
72. K. Burgess, B. F. G. Johnson and J. Lewis, *J. Organomet. Chem.*, 1982, **233**,

C55.

73. N. Lugan, F. Laurent, G. Lavigne, T. P. Newcomb, E. W. Liimatta and J. J. Bonnet, *J. Am. Chem. Soc.*, 1990, **112**, 8607.
74. A. J. Deeming, M. Karim, P. A. Bates and M. B. Hursthouse, *Polyhedron*, 1988, **7**, 1401.
75. A. J. Deeming, M. Karim, N. I. Powell and K. I. Hardcastle, *Polyhedron*, 1990, **9**, 623.
76. B. R. Cockerton, A. J. Deeming, M. Karim and K. I. Hardcastle, *J. Chem. Soc., Dalton Trans.*, 1991, 431.
77. M. A. Ciriano, F. Viguri, F. J. Lahoz, L. A. Oro, A. Tiripicchio and M. Tiripicchio-Camellini, *Nouv. J. Chim.*, 1986, **10**, 75.
78. N. Lenhart and H. Singer, *Z. Naturforsch.*, 1975, **B30**, 284.
79. A. J. Deeming, K. I. Hardcastle and M. M. Karim, *Inorg. Chem.*, 1992, **31**, 4792.
80. A. J. Deeming, M. N. Meah, P. A. Bates and M. B. Hursthouse, *J. Chem. Soc., Dalton Trans.*, 1988, 235.
81. M. Kasuhisa, A. Matsuda and T. Masuda, *Jpn. Kokai Tokkyo Koho*, Japanese Patents, JP 63,179,841; *Chem. Abs.*, 1989, **110**, 7670s.
82. A. Albert, *Heterocyclic Chemistry*, The Athlone Press, University of London, 1968, pp.68-74, 155.
83. *Comprehensive Organometallic Chemistry*, Eds. G. Wilkinson, F. G. A. Stone and E. W. Abel, Vols. 1 and 2.
84. a. W. Sliwa, *Transition Met. Chem.*, 1989, **14**, 321, and references therein.
b. W. Sliwa, *Transition Met. Chem.*, 1988, **13**, 161.
85. D. Mandler and I. Willnar, *J. Phys. Chem.*, 1987, **91**, 3600.

86. B. Crociani, F. Di Bianca, A. Giovenco, A. Berton and R. Bertani, *J. Organomet. Chem.*, 1989, **361**, 255.
87. A. Mantovani, *J. Organomet. Chem.*, 1983, **255**, 385.
88. K. Isobe, E. Kai, Y. Nakamura, K. Hishimoto, T. Miwa, S. Kawaguchi, K. Kinoshita and K. Nakatsu, *J. Am. Chem. Soc.*, 1980, **102**, 2475.
89. a. K. Isobe, Y. Nakamura and S. Kawaguchi, *Bull. Chem. Soc. Japan*, 1980, **53**, 139.
b. K. Isobe, Y. Nakamura and S. Kawaguchi, *Chem. Lett.*, 1977, 1383.
90. B. Crociani, F. Di Bianca, A. Giovenco and A. Berton, *J. Organomet. Chem.*, 1987, **323**, 123.
91. a. K. Nakatsu, K. Kinoshita, H. Kanda, K. Isobe, Y. Nakamura and S. Kawaguchi, *Chem. Lett.*, 1980, 913.
b. K. Isobe and S. Kawaguchi, *Heterocycles*, 1981, **16**, 1603.
92. a. J. Halpern and J. P. Maher, *J. Am. Chem. Soc.*, 1965, **87**, 5361.
b. W. W. Adams and P. G. Lenhert, *Acta Crystallogr., Sect. B*, 1970, **29**, 2412.
93. a. L. G. Vaughan, *J. Am. Chem. Soc.*, 1970, **92**, 730.
b. L. G. Vaughan, *J. Organomet. Chem.*, 1980, **190**, C56.
94. J. Cook, M. Green and F. G. A. Stone, *J. Chem. Soc. (A)*, 1968, 173.
95. G. Conole, M. McPartlin, H. R. Powell, T. Dutton, B. F. G. Johnson and J. Lewis, *J. Organomet. Chem.*, 1989, **379**, C1.
96. a. R. D. Adams and D. F. Foust, *Organometallics*, 1983, **2**, 323.
b. R. D. Adams, Z. Dawoodi, D. F. Foust and B. E. Segmüller, *J. Am. Chem. Soc.*, 1983, **105**, 831.
97. G. A. Foulds, B. F. G. Johnson and J. Lewis, *J. Organomet. Chem.*, 1985,

- 296, 147.
98. M. I. Bruce, M. G. Humphrey, M. R. Snow, E. R. T. Tiekink and R. C. Wallis, *J. Organomet. Chem.*, 1986, **314**, 311.
99. A. Eisenstadt, C. M. Giandomenico, M. F. Frederick and R. M. Laine, *Organometallics*, 1985, **4**, 2033.
100. C. Choo Yin and A. J. Deeming, *J. Chem. Soc., Dalton Trans.*, 1975, 2091.
101. P. O. Nubel, S. R. Wilson and T. L. Brown, *Organometallics*, 1983, **2**, 515.
102. a. B. Klei and J. H. Teuben, *J. Chem. Soc., Chem. Commun.*, 1978, 659.
b. B. Klei and J. H. Teuben, *J. Organomet. Chem.*, 1981, **214**, 53.
103. P. L. Watson, *J. Chem. Soc., Chem. Commun.*, 1983, 276.
104. M. E. Thompson, S. M. Baxter, A. R. Bulls, B. J. Burger, M. C. Nolan, B. D. Santarsiero, W. P. Schaefer and J. E. Bercaw, *J. Am. Chem. Soc.*, 1987, **109**, 203.
105. F. P. Netzer and G. Rangelov, *Surface Science*, 1990, **225**, 260.
106. V. H. Grassian and E. L. Muetterties, *J. Phys. Chem.*, 1986, **90**, 5900.
107. E. L. Muetterties, T. N. Rhodin, E. Band, C. F. Brucker and W. R. Pretzer, *Chem. Rev.*, 1979, **79**, 91.
108. R. Whyman in *Transition Metal Clusters*, Ed. B. F. G. Johnson, Wiley, 1980, Chapter 8.
109. R. D. Adams, Z. Dawoodi, D. F. Foust and B. E. Segmüller, *Organometallics*, 1983, **2**, 315.
110. R. D. Adams, *Polyhedron*, 1985, **4**, 2003.
111. R. D. Adams, I. T. Horváth and P. Mathur, *J. Am. Chem. Soc.*, 1983, **105**, 7202.
112. R. D. Adams, J. E. Babin and M. Tasi, *Inorg. Chem.*, 1988, **27**, 2618.

113. P. R. Raithby in *Transition Metal Clusters*, ed B. F. G. Johnson, Wiley, 1980, Section 2.10.
114. S. Martinengo, P. Chini, V. G. Albano, F. Cariati and T. Salvatori, *J. Organomet. Chem.*, 1973, **59**, 379.
115. J. Knight and M. J. Mays, *J. Chem. Soc. (A)*, 1970, 654.
116. J. Knight and M. J. Mays, *J. Chem. Soc., Dalton Trans.*, 1972, 1022.
117. G. L. Geoffroy and W. L. Gladfelter, *J. Am. Chem. Soc.*, 1977, **99**, 304.
118. e.g. M. J. Mays, P. R. Raithby, P. L. Taylor and K. Henrick, *J. Chem. Soc., Dalton Trans.*, 1984, 959.
119. a. M. R. Churchill, F. J. Hollander and R. A. Lashewycz, *J. Am. Chem. Soc.*, 1981, **103**, 2430.
b. J. R. Shapley, G. A. Pearson, M. Tachikawa, G. E. Schmidt, M. R. Churchill and F. J. Hollander, *J. Am. Chem. Soc.*, 1977, **99**, 8064.
120. W. L. Gladfelter and G. L. Geoffroy in *Comprehensive Organometallic Chemistry*, Eds. G. Wilkinson, F. G. A. Stone and E. W. Abel, Pergamon, Oxford, 1982, vol. 6, ch. 40.
121. a. E. L. Muetterties, *Angew. Chem. Int. Ed. Engl.*, 1978, **17**, 545.
b. E. L. Muetterties, *Science*, 1977, **196**, 839.
122. G. Huttner, J. Schneider, H.-D. Müller, G. Mohr, J. V. Seyerl and L. Wohlfahrt, *Angew. Chem. Int. Ed. Engl.*, 1979, **18**, 76.
123. C. U. Pitman Jr., G. M. Wilemon, W. D. Wilson and R. C. Ryan, *Angew. Chem. Int. Ed. Engl.*, 1980, **19**, 478.
124. Y. Chi, G.-H. Lee, S.-M. Peng and C.-H. Wu, *Organometallics*, 1989, **8**, 1574.
125. Y. Chi, G.-H. Lee, B.-J. Liu and S.-M. Peng, *Polyhedron*, 1989, **8**, 2003.

126. J. A. Connor in *Transition Metal Clusters*, ed B. F. G. Johnson, Wiley, 1980, p. 358.
127. J. A. Smieja and W. L. Gladfelter, *Inorg. Chem.*, 1986, **25**, 2667.
128. Y. Chi, D.-K. Hwang, S.-F. Chen, L.-K. Liu, *J. Chem. Soc., Chem. Commun.*, 1989, 1540.
129. a. A. J. Deeming, M. S. B. Felix, P. A. Bates and M. B. Hursthouse, *J. Chem. Soc., Chem. Commun.*, 1987, 461.
b. A. J. Deeming and M. Underhill, *J. Chem. Soc., Dalton Trans.*, 1973, 2727.
130. Y. Chi, L.-K. Liu, G. Huttner and L. Zsolnai, *J. Organomet. Chem.*, 1990, **390**, C50.
131. R.-C. Lin, Y. Chi, S.-M. Peng and G.-H. Lee, *Inorg. Chem.*, 1992, **31**, 3818.
132. A. J. Carty, S. A. MacLaughlin and N. J. Taylor, *J. Organomet. Chem.*, 1981, **204**, C27.
133. M. Lanfranchi, A. Tiripicchio, E. Sappa, S. A. MacLaughlin and A. J. Carty, *J. Chem. Soc., Chem. Commun.*, 1982, 538.
134. M. R. Churchill, F. J. Hollander and J. P. Hutchinson, *Inorg. Chem.*, 1977, **16**, 2655.
135. B. F. G. Johnson, R. D. Johnston and J. Lewis, *J. Chem. Soc. (A)*, 1968, 2865.
136. M. R. Churchill, K. N. Amoh and H. J. Wasserman, *Inorg. Chem.*, 1981, **20**, 1609.
137. M. Herberhold, D. Reiner, K. Ackermann, U. Thewalt and T. Debaerdemaker, *Z. Naturforsch.*, 1984, **B39**, 1199.
138. M. R. Churchill in *Transition Metal Hydrides*, Ed. R. Bau.

139. R. D. Adams, D. F. Foust and B. E. Segmüller, *Organometallics*, 1983, **2**, 308.
140. M. R. Churchill and B. G. DeBoer, *Inorg. Chem.*, 1977, **16**, 878.
141. G. M. Sheldrick, SHELXTL PLUS, An intergrated system for refining and displaying crystal structures from diffraction data, University of Göttingen, 1986.
142. B. F. G. Johnson, R. D. Johnston, J. Lewis, B. H. Robinson and G. Wilkinson, *J. Chem. Soc. (A)*, 1968, 2856.
143. B. F. G. Johnson, J. Lewis and P. A. Kilty, *J. Chem. Soc. (A)*, 1968, 2859.
144. C. R. Eady, P. F. Jackson, B. F. G. Johnson, J. Lewis, M. C. Malatesta, M. McPartlin and W. J. H. Nelson, *J. Chem. Soc., Dalton Trans.*, 1980, 383.
145. a. M. I. Bruce in *Comprehensive Organometallic Chemistry*, Eds. G. Wilkinson, F. G. A. Stone, E. W. Abel, Pergamon, 1982, Chapter 32.6.
b. B. F. G. Johnson, J. Lewis, M. McPartlin, J. Morris, G. L. Powell, P. R. Raithby and M. D. Vargas, *J. Chem. Soc., Chem. Commun.*, 1986, 429.
146. P. Chini, *J. Organomet. Chem.*, 1980, **200**, 37-61.
147. M. D. Vargas and J. N. Nicholls, *Adv. Inorg. Chem. Radiochem.*, 1986, **30**, 123.
148. P. Chini, G. Longoni and V. G. Albano, *Adv. Inorg. Chem. Radiochem.*, 1976, **14**, 285.
149. S.-H. Han, S. T. Nguyen and G. L. Geoffroy, *Organometallics*, 1988, **7**, 2034.
150. A. J. Arce, P. Arrojo, A. J. Deeming and Y. De Sanctis, *J. Chem. Soc., Dalton Trans.*, 1992, 2423.
151. D. McIntosh and G. A. Ozin, *J. Am. Chem. Soc.*, 1976, **98**, 3167.

152. C.-M. T. Hayward and J. R. Shapley, *J. Am. Chem. Soc.*, 1982, **104**, 7347.
153. P. F. Jackson, B. F. G. Johnson, J. Lewis, W. J. H. Nelson and M. McPartlin, *J. Chem. Soc., Dalton Trans.*, 1982, 2099.
154. S. R. Bunkhall, H. D. Holden, B. F. G. Johnson, J. Lewis, G. N. Pain, P. R. Raithby and M. J. Taylor, *J. Chem. Soc., Chem. Commun.*, 1984, 25.
155. G. Ciani, A. Magni and A. Sironi, *J. Chem. Soc., Chem. Commun.*, 1981, 1280.
156. a. G. Ciani, L. Garlaschelli, A. Sironi and S. Martinengo, *J. Chem. Soc., Chem. Commun.*, 1981, 563.
b. N. N. Greenwood and A. Earnshaw, *Chemistry of the Elements*, Pergamon, 1984, p1326.
157. G. Ciani, A. Sironi and S. Martinengo, *J. Chem. Soc., Chem. Commun.*, 1982, 1099.
158. J. L. Vidal, R. A. Fiato, L. A. Cosby and R. L. Pruett, *Inorg. Chem.*, 1978, **17**, 2574.
159. P. Braunstein, *Nouv. J. Chim.*, 1986, **10**, 365.
160. M. Fajardo, H. D. Holden, B. F. G. Johnson, J. Lewis and P. R. Raithby, *J. Chem. Soc., Chem. Commun.*, 1984, 24.
161. F. Bachechi, J. Ott and L. M. Venanzi, *J. Am. Chem. Soc.*, 1985, **107**, 1760.
162. a. A. Ceriotti, F. Demartin, G. Longoni, M. Manassero, M. Marchionna, G. Piva and M. Sansoni, *Angew. Chem. Int. Ed. Eng.*, 1985, **24**, 697.
b. D. Fenske, J. Ohmer and J. Hachgenei, *Angew. Chem. Int. Ed. Eng.*, 1985, **24**, 993.
163. M. J. Freeman, A. D. Miles, M. Murray, A. G. Orpen and F. G. A. Stone, *Polyhedron*, 1984, **3**, 1093.

164. L. F. Rhodes, J. C. Huffman and K. G. Caulton, *J. Am. Chem. Soc.*, 1983, **105**, 5137.
165. G. Doyle, B. T. Heaton and E. Occhiello, *Organometallics*, 1985, **4**, 1224.
166. J. S. Field, R. J. Haines, E. Minshall and D. N. Smit, *J. Organomet. Chem.*, 1986, **310**, C69.
167. J. S. Field, R. J. Haines and D. N. Smit, *J. Chem. Soc., Dalton Trans.*, 1988, 1315.
168. J. Lunniss, S. A. MacLaughlin, N. J. Taylor, A. J. Carty and E. Sappa, *Organometallics*, 1985, **4**, 2066.
169. A. J. Carty, S. A. MacLaughlin, J. Van Wagner and N. J. Taylor, *Organometallics*, 1982, **1**, 1013.
170. a. M. I. Bruce, M. J. Liddell and E. R. T. Tiekink, *J. Organomet. Chem.*, 1990, **391**, 81.
b. M. I. Bruce, M. J. Liddell, B. W. Skelton and A. H. White, *Organometallics*, 1991, **10**, 3282.
171. M. I. Bruce, M. L. Williams, J. M. Patrick and A. H. White, *J. Chem. Soc., Dalton Trans.*, 1985, 1229.
172. J. S. Field, R. J. Haines and D. N. Smit, *J. Organomet. Chem.*, 1982, **224**, C49.
173. K. Natarajan, L. Zsolnai and G. Huttner, *J. Organomet. Chem.*, 1981, **209**, 85.
174. F. Van Gastel, N. J. Taylor and A. J. Carty, *J. Chem. Soc., Chem. Commun.*, 1987, 1049.
175. F. Van Gastel, N. J. Taylor and A. J. Carty, *Inorg. Chem.*, 1989, **28**, 384.
176. L. M. Bullock, J. S. Field, R. J. Haines, E. Minshall and D. N. Smit, *J.*

Organomet. Chem., 1986, **310**, C47.

177. S. Rossi, J. Pursiainen and T. A. Pakkenen, *Organometallics*, 1991, **10**, 1390.
178. B. F. G. Johnson, J. Lewis, K. Wong and M. McPartlin, *J. Organomet. Chem.*, 1980, **185**, C17.
179. a. G. Süss-Fink, U. Bodensieck, L. Hoferkamp, G. Rheinwald and H. Stoeckli-Evans, *J. Cluster Science*, 1992, **3**, 469.
b. G. Süss-Fink, U. Bodensieck, L. Hoferkamp and H. Stoeckli-Evans, *J. Chem. Soc., Dalton Trans.*, 1993, 127.
180. S. Jeannin, Y. Jeannin and G. Lavigne, *Inorg. Chem.*, 1978, **17**, 2103.
181. a. M. R. DuBois, M. C. Van Derveer, D. L. DuBois, R. C. Haltiwanger and W. K. Miller, *J. Am. Chem. Soc.*, 1980, **102**, 7456.
b. H. Alper and H.-N. Paik, *J. Org. Chem.*, 1977, **42**, 3522.
182. R. D. Adams, J. E. Babin and M. Tasi, *Inorg. Chem.*, 1986, **25**, 4514.
183. R. D. Adams, J. E. Babin and M. Tasi, *Inorg. Chem.*, 1986, **25**, 4460.
184. R. D. Adams, J. E. Babin and M. Tasi, *Inorg. Chem.*, 1987, **26**, 2807.
185. a. R. D. Adams, J. E. Babin and M. Tasi, *Organometallics*, 1988, **7**, 503.
b. R. D. Adams, J. E. Babin, M. Tasi and T. A. Wolfe, *Polyhedron*, 1988, **7**, 1071.
c. R. D. Adams, J. E. Babin, M. Tasi and T. A. Wolfe, *New J. Chem.*, 1988, **12**, 481.
186. a. R. D. Adams, T. A. Wolfe and W. Wu, *Polyhedron*, 1991, **10**, 447.
b. R. D. Adams, J. E. Babin and J.-G. Wang, *Polyhedron*, 1989, **8**, 2351.
187. U. Bodensieck, C. Meister, H. Stoeckli-Evans and G. Süss-Fink, *J. Chem. Soc., Dalton Trans.*, 1992, 2131.

188. a. R. J. Goudsmit, B. F. G. Johnson, J. Lewis, P. R. Raithby and K. H. Whitmore, *J. Chem. Soc., Chem. Commun.*, 1982, 640.
b. G. Longoni, M. Manassero and M. Sironi, *J. Am. Chem. Soc.*, 1980, **102**, 7973.
189. S. Bhaduri, K. Sharma and P. G. Jones, *J. Chem. Soc., Chem. Commun.*, 1987, 1769.
190. N. M. Boag, C. B. Knobler and H. D. Kaesz, *Angew. Chem. Int. Ed. Engl.*, 1983, **22**, 249.
191. M. I. Bruce, M. P. Cifuentes and M. G. Humphrey, *Polyhedron*, 1991, **10**, 277.
192. S. R. Drake and R. Khattar, *Organomet. Synth.*, 1988, **4**, 234.
193. G. A. Foulds, B. F. G. Johnson and J. Lewis, *J. Organomet. Chem.*, 1985, **224**, 123.
194. H. Bantel, B. Hansert, A. K. Powell, M. Tasi and H. Vahrenkamp, *Angew. Chem. Int. Ed. Engl.*, 1989, **28**, 1059.
195. R. D. Adams, J. E. Babin and J. Tanner, *Organometallics*, 1988, **7**, 765.
196. R. D. Adams, J. E. Babin and J. Tanner, *Organometallics*, 1988, **7**, 2027.
197. J. A. Smieja, R. E. Stevens, D. E. Fjare and W. L. Gladfelter, *Inorg. Chem.*, 1985, **24**, 3206.
198. a. C. E. Anson, J. P. Attard, B. F. G. Johnson, J. Lewis, J. M. Mace and D. B. Powell, *J. Chem. Soc., Chem. Commun.*, 1986, 1715.
b. M. A. Collins, B. F. G. Johnson, J. Lewis, J. M. Mace, J. Morris, M. McPartlin, W. J. H. Nelson, J. Puga and P. R. Raithby, *J. Chem. Soc., Chem. Commun.*, 1983, 689.
199. K. Henrick, B. F. G. Johnson, J. Lewis, J. M. Mace, M. McPartlin and J.

- Morris, *J. Chem. Soc., Chem. Commun.*, 1985, 1617.
200. B. F. G. Johnson, J. Lewis, W. G. H. Nelson, J. Puga, P. R. Raithby, M. Braga, M. McPartlin and W. Clegg, *J. Organomet. Chem.*, 1983, **243**, C13.
201. B. F. G. Johnson, J. Lewis, W. G. H. Nelson, J. Puga, M. McPartlin and A. Sironi, *J. Organomet. Chem.*, 1983, **253**, C5.
202. M. P. Gomez-Sal, B. F. G. Johnson, J. Lewis, P. R. Raithby and S. N. A. B. Syed-Mustaffa, *J. Organomet. Chem.*, 1984, **272**, C21.
203. B. R. Cockerton and A. J. Deeming, *J. Organomet. Chem.*, 1992, **426**, C36.
204. V. A. Maksakov, V. A. Ershova, V. P. Kirin, I. F. Golavaneva, A. Ya. Mikhailova and A. P. Klyagina, *Dokl. Akad. Nauk SSSR*, 1988, **299**, 116.
205. J. M. Coleman, A. Wojcicki, P. J. Pollick and L. F. Dahl, *Inorg. Chem.*, 1967, **6**, 1236.
206. R. D. Adams, D. Männig and B. E. Segmüller, *Organometallics*, 1983, **2**, 149.
207. R. D. Adams, Z. Dawoodi and D. F. Foust, *Organometallics*, 1982, **1**, 411.
208. R. D. Adams, I. T. Horváth, P. Mathur and B. E. Segmüller, *Organometallics*, 1983, **2**, 996.
209. P. Parhami and B. M. Fung, *J. Am. Chem. Soc.*, 1985, **107**, 7304.
210. A. J. Deeming and R. Vaish, unpublished results.
211. E. G. Bryan, B. F. G. Johnson, J. W. Kelland, J. Lewis and M. McPartlin, *J. Chem. Soc., Chem. Commun.*, 1974, 254.
212. B. F. G. Johnson, J. Lewis and D. A. Pippard, *J. Chem. Soc., Dalton Trans.*, 1981, 407.
213. a. E. C. Constable, *Polyhedron*, 1984, **3**, 1037.
b. J. Shapley, D. Samkoff, C. Bueno and M. R. Churchill, *Inorg. Chem.*,

- 1982, **21**, 634.
214. J. A. Cabeza, L. A. Oro, A. Tiripicchio and M. Tiripicchio-Camellini, *J. Chem. Soc., Dalton Trans.*, 1988, 1437.
215. T. Venäläinen, J. Pursiainen and T. A. Pakkanen, *J. Chem. Soc., Chem. Commun.*, 1982, 1348.
216. A. J. Deeming, R. Peters, M. B. Hursthouse and J. D. J. Backer-Dirks, *J. Chem. Soc., Dalton Trans.*, 1982, 787.
217. K. Nomiya and H. Suzuki, *Bull. Chem. Soc. Japan*, 1979, **52**, 623.
218. a. E. Alessio, G. Clauti and G. Mestroni, *J. Mol. Catal.*, 1985, **29**, 77.
b. E. Alessio, G. Zassinovich and G. Mestroni, *J. Mol. Catal.*, 1983, **18**, 113.
219. A. J. Arce, A. J. Deeming, M. B. Hursthouse, L. New, N. P. C. Walker, C. C. Yin, unpublished results.
220. M. Hansen and H. J. Jakobsen, *J. Magn. Res.*, 1973, **10**, 74.
221. Ch. Elschenbroich and A. Salzer, *Organometallics*, VCH Publishers New York, 1989, p298.
222. F. Neumann and G. Süss-Fink, *J. Organomet. Chem.*, 1989, **367**, 175.
223. M. Langenbahn, H. Stoeckli-Evans and G. Süss-Fink, *J. Organomet. Chem.*, 1990, **397**, 347.
224. F. Neumann, H. Stoeckli-Evans and G. Süss-Fink, *J. Organomet. Chem.*, 1989, **379**, 139.
225. a. E. O. Fischer, V. Kiener, D. St. P. Bunbury, E. Frank, P. F. Lindley and O. S. Mills, *J. Chem. Soc., Chem. Commun.*, 1968, 1378.
b. E. O. Fischer and V. Keiner, *J. Organomet. Chem.*, 1970, **23**, 215.
226. E. O. Fischer and V. Keiner, *J. Organomet. Chem.*, 1972, **42**, 447.

227. T. A. Stephenson and G. Wilkinson, *J. Inorg. Nucl. Chem.*, 1966, **28**, 945.
228. S. D. Robinson and G. Wilkinson, *J. Chem. Soc. (A)*, 1966, 300.
229. D. M. Adams, *Metal-Ligand and Related Vibrations*, Arnold, London, 1967, Chapters 2 and 3.
230. K. Nakamoto, *Infrared and Raman Spectra of Inorganic and Coordination Compounds.*, Wiley-Interscience, New York, Fourth Ed., 1986, pp. 324-9.
231. S. N. Vinogradov and R. H. Linnell, *Hydrogen Bonding*, Van Nostrand Reinhold Company, New York, 1971.
232. B. R. Sutherland and M. Cowie, *Organometallics*, 1985, **4**, 1637.
233. J. Lewis and B. F. G. Johnson, *Pure and Appl. Chem.*, 1982, **54**, 97.
234. C.-M. T. Hayward and J. R. Shapley, *Inorg. Chem.*, 1982, **21**, 3816.
235. R. D. Adams, I. T. Horvath and L.-W. Wang, *J. Am. Chem. Soc.*, 1983, **105**, 1533.
236. A. J. Deeming, *J. Cluster Science*, 1992, **3**, 347.
237. K. I. Hardcastle, T. McPhillips, A. J. Arce, Y. De Sanctis, A. J. Deeming and N. I. Powell, *J. Organomet. Chem.*, 1990, **389**, 361.
238. A. J. Deeming and N. I. Powell, unpublished work.
239. A. J. Deeming, S. Doherty, M. W. Day, K. I. Hardcastle and H. Minassian, *J. Chem. Soc., Dalton Trans.*, 1991, 1273.
240. a. C. J. Cardin, S. B. Colbran, B. F. G. Johnson, J. Lewis and P. R. Raithby, *J. Chem. Soc., Chem. Commun.*, 1986, 1288.
- b. S. B. Colbran, C. M. Hay, B. F. G. Johnson, F. J. Lahoz, J. Lewis and P. R. Raithby, *J. Chem. Soc., Chem. Commun.*, 1986, 1766.
241. A. J. Deeming, S. Doherty and N. I. Powell, *Inorg. Chim. Acta*, 1992, **198-200**, 469

242. D. H. Williams and I. Fleming, *Spectroscopic Methods in Organic Chemistry*, McGraw Hill 1989.
243. A. G. Cowie, B. F. G. Johnson, J. Lewis, J. N. Nicholls, P. R. Raithby and M. J. Rosales, *J. Chem. Soc., Dalton Trans.*, 1983, 2311.
244. D. Rabinovich and G. Parkin, *J. Am. Chem. Soc.*, 1991, **113**, 5904.
245. L. J. Bellamy, *The Infrared Spectra of Complex Molecules*, Methuen, 1962, pp.350.
246. R. D. Adams, I. T. Horvath, B. E. Segmüller, L.-W. Wang, *Organometallics*, 1983, **2**, 1301.
247. G. Hogarth, J. A. Phillips, F. Van Gestel, N. J. Taylor, T. B. Marder and A. J. Carty, *J. Chem. Soc., Chem. Commun.*, 1988, 1570.
248. L. R. Martin, F. W. B. Einstein and R. K. Pomeroy, *Organometallics*, 1988, **7**, 294.
249. R. D. Adams and L.-W. Wang, *J. Am. Chem. Soc.*, 1983, **105**, 235.
250. A. J. Carty, *Pure and Appl. Chem.*, 1982, **54**, 113.
251. L. H. Staal, L. H. Polm, K. Vrieze, F. Ploeger and C. H. Stam, *Inorg. Chem.*, 1981, **20**, 3590.
252. A. J. Carty, S. A. MacLaughlin J. Van Wagner and N. J. Taylor, *Organometallics*, 1982, **1**, 1013.
253. R. D. Adams and I. T. Horvath, *J. Am. Chem. Soc.*, 1984, **106**, 1869.
254. P. D. Frisch and L. F. Dahl, *J. Am. Chem. Soc.*, 1972, **94**, 5082.
255. K. Wade in *Transition Metal Clusters*, Ed. B. F. G. Johnson, Wiley NY, 1980, Chapter 3.
256. R. D. Adams, J. E. Babin and M. Tasi, *Inorg. Chem.*, 1987, **26**, 2561.
257. G. Gervasio, R. Rossetti, P. L. Stanghellini and G. Bor, *Inorg. Chem.*,

1984, **23**, 2073.

258. R. D. Adams and D. A. Katahira, *Organometallics*, 1982, **1**, 53.
259. M. N. Meah, Ph.D. thesis, University College London, 1986.
260. D. R. Neithamer, L. Párkányi, J. F. Mitchell and P. T. Wolczanski, *J. Am. Chem. Soc.*, 1988, **110**, 4421.
261. M.-D. Su and S.-Y. Chu, *J. Phys. Chem.*, 1989, **93**, 6043.
262. R. H. Morris and J. M. Ressler, *J. Chem. Soc., Chem. Commun.*, 1983, 909.
263. H. W. Choi and M. S. Sollberger, *J. Organomet. Chem.*, 1983, **243**, C39.
264. H.-G. Biedermann, K. Öfele, N. Schuhbauer and J. Tajtelbaum, *Z. Naturforsch.*, 1976, **B31**, 321
265. H.-G. Biedermann, K. Öfele, N. Schuhbauer and J. Tajtelbaum, *Angew. Chem. Int. Ed.*, 1975, **14**, 639.
266. P. L. Timms, *Angew. Chem. Int. Ed.*, 1975, **14**, 273.
267. a. E. H. Wucherer and E. L. Muetterties, *Organometallics*, 1987, **6**, 1691.
b. E. H. Wucherer and E. L. Muetterties, *Organometallics*, 1987, **6**, 1696.
268. a. L. H. Simons, P. E. Riley, R. E. Davis and J. J. Lagowski, *J. Am. Chem. Soc.*, 1976, **98**, 1044.
b. P. E. Riley and R. E. Davis, *Inorg. Chem.*, 1976, **15**, 2735.